SOME OTHER ELBS LOW-PRICED EDITIONS

Anderson, Leaver, Alexander and Rawlings	MATERIALS SCIENCE	*Van Nostrand Reinhold (UK)*
Bishop and Henkel	THE MEASUREMENT OF SOIL PROPERTIES IN THE TRIAXIAL TEST	*Edward Arnold*
Case and Chilver	STRENGTH OF MATERIALS AND STRUCTURES	*Edward Arnold*
Coates, Coutie and Kong	STRUCTURAL ANALYSIS	*Van Nostrand Reinhold (UK)*
Jackson	CIVIL ENGINEERING MATERIALS	*Macmillan*
John	INTRODUCTION TO ENGINEERING MATERIALS	*Macmillan*
Lambert	STRUCTURAL STEELWORK	*Longman*
Marshall and Nelson	STRUCTURES	*Pitman*
Neidle	ELECTRICAL INSTALLATION TECHNOLOGY	*Butterworth*
Neville	PROPERTIES OF CONCRETE	*Pitman*
Reeves	NEWNES ELECTRICAL POCKET BOOK	*Butterworth*
Ryder	STRENGTH OF MATERIALS	*Macmillan*
Smith	SOIL MECHANICS	*Longman*
Tomlinson	FOUNDATION DESIGN AND CONSTRUCTION	*Pitman*
Young, Griffiths and Fardon	AUTOMOBILE ELECTRICAL AND ELECTRONIC EQUIPMENT	*Butterworth*

a short course in FOUNDATION ENGINEERING

N.E.SIMONS and B.K.MENZIES

BUTTERWORTHS
London Boston Durban Singapore Sydney Toronto Wellington

First published 1975 by IPC Science and Technology Press
Reprinted 1976, 1977, 1980, 1982, 1986

ISBN 0 408 00295 6

Photoset by Butterworths Litho Preparation Department
Printed in England by J. W. Arrowsmith Ltd., Bristol BS3 2NT

Recommended list of units, unit abbreviations, quantity symbols and conversion factors for use in soil and rock mechanics. Part 1. SI base units, derived units and multiples

Quantity and symbol	Units and multiples	Unit abbreviation	Conversion factors for existing units	Remarks
Length (various)	kilometre metre millimetre micrometre	km m mm μm	1 mile = 1.609 km 1 yard = 0.9144 m 1 ft = 0.3048 m 1 in = 25.40 mm	1 micrometer = 1 micron
Area (A)	square kilometre square metre square millimetre	km^2 m^2 mm^2	1 mile^2 = 2.590 km^2 1 yd^2 = 0.8361 m^2 1 ft^2 = 0.09290 m^2 1 in^2 = 645.2 mm^2	
Volume (V)	cubic metre cubic centimetre cubic millimetre	m^3 cm^3 mm^3	1 yd^3 = 0.7646 m^3 1 ft^3 = 0.02832 m^3 1 in^3 = 16.39 cm^3 1 UK gallon = 4546 cm^3	To be used for solids and liquids
Mass (m)	megagram (or tonne) kilogram gram	Mg (t) kg g	1 ton = 1.016 Mg 1 lb = 0.4536 kg	Megagram is the SI term
Unit weight (γ)	kilonewton per cubic metre	kN/m^3	100 lb/ft^3 = 15.708 kN/m^3 (62.43 lb/ft^3 pure water = 9.807 kN/m^3 = specific gravity 1.0 approx.)	Unit weight is weight per unit volume
Force (various)	meganewton kilonewton newton	MN kN N	1 tonf = 9.964 kN 1 lbf = 4.448 N 1 kgf = 9.807 N	
Pressure (p, u)	meganewton per square metre	MN/m^2	1 tonf/in^2 = 15.44 MN/m^2 (1 MN/m^2 = 1 N/mm^2)	To be used for shear strength, compressive strength, bearing capacity, elastic moduli and laboratory pressures of rock
Stress (σ, τ) and Elastic moduli (E, G, K)	kilonewton per square metre	kN/m^2	1 lbf/in^2 = 6.895 kN/m^2 1 lbf/ft^2 = 0.04788 kN/m^2 1 tonf/ft^2 = 107.3 kN/m^2 1 bar = 100 kN/m^2 1 kgf/cm^2 = 98.07 kN/m^2	Ditto for soils
Coefficient of volume compressibility (m_v) or swelling (m_s)	square metre per meganewton square metre per kilonewton	m^2/MN m^2/kN	1 ft^2/tonf = 9.324 m^2/MN = 0.009324 m^2/kN	
Coefficient of water permeability (k_w)	metre per second	m/s	1 cm/s = 0.010 m/s	This is a velocity, depending on temperature and defined by Darcy's law $V = k_w \frac{\delta h}{\delta s}$ V = velocity of flow $\frac{\delta h}{\delta s}$ = hydraulic gradient
Absolute permeability (k)	square micrometre	μm^2	1 Darcy = 0.9869 μm^2	This is an area which quantifies the seepage properties of the ground independently of the fluid concerned or its temperature $V = \frac{k\rho g}{\eta} \frac{\delta h}{\delta s}$ ρ = fluid density g = gravitational acceleration η = dynamic viscosity
Dynamic viscosity (η)	millipascal second (centipoise)	mPas (cP)	1 cP = 1 mPas (1 Pa = 1 kN/m^2)	Dynamic viscosity is defined by Stokes' Law. A pascal is a kilonewton per square metre

Quantity and symbol	Units and multiples	Unit abbreviation	Conversion factors for existing units	Remarks
Kinematic viscosity (ν)	square millimetre per second (centistoke)	mm^2/s (cSt)	1 cSt = $1 mm^2/s$	$\nu = \eta/\rho$
Celsius temperature (t)	degree Celsius	°C	t°F = 5 (t – 32)/9°C	The Celsius temperature t is equal to the difference $t = T - T_0$ between two thermodynamic temperatures T and T_0 where T_0 = 273.15 K (K = Kelvin)

Part 2. Other units

Plane angle (various)	degree minute second (angle)	° ′ ″		To be used for angle of shearing resistance (ϕ) and for slopes
Time (t)	year day hour second (time)	year d h s	1 year = 31.557×10^6 s 1 d = 86.40×10^3 s 1 h = 3600 s	'a' is the abbreviation for year The second (time) is the SI unit
Coefficient of consolidation (c_v) or swelling (c_s)	square metre per year	m^2/year	1 ft^2/year = 0.09290 m^2/year	

Preface

This book is based on a series of lectures given to practising civil engineers attending residential courses on foundation engineering at the University of Surrey, UK. Attention has been concentrated on methods for predicting the failure loads, and the deformations at working loads, of piled and non-piled foundations. It must be emphasized that a knowledge of these methods alone will not enable an engineer to become a reliable practitioner of the art of foundation engineering. Peck (1962) has listed the attributes necessary for the successful practice of subsurface engineering as follows:

- A knowledge of precedents
- A working knowledge of geology
- Familiarity with soil mechanics.

By concentrating on the third point (because of time and space limitations) the authors are not suggesting that it is the most significant factor. Without doubt, a knowledge of precedents is by far the most important; such experience is a necessary and priceless asset of a good foundation engineer. Also, a working knowledge of geology is as basic to foundation engineering as is familiarity with soil mechanics methods. It makes one aware of the departures from reality inherent in simplifying assumptions which have to be made before computations can be performed. The geology of a site must be understood before any reasonable assessment can be made of the errors involved in calculations and predictions. Moreover, intelligent subsurface exploration is impossible without a working knowledge of geology.

It is hoped that this book will reflect the authors' experience of teaching, research and consulting and may, therefore, appeal to both students and practising engineers.

The book is written in the belief that brevity is a virtue. To facilitate the extraction and use of information the authors have endeavoured to concentrate information in tables and in charts.

The book uses SI units. Gravitational units have been used throughout with weight per unit volume being expressed as unit weight (kN/m^3) rather than in terms of mass density (Mg/m^3). As a helpful simplification, the unit weight of water is taken as 10 kN/m^3. For units of stress, kilonewtons per square metre (kN/m^2) have been preferred to kilopascals (kPa).

The authors are most grateful to Margaret Harris who did the drawings, and to Corrie Niemantsverdriet and Carole Cox who typed the script.

N. E. Simons, B. K. Menzies
University of Surrey,
Guildford, 1975

1 Effective stress

1 Definition

Effective stress in any direction is defined as the difference between the total stress in that direction and the pore-water pressure. The term *effective stress* is, therefore, somewhat of a misnomer, its meaning being a stress difference.

2 The nature of effective stress

Soil is a skeletal structure of solid particles in contact, forming an interstitial system of interconnecting voids or pores. The pores are filled partially or wholly with water. The interaction between the soil structure and the pore fluid determines the unique time-dependent engineering behaviour of the soil mass.

The deformability of a soil subjected to loading or unloading is, in the main, its capacity to deform the voids, usually by displacement of water. The strength of a soil is its ultimate resistance to such loading.

Shear stresses can be carried only by the structure of solid particles, the water having no shear strength. On the other hand, the normal stress on any plane is the sum of two components: owing to both the load transmitted by the solid particles of the soil structure and to the pressure in the fluid in the void space (Bishop and Henkel, 1962).

The deformability and strength of a soil are dependent on the difference between the applied external total loading stress, σ, and the pore-water pressure, u. This difference is termed the *effective stress* and is written $(\sigma - u)$.

The physical nature of this parameter may be intuitively understood by considering the saturated soil bounded by a flexible impermeable membrane as shown in Fig.1.1. The external applied total pressure is σ normal to the boundary. The pore-water pressure is u ($<\sigma$) which, being a hydrostatic pressure, acts with equal intensity in all directions, giving a pressure of u

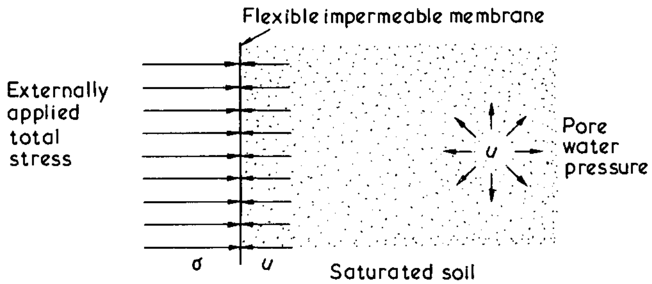

Fig. 1.1 Intuitive soil model demonstrating the nature of effective stress

normal to the boundary. By examining the stresses normal to the boundary it may be seen by inspection that the disparity in stresses $(\sigma - u)$ is transmitted across the boundary into the soil structure, assuming an equilibrium condition. Thus, *the effective stress* $(\sigma - u)$ *is a measure of the loading transmitted by the soil structure.*

3 The principle of effective stress

The principle of effective stress was stated by Bishop (1959) in terms of two simple hypotheses:

- Volume change and deformation in soils depends on the difference between the total stress and the pressure set up in the fluid in the pore space, not on the total stress applied. This leads to the expression

$$\sigma' = \sigma - u \tag{1.1}$$

  where σ denotes the total normal stress, u denotes the pore pressure, and σ' is termed the effective stress

- Shear strength depends on the effective stress, not on the total normal stress on the plane considered. This may be expressed by the equation

$$\tau_f = c' + \sigma' \tan \phi' \tag{1.2}$$

  where τ_f denotes the shear strength, σ' the effective stress on the plane considered, c the apparent cohesion, ϕ' the angle of shearing resistance.

The principle of effective stress, as expressed above, has proved to be vital in the solution of practical problems in soil mechanics.

In seeking a physical concept of the stress difference $(\sigma - u)$, an idealized soil model was proposed in which the intergranular forces normal to a horizontal plane were examined, an approach similar to that adopted by Skempton and Bishop (1954). It was found that the average intergranular force per unit global area of a horizontal plane through the soil model, while often termed the *effective stress*, only approximated to $(\sigma - u)$, the force being dependent on the contact area between particles – the smaller the contact area per unit global area, the closer the approximation.

It must be emphasized that effective stress is simply a stress difference $\sigma' = (\sigma - u)$ and is not the intergranular stress or the intergranular force per unit cross sectional area. To illustrate this point, consider a saturated soil confined laterally and loaded vertically by a total stress, σ. Let u = pore pressure; A = cross sectional area; a = area of contact of grains per unit cross sectional area; σ_g = average vertical component of the intergranular stress; σ_{ga} = average vertical component of the intergranular force per unit global horizontal cross sectional area. For force equilibrium in the vertical direction

$$\sigma . A = \sigma_{ga} A + u(1 - a)A$$

whence

$$\sigma_{ga} = \sigma - u(1 - a) \tag{1.3}$$

similarly,

$$\sigma . A = \sigma_g . a . A + u(1 - a)A$$

whence

$$\sigma_g = \frac{1}{a}(\sigma - u(1 - a)) \tag{1.4}$$

To use realistic numbers let $\sigma = 100$ kN/m^2, $u = 50$ kN/m^2, and let $a = 0.01$ (clay) and 0.3 (lead shot), respectively.

From equation (1.3) $\sigma_{ga} = 50.5$ kN/m^2 and 65 kN/m^2, respectively.

From equation (1.4) $\sigma_g = 5050$ kN/m^2 and 216.7 kN/m^2, respectively.

The effective stress if $\sigma' = (\sigma - u) = 50$ kN/m^2

In an elegant experiment performed on lead shot, Bishop (1966) showed clearly that, in spite of significant contact areas between the particles, volume change and shear strength were still governed by the simple expression for effective stress, namely, $\sigma' = (\sigma - u)$.

The important implication the principle of effective stress has on the strength is that a change in effective stress results in a change of strength, and the corollary follows, that if there is no change in effective stress, then there is no change in strength. While it is true that a change in volume will always be accompanied by a change in effective stress, it is not necessarily true, however, that a change in effective stress will produce a change in volume.

Consider, for example, the undrained triaxial test on a saturated soil. During the test, while there is no change in water content and therefore in volume, the pore pressures do change and alter the vertical or horizontal effective stress, or both. At failure, the effective stress throughout the sample will have changed considerably from that pertaining before the axial loading stage of the test. These changes in effective stress are accompanied by specimen deformation by the change of shape. It follows, therefore, that *the sufficient and necessary condition for a change in the state of effective stress to occur is that the soil structure deforms.* Deformation may occur by volumetric strain, by shear strain or by both. The corollary follows that deformation is induced by a change in the state of effective stress, whether or not there is a change in volume.

This implication of the principle of effective stress is of interest. Consider for example, the interrelation of stress changes in the oedometer or under uniform global loading conditions in the field, for a saturated clay.

Let $\Delta\sigma_v$ be the change in vertical total stress, $\Delta\sigma_h$ be the change in horizontal total stress, and Δu be the change in pore-water pressure. At the moment of applying the vertical stress increment there is no deformation, and it thus follows that there is no change in effective stress in any direction and therefore

$$\Delta u = \Delta\sigma_v = \Delta\sigma_h \tag{1.5}$$

This expression has been proved by Bishop (1958) for soft soils. Bishop (1973) has shown that, for porous materials of very low compressibility, equation (1.5) is modified. Equation (1.5) is valid, of course, independently of the value of the pore pressure parameter, A.

As a consequence of this, during drainage the stress path followed in the oedometer is quite complex. At the start of the consolidation stage, it has been shown that the oedometer ring applies a stress increment to the sample equal to the increment in vertical stress. During consolidation, however, the horizontal stress decreases to a value, at the end of pore pressure dissipation, equal to K_0 times the vertical stress (Simons and Menzies, 1974).

4 The computation of effective stress

4.1 Introduction

The computation of effective stress requires the separate determination of the total stress, σ, and of the pore-water pressure, u. The effective stress is then found as $\sigma' = \sigma - u$.

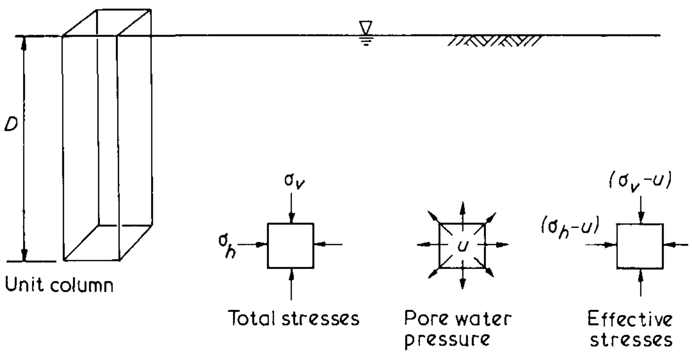

Fig. 1.2 'At rest' in situ stresses due to self-weight of soil

4.2 The determination of vertical total stress

Consider the typical *at rest* ground condition shown in Fig. 1.2. This is a *global* loading condition.

Consider an element of soil at a depth D metres. The water level is at the surface. The bulk unit weight of the soil (i.e. including solids and water) is γ kN/m^3. The total vertical stress σ_v is computed by finding the total weight of a vertical column subtended by unit horizontal area (1 m^2) at depth D. The weight of this column divided by its base area is γD kN/m^2 and is the vertical total stress acting on a horizontal plane at depth D.

The vertical total stress σ_v, and the horizontal total stress σ_h are principal stresses. In general, $\sigma_v \neq \sigma_h$.

For *local* loading, the total stresses may be estimated using elastic theory as discussed in Chapter 3.

4.3 The determination of pore-water pressure

Referring to Fig. 1.2, the pore-water pressure, u, is found by considering a vertical unit column of water only. The presence of the soil structure has no effect on the pore-water pressure. Thus, $u = \gamma_w D$, where γ_w is the unit weight of water. A helpful approximation is to take γ_w = 10 kN/m^3 (more accurately, γ_w = 9.807 kN/m^3).

For a clay layer rapidly loaded locally, the viscous retardation of pore-water flow in the fine-grained soil gives a build-up of pore pressure. Water will eventually flow out of the zone of loading influence to the ground surface and into surrounding soil unaffected by the loading. This flow or consolidation takes place under the load-induced hydraulic gradient which is itself reduced by the flow as the consolidation of the soil structure allows it to support more load. The law of diminishing returns thus applies and there is an exponential decay in the excess or load-generated pore pressure. This effect is illustrated in Fig. 1.3 where a saturated clay layer is rapidly loaded by the building-up of an embankment. The distribution of pore pressure with time (isochrones) is shown by the relative heights of piezometric head in the standpipes.

In real soils subjected to rapid local loading, the effects of deformation of the soil structure at constant volume, the compressibility of the pore fluid in practice and the dependence of the structural properties of the soil skeleton upon the mean stress, all mean that initially the loading change is shared between the soil structure and the generated pore pressure change. The generated pore pressure change is thus not only a function of the loading change but also a function of the soil properties. These properties are experimentally determined and are called the *pore pressure parameters A and B*.

Consider the loading increment applied to a cylindrical soil element shown in Fig. 1.4. The loading change is in triaxial compression, the major vertical total stress increasing by $\Delta\sigma_1$, while the minor horizontal (or radial) total stress increases by $\Delta\sigma_3$. An excess pore pressure, i.e. greater than the existing pore pressure, of Δu is generated by the loading increment.

The generalized loading system of Fig.1.4 may be split into two components consisting of an isotropic change of stress $\Delta\sigma_3$ generating an excess pore pressure Δu_b and a uniaxial change of stress $(\Delta\sigma_1 - \Delta\sigma_3)$ generating an excess pore pressure Δu_a.

By the principle of superposition

$$\Delta u = \Delta u_b + \Delta u_a \tag{1.6}$$

Assuming that the excess pore pressure generated by the loading increment is a simple function of that loading increment we have,

$$\Delta u_b = B\Delta\sigma_3 \tag{1.7}$$

and

$$\Delta u_a = \bar{A}(\Delta\sigma_1 - \Delta\sigma_3) \tag{1.8}$$

where $\bar{A}$ and B are experimentally determined pore pressure parameters.

Thus, the total pore pressure change is made up of two components: one that is B times the isotropic stress change, and the other that is $\bar{A}$ times the change in principal stress difference.

Hence,

$$\Delta u = B\Delta\sigma_3 + \bar{A}(\Delta\sigma_1 - \Delta\sigma_3) \tag{1.9}$$

(Note that Skempton (1954) gives $\Delta u = B[\Delta\sigma_3 + A(\Delta\sigma_1 - \Delta\sigma_3)]$ i.e. $\bar{A} = A \,.\, B$)

The pore pressure parameters may be measured in the triaxial compression test where a cylindrical soil sample is tested in two stages. In the first stage, the sample is subjected to an increment of all-round pressure and the pore pressure increase measured. In the second stage, the sample is loaded axially and the pore pressure increase measured. For a saturated soil, $B = 1$ and $\bar{A} = A$.

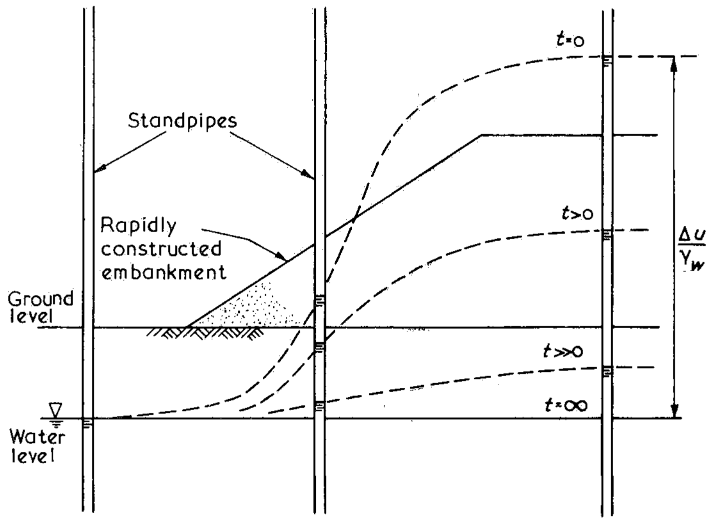

Fig. 1.3 Pore pressure response of a saturated clay to rapid local loading

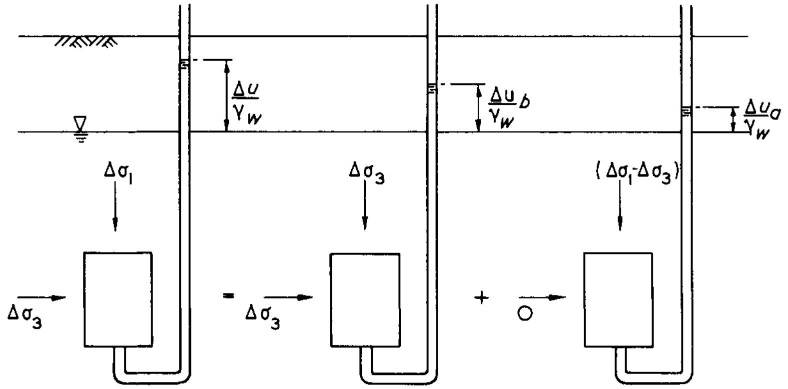

Fig. 1.4 Components of excess pore pressure generated by a loading increment ($\Delta\sigma_1 > \Delta\sigma_2 = \Delta\sigma_3$)

4.4 Worked example

Question

The strata in the flat bottom of a valley consist of 3 m of coarse gravel overlying 12 m of clay. Beneath the clay is fissured sandstone of relatively high permeability.

The water table in the gravel is 0.6 m below ground level. The water in the sandstone is under artesian pressure corresponding to a standpipe level of 6 m above ground level.

The unit weights of the soil are:

Gravel – above water table	16 kN/m^3
– below water table (saturated)	20 kN/m^3
Clay – saturated	22 kN/m^3

1. Plot total stresses, pore-water pressures and effective vertical stresses against depth:
   (a) With initial ground water levels,
   (b) Assuming that the water level in the gravel is lowered 2 m by pumping, but the water pressure in the sandstone is unchanged,
   (c) Assuming that the water level in the gravel is kept as for (b), but that relief wells lower the water pressure in the sandstone by 5.5 m,
   (d) Assuming that the relief wells are then pumped to reduce the water level in the sandstone to 15 m below ground level.

   Note that for (b), (c) and (d), stresses are required both for the short-term and the long-term conditions.

2. To what depth can a wide excavation be made into the clay before the bottom *blows up* (neglect side shear) assuming the initial ground water level
   (a) With initial artesian pressure in sandstone?
   (b) With relief wells reducing the artesian pressure to 0.6 m above ground level?
   (c) With relief wells pumped to reduce the pressure to 15 m below ground level?

3. An excavation 9 m in depth (below ground level) is required. If a ratio of total vertical stress to uplift pressure of 1.3 is required for safety, to what depth must the piezometric head in the sandstone be lowered?

4. If the coefficient of volume change of the clay is 0.0002 m^2/kN to what extent would the

clay layer in the locality eventually decrease in thickness if the artesian pressure were permanently lowered by this amount?

5. If, on the other hand, the water level in the sandstone were raised to 15 m above ground level owing to the impounding behind a dam upstream of the site, at what depth in the undisturbed clay would the vertical effective stress be least and what would this value be?

Answer

1. See Fig.1.5. Note that rapid changes of global total stress do not cause immediate changes in effective stress within the clay layer.

2. (a) Let the excavation proceed to a depth D below ground level. The bottom will *blow up* when the total stress, diminished by excavation, equals the water pressure in the sandstone, that is, when $(15 - D)22 = 21 \times 10$ assuming the excavation is kept pumped dry. Thus, $D = 5.454$ m.
   (b) Similarly, $(15 - D)22 = 15.6 \times 10$. Thus, $D = 7.909$ m.
   (c) By inspection, $D = 15$ m.

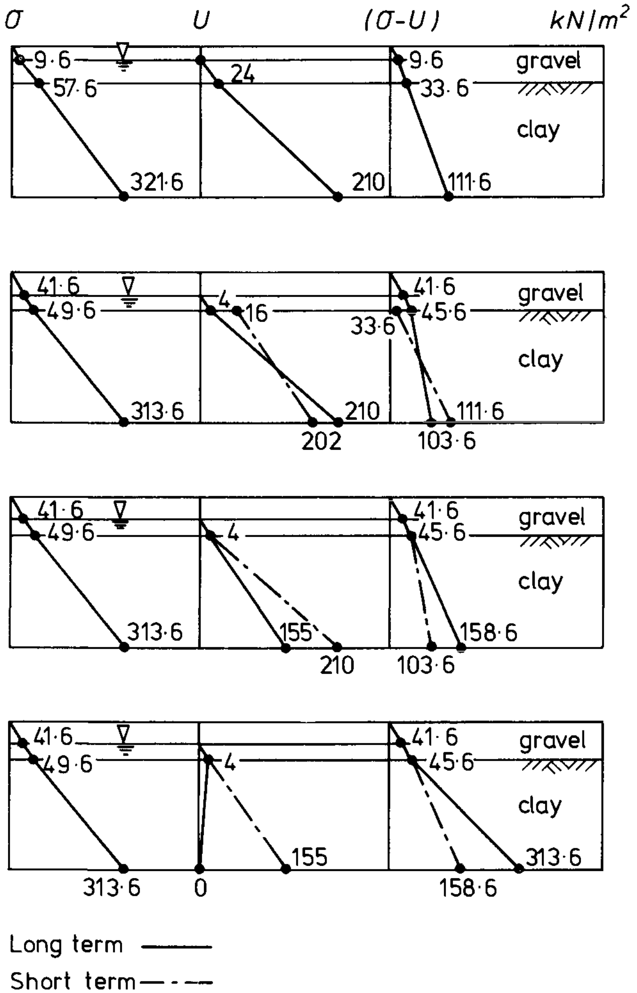

Fig. 1.5 Solution to worked example, section 1

3. By inspection, $(6 \times 22)/10p = 1.3$, where p is the total piezometric head in the sandstone, whence $p = 10.153$ m, i.e. the piezometric head in the sandstone must be lowered to $(15 - 10.153) = 4.847$ m below ground level.

4. The change in effective stress is $(21 - 10.153)\ 10/2 = 54.235\ kN/m^2$, whence the change in thickness of the clay layer is $0.0002 \times 54.235 \times 12 = 0.130$ m.

5. The pore pressure at the base of the clay layer will be $(15 + 15)\ 10 = 300\ kN/m^2$ giving a minimum vertical effective stress of $21.6\ kN/m^2$ at 15 m depth.

2 Shear strength

1 The definition of shear strength

The shear strength of a soil in any direction is the maximum shear stress that can be applied to the soil structure in that direction. When this maximum has been reached, the soil is regarded as having *failed*, the strength of the soil having been fully mobilized.

2 The nature of shear strength

When soil fails it does so by means of some plastic failure mechanism involving shear. The shear strength of a soil is derived from the structural strength alone, the pore-water having no shear strength. The resistance of the soil structure to shear arises from the frictional resistance, F, generated by the interparticle forces, N (Fig.2.1). In the soil mass, the loading transmitted by the soil structure normally to the shear surface is an integrated measure of these interparticle forces. Thus, the shear strength, τ_f (shear stress at failure), on any plane in a soil, is some function of the effective stress normal to that plane. Assuming a linear relationship gives

$$\tau_f = k_1 + k_2(\sigma_n - u) \tag{2.1}$$

where σ_n is the total stress normal to the plane, u is the pore-water pressure, and k_1 and k_2 are two experimentally determined constants.

Experiment has shown this expression to be substantially correct over a wide range of soils for a limited range of stresses.

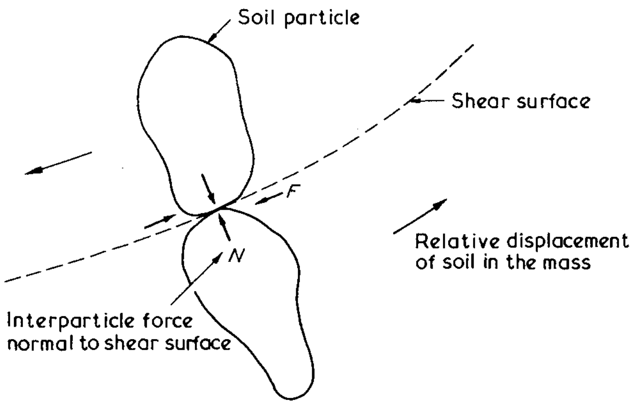

Fig. 2.1 Forces arising at inter-particle slip

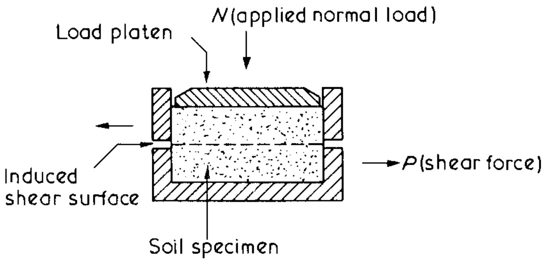

Fig.2.2 A schematic section through the direct shear box

Common usage has

$$k_1 = c' \tag{2.2}$$

$$k_2 = \tan\phi' \tag{2.3}$$

whence

$$\tau_f = c' + (\sigma_n - u)\tan\phi' \tag{2.4}$$

where c' is the cohesion intercept and ϕ' is the angle of shearing resistance, with respect to effective stress.

3 The measurement of shear strength

3.1 Direct and indirect measurements

If the effective stress shear strength parameters c' and $\tan\phi'$ are known, the shear strength on any plane may be estimated from a knowledge of the effective stress normal to that plane $(\sigma_n - u)$. In this way, the shear strength is evaluated indirectly by using the experimentally determined values of c' and $\tan\phi'$, and estimating or measuring the total normal stress σ_n and the pore-water pressure u, whence $\tau_f = c' + (\sigma_n - u)\tan\phi'$.

It is also possible to measure the peak shear strength, τ_f, directly. A device which does this is the direct shear box (Fig.2.2) which tests a prismoidal specimen of soil contained in a rigid box which is split in a horizontal mid-section. The top half of the box is free to move relative to the bottom half. The box is open at the top where the soil specimen is loaded vertically by a horizontal rigid platen. By constraining one half of the box to move relative to the other half, the soil specimen is sheared on a horizontal plane. The peak shear strength is found directly by measuring the maximum shear stress required for the relative displacement.

The relationship between the direct and indirect measurements of shear strength may now be examined in more detail.

Consider a saturated clay specimen confined in a direct shear box and loaded vertically on a horizontal midsection with a total stress of σ_v (Fig.2.3). The box is contained in an open cell which is flooded to a constant depth. The pore pressure has the equilibrium value, u_0. The shear strength may be found directly by shearing the specimen. By shearing the specimen rapidly, the undrained condition is simulated, that is, there is no change in water content and therefore no change in overall volume, owing to the viscous resistance to rapid displacement of pore water in a fine grained soil.

The shearing distortion of the soil structure in the shear zone generates an excess pore-water pressure, which at failure is Δu_f.

The shear strength directly obtained is, therefore, the undrained shear strength,

$$s_u = c' + (\sigma_v - u_0 - \Delta u_f) \tan \phi' \tag{2.5}$$

It can be seen, therefore, that the undrained shear strength, s_u, simply provides a direct measure of the shear strength of a soil structure which is rapidly sheared. This strength may also be deduced from a knowledge of the effective stress at failure and the relationship between effective stress and shear strength for the soil embodied in the parameters c' and $\tan \phi'$.

3.2 Drained and undrained measurements

If a fine-grained saturated soil is rapidly loaded (e.g. rapidly filling a large oil tank), in the short term the soil is effectively undrained because of the viscous forces resisting pore-water flow within the soil. The excess pore pressure generated by the *sudden* application of load dissipates by drainage or consolidation over a period of time which may, in the case of clays, extend for many tens or even hundreds of years. Hence, the terms *short* and *sudden* are relative and a load application over several months during a construction period may be relatively rapid with the short term, end-of-construction, condition approximating to the undrained case. In positive loading conditions such as embankments and footings, the subsequent consolidation under the influence of the increased load gives rise to increased strength and stability. The lowest strength and, therefore, the most critical stability condition consequently holds at the end of construction when loading is completed. The critical strength is thus the undrained shear strength before consolidation. One way of measuring the strength is to build-up rapidly the load in a full scale field test until the soil fails and this is sometimes done, particularly in earthworks, by means of trial embankments. However, such full scale testing is very expensive and only really applicable to large and costly projects where the subsoil is uniform. For variable subsoils and cases where large expenditure on soil testing is unlikely to effect large economies in design, small scale testing is more appropriate. A rapid test in the direct shear box, for example, presents a convenient, though vastly simplified small scale simulation or model of the likely full scale field or prototype failure. It was seen in the preceding section 3.1 that this rapid direct measure of shear strength gave the undrained shear strength, s_u. However, if the test is carried out slowly, the distortion of the soil structure in the shear zone produces an insignificantly small excess pore-water pressure. This is because any slight increase in pore pressure has time to dissipate by drainage, that is, the slow test is *drained* as opposed to *undrained* in the quick test. Hence, the pore pressure remains at almost u_0 throughout the test (Fig.2.4). The soil structure in the shear zone is able to change its volume by drainage. Hence the shear distorted structure in the drained test will be different from that of the undrained test, giving a different strength, the drained shear strength,

$$s_d = c' + (\sigma_v - u_0) \tan \phi' \tag{2.6}$$

The essential feature is that, generally

$$s_u \neq s_d$$

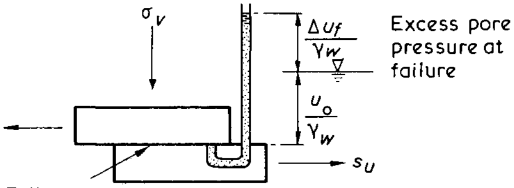

Fig.2.3 Stresses at undrained failure in the direct shear box

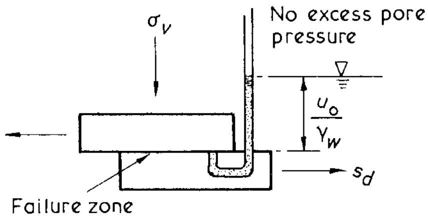

Fig.2.4 Stresses at drained failure in the direct shear box

for although it is the one soil which is being tested, the soil structures in the failure zones are different in each case.

In the drained direct shear test therefore, the pore pressure is almost zero and therefore the effective stresses are known. From this, the effective stress shear strength parameters c' and $\tan\phi'$ may be deduced from two or more such tests. Hence this test not only directly measures the drained shear strength for the particular consolidation pressures, σ_v, of each test but, in furnishing c' and ϕ', it also allows the shear strength to be estimated for any loading condition.

3.3 Methods of measurement

3.3.1 The direct shear box

The direct shear box test, introduced in the preceding section, represents a simple and direct shear test. As shown in Fig.2.5, the relationship between strength and effective stress,

$$\tau_f = c' + (\sigma_n - u_f)\tan\phi' \tag{2.4}$$

plots as a straight line in τ, $(\sigma - u)$ co-ordinates, with a slope of $\tan\phi'$ and an intercept on the shear stress axis of c'. This line or *failure envelope* may be evaluated by the drained direct shear test by applying a different vertical stress in each test and measuring the shear stress up to and beyond the peak value.

After exceeding the peak shear strength clays strain-soften to a residual value of strength corresponding to the resistance to sliding on an established shear plane. Large displacements are necessary to achieve this minimum ultimate strength requiring multiple reversals in the direct shear box or, more appropriately, use of the ring shear apparatus (Bishop *et al*, 1971). As shown in Fig.2.5, the peak and residual strengths may be displayed as failure and post-failure envelopes

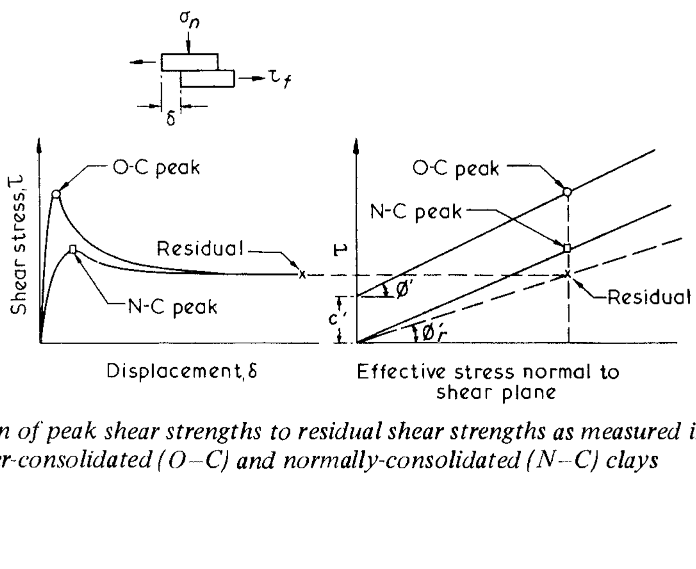

Fig.2.5 Relation of peak shear strengths to residual shear strengths as measured in the direct shear box for over-consolidated (O–C) and normally-consolidated (N–C) clays

giving the residual shear strength

$$s_r = c_r' + (\sigma_n - u)\tan\phi_r' \tag{2.7}$$

where c_r' is the residual cohesion intercept and ϕ_r' is the residual angle of shearing resistance. Soft, silty clays may show little difference between the peak and residual strengths. As the plasticity index of the clay increases, the difference tends to increase, even in the normally consolidated condition, and the decrease in strength is associated with re-orientation of the clay particles along the slip surface. Most over-consolidated clays show a marked decrease in strength from peak to residual, resulting partly from particle orientation and partly from an increase in water content owing to dilatancy within the zone of shearing. These effects increase with clay content and the degree of over-consolidation.

In a field failure, the average shear strength is the integrated sum of all the elements around the slip surface. This strength will lie between the peak and residual strengths. It is assessed from field failures and expressed in terms of a *residual factor* (Skempton, 1964),

$$R = \frac{s_f - \bar{s}}{s_f - s_r} \tag{2.8}$$

where s_f is the peak shear strength, s_r is the residual shear strength, and $\bar{s}$ is the average shear strength around the failure surface.

In clays, the fall-off in strength from the peak to the residual value may be expressed in terms of a *brittleness index*, I_B, which is the ratio of the reduction in strength from peak to residual to the peak strength and is written

$$I_B = \frac{s_f - s_r}{s_f} \tag{2.9}$$

As shown in Fig.2.5, the soft plastic normally consolidated soil has a low brittleness index whereas the stiff over-consolidated soil has a high brittleness index.

The consequence of this strain-softening behaviour of stiff clays is the practical phenomenon of *progressive failure*. If for any reason a clay is forced to exceed the peak strength at some particular point within its mass, the strength at that point will decrease. This action will put additional stress on to the clay at some other point along the potential failure surface, causing the peak to be passed at that point also. In this way a progressive failure can be initiated and, in the limit, the strength along the entire length of a slip surface will fall to the residual value.

The *ring shear apparatus* (Bishop, *et al.*, 1971) may be used to determine the full shear stress-displacement relationship of an annular ring-shaped soil specimen subjected to a constant normal stress, confined laterally and ultimately caused to rupture on a horizontal plane of relative rotary motion. The apparatus may be considered as a conventional direct shear box extended round into a ring. Each revolution of one half of the specimen relative to the other represents a displacement of one perimeter. Consequently, large actual displacements may be obtained in the one direction, and, indeed, large displacements may be necessary to realize the residual shear strength.

3.3.2 The triaxial compression test

A more versatile soil testing apparatus than the direct shear box is the triaxial cell (Fig.2.6).

In this test, a right cylindrical column of saturated soil is tested in triaxial compression with $\sigma_1 > \sigma_2 = \sigma_3$, the axial principal stress σ_1 acting vertically. Triaxial extension. $\sigma_1 = \sigma_2 > \sigma_3$ is also possible. The stress system is mixed, σ_1 being generated by the displacement of a rigid platen, whereas σ_3 is directly applied by hydrostatic fluid pressure against a flexible rubber membrane.

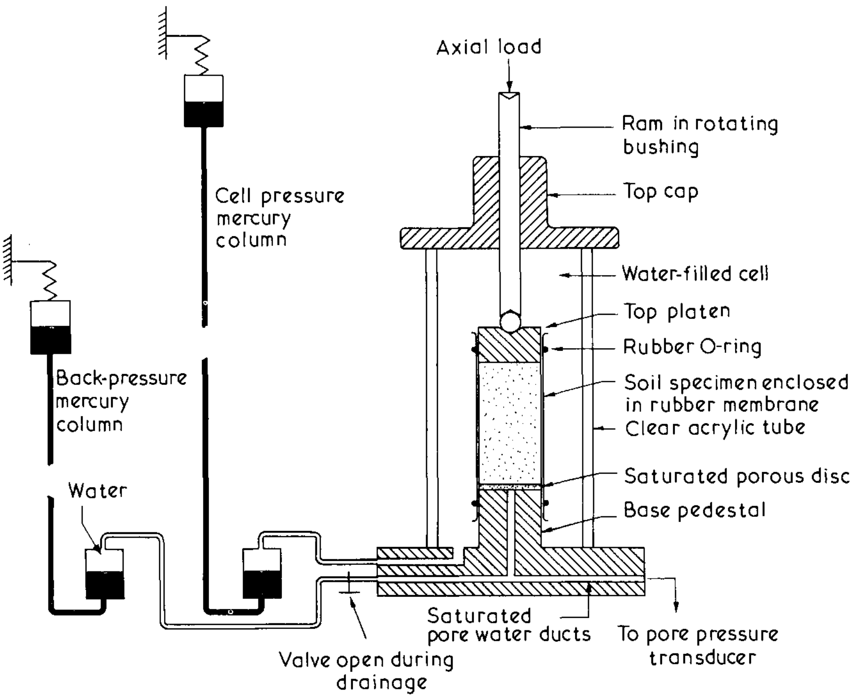

Fig. 2.6 Typical set-up for triaxial compression tests

The specimen, enclosed in a rubber membrane, is mounted on a saturated porous disc resting on the base pedestal of the cell. The cell water, which applies σ_3, is isolated from the pore-water by the rubber membrane. The porous disc allows the pore-water to communicate with the saturated water ducts in the base of the cell. One of these ducts is connected to the pore pressure transducer, the other duct being connected to a back-pressure of $p < \sigma_3$, which is the datum of pore pressure measurement. The back-pressure ensures both saturation of the specimen by dissolving any residual air and also that any pore pressure reduction owing to incipient dilation of the soil does not give rise to a negative gauge pressure and cause cavitation. However, if these considerations do not arise, then $p = 0$ may be obtained during drainage by connecting the pore pressure duct to a free water surface in a burette level with the mid-height of the test specimen. The cell pressure is maintained by a mercury column constant pressure device at σ_3. The soil structure is thus consolidated to an effective stress of $(\sigma_3 - p)$.

The specimen is tested at a constant strain rate by a motorized loading frame. The cell is driven upwards, the loading ram bearing against a proving ring fixed to the testing frame. The proving ring compression registers the load applied to the specimen by means of a dial gauge which may be coupled in parallel to a displacement transducer thus giving a load cell. The load measured by the proving ring per unit specimen cross-sectional area is the principal stress difference, $(\sigma_1 - \sigma_3)$.

The great advantage of the triaxial cell over the shear box is the control of drainage through the base pore-water ducts. It is therefore possible to measure the total specimen volume change by measuring the water imbibed or expelled in the drained case, or, in the undrained case, it is possible to measure the pore pressure. Another advantage of the triaxial test is that the applied stresses are principal stresses. This is not true near the specimen ends because of the frictional *end restraint* of the rigid platens.

The triaxial test gives an indirect measure of shear strength, providing the undrained shear strength from a Mohr's circle construction in terms of total stress from unconsolidated-undrained tests, and also providing the effective stress shear strength parameters c' and $\tan\phi'$ from consolidated-undrained or drained tests, by invoking the Mohr–Coulomb failure criterion in terms of effective stress. The inter-relationships of various triaxial and uniaxial tests are demonstrated in Fig.2.7. It can be seen that the Mohr–Coulomb failure criterion requires the Mohr's circles at failure to be tangential to the failure envelope.

3.3.2.1 The triaxial compression test – example. Consider nine identical saturated clay specimens removed from the same borehole at the same depth where, for example, it is assumed that the mean effective stress is 50 kN/m^2. The specimens are removed from their capped sampling tubes and immediately encased in impermeable rubber sheaths. In the transition from the ground to the laboratory table, the water content has remained unaltered while the external total stresses have been reduced to zero. Assuming the sampling disturbance has not significantly distorted the specimens, the constant water content and therefore constant volume suggests that the state of effective stress has changed little, the pore pressure being reduced to give a suction of about −50 kN/m^2 gauge pressure (Fig.2.8(a)).

Undrained test. The specimens are now placed in three identical triaxial cells at cell pressures of 200, 400 and 600 kN/m^2, still undrained. Because the soil structure is saturated with relatively incompressible water (relative to the soil skeleton), the cell pressure is transmitted across the flexible impermeable rubber membrane increasing the pore pressure by the respective cell pressures. The specimen volume and shape remain the same as no drainage is permitted and the effective stress is unaltered at 50 kN/m^2 (Fig.2.8(b)).

The still identical specimens are then loaded axially to failure. As the load-deformation properties of soil depend uniquely on the effective stress the specimens originally possessing the same structure and therefore effective stress, undergo the same changes in shape, generating the same changes in effective stress and therefore pore pressure (Fig.2.8(c)). Thus, the structural strengths are the same for each specimen to give a unique Mohr's circle in terms of effective stress (Fig.2.9).

It can be seen that undrained isotropic changes in stress do not alter the effective stress; this only happens for a saturated specimen, when one of the two principal stresses is changed with

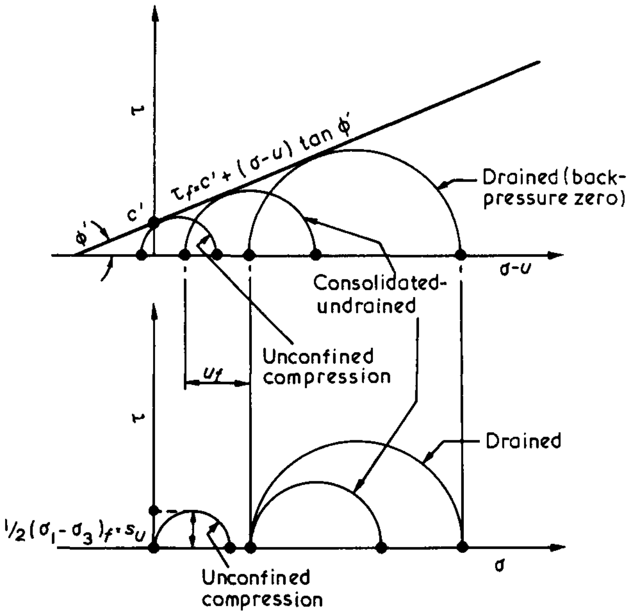

Fig.2.7 Correlation between axial compression tests

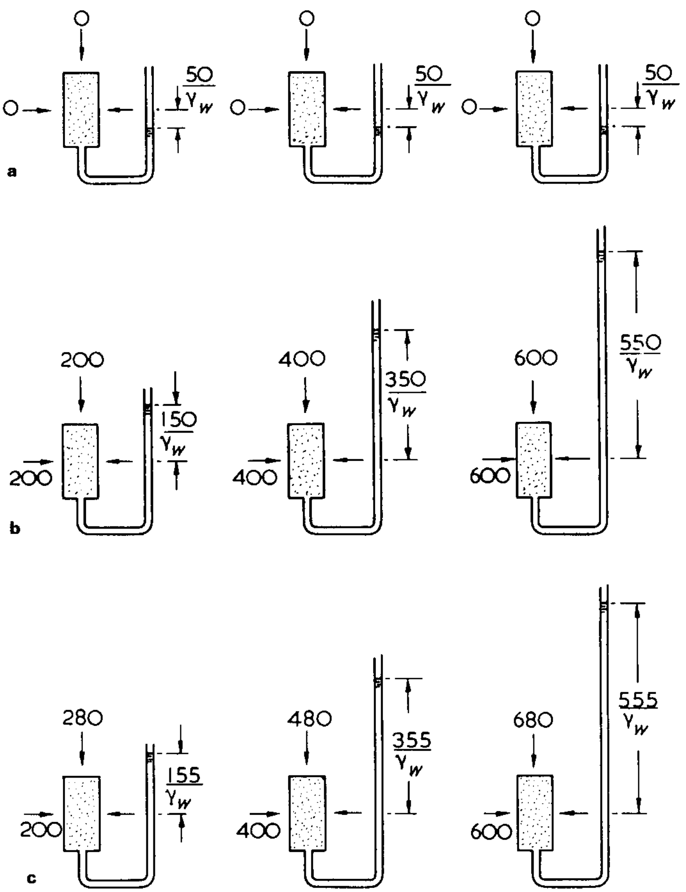

Fig.2.8 Stress diagrams for the undrained test. (a) total stresses and pore pressures after removal from ground; (b) application of cell pressure, undrained; (c) application of axial load to failure, undrained

respect to the other to give rise to a principal stress difference of ($\sigma_1 - \sigma_3$). The compressive strength of the soil specimen is $(\sigma_1 - \sigma_3)_f$, that is, the principal stress difference at failure.

Because only one Mohr's circle with respect to effective stress results, an envelope cannot be obtained. In order to separate the Mohr's circles and obtain an envelope, the consolidated-undrained test is used.

Consolidated-undrained test. Each originally identical specimen has its structure altered in turn by allowing it to drain under the cell pressure against a back-pressure of 100 kN/m^2 (Fig.2.10(a)).

This consolidation stage increases the effective stresses to the difference between the respective cell pressures and the back-pressure, the pore volume decreasing by drainage of pore-water out of the specimen, increasing the stiffness and strength of the consequently denser structure.

When the consolidation stage is completed, drainage during axial loading is not allowed and the specimens are loaded axially to failure in the undrained condition as before (Fig.2.10(b)). However, in this case, the different soil structures respond to the deformation with different strengths giving rise to Mohr's circles of different location and diameter (Fig.2.9).

Drained test. The effective stress shear strength parameters may also be obtained by carrying out drained tests. Here, as the name suggests, the specimen is drained the whole time, that is during the cell pressure application (Fig.2.11(a)) and during axial loading to failure (Fig.2.11(b)). As the pore pressures are set to the back pressure, the effective stresses are readily obtained from the total stresses (Fig.2.12).

The correlation between the various tests may be seen by considering, say, specimen number 2 (Fig.2.13).

Unconfined compression test. A further axial compression test is *unconfined compression* which may be regarded as a forerunner of the triaxial compression test. The cylindrical specimen of saturated clay is rapidly loaded axially but is not sheathed in a rubber membrane and is not confined by a cell pressure, that is, $\sigma_3 = 0$. The test is undrained and the undrained shear strength is $s_u = \tau_{max} = \sigma_1/2$ as shown in Fig.2.7.

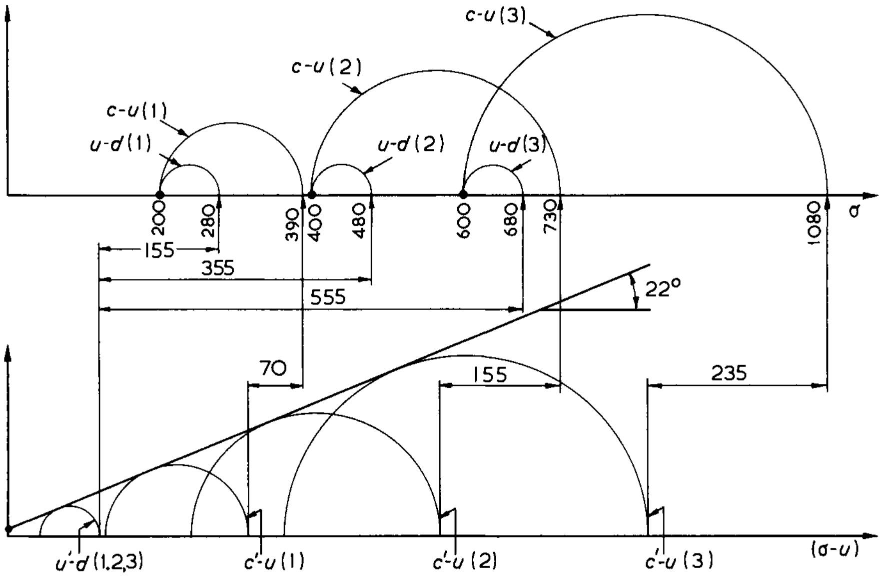

Fig.2.9 Typical undrained (u-d) and consolidated undrained (c-u) triaxial compression test Mohr's circles in terms of total stress and effective stress

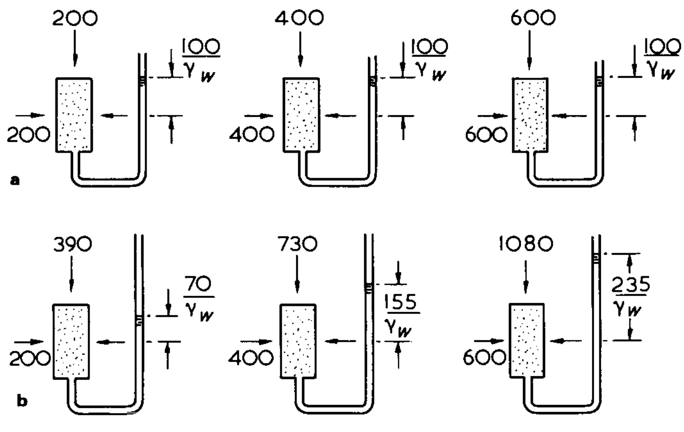

Fig.2.10 Stress diagrams for the consolidated-undrained test. (a) application of cell pressure. Drainage to back pressure of 100 kN/m²; (b) application of axial load to failure, undrained

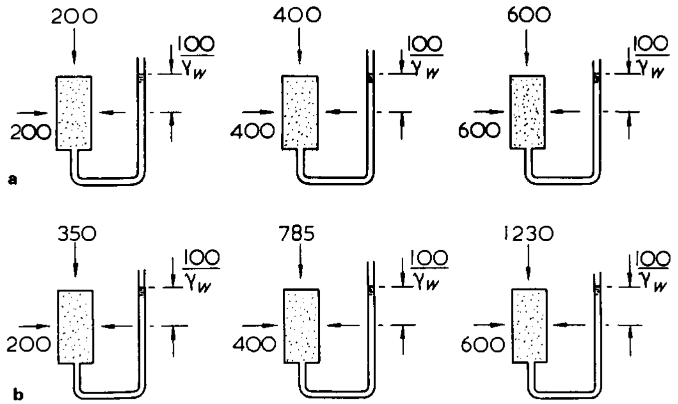

Fig.2.11 Stress diagrams for drained test. (a) application of cell pressure. Drainage to back pressure of 100 kN/m²; (b) application of axial load to failure. Drainage to back pressure of 100 kN/m²

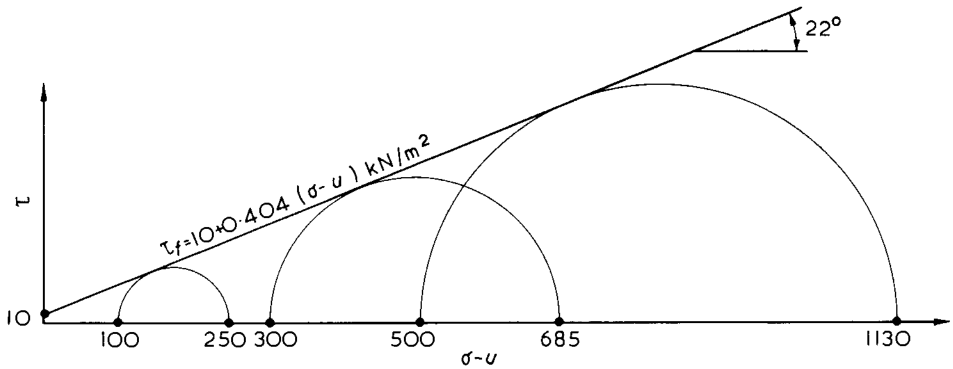

Fig.2.12 Failure envelope for drained triaxial compression test

3.3.2.2 Stress paths in the triaxial test

The plotting of several Mohr's circles to determine the failure envelope can lead to a confusing number of circles. One way of overcoming this problem is to plot one point only. It is useful to plot the topmost point of the Mohr's circle as shown in Fig.2.14. Typical effective stress paths for soft and stiff soils in the consolidated-undrained triaxial test are given in Fig.2.15.

To obtain the effective stress shear strength parameters a *failure line* is drawn tangential to the steady or *failure* portion of the stress path. Taking the slope of this line as θ and the intercept of the maximum shear stress axis as K gives

$$c' = K \sec\phi' \tag{2.10}$$

$$\phi' = \sin^{-1}(\tan\theta). \tag{2.11}$$

Plotting triaxial test results in this way gives a clear and unambiguous indication of failure.

3.3.3 Field measurements of undrained shear strength

The triaxial and unconfined compression tests and the laboratory direct shear box test rely on obtaining samples of soil from the ground by sampling from boreholes or trial pits and sealing and transporting these samples to the laboratory. The degree of disturbance affecting the samples will vary according to the type of soil, sampling method and skill of the operator. At best, there will be some structural disturbance simply from the removal of the *in situ* stresses during sampling and laboratory preparation even if these *in situ* stresses are subsequently re-applied as a first stage of the test. There is, therefore, considerable attraction in measuring shear strength in the field, *in situ*.

The determination of the undrained shear strength is only appropriate in the case of clays which, in short term loading, may approximate in the field to the undrained condition. A typical variation of undrained shear strength with depth is shown in Fig.2.16, for both normally-consolidated and heavily over-consolidated clay.

An indication of undrained shear strength may be obtained from plasticity tests. For example, Fig.2.17 shows the relationship between the ratio of the undrained shear strength to the effective overburden pressure, s_u/p', and the plasticity index, PI, for several marine clays.

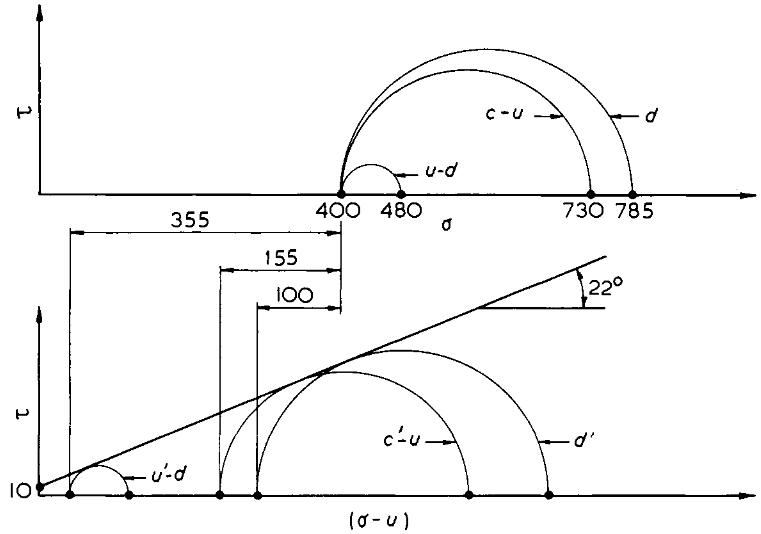

Fig.2.13 Correlation between undrained (u-d), consolidated-undrained (c-u) and drained (d) triaxial compression tests for specimen number 2

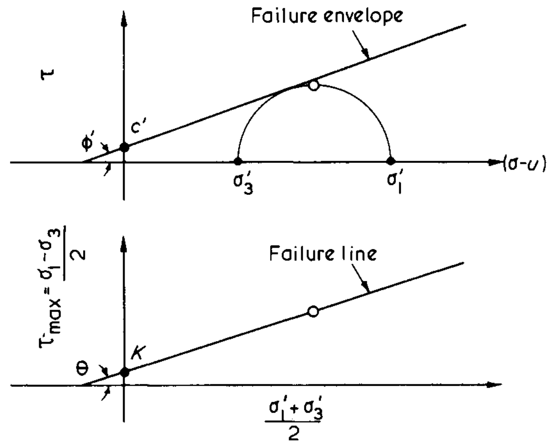

Fig.2.14 Stress-path representation of top point of Mohr's circle at failure

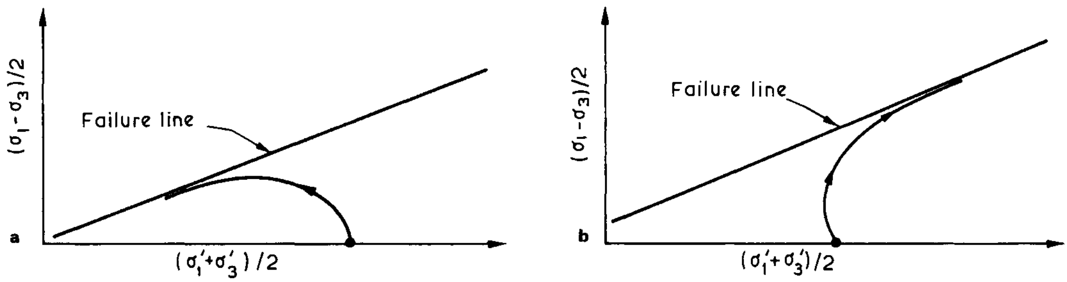

Fig.2.15 Typical effective stress paths for undrained triaxial compression tests on (a) loose sand/soft clay; (b) dense sand/stiff clay

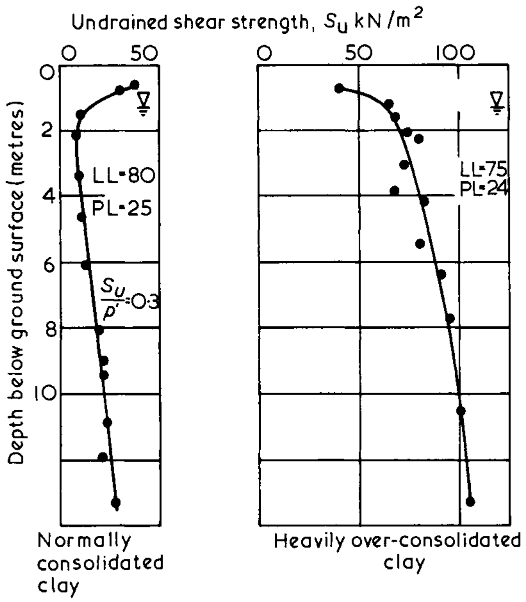

Fig.2.16 Typical variations of undrained shear strength with depth, after Bishop and Henkel (1962)

As shown in Table 2.1, the relationship between consistency and strength may be generalized to give a rough guide of strength from field inspection.

3.3.4 The in situ shear vane

The field shear vane is a means of determining the *in situ* undrained shear strength. This consists of a cruciform vane on a shaft (Fig.2.18). The vane is inserted into the clay soil and a measured increasing torque is applied to the shaft until the soil fails as indicated by a constant or dropping torque by shearing on a circumscribing cylindrical surface. The test is carried out rapidly. Now, if s_{u_v} is the undrained shear strength in the vertical direction, and s_{u_h} is the undrained shear strength in the horizontal direction, then the maximum torque is

$$T = \frac{\pi D^2}{2}\left(Hs_{u_v} + \frac{D}{3}s_{u_h}\right) \tag{2.12}$$

where H is the vane height and D is the vane diameter, and assuming peak strengths are mobilized simultaneously along all vane edges.

This equation in two unknowns, s_{u_v} and s_{u_h} can only be solved if the torque is found for two vanes with different height to diameter ratios.

It is often incorrectly assumed that the soil is isotropic and

$$s_{u_v} = s_{u_h} = s_u$$

whence,

$$T = \frac{\pi D^2}{2} (H + D/3)s_u = ks_u$$

where k is a geometrical constant of the vane.

The *in situ* shear vane may be used in inspection pits and down boreholes for the extensive determination of *in situ* strength profiles as part of a site investigation programme.

Some types of shear vane equipment have the extension rods in an outer casing with the vane fitting inside a driving shoe. This type of vane may be driven to the desired depth, the vane

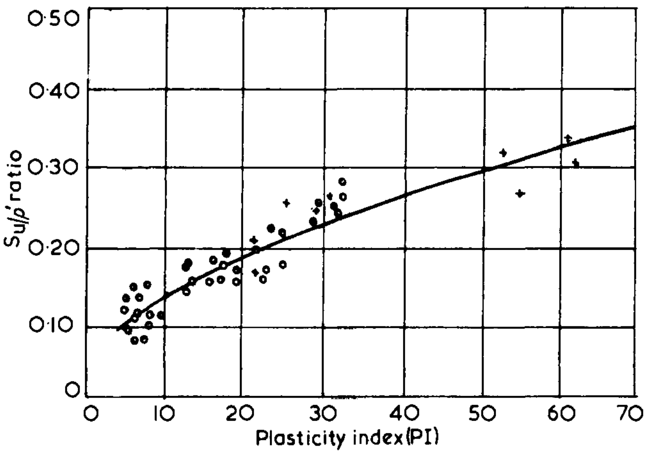

Fig.2.17 Relationship between s_u/p' and Plasticity index, after Bjerrum and Simons (1960)

Table 2.1 Consistency–strength relationship from field inspection (after CP 2004)

Consistency	Field indications	Undrained shear strength – kN/m^2
Very stiff	Brittle or very tough	>150
Stiff	Cannot be moulded in the fingers	75–150
Firm	Can be moulded in the fingers by strong pressure	40–75
Soft	Easily moulded in the fingers	20–40
Very soft	Exudes between the fingers when squeezed in the fist	<20

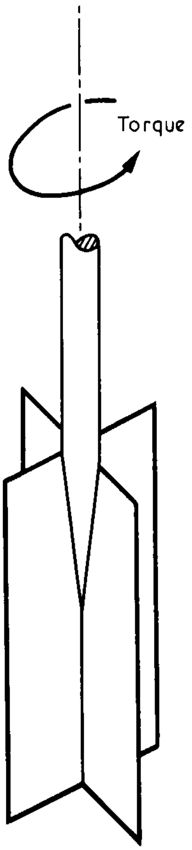

Fig.2.18 Representation of the shear vane

extended from the shoe and the test carried out. The vane may then be retracted and driving continued to a lower depth.

It must be emphasized that the *in situ* vane provides a direct measure of shear strength and because the torque application is hand operated, it is a relatively rapid strength measure, therefore giving the undrained shear strength.

3.3.5 The large diameter plate loading test

In some over-consolidated clays such as London clay, the release of previous overburden pressure allows the soil mass to expand vertically causing cracks or fissures to form. In stiff fissured clay of this kind, therefore, the difficulty in shear testing is to ensure that the specimen or zone tested is representative of the fissured soil mass as a whole and not reflecting the behaviour of intact lumps. Small scale testing can, in these circumstances, be dangerously misleading as demonstrated in Fig.2.19. The penetration test where a penetrometer with a conical point is loaded in a standard way and the penetration is measured, provides indications of strength of intact lumps. The triaxial compression tests on 38 mm and 98 mm diameter specimens fail to include sufficiently the effect of the fissures. Only the large diameter (865 mm) *in situ* plate loading tests, carried out in the bottom of a borehole, tests a truly representative zone of soil. In this test, the plate is loaded and its deflection measured to give bearing pressure–settlement relationships. At failure, bearing capacity theory is invoked to provide the field undrained shear strength. The line representing this undrained shear strength in Fig.2.19 is the *lower bound* of the scatter of the triaxial test results and is the most appropriate value to use in a bearing capacity calculation.

3.4 Factors affecting the measurement of shear strength

The factor which most significantly affects the measurement of shear strength is the mode of test, that is, whether the test is drained or undrained and this has been considered previously. Further significant factors which affect the measurement of shear strength, particularly undrained shear strength, are the type of test, that is, whether by direct shear box, triaxial compression, *in situ* shear vane etc; the effects of the orientation of the test specimen or test zone, that is, the effect of anisotropy; time to failure; sampling disturbance and size of test specimen or test zone; time between sampling and testing. These factors are now discussed.

3.4.1 Strength anisotropy

Soil strength anisotropy arises from the two interacting anisotropies of geometrical anisotropy, that is, preferred particle packing; and of stress anisotropy. The geometrical anisotropy arises at deposition when the sedimented particles tend to orientate with their long axes horizontal seeking packing positions of minimum potential energy. The horizontal layering or bedding which results is further established by subsequent deposition which increases the overburden pressure. The stress anisotropy arises because of a combination of stress history and the geometrical anisotropies of both the particles themselves and of the packed structure they form. The net effect is a clear strength and stress–strain anisotropy.

Consider, for example, the drained triaxial compression tests carried out on a dense dry rounded sand in a new cubical triaxial cell described by Arthur and Menzies (1972). The cubical specimen was stressed on all six faces with flat, water-filled, pressurized rubber bags. The test specimen was prepared by pouring sand through air into a tilted former. In this way, it was possible to vary the direction of the bedding of the particles which was normal to the direction of deposition. A clear stress–strain anisotropy was measured, the strain required to mobilize a given strength being greater for the bedding aligned in the vertical major principal stress direction than for the conventional case of the bedding aligned horizontally in the test specimen.

Parallel tests were carried out by Arthur and Phillips (1972) in a conventional triaxial cell testing a prismatic specimen with lubricated ends. It can be seen from Fig.2.20(a) that remarkably similar anisotropic strengths have been measured in different apparatus. The major dif-

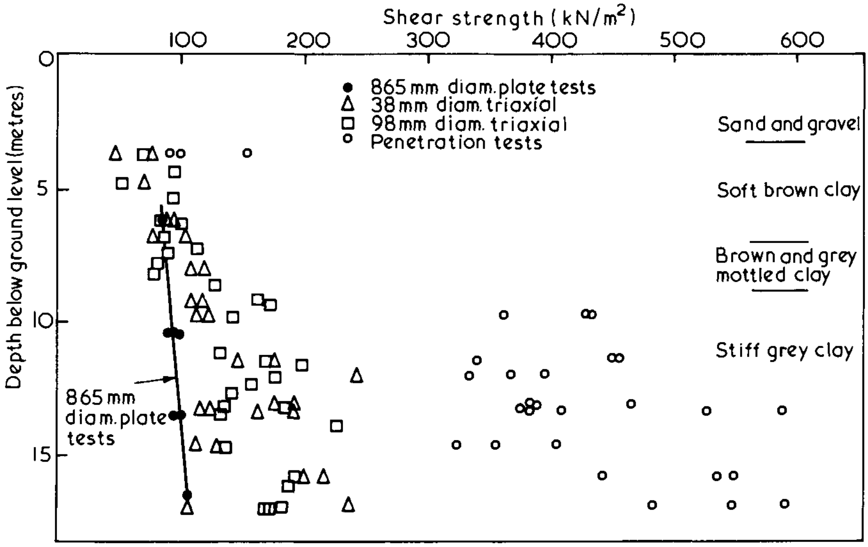

Fig.2.19 Comparison of undrained shear strengths estimated from 865 mm diameter plate tests and triaxial tests on 38 mm and 98 mm diameter specimens in London clay at Chelsea, after Marsland (1971(a))

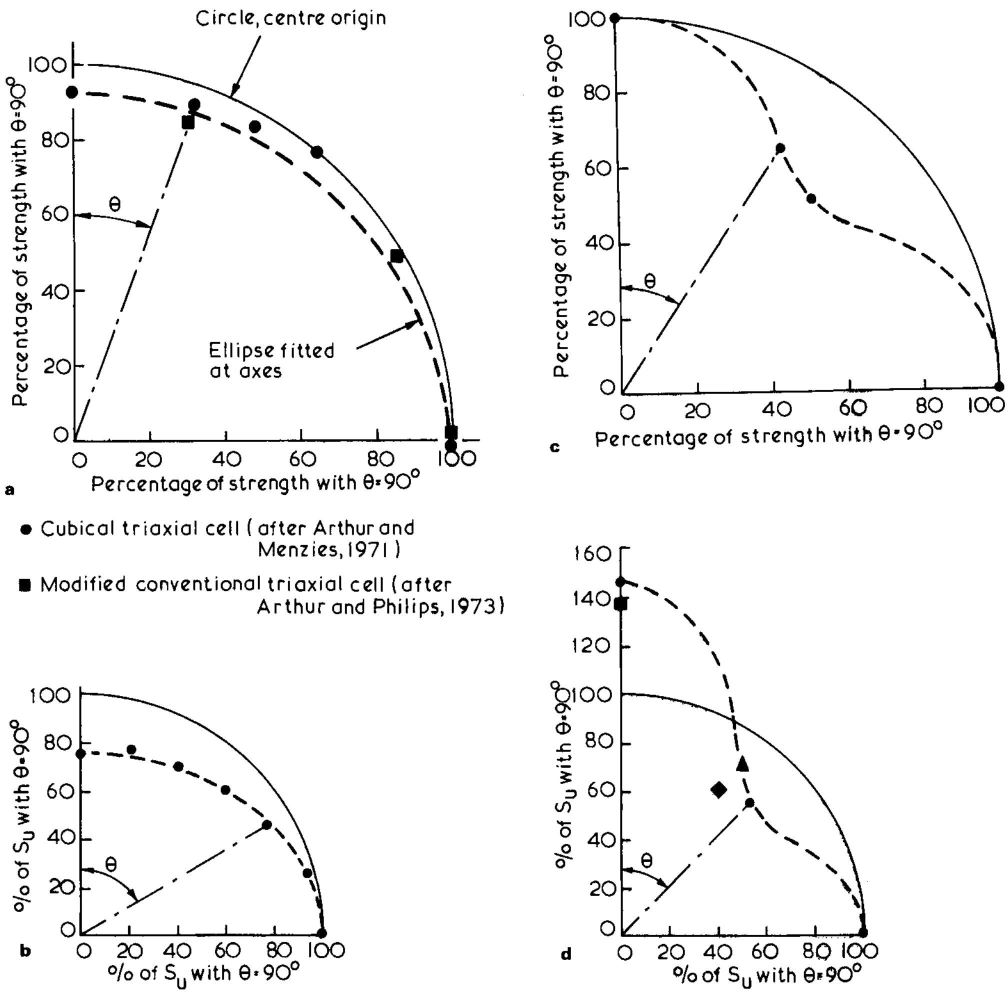

Fig.2.20 Polar diagrams showing variations of soil strength measured in compression tests: θ denotes inclination of bedding with respect to vertical axis of test specimen. (a) drained tests on dense rounded Leighton Buzzard sand, after Arthur & Menzies (1971); (b) undrained tests on lightly over-consolidated Welland clay, after Lo (1965); (c) undrained tests on heavily over-consolidated blue London clay, after Simons (1967); (d) undrained tests on heavily over-consolidated London clay, after Bishop (1967)

ferences in type of apparatus include the control of deformation (one stress control, the other, displacement control), the geometric proportions of the specimens, and the application of the boundary stresses (one with uniform pressures on each face and one with rigid ends). It would appear, therefore, that drained triaxial compression tests on a dry, rounded sand give similar measures of the strength anisotropy despite fundamental differences in the type of triaxial apparatus used. It is of interest to note that fitting an ellipse to the strength distribution of Fig.2.20(a) adequately represents the variation. An elliptical variation of strength with direction was first proposed by Casagrande and Carillo (1944) in a theoretical treatment. Lo (1965) found an elliptical-like variation in the undrained shear strength of a lightly over-consolidated Welland clay (Fig.2.20(b)). Simons (1967) on the other hand, found a non-elliptical variation

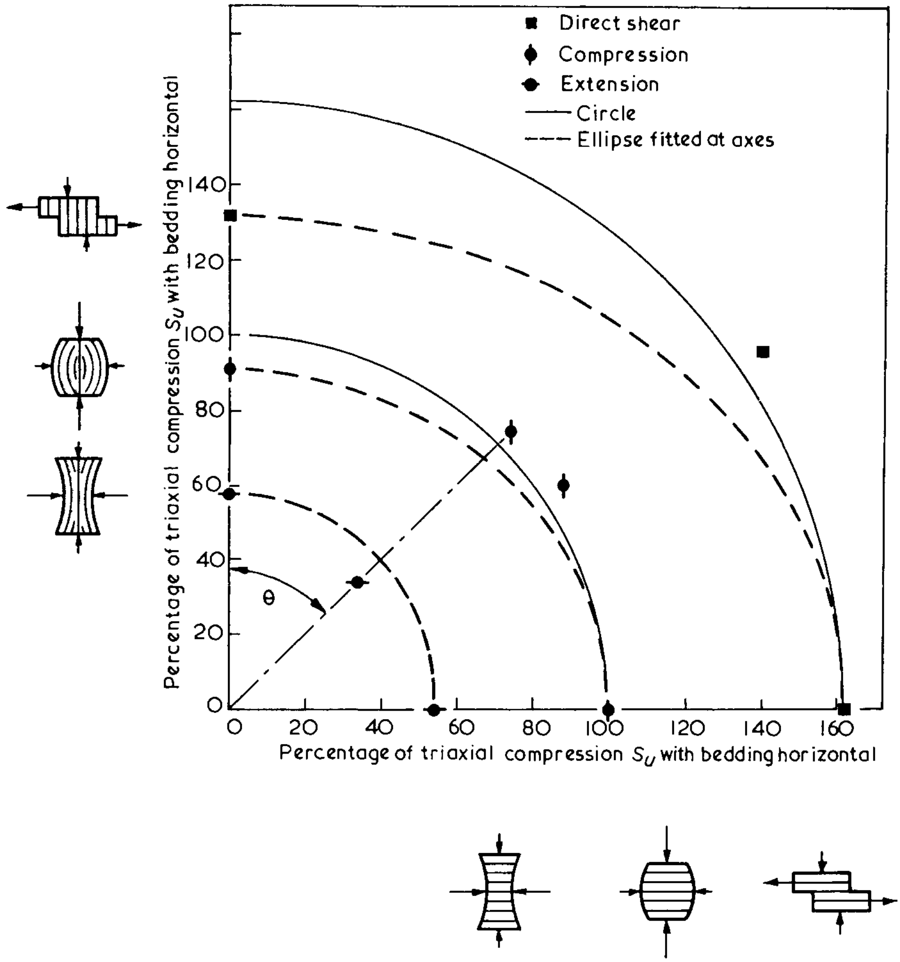

Fig. 2.21 Polar diagram showing the variation in undrained shear strength with test type and specimen orientation for a soft clay from Kings Lynn, Norfolk, after Madhloom (1974)

Table 2.2 Comparison between the results of compression and extension tests, direct simple shear tests, and in situ vane tests on soft clay, after Bjerrum (1972 (a))

Type of soil	Index properties %				Triaxial test τ/p'_0		Simple shear test τ_f/p'_0	Vane tests s_u/p'_0	
	Water content, w	Liquid limit w_l	Plastic limit w_p	Plasticity index I_p	Compression	Extension		Observed	Corrected for rate
Bangkok clay	140	150	65	85	0.70	0.40	0.41	0.59	0.47
Matagami clay	90	85	38	47	0.61	0.45	0.39	0.46	0.40
Drammen plastic clay	52	61	32	29	0.40	0.15	0.30	0.36	0.30
Vaterland clay	35	42	26	16	0.32	0.09	0.26	0.22	0.20
Studentertunden	31	43	25	18	0.31	0.10	0.19	0.18	0.16
Drammen lean clay	30	33	22	11	0.34	0.09	0.22	0.24	0.21

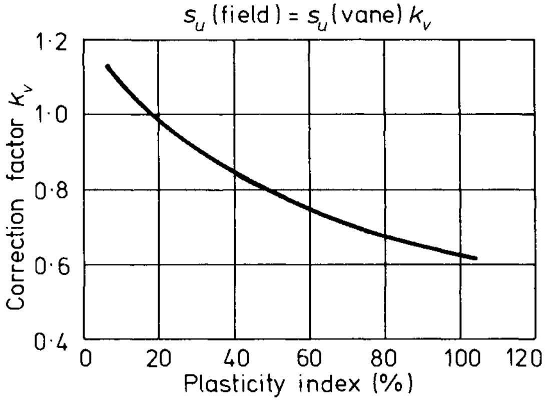

Fig. 2.22 Vane strength correction factor for soft clays (after Bjerrum, 1973)

in the undrained shear strength of a heavily over-consolidated London clay (Fig.2.20(c)). Results summarized by Bishop (1966) are similar (Fig.2.20(d)).

Geometrical anisotropy, or *fabric* as it is sometimes called, not only gives rise to strength variations with orientation of the test axes but is also probably partly the cause of undrained strength variations between test type. Madhloom (1973) carried out a series of undrained triaxial compression tests, triaxial extension tests and direct shear box tests using specimens of a soft, silty clay from Kings Lynn, Norfolk. The soil was obtained by using a Geonor piston sampler. Samples were extruded in the laboratory and hand-trimmed to give test specimens in which the bedding was orientated at different angles to the specimen axes. A polar diagram showing the variation of undrained shear strength with test type and specimen orientation is given in Fig.2.21.

It is clear that the magnitude of undrained strength anisotropy in clays is much greater than drained strength anisotropy in sands. It can be seen that generally for this type of clay the triaxial compression test indicates a strength intermediate between that indicated by the triaxial extension test and the direct shear box test. This was not the case, however, in tests on soft marine clays reported by Bjerrum (1972a) and given in Table 2.2. Here the direct shear box (and the corrected shear vane) indicated strengths intermediate between the triaxial extension and compression tests.

Bjerrum (1972) found that using the undrained shear strength measured by the vane in a conventional limit analysis gave varying estimates of the actual stability depending on the plasticity of the clay. The disparity between $s_{u(\text{field})}$ and $s_{u(\text{vane})}$ may be partly accounted for by the combined effects of anisotropy and testing rate. The correlation

$$s_{u(\text{field})} = s_{u(\text{vane})} \cdot K_v$$

for soft clays is given in Fig.2.22.

3.4.2 Time to undrained failure

As demonstrated by Bjerrum, Simons and Torblaa (1958), the greater the time to undrained failure, the lower will be undrained strength (Fig.2.23(a)). It is therefore necessary to take this factor into account when using the results of *in situ* vane tests or undrained triaxial compression tests, with a failure time of the order of 10 min, to predict the short term stability of cuttings and embankments, where the shear stresses leading to failure may be gradually applied over a period of many weeks of construction.

The greater the plasticity index of the clay, the greater is the reduction factor which should be applied to the results of the tests with small times to failure. As shown in Fig.2.23(b) most of the reduction in undrained shear strength is because of an increase in the pore-water pressure as the time to failure increases.

A further factor to be considered is the elapsed time between taking up a sample, or opening a test pit, and performing strength tests. No thorough study of this aspect has been made to date but it is apparent that the greater the elapsed time, for a stiff, fissured clay, the smaller is the measured strength. Marsland (1971, b) noted that from loading tests made on 152 mm diameter plates at Ashford Common, strengths measured 4–8 hours and 2.5 days after excavation were approximately 85% and 75%, respectively, of those measured 0.5 hour after excavation. Other evidence was provided by laboratory tests on 38 mm diameter specimens cut from block samples of fissured clay from Wraysbury, which were stored for different periods before testing. Strengths of specimens cut from blocks stored for about 150 days before testing were only about 75% of the strengths of specimens prepared from blocks within 5 days of excavation from the shaft. This could be attributed to a gradual extension of fissures within the specimens.

3.4.3 Sampling disturbance and test specimen size

If the test specimen is disturbed by the sampling process, the measured undrained shear strength will generally be lower than the *in situ* value for a given test apparatus and procedure. Thin-walled piston samples jacked into the ground cause very little disturbance and this technique, together with careful handling in the field, during transit, and in the laboratory, are believed to give reasonably reliable measurements of the undrained shear strength of clay. Equally well, hand-cut block samples of clay taken from open excavation may be used. In Table 2.3, which shows results reported by Simons (1967), the undrained shear strength of various sized test specimens of London clay is compared with that obtained from the customary 38 mm dia X

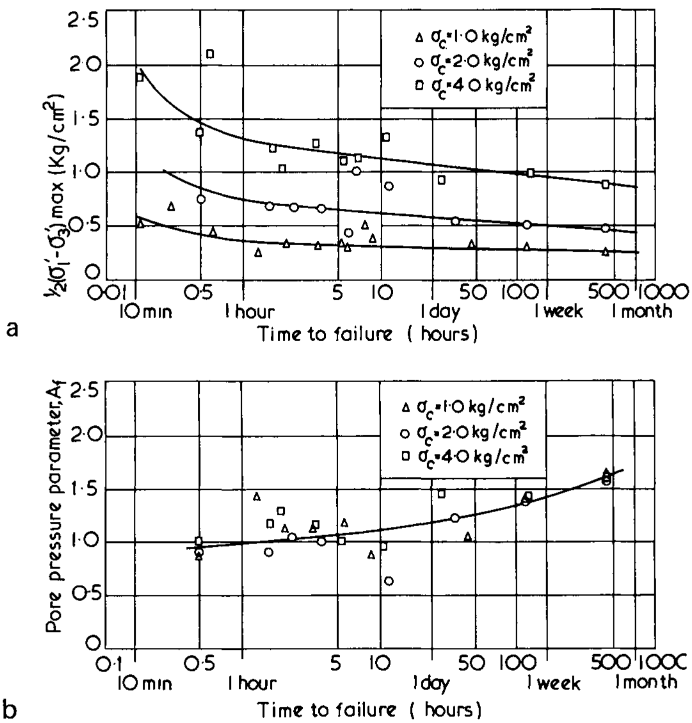

Fig.2.23 The effect of time to failure on undrained shear strength and pore pressure generation, after Bjerrum, Simons and Torblaa (1958); (a) undrained shear strength plotted against time to failure; (b) pore pressure parameter A_f plotted against time to failure

Table 2.3 Effect of test specimen size and time to failure on undrained shear strength of triaxial compression test specimens cut from intact blocks of blue London clay, after Simons (1967)

Size of triaxial test specimen (mm)	Number of tests	Water content w%	Time to failure t_f min.	s_u kN/m^2	s_u (m_c = 28%) kN/m^2	Strength ratio
305 × 610	5	28.2	63	48.8	50.7	0.62
152 × 305	9	27.1	110	51.5	46.0	0.56
102 × 203	11	27.7	175	47.9	46.4	0.57
38 × 76 (U-4)	36	26.9	8	93.4	81.9	1.00
38 × 76 (blocks)	12	28.1	7	116.3	117.3	1.43
13 × 25 (intact)	19	26.6	10	262.4	219.3	2.68

Table 2.4 Comparison of undrained shear tests on blue London clay, with strength estimated from a field failure, after Simons 1967)

Test	w% water content	t_f time to failure (min)	s_u kN/m^2	s_u (w = 28%) kN/m^2	s_u (w = 28%) (t_f = 4000 min) kN/m^2	Strength ratio
Slip	29.3	4000	30.1	35.4	35.4	1.00
610 mm × 610 mm shear box	28.1	71	47.9	48.3	41.2	1.16
305 mm × 610 mm triaxial	28.2	63	48.8	50.8	43.1	1.21
38 mm × 76 mm triaxial	26.9	8	93.4	81.8	65.6	1.85

76 mm triaxial specimens extracted from a U-4 sampling tube. The strength of 38 mm × 76 mm triaxial specimens taken from hand-cut blocks is 143% of the strength obtained from 38 mm × 76 mm specimens taken from U-4 sampling tubes. This difference results from the greater disturbance caused by using the U-4 sampling tubes.

From Table 2.3 it may also be seen that the size of specimen is of crucial importance. With stiff, fissured clays, the size of the test specimen must be large enough to ensure that the specimen is fully representative of the structure of the clay in the mass. If specimens are too small, the measured strength will be greater than that which can be relied on in the field.

In addition to the laboratory tests given in Table 2.3, Simons (1967) compared the results obtained from an analysis of a slip on the same site with 610 mm × 610 mm square *in situ* shear box tests, the 305 mm by 610 mm vertical triaxial specimens and the 38 mm × 76 mm vertical specimens from U-4 samples, the latter representing standard practice. These results are given in Table 2.4. Corrections have been made for the different water contents and times to failure, assuming purely undrained shear. The main points to note are:

- The standard 38 mm × 76 mm specimens give a strength 185% times that indicated by an analysis of the slip. If no corrections are made for water content and time to failure, this ratio would be 310%;
- The 305 mm × 610 mm triaxial specimens show a strength 21% higher than that indicated by the slip analysis. Of course, part of this difference is due to the different inclinations of the failure surfaces as discussed in section 3.4.1;
- The 610 mm × 610 mm *in situ* shear box tests give a strength 16% higher than that from slip analysis.

Bearing in mind the approximate nature of the corrections made for water content and time to failure, and the possibility that slight restraint imposed by the shear box may have resulted in a higher measured strength, reasonable agreement between the *in situ* shear box tests and the slip analysis is indicated.

To summarize, the standard undrained triaxial tests carried out on 38 mm × 76 mm specimens taken from U-4 samples greatly overestimates the *in situ* strength of the London clay as indicated by an analysis of the end of construction slip. Much better agreement is obtained from the results of triaxial specimens 100 mm diameter by 200 mm high and larger, and 610 mm × 610 mm *in situ* shear tests.

3 Immediate settlement

1 Introduction

Generally, the settlement of foundations may be regarded as consisting of three separate components of settlement, giving

$$\delta = \delta_i + \delta_c + \delta_s \tag{3.1}$$

where δ = total ultimate settlement, δ_i = *immediate* settlement resulting from the constant volume distortion of the loaded soil mass, δ_c = *consolidation* settlement resulting from the time dependent flow of water from the loaded area under the influence of the load generated excess pore pressure which is itself dissipated by the flow, δ_s = *secondary* settlement, or creep which is also time dependent but may occur at essentially constant effective stress.

This chapter covers the most convenient methods currently used to estimate the magnitude of the immediate or undrained settlement, δ_i. As a useful aside, some methods for estimating vertical foundation stresses are also given. The methods for estimating foundation settlement and stresses are based on the results of elastic theory.

2 The use of elastic theory in soil mechanics

In soil mechanics, foundation settlement and stresses under local loading (as against uniform global loading) conditions are determined from the established procedures of the mathematical theory of elasticity. Changes in foundation stresses caused by changes in applied loading are obtained in terms of total stress and the measured or computed pore pressure changes must be subtracted to yield the resulting changes in effective stress. The mathematical theory of elasticity furnishes the engineer with displacements and distributions of stresses caused by loads covering flat, flexible and rigid areas of various geometrical shapes, either on or in the horizontal surfaces of semi-infinite or layered elastic solids of wide extent. The procedure uses the assumption of constant soil parameters Youngs Modulus, E, and Poissons Ratio, υ. These parameters vary with time from the undrained values at the instant of loading ($\upsilon = 0.5$ for the idealized undrained case) to the drained values at the end of dissipation of the excess pore pressure. As pointed out by Davis and Poulos (1968) the assumption of constant elastic soil parameters does not imply that real soil behaves as an ideal elastic solid. Nevertheless, similarities exist between the behaviour of real soil and ideal elastic solids. Elastic-type behaviour may be simulated at small strains, that is, under loading conditions which ensure a high factor of safety against failure. This is reasonably true, for example, for foundations where the factor of safety is of the order of three, but is unlikely for embankments where the factor of safety is of the order of 1.5. Generally, however, soil stresses will decrease away from the loading in much the same way as in an elastic medium. The elastic soil *constants* must be experimentally determined under conditions which simulate the range of stresses and type of deformation encountered in the

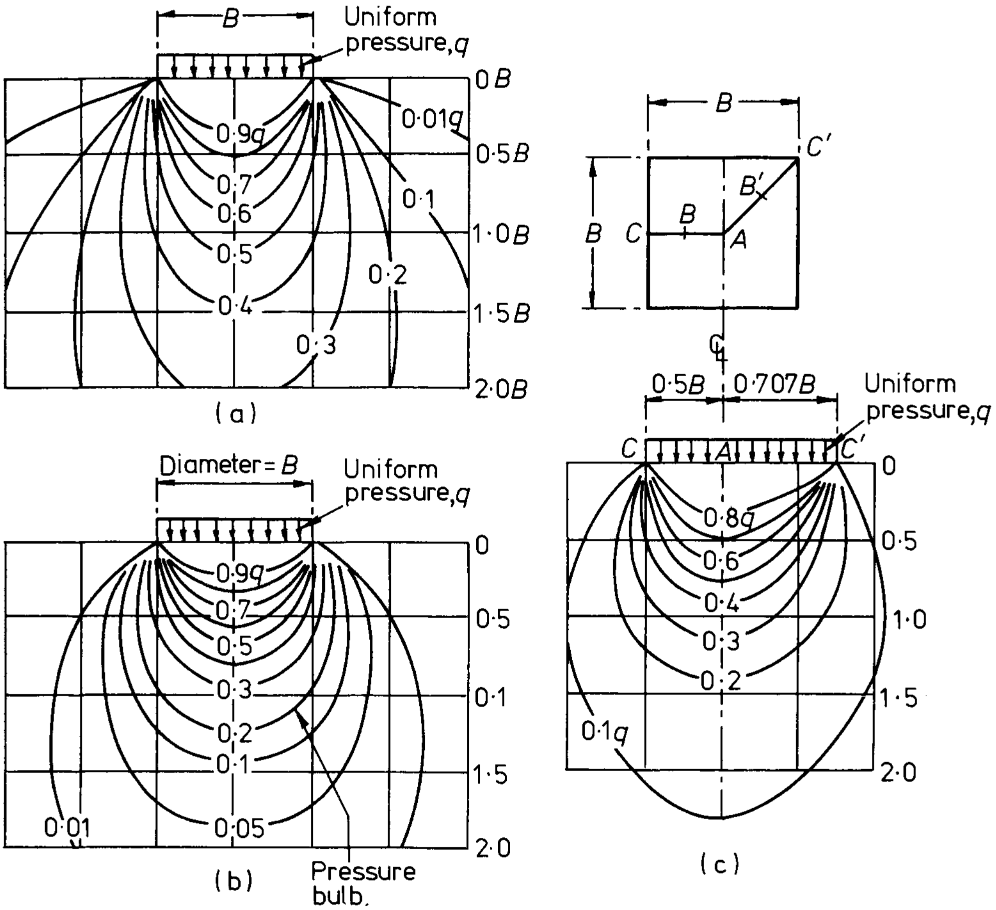

Fig.3.1 Vertical stresses under uniformly loaded flexible footings resting on a deep wide homogeneous isotropic elastic solid, after Teng (1962): (a) strip footing; (b) circular footing; (c) square footing

field, thereby justifying the use of the elastic analytical model for predicting stresses and settlements.

Distributions of stress and displacement in an elastic solid caused by a distributed load are based on integrations of the effect of a vertical point load. There are solutions to various problems and most of these may be found in the comprehensive digests by Lysmer and Duncan (1972) and by Poulos and Davis (1974).

In the following sections, a limited selection may be found of the results for vertical loadings applied to an elastic solid of wide extent. From these results, foundation settlements and distributions of vertical stresses beneath foundations may be estimated.

3 Elastic stress distributions

Stress distributions may be obtained in the form of contours of equal stresses (Fig.3.1) or *pressure bulbs* which serve as a useful qualitative conceptual aid. For example, it can be seen from Fig.3.1(a) that the influence of a flexible strip footing does not extend much beyond a depth of about twice the footing width.

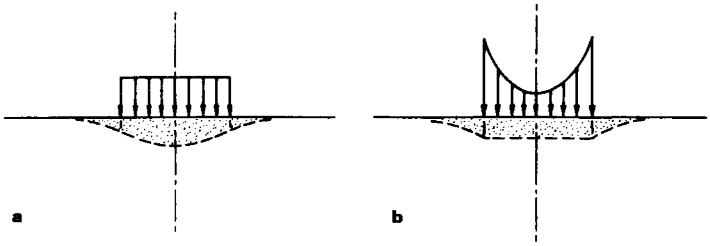

Fig.3.2 Settlements and contact stresses for uniformly loaded circular areas resting on a deep wide homogeneous isotropic elastic solid. (a) flexible footings; (b) rigid footings

The distribution of contact pressure under a uniformly loaded, flexible circular area usually produces a bowl-shaped settlement of the loaded area (Fig.3.2(a)). This is not always the case. The deformed shape will depend on the variation with depth of the moduli and on the relative magnitudes of the horizontal and vertical moduli (Fig.3.14).

In order to produce a uniform settlement, the unit load on a circular area must be very much greater at the rim than at the centre. Hence, if a perfectly uniform settlement is enforced by the absolute rigidity of a footing, the contact pressure must increase from the centre of the base of the footing toward the rim, provided the supporting material is perfectly elastic (Fig.3.2(b)). Thus the contact pressure of real rigid footings will be different from that of the idealized flexible footings. However, by St Venants principle, the stress distributions will be much the same. This principle states that:

> *If forces acting on a small portion of the surface of an elastic body are replaced by another statically equivalent system of forces acting on the same portion of the surface, this redistribution of loading produces substantial changes in the stresses locally but has a negligible effect on the stresses at distances which are large in comparison with the linear dimensions of the surface on which the forces are changed.* (Timoshenko and Goodier [1951].)

3.1 Design charts for estimating foundation stresses

Probably the most useful design chart for estimating foundation stresses is that given by Janbu, Bjerrum and Kjaernsli (1956) and shown in Fig.3.3. This chart gives the increase in vertical stress beneath the *centre* of a uniformly loaded flexible area of strip, rectangular or circular shape.

The design chart of Fadum (1948) given in Fig.3.4 is of classical interest. It provides estimates of vertical stress beneath the *corner* of uniformly loaded flexible rectangular areas. It may also be used for stress determination beneath any point on a uniformly loaded area of a shape amenable to subdivision into rectangular areas. The subdivision is carried out in such a way that the point under consideration forms a common corner. The contribution from each area is computed and summed, invoking the principle of superposition. The technique may be extended to include a point outisde the area. In this case, the area is extended to include the point with subdivision and computation carried out as before except that the contribution of the fictitious area is subtracted.

For estimating vertical stresses beneath flexible, uniformly loaded areas of shapes not amenable to treatment by Figs.3.3 or 3.4, the chart given by Newmark (1942) and shown in Fig.3.5 may be used. In this case, the area is drawn to scale on transparent paper such that the depth at which the stress change is required equals the scale datum AB (Fig.3.5). The scale drawing is positioned on the chart with the point in question (either inside or outside the area) located on the centre spot. An estimate is then made of the number of segments and fractions of segments, N, of the chart enclosed by the boundary of the scaled area. If the loading intensity is q kN/m^2, then the stress at the required depth below the point in question is computed as $\sigma_v = 0.001\,Nq$ kN/m^2.

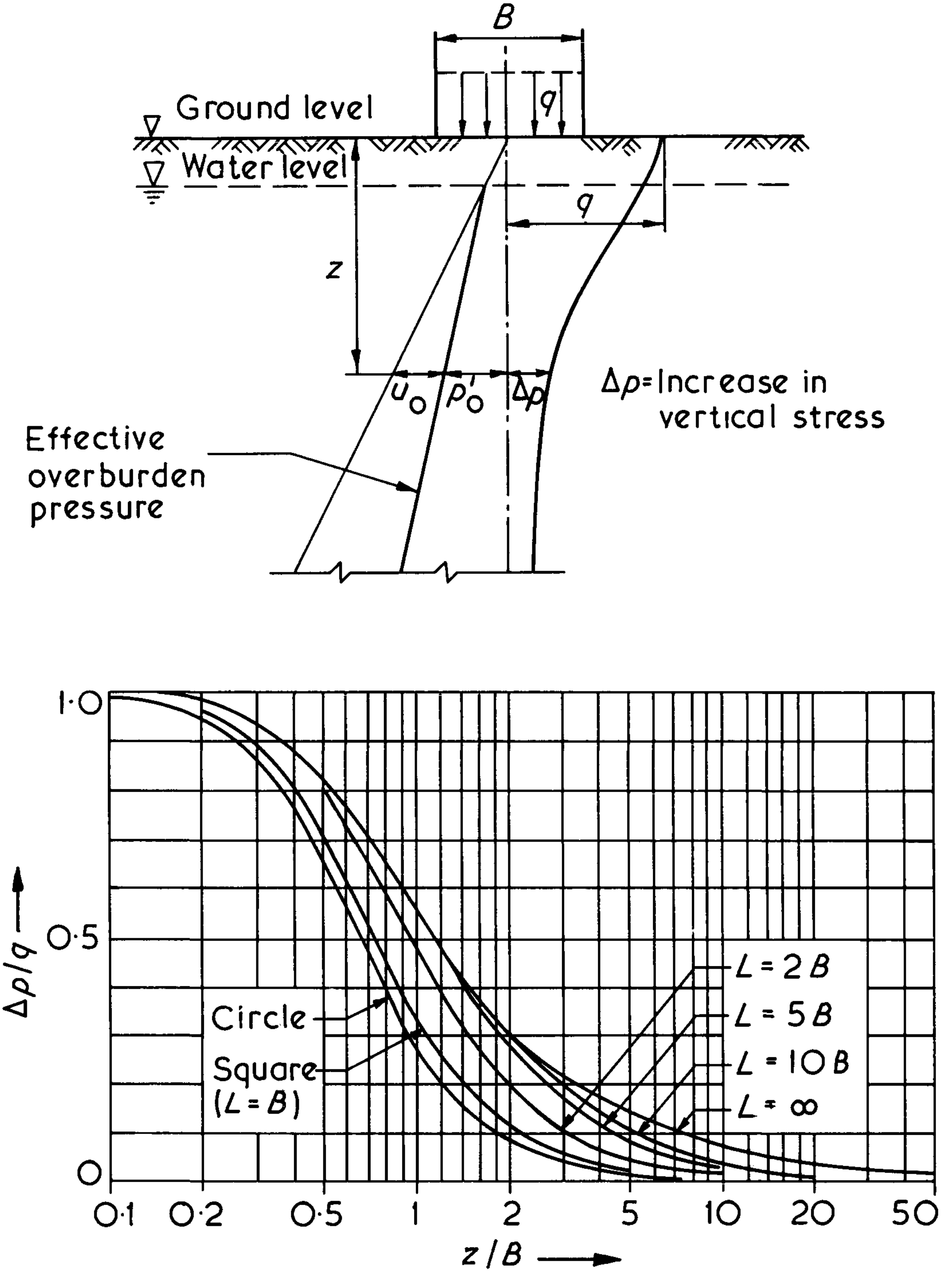

Fig. 3.3 Determination of increase in vertical stress under the centre of uniformly loaded flexible footings, after Janbu, Bjerrum and Kjaernsli (1956)

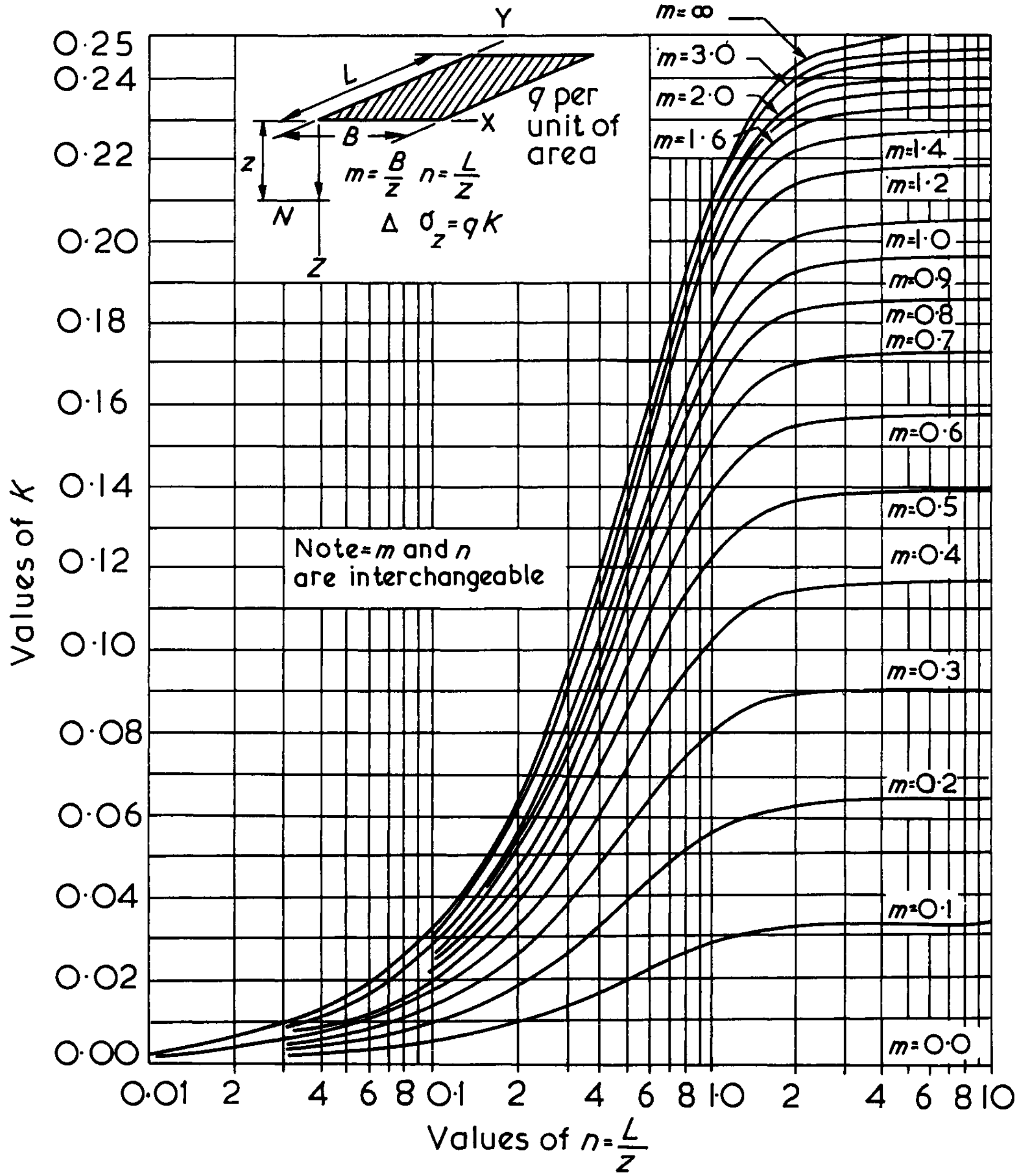

Fig.3.4 Influence coefficients for the increase in vertical stress under the corner of a uniformly loaded flexible rectangular footing, after Fadum (1948)

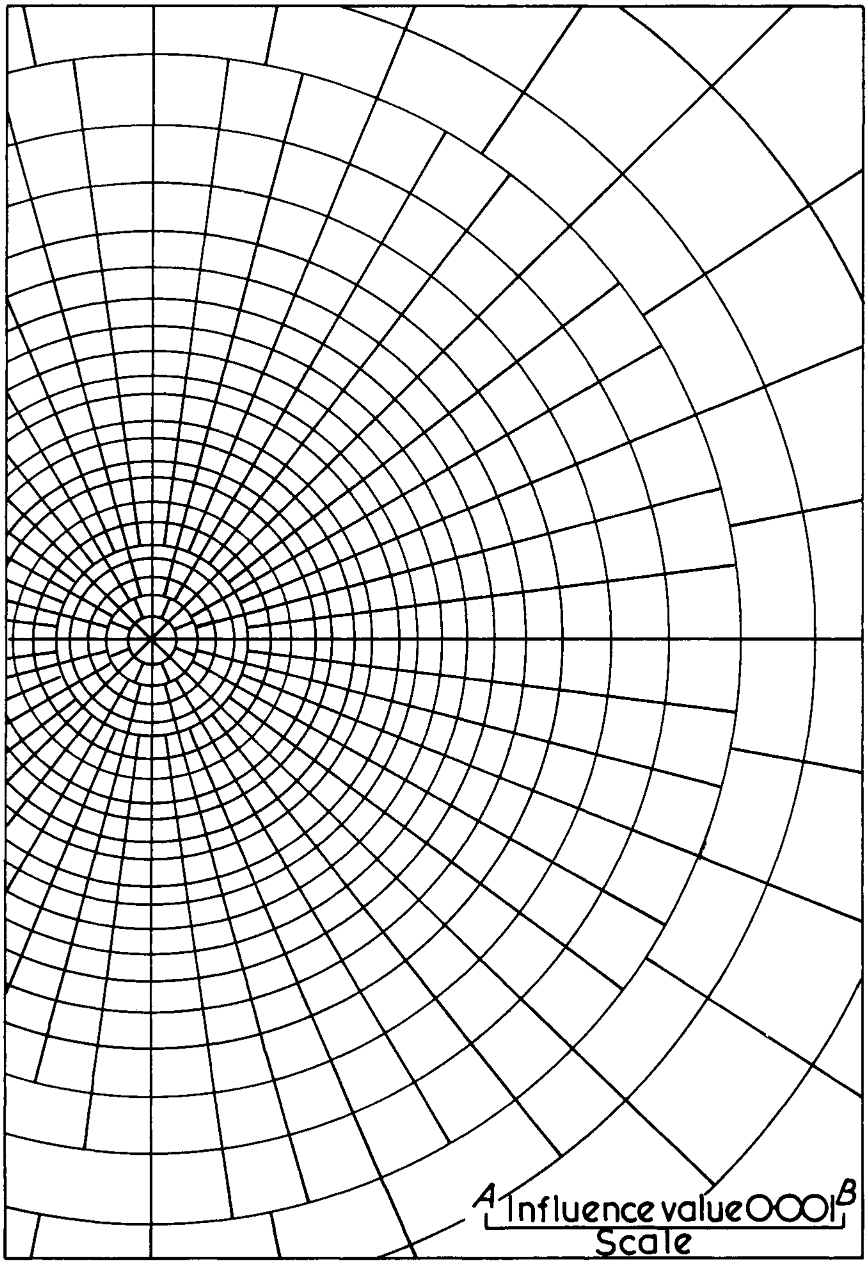

Fig. 3.5 Influence chart for the increase in vertical stress under a uniformly loaded flexible footing, after Newmark (1942)

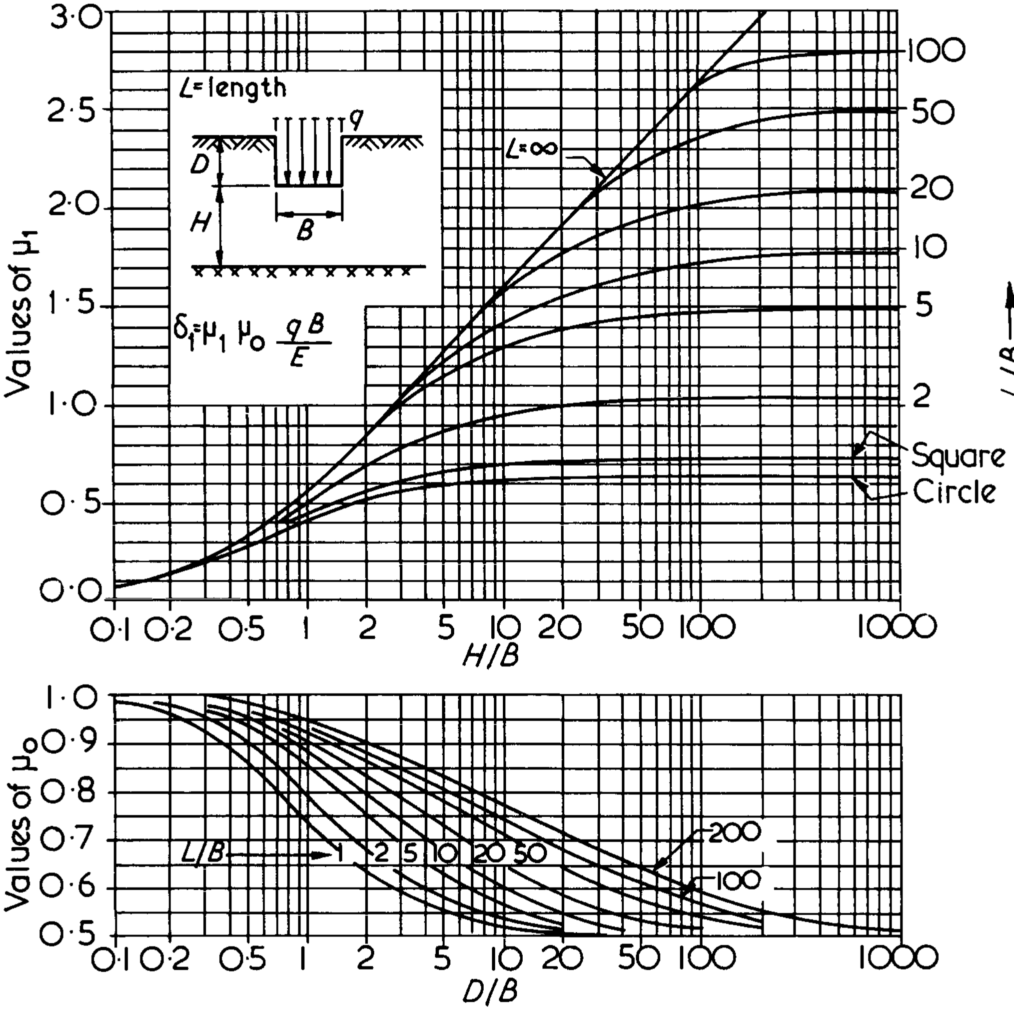

Fig. 3.6 Diagrams for the factors μ_0 and μ_1 used in the calculation of the immediate average settlement of uniformly loaded flexible areas on homogeneous isotropic saturated clay, after Janbu, Bjerrum and Kjaernsli (1956)

4 Elastic settlements

As pointed out by Davis and Poulos (1968), in a layered soil the total final settlement may be obtained by summation of the vertical strains in each layer whence generally

$$\delta_z = \sum \frac{1}{E'} (\sigma_z - \upsilon'\sigma_x - \upsilon'\sigma_y)\delta h \tag{3.2}$$

where E' and υ' are the elastic parameters for the soil structure appropriate to the stress changes in each layer; σ_x, σ_y and σ_z, are the stresses owing to the foundation, and δh is the thickness of each layer.

If, however, the soil profile is, for example, a reasonably homogeneous clay stratum, then appropriate values of E' and υ' can be assigned to the clay for the whole depth of the stratum, giving

$$\delta_z = \frac{qBI}{E'} \tag{3.3}$$

where q is the foundation pressure, B is some convenient dimension of the foundation and I is an influence factor given by elastic theory.

4.1 Undrained or immediate settlements

If an incompressible elastic solid of wide extent is locally loaded, local deformations will occur at constant volume. If a saturated clay layer is rapidly loaded locally, the low permeability of the clay retards drainage of water out of the pores and the clay deforms in the undrained or constant volume mode. The similarity is thus apparent between a loaded incompressible (i.e. $\upsilon = 0.5$) elastic solid and a loaded *end of construction* saturated clay. The appropriate form, therefore, of equation (3.3) is

$$\delta_i = \delta_u = \frac{qBI_u}{E_u} \tag{3.4}$$

where I_u is the influence factor for $\upsilon = \upsilon_u = 0.5$ and E_u is the modulus determined from undrained triaxial tests.

4.2 Design charts for estimating immediate settlements

Probably the most useful chart is that given by Janbu, Bjerrum and Kjaernsli (1956) and shown in Fig.3.6. The chart provides estimates of the *average* immediate settlement of uniformly loaded, flexible areas of strip, either rectangular or circular in shape. The average settlements are obtained from equation (3.4) putting $I_u = \mu_0 \mu_1$.

Generally, real soil profiles which are deposited naturally consist of layers of soils of different properties underlain ultimately by a *hard* stratum. Within these layers, strength and moduli generally increase with depth. Gibson (1967) has shown that the variation of modulus with depth has little effect on the distribution of stresses but has a marked effect on surface displacements which are concentrated within the loaded area for an incompressible medium. The chart given in Fig.3.6 may be used to accommodate a variation of E with depth by replacing the multilayered system with one hypothetical layer on a rigid base. The depth of this hypothetical layer is successively extended to incorporate each *real* layer, the corresponding values of E being ascribed in each case and settlements calculated. By subtracting the effect of the hypothetical

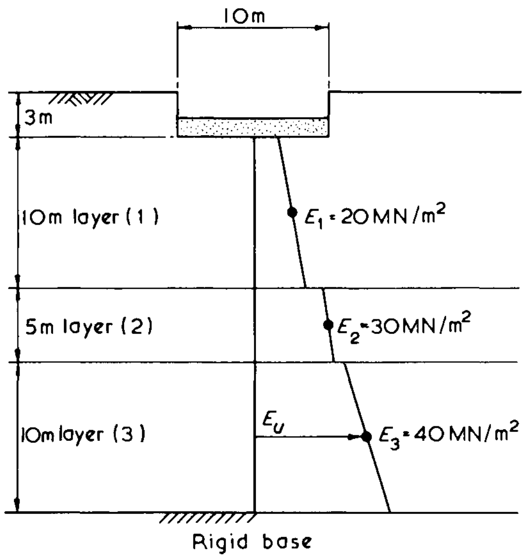

Fig.3.7 Rectangular footing, 10 m × 40 m, uniformly loaded with net intensity 50 kN/m²

layer above each *real* layer, the separate compression of each layer may be found and summed to give the overall total settlement.

Consider the typical example given in Fig.3.6, $D/B = 0.3$, $L/B = 4$, whence $\mu_0 = 0.96$. For layer (1) $H/B = 1$, whence $\mu_1 = 0.55$.

The compression of layer (1) if it had a rigid base is therefore,

$$\delta_{(1)_{20}} = 0.55 \times 0.96 \times \frac{0.05 \times 10}{20} = 0.013 \text{ m}$$

Assuming that layer (2) extends to the surface and has a rigid base gives $H/B = 1.5$ whence $\mu_1 = 0.67$.

The combined compression of layer (1) and (2) if $E_1 = E_2 = 30$ MN/m^2 and if layer (2) had a rigid base is, therefore,

$$\delta_{(1,2)_{30}} = 0.96 \times 0.67 \times \frac{0.05 \times 10}{30} = 0.011 \text{ m}$$

The compression of layer (1) if $E_1 = E_2 = 30$ MN/m^2 and if it had a rigid base is

$$\delta_{(1)_{30}} = 0.55 \times 0.96 \times \frac{0.05 \times 10}{30} = 0.009 \text{ m}$$

Assuming that layer (3) extends to the surface gives $H/B = 2.5$ whence $\mu_1 = 0.88$.
The compression of layers (1), (2) and (3) if $E_1 = E_2 = E_3 = 40$ MN/m^2 is, therefore,

$$\delta_{(1,2,3)_{40}} = 0.88 \times 0.96 \times \frac{0.05 \times 10}{40} = 0.011 \text{ m}$$

The combined compression of layers (1) and (2) if $E_1 = E_2 = 40$ MN/m^2 and if layer (2) has a rigid base is

$$\delta_{(1,2)_{40}} = 0.67 \times 0.96 \times \frac{0.05 \times 10}{40} = 0.008 \text{ m}$$

The overall total settlement is, therefore,

$$\delta_{(1)_{20}(2)_{30}(3)_{40}} = \delta_{(1)_{20}} + \delta_{(1,2)_{30}} - \delta_{(1)_{30}} + \delta_{(1,2,3)_{40}} - \delta_{(1,2)_{40}}$$

$$= (0.013 + 0.011 - 0.009 + 0.011 - 0.008) \text{ m} = 18 \text{ mm}$$

Butler (1974) has adopted a similar approach using a simple extrapolation of Steinbrenners (1934) approximation. The Boussinesq (1885) displacements for an infinite depth of soil are used, and the effect of the rigid base is simulated by the approximation that the compression of a finite layer of depth z metres on a rigid base is the same as the compression within the top z metres of an infinitely deep deposit.

Butler gives charts which enable estimates to be made of the settlement of the corner of a uniformly loaded, flexible rectangular area resting on the surface of a heterogeneous elastic layer. It is assumed that the modulus increases linearly with depth. Butler's charts for immediate (undrained) settlement are given in Fig.3.8(a),(b) and (c).

Consider the case shown in Fig.3.10. The settlement at the centre may be found by subdividing the loaded area as shown and using superposition.

Referring to Fig.3.8, for $L/B = 2$, $k = 0.5$, $z/b = 8$, we have

$I = 0.23$.

The settlement of the corner of a rectangle 5 m $\times$ 10 m is

$$\delta_{\text{corner}} = \frac{BqI}{E_0} = \frac{5 \times 0.05}{10} \times 0.23 = 0.00575 \text{ m.}$$

By superposition, the settlement in the centre of a rectangle 10 m $\times$ 20 m is

$$\delta_{\text{centre}} = 4\delta_{\text{corner}} = 4 \times 0.00575 = 0.023 \text{ m.}$$

This kind of problem may be dealt with using the chart given in Fig.3.6 and *layering* the soil as shown in Fig.3.10.

Noting that $L/B = 2$, $D/B = 0$, i.e. $\mu_0 = 1$, then for the four layers shown we have by Fig.3.6

H/B	μ_1
layer 1	0.5
layer 2	0.7
layer 3	0.8
layer 4	0.85

Therefore,

$$\delta_{average} = 0.05 \times 10 \left[\frac{0.5}{15} + \left(\frac{0.7}{25} - \frac{0.5}{25}\right) + \left(\frac{0.8}{35} - \frac{0.7}{35}\right) + \left(\frac{0.85}{45} - \frac{0.8}{45}\right)\right] = 0.022 \text{ m.}$$

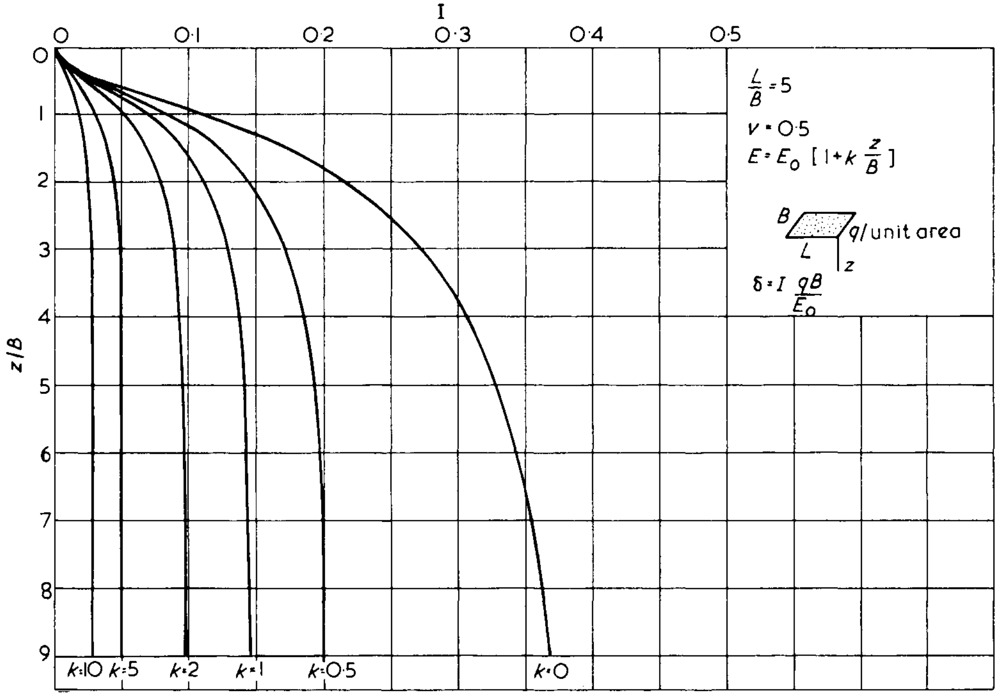
I
0
0·1
0·2
0·3
0·4
0·5
z/B
$\frac{L}{B}=5$
$\nu=0·5$
$E=E_0\,[1+k\,\frac{z}{B}]$
B
L
q/unit area
z
$\delta=I\,\frac{qB}{E_0}$
k=10
k=5
k=2
k=1
k=0·5
k=0

a

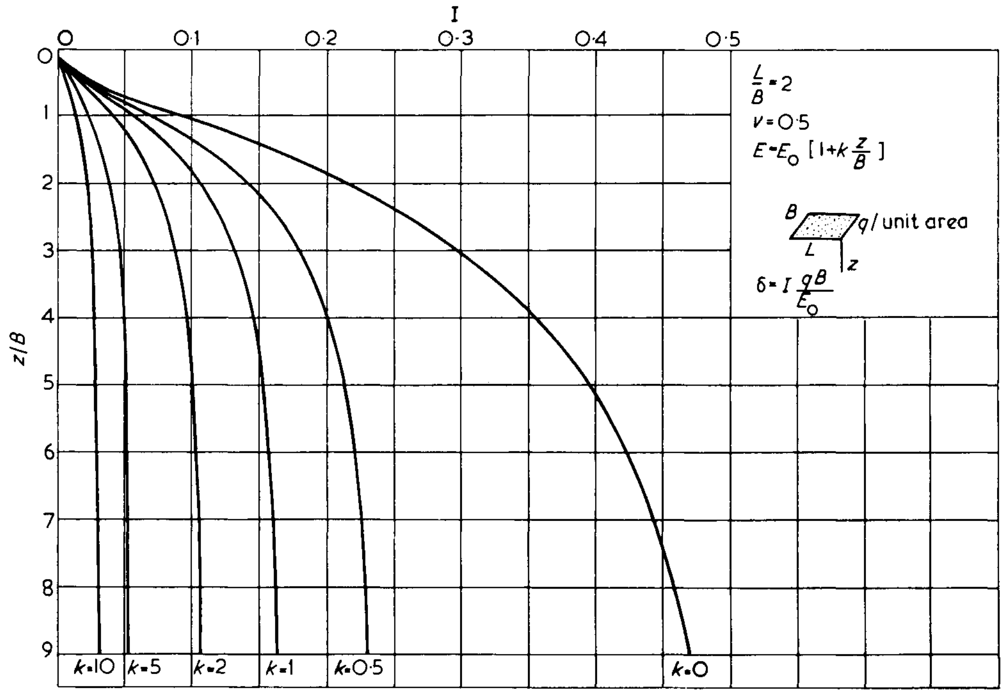
I
0
0·1
0·2
0·3
0·4
0·5
z/B
$\frac{L}{B}=2$
$\nu=0·5$
$E=E_0\,[1+k\,\frac{z}{B}]$
B
L
q/unit area
z
$\delta=I\,\frac{qB}{E_0}$
k=10
k=5
k=2
k=1
k=0·5
k=0

b

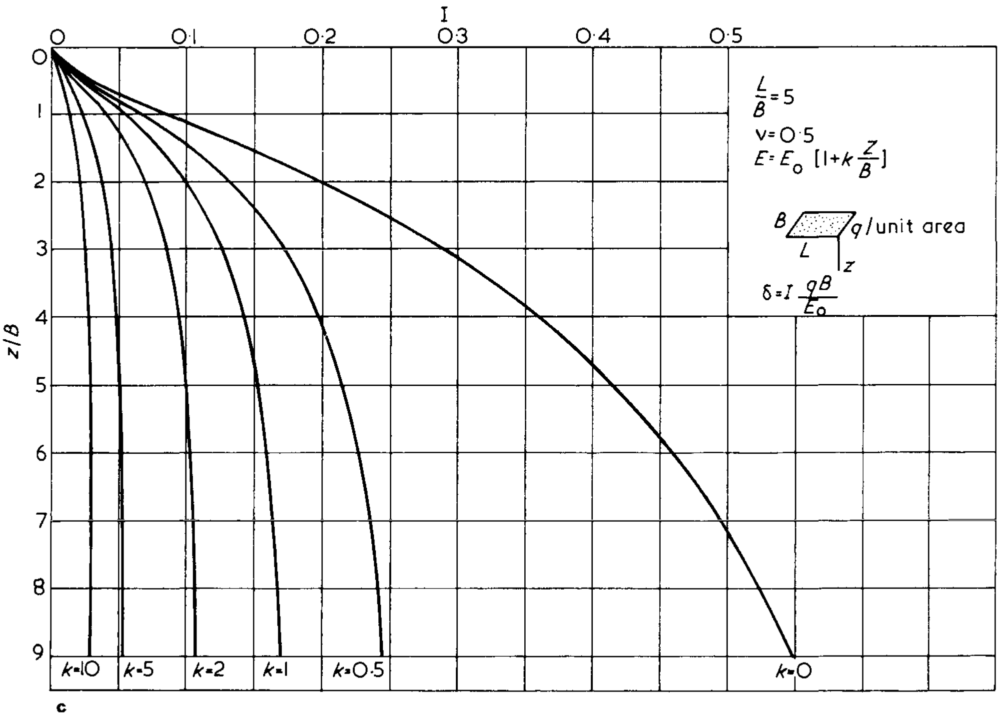

Fig. 3.8 Influence coefficients for immediate settlement of the corner of a flexible uniformly loaded rectangle on the surface of a saturated clay with Youngs modulus increasing linearly with depth, after Butler (1975); (a) length to breadth ratio L/B = 1; (b) length to breadth ratio L/B = 2; (c) length to breadth ratio L/B = 5

This result tends to confirm the rough guide relating the relative settlements given by the expression

$$\delta_{(flexible, average)} \approx 0.9\ \delta_{(flexible, maximum)}$$

$$\approx 1.1\ \delta_{(rigid)}$$

Davis and Poulos (1968) give the following expressions effectively relating rigid footing settlements to flexible footing settlements.

For a circle,

$$\delta_{(rigid)} \approx \tfrac{1}{2}(\delta_{centre} + \delta_{edge})_{flexible}$$

For a rectangle,

$$\delta_{rigid} \approx \tfrac{1}{3}(2\delta_{centre} + \delta_{corner})_{flexible}$$

For a strip,

$$\delta_{rigid} \approx \tfrac{1}{2}(\delta_{centre} + \delta_{edge})_{flexible}$$

As far as the footing roughness is concerned, it should be noted that an analysis of a rigid circular plate resting on a heterogeneous elastic half-space (Carrier and Christian, 1973) showed

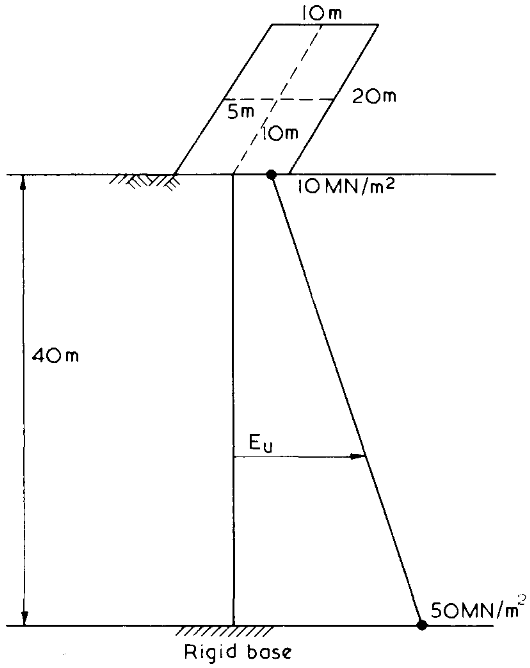

Fig. 3.9 Subdivision of rectangular area loaded uniformly with intensity 50 kN/m²

that for most practical problems the solution for a rough plate was the same as the solution for a smooth plate.

5 Heave of excavations

When an excavation is opened, load is removed from the soil and *heave* may therefore be expected. This heave can be considered as occurring without change in volume of the soil, provided that no water is allowed to accumulate in the excavation, and that the excavation is kept open for a reasonably short period. The calculations of immediate heave may therefore be made in exactly the same way as for immediate settlement, considering the soil weight removed as a negative load. If water is allowed to remain in an excavation in clay for even a short time, not only will a greater heave be experienced owing to the soil increasing in volume by taking up water, but the shear strength, and hence the bearing capacity, will also be reduced.

There are two additional points to bear in mind when considering immediate heave:

- The value for E_u for unloading is generally greater than the value of E_u for loading;
- Any de-watering has a very great effect on the magnitude of the heave. Lowering the ground water table increases the effective stresses in the underlying soil and this leads to settlement which tends to reduce the magnitude of the elastic heave.

Reference may be made to Serota and Jennings (1959).

6 Estimates of undrained modulus

Clearly, the success of the preceding methods in predicting undrained settlements rests crucially on the use of appropriate values of the undrained modulus, E_u. Indeed, the analytical sophistication of many methods presupposes, by implication, unrealistically accurate values of E_u.

Traditionally, E_u has been estimated from conventional undrained triaxial tests, where E_u is determined over a range of axial loading equal to half the ultimate. A worthwhile refinement is to determine E_u over the range of stress relevant to the particular problem, because the experimental stress–strain relationship may not be linear even for stresses less than 50% of the ultimate. Davis and Poulos (1968) suggest that the *undisturbed* triaxial specimen is given a preliminary consolidation under K_0 conditions and with an axial stress equal to the effective overburden pressure at the sampling depth. This procedure attempts to return the specimen to its original state of effective stress in the ground, assuming that the horizontal effective stress in the ground was the same as that produced by the laboratory K_0 condition. There is some evidence (Skempton and Sowa, 1963) to suggest that is not generally the case. Simons and Som (1970) have shown that triaxial tests on London clay in which the specimens are brought back to their original *in situ* stresses give elastic moduli which are much higher than those determined from conventional undrained triaxial tests. This has been confirmed by Marsland (1971) who carried out 865 mm diameter plate loading tests in 900 mm diameter bore holes in London clay. Marsland found that the average moduli determined from the loading tests on 865 mm diameter plates in well-prepared boreholes were between 1.8–4.8 times those obtained from undrained triaxial tests (see Fig.3.11).

Sample disturbance is known to affect considerably the value of modulus obtained (Simons, 1957; Ladd, 1969; Raymond *et al*, 1971). For example, it was found that for two structures in Norway (Simons, 1957), the E_u values obtained by carefully-conducted, unconfined compression tests carried out on samples obtained by a 54 mm thin-walled stationary piston sampler, were about one third of the values which could be estimated from the settlement observations. Ladd (1969) suggested that sample disturbance can be partly overcome by proper reconsolidation in the laboratory.

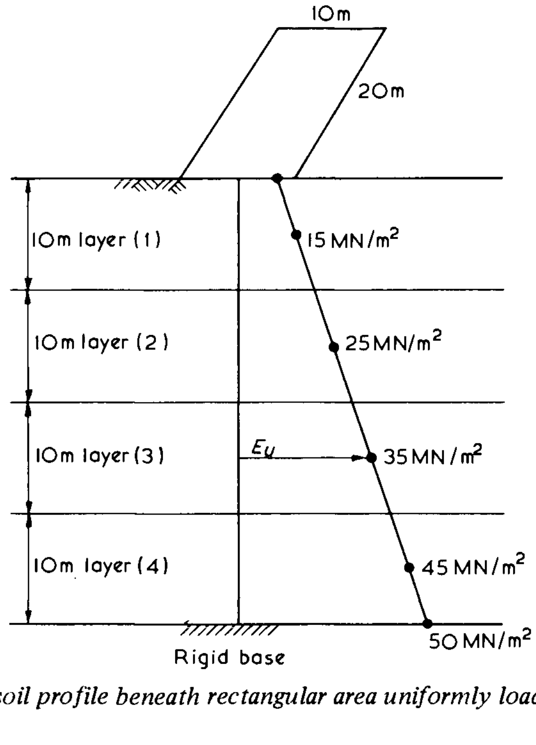

Fig.3.10 Layering of soil profile beneath rectangular area uniformly loaded with intensity 50 kN/m²

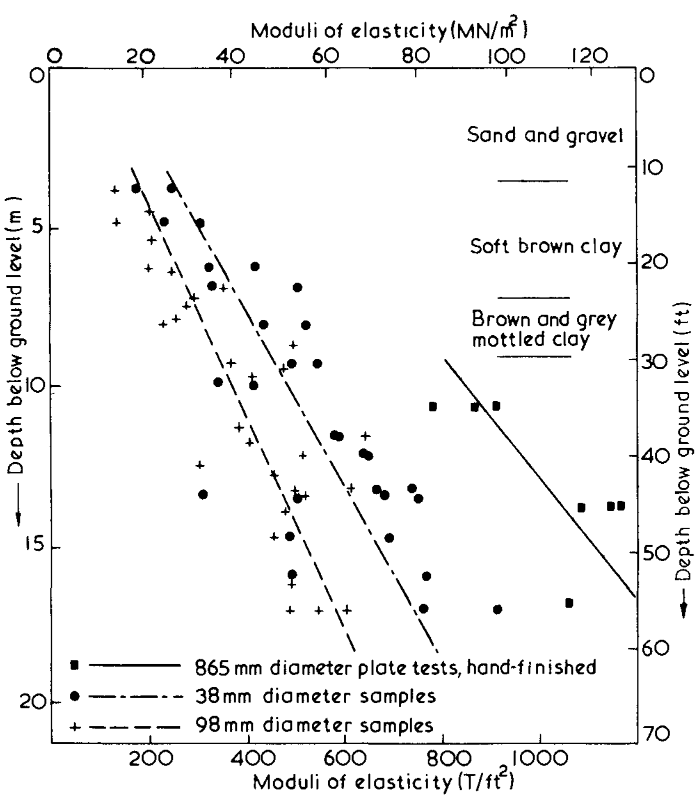

Fig. 3.11 Moduli determined from triaxial tests on 38 mm and 98 mm diameter specimens, and from 865 mm diameter plate tests on London clay at Chelsea, after Marsland (1971 (c))

It has been suggested that more realistic determinations of E_u will be obtained if:

- Samples are reconsolidated under a stress system equal to that existing in the field, e.g. Simons (1957) and Berre (1973) or
- Samples are reconsolidated isotropically to a stress equal to $\frac{1}{2}$ to $\frac{2}{3}$ of the *in situ* vertical stress, Raymond *et al* (1971).

However, if samples of sensitive clays in particular are significantly disturbed, then reconsolidation may well lead to changes in moisture content, and hence a stiffer structure, with E_u determinations which are on the high side.

Factors which should be considered when using consolidated undrained tests to estimate the deformation are: type of consolidation, that is, whether isotropic or anisotropic; the stress level; consolidation period; the stress path followed; the rate of strain; the elapsed times between opening up a test pit or drilling a borehole, taking a sample, and then testing it; the size of the sample; orientation of the sample.

Reference may be made to Marsland (1971), Ward (1971), Berre and Bjerrum (1973), Bjerrum (1973) and Lambe (1973[a,b]).

Of particular importance is the shear stress level. The field loading tests which have been carried out over the past few years in Norway have yielded invaluable information. Two field loading tests on a soft quick clay were carried out at Asrum by Høeg, Andersland and Rolfsen (1969), another at Mastermyr by Frimann Clausen (1969, 1970) and two at Sunderland by Engesgaar (1970). These tests showed clearly that for surface loads up to approximately one third to one half of the failure load, the measured undrained settlements (and the induced pore-water pressures) were small; as the loading approached failure much larger settlements were naturally observed. The corresponding E_u values were thus shown to be very sensitive to the shear stress level. Even though the filling was placed on peat and soft quick clay with a total thickness of some 19 m, very small settlements were recorded during the early stages of the test at Mastermyr.

Carefully conducted laboratory tests on a variety of clays by Berre (1973), confirm the conclusion. In addition, Berre found that the undrained stress–strain relationships were somewhat anisotropic and also time-dependent, the smaller the strain rate the smaller the E_u value by a factor of approximately one third per log-cycle of time. It should, however, be pointed out that the E_u value for the Fornebu clay was not found to be dependent on the strain rate. Bjerrum, Simons and Torblaa (1957), and Madhloom (1973) found an increase in E_u with increasing time to failure.

Because of the many difficulties faced in selecting a modulus value from the results of laboratory tests, it has been suggested that a correlation between the deformation modulus and the undrained shear strength, may provide a basis for a settlement calculation. Different authors have quoted different values for the ratio of E_u/s_u, for example Bjerrum (1964), 250–500; and Bjerrum (1972), 500–1500.

Table 3.1 shows values of the E_u/s_u ratio for a number of structures on normally and slightly over-consolidated clay, and the ratio ranges from 40–3000. As discussed earlier, the shear stress level is a factor which has great influence on E_u; low values of E_u/s_u would be expected for highly plastic clays with a high shear stress level, and higher values for lightly-loaded clays of small plasticity (Ladd, 1964; Bjerrum, 1972).

The use of the Menard pressuremeter has also been advocated for the determination of the undrained modulus of clay (Hobbs, 1971; Calhool, 1972). In principle, the pressuremeter, which tests a comparatively large volume of soil *in situ*, should provide a reliable basis for calculating the initial settlement, provided the soil is not greatly anisotropic with respect to E_u. It is of interest to note that Calhoon (1972) found that initial settlements computed from pressuremeter data are of the same order of magnitude as initial settlements computed for E_u values in the range 500–1000 times the undrained shear strength.

The Norwegian field compressometer (Janbu and Senneset, 1973), may well provide a reli-

Table 3.1 Values of the ratio of undrained modulus to undrained shear strength, after Simons (1974)

Site	E_u/s_u	Reference
Test embankment	40	Wilkes (1974)
Oil tanks, Arabian Gulf	50–70 (depending on factor of safety)	Meigh & Corbett (1970)
Skabo Office Building, Oslo	150	Simons (1957)
Turnhallen (Heavy) Drammen	190	Simons (1957)
Tank, Shellhaven	220	Bjerrum (1964)
Northeast Test Embankment, Boston	240	Lambe (1973[a])
Preload test, Lagunillas	250	Lambe (1973[a])
Preload test, Amuay	250	Lambe (1973[a])
Loading test, Skå Edeby	340	Bjerrum (1964)
Storage tanks, South Portland	400	Liu and Dugan (1974)
Satellite antenna tower Fucino plains	450	D'Elia and Grisolia (1974)
Loading test, Fornebu	500	Bjerrum (1964)
Loading test, Åsrum	1000	Høeg, Andersland & Rolfsen (1969)
Økernbråten, Oslo	1500	Simons (1963)
Loading test, Mastemyr	3000	Frimann Clausen (1969, 1970)

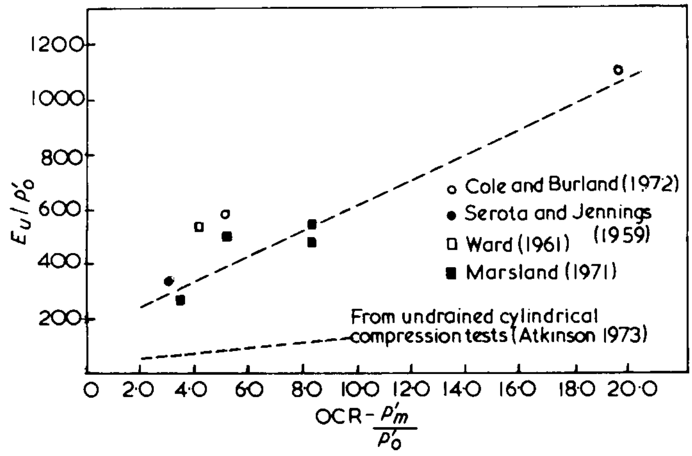

Fig.3.12 Values of E_u/p'_o plotted against OCR, after Atkinson (1974)

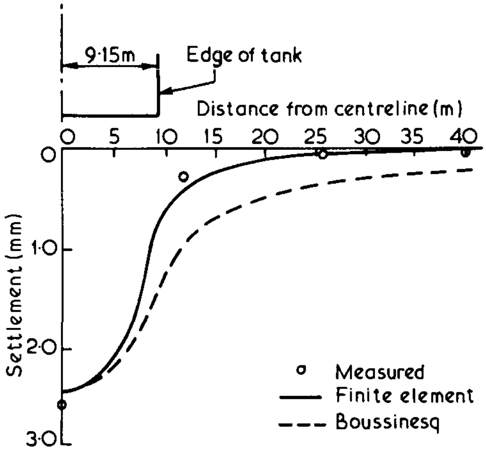

Fig.3.13 Effect of heterogeneity on ground surface deformation, after Burland, Sills and Gibson (1973)

able method for obtaining the undrained deformation modulus of clays, although up to the present it has been mainly used in sands and silts.

An investigation into the undrained deformation properties of a clay crust has been carried out by Bauer, Scott and Shields (1973). They found that *in situ* plate loading tests, using a rigid 460 mm diameter steel plate, gave a good correlation with the results from a 3.1 m X 3.1 m heavily reinforced rigid footing, 660 mm thick, while values deduced from laboratory tests were generally too low and erratic.

For London clay, Wroth (1971) demonstrated that deformation moduli measured in a consistent way are dependent on the mean stress at the start of shear (p'_0) and, to a lesser extent, on the over-consolidation ratio (OCR = p'_m/p'_0 where p'_m is the maximum mean stress experienced by the soil). Burland (1974) has emphasized the usefulness of field observations from which *in situ* properties may be back-analysed.

Atkinson (1974) has compared the values of the *in situ* E_u values calculated in the above way with the values determined from undrained cylindrical compression tests. As shown in Fig.3.12 the relationship suggested by Wroth is well-defined but the moduli determined from field measurements are approximately five times the moduli determined from laboratory measurements.

Values for the field E_u were obtained from plate loading tests at Chelsea and Hendon (Marsland, 1971); from observations of the heave of a deep excavation (Serota and Jennings, 1959); from the deflections of a retaining wall (Cole and Burland, 1972); and from the deflections of a tunnel below an excavation (Ward, 1961). With the exception of the Hendon plate loading tests, these sites were in or near central London.

Atkinson (1974) observes that the significant difference between the laboratory and field measured values of the same soil parameter, E_u, can be partly explained by allowing for elastic anisotropy in analysing the field data. By assuming a degree of undrained anisotropy of 0.6 (Atkinson, 1973) the field moduli could be reduced by about 30%. The balance of the disparity between laboratory and field measured E_u may be attributed to sampling disturbance, test machine interference, and an isotropic starting state of stress in the laboratory tests.

Apart from difficulties in obtaining undisturbed, representative, triaxial specimens and restoring them to their *in situ* effective stresses prior to testing, there is the problem of carrying out appropriate measurements of axial strain during the test. The frictional restraint of the end platens cause the specimen to deform under axial loading in the characteristically *barrelled* fashion, with the deformation concentrated in the middle third of the specimen. To base axial strain measurements, therefore, on the displacement of the top platen, gives a low estimate of the true axial strain (Arthur and Menzies, 1968) giving an overestimate of E_u. Even using lubricated *free end* platens (Rowe and Barden, 1965) does not exclude the possibility of local strains exceeding the integrated value (Arthur and Phillips, 1972). Axial strains must therefore be measured locally.

7 The effects of heterogeneity and anisotropy

Although the use of an average value of E_u may, with experience, give a reasonable estimate of the average initial settlement of a structure, if it is necessary to predict the initial deflected

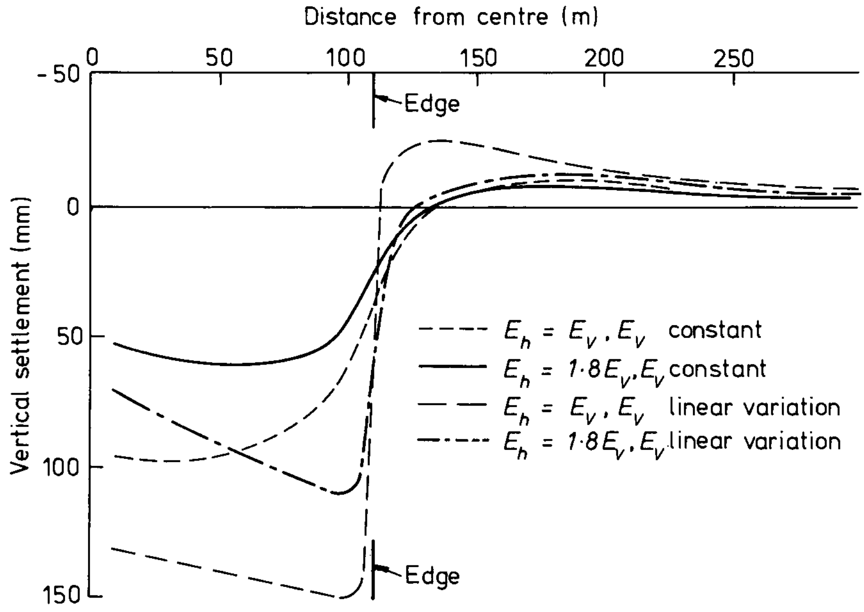

Fig. 3.14 Vertical settlement of a uniformly loaded flexible circular area resting on a wide deep elastic solid of specified anisotropy and heterogeneity, after Rodrigues (1975)

shape, then heterogeneity and anisotropy must be taken into account. The effects of heterogeneity and anisotropy have been considered, for example, by Lambe (1964), Gibson (1967), Davies and Poulos (1968), Gibson and Sills (1971), Burland, Sills and Gibson (1973), Carrier and Christian (1973), and solutions to a limited number of problems are available.

An example of the influence of heterogeneity is given in Fig.3.13, taken from Burland, Sills and Gibson (1973). The theoretical deflected shapes of the ground surface for the Mundford tank, founded on chalk (Ward, Burland and Gallois, 1968) are compared with the observed displacements. It can be seen that the settlement of the ground surface is localized around the loaded area much more than the simple elastic Boussinesq theory predicts – an effect accounted for almost entirely by the influence of inhomogeneity.

The deformed shape of the ground surface depends on the variation of the moduli with depth and the relative magnitudes of the horizontal and vertical moduli. Rodrigues (1975), for example, has shown (Fig.3.14) by a finite element stress analysis that the maximum settlement of a flexible loaded area may occur nearer the edges than in the middle, an effect predicted by Gibson (1974).

Two important points to emerge are:

- The vertical settlement is generally very sensitive to the horizontal modulus E_h.
- For $E_v = 0$ at the surface and E_v increasing with depth, the maximum settlement is near the edge because of the large lateral strains existing at the edge.

4 Bearing capacity of footings

1 Introduction

Foundation engineering may be defined as the art of applying – economically – structural loads to the ground in such a manner as to avoid excessive deformations. It should be noted that unless foundations are placed on hard sound rock, some measurable settlement will always occur. In particular, differential settlements must be kept within tolerable bounds, although if total settlements become too large, damage to services may occur, and tall buildings may tilt.

When designing foundations, there are two criteria which must be considered and satisfied separately:

- There must be an adequate factor of safety against a bearing capacity failure in the soil
- The settlements, and particularly the differential settlements, must be kept within reasonable limits.

For foundations on clays, either bearing capacity or settlement may govern the foundation design; it will be found that with foundations on granular soils, however, the choice of allowed bearing pressure will, on virtually every occasion, be controlled by settlement.

Deformation of an element of soil is a function of a change in effective stress, not a change in total stress. Various causes of deformation of a structure are listed as follows:

- Application of structural loads
- Lowering of the ground water table
- Collapse of soil structure on wetting
- Heave of swelling soils
- Fast growing trees on clay soils
- Deterioration of the foundation (sulphate attack of concrete, corrosion of steel piles, decay of timber piles)
- Mining subsidence
- Sinkholes
- Vibrations in sandy soils
- Heave of clay soils after clearance of trees
- Seasonal moisture movements
- The effects of frost action.

The settlement of a foundation on a saturated soil may be considered as consisting of three different types:

- The immediate, elastic, or initial settlement which occurs immediately upon load application, under conditions of no change in volume.
- The primary consolidation settlement which develops as the volume changes as a consequence of the dissipation of excess pore-water pressures.
- The secondary settlement, which is a creep phenomenon and occurs under conditions of practically zero excess pore-water pressure.

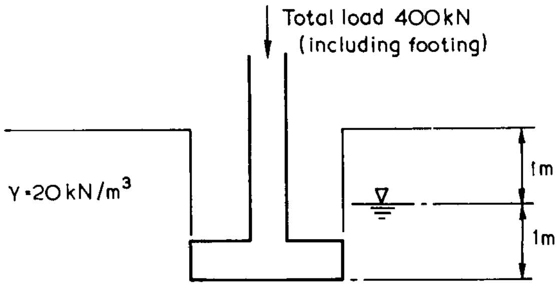

Fig.4.1 Example of gross and net pressures

The bearing capacity of a soil is related to shear failure in the ground. For foundations on clays, the undrained shear strength is usually the controlling factor, because clays are of low permeability and the construction of the structure generally occurs under undrained conditions. The clay will then consolidate with time, gain strength and so the bearing capacity will increase with time. The *end of construction* case is almost always critical. Granular soils are of high permeability, however, and by the end of construction, the drained condition has already been reached. The applied structural load, therefore, increases not only the shear stresses in the soil, but also the effective stresses and hence the strength. This is the main reason why sands and gravels have higher bearing capacities than clays.

It is vital to distinguish between gross and net foundation pressures. The *gross* foundation pressure, q, at foundation level is the total applied load divided by the area of the foundation. The *net* foundation pressure, q_n, (or the net loading intensity) is the net increase in pressure at foundation level, and is the pressure causing consolidation settlement, and shear failure in the soil.

Example

Determine the gross and net foundation pressures for the example shown in Fig.4.1. The initial total overburden pressure at foundation is

$$p_0 = 2 \times 20 = 40 \text{ kN/m}^2.$$

For simplicity it is assumed that the soil is fully saturated above the water table to the ground surface and hence the bulk unit weight is the same above and below the water table. The water table is the line where the water pressure equals atmospheric pressure and fine-grained soils can be fully saturated above the water table, the water being held by capillary tension.

The gross foundation pressure = q = 400/2 = 200 kN/m^2.

The net foundation pressure = $q_n = q - p_0$ = 200 − 40 = 160 kN/m^2. It can be seen that this is the net increase in effective stress at foundation level.

The final effective stress at foundation after dissipation of excess pore-water pressure is

$$p'_f = q - u = 200 - 10 = 190 \text{ kN/m}^2.$$

Since p'_0 = 30 kN/m^2, the net increase in effective stress at foundation level is 190 − 30 = 160 kN/m^2.

1.1 Various definitions

1.1.1 The ultimate bearing pressure, q_f, is the value of the bearing pressure at which the ground fails in shear.

1.1.2 The maximum safe bearing pressure, q_s, is the intensity of applied pressure that the soil will safely support without risk of a shear failure, irrespective of the settlement which may develop, that is

$$q_s = q_f/F$$

where F is the load factor, which generally varies from 1.75 to 3.0. A value of 1.75 would be chosen where there is considerable experience of the soil under consideration and where strict settlement criteria do not apply, and a figure of 3.0 would be taken where little is known of the field behaviour of the soil and where settlements must be kept to a minimum.

1.1.3 The allowable bearing pressure, q_a, is the allowed intensity of applied pressure, taking into account both bearing capacity and settlement.

In this chapter, methods of determining the *safe* bearing pressure (i.e. governed by the strength of the soil) of footings are outlined.

Charts for estimating the distribution of vertical stresses below a foundation are given in Chapter 3, together with procedures for estimating initial undrained settlements.

Settlement analysis is covered in Chapter 5.

2 Ultimate bearing capacity

The ultimate bearing capacity of a footing may be determined using bearing theory, whereby a failure mechanism is postulated and the pressure causing failure in the soil is expressed in terms of the shear strength mobilized at failure and the geometry of the problem. Several bearing capacity theories have been proposed and the one most commonly adopted for shallow footings is that of Terzaghi (1942).

By considering a strip footing, neglecting the strength of the soil above foundation level, Terzaghi arrived at the following solution for a strip footing for a soil having a cohesion intercept, c, and an angle of shearing resistance, ϕ.

$$q_f = c \,.\, N_c + \gamma \,.\, D \,.\, N_q + ½ \,.\, B \,.\, \gamma \,.\, N_\gamma \tag{4.1}$$

where N_c, N_q, N_γ are bearing capacity factors depending on the value of ϕ, and are reproduced in Fig.4.2. These factors are valid for strip footings and require to be adjusted for rectangular

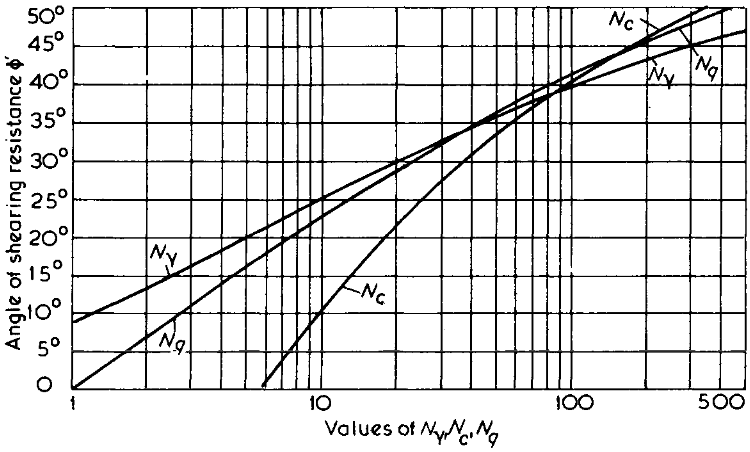

Fig.4.2 Bearing capacity factors, N_c, N_q, N_γ, *after Terzaghi (1943)*

and circular footings as follows:

Rectangular footings

$$N_c\, rect = N_c\, strip\,(1 + 0.2\,(B/L))$$

$$N_\gamma\, rect = N_\gamma\, strip\,(1 - 0.2\,(B/L))$$

$$N_q\, rect = N_q\, strip$$

Circular footings

$$N_c\, circle = 1.3 \times N_c\, strip$$

$$N_\gamma\, circle = 0.6 \times N_\gamma\, strip$$

$$N_q\, circle = N_q\, strip$$

In the form presented by Terzaghi, the bearing capacity solution can be applied strictly only to cases where the ground water table is deep; total stresses equal effective stresses everywhere and the shear stress parameters should be expressed in terms of effective stress.

The Terzaghi solution could also be applied to an undrained, total stress condition, using in this case, shear strength parameters in terms of total stress, c_u and ϕ_u.

For free draining soils, that is, the excess pore water pressures under the footing are zero at the end of load application, the bearing capacity equation is most usefully expressed as follows for the case of high ground water table:

$$q_f = c' \,.\, N_c + p' \,.\, (N_q - 1) + \tfrac{1}{2} \,.\, B \,.\, \gamma' \,.\, N_\gamma + p \tag{4.2}$$

where p' = initial effective overburden pressure at foundation level, p = initial total overburden pressure at foundation level, and γ' = submerged unit weight.

If the ground water table is low then the equation can be written:

$$q_f = c' \,.\, N_c + p(N_q - 1) + \tfrac{1}{2}B\gamma \,.\, N_\gamma + p \tag{4.3}$$

When using the bearing capacity equation to solve a problem in practice, it is necessary to consider whether the material is so permeable that the excess pore pressures dissipate immediately the load is applied, that is, consolidation and gain in strength are complete at the end of the construction period, or whether the permeability is so low that very little pore pressure dissipation occurs during construction, no gain in soil strength can be relied upon and the condition is essentially undrained. The first possibility will apply to sands and gravels and can be analysed using a drained analysis in terms of effective stress; and the second applies to clays and can be analysed using an undrained analysis in terms of total stress. Of course, with time, a clay under load will consolidate and gain in strength and the long-term bearing capacity will, in general, be greater than the short-term undrained bearing capacity, and if necessary could be determined from an effective stress analysis. Examples are given below.

Granular soils

Consider a strip loading applied at a depth D below the surface of a sand deposit with the ground water table at the ground surface. Equation 4.2 can then be written as follows:

$$q_f = p'(N_q - 1) + \tfrac{1}{2} \,.\, B \,.\, \gamma' \,.\, N_\gamma + p \tag{4.4}$$

The following points should be noted:

- The ultimate bearing pressure, q_f, depends on the initial effective overburden pressure, p', at foundation level; for a greater depth of footing or if ground water is absent (both increasing p'), then q_f will be increased.
- q_f depends on the submerged unit weight, γ'. If the ground water table is deep, greater than for example, 2 B, below the foundation level and will always remain below that depth, then the bulk unit weight, γ, can be inserted instead of γ', resulting in increased bearing capacity.
- q_f is very sensitive to ϕ', particularly for large values of ϕ'; small increases in ϕ' will lead to large increases in N_q and N_γ and hence to large increases in q_f. For this reason, caution must be exercised when estimating the value of ϕ' to be inserted in equation (4.4).

Example

Consider a strip footing 2 m wide founded at a depth of 1.5 m below the surface of a dense sand with $\phi' = 42°$. The ground water table is at foundation level, and $\gamma = 20$ kN/m^3 and $\gamma' =$ 10 kN/m^3, see Fig.4.3. Determine the safe bearing pressure for $\phi' = 42°$, $N_\gamma = 140$ and $N_q = 110$, from Fig.4.2,

$$q_f = 1.5 \times 20(110 - 1) + ½ \times 2 \times 10 \times 140 + 1.5 \times 20$$

$$= 4700 \text{ kN/m}^2$$

Applying a load factor of two to determine the working load

$$q_s = 2350 \text{ kN/m}^2.$$

If, at a particular location along the strip footing, the sand is locally a little looser, with an angle of shearing resistance 10% less than the 42° used in the calculations, i.e. 37.8°, what is the load factor for the design loading of 2105 kN/m^2? For $\phi' = 37.8°$, $N_\gamma = 75$, $N_q = 63$, from Fig.4.2,

$$q_f = 1.5 \times 20 \times (63 - 1) + ½ \times 2 \,.\, 10 \times 75 + 1.5 \times 20$$

$$= 2640 \text{ kN/m}^2$$

The load factor is therefore

$$\frac{2640}{2350} = 1.12$$

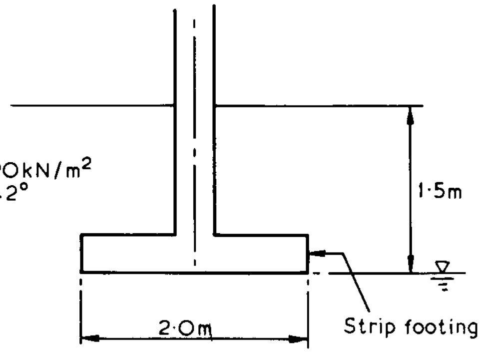

Fig.4.3 Example of bearing capacity calculation

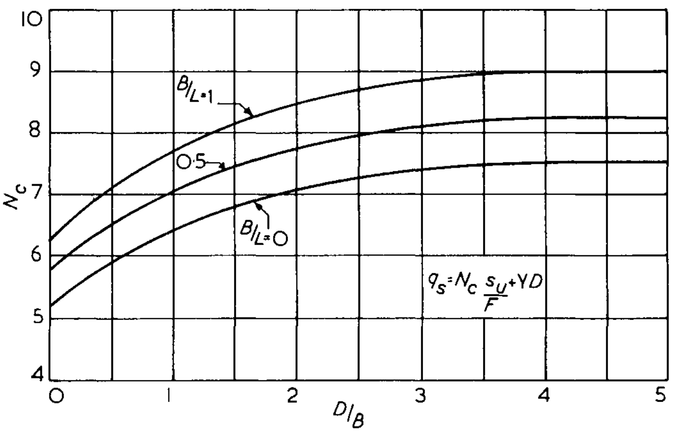

Fig. 4.4 Bearing capacity factor, N_c, for undrained analysis, after Skempton (1951)

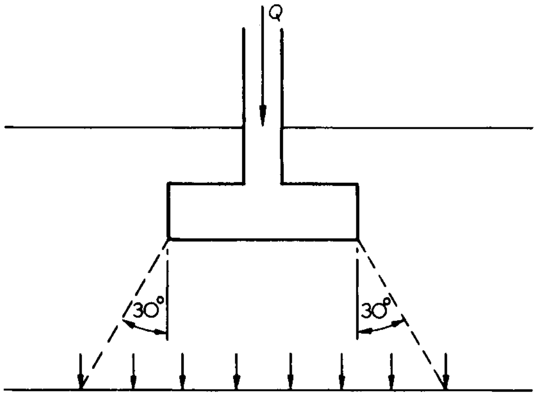

Fig. 4.5 Spread of load onto underlying layer

This example is somewhat artificial but has been chosen to illustrate two main points:

- For most footings on granular materials, the bearing pressure is extremely high in terms of bearing capacity, so that the allowed bearing pressure in a practical problem is determined by consideration of *settlement*, rather than strength. The only possible exception to this statement would be a very narrow foundation, founded just below the surface of a loose sand with a very high ground water table.
- In bearing capacity calculations, the load factor is by no means equal to the factor of safety on shear strength. The example shows that even if a load factor of two is adopted, soil failure can be approached if the shearing resistance is only 10% less than that used in the design calculation. Since difficulties lie in assessing correctly soil strength, a more practical and safer approach is to place a factor of safety on the shear strength of the soil and to use the factored strength in bearing capacity calculations to obtain safe bearing pressures. This point is also particularly relevant when making passive earth pressure calculations, particularly for high values of shearing resistance and wall friction.

Example

Consider the end of construction stability of a saturated clay owing to foundation loading. This is the undrained condition and the problem is analysed in terms of total stress, taking $\phi = 0$.

Equation 4.2 can be written as follows:

$$q_f = c \, . \, N_c + p \tag{4.5}$$

or

$$q_f = s_u \, . \, N_c + \gamma D$$

where s_u = undrained shear strength, γ = bulk unit weight, D = depth of footing below ground surface, and N_c = bearing capacity factor depending only on the geometry, and is given in Fig.4.4. The ultimate bearing capacity is independent of the breadth, B.

In many practical cases, the undrained shear strength varies with depth below a foundation, and in this case, the average value of s_u should be taken over a depth below foundation level equal to 2/3 B, provided the shear strength of any layer does not depart from the average strength by more than ±50%. If a softer layer is present under a foundation, its effect can be assessed by assuming a spread of load from the foundation down to the surface of the softer material, as shown in Fig.4.5, and then carrying out a bearing capacity calculation in the usual way.

A particular problem which must be treated with caution is the case of an oil tank on a soft clay deposit. Because of the flexibility of the base, it is possible for a local failure to occur, for example, a strip near the edge. In such cases, the shear strength must not be averaged over a depth equal to 2/3 of the tank diameter. Local failure must be considered and trial strips analysed until a minimum factor of safety is obtained. The procedure is indicated in Fig.4.6.

A classic paper covering the failure of an oil tank in detail has been published by Bjerrum and Øverland (1957). By back-analysing the failure of an oil tank at Frederikstad the authors found that the minimum calculated factor of safety against a local failure was 1.05, while a value of 1.72 was found for an overall failure of the tank.

2.1 Eccentric loading

Meyerhof (1953) has shown that, as a reasonably good approximation, the influence of an eccentric load with eccentricity, e, measured from the axis of symmetry of a foundation of width B, can be accounted for by using a reduced width, B', in the bearing capacity calculations, where

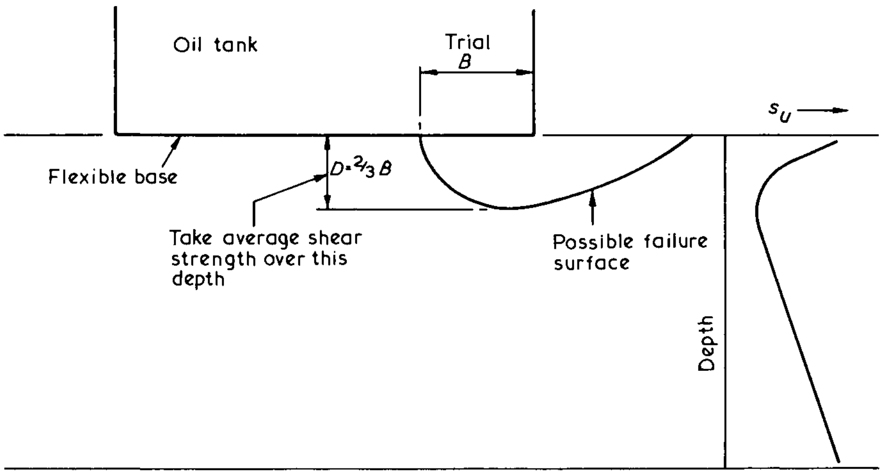

Fig.4.6 Bearing capacity calculations for an oil tank, after Bjerrum and Øverland (1957)

Table 4.1 λ factor for inclined loading bearing capacity calculations, after Brinch Hansen (1955)

$\tan\phi'/F$	0	0.2	0.4	0.6	0.8	1.0
λ	1.4	1.8	2.3	2.8	3.3	3.9

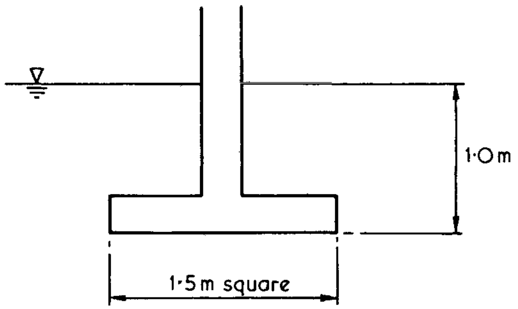

Fig.4.7 Example of short term and long term bearing capacity calculations

$$B' = B - 2e \tag{4.6}$$

and then considering the loading to be symmetrical.

2.2 Inclined loading

For the case of inclined loading, with a vertical component P_v and an horizontal component P_h, Brinch Hansen (1955) proposed operating with an equivalent vertical applied foundation pressure, q_e, where

$$q_e = \frac{P_v + \lambda \, . \, P_h}{A} \tag{4.7}$$

where A = area of the base and λ = dimensionless constant depending on the angle of shearing resistance. Values of λ are given in Table 4.1.

Example

Determine the short-term, undrained, and the long-term, fully drained bearing capacities of the square footing shown in Fig.4.7. Short term condition:

$s_u = 70$ kN/m^2, $\phi_u = 0$

$\gamma = 20$ kN/m^3

$N_c = 7.2$ (Fig.4.4 for $D/B = 0.67$)

$q_f = s_u \, . \, N_c + \gamma D = 70 \times 7.2 + 20 \times 1 = 524$ kN/m^2

Long term condition:

$c' = 10$ kN/m^2, $\phi' = 30°$

$\gamma = 20$ kN/m^3, $\gamma' = 10$ kN/m^3

$N_c = 36 \times (1 + 0.2) = 43.2$

$N_q = 22 \times 1 = 22$

$N_\gamma = 20 \times (1 - 0.2) = 16$

Values of N_c, N_q, and N_γ from Fig.4.2, and adjusted for the square footing.

$$q_f = c' . N_c + p' . (N_q - 1) + ½ . B . \gamma' . N_\gamma + p$$

$$= 10 \times 43.2 + 1 \times 10 \times 21 + ½ \times 1.5 \times 10 \times 16 + 1 \times 20$$

$$= 702 \text{ kN/m}^2$$

This calculation merely confirms that, in general, the long-term bearing capacity of a clay foundation after consolidation is greater than the short-term bearing capacity. Possible exceptions to this general proposition are:

- Where lateral dissipation of excess pore-water pressure from under a large loaded area e.g. an oil tank or an embankment, may give rise to increases in pore pressure outside the loaded area, reaching a critical value some time after the end of construction
- In a thick clay deposit where a decrease in the undrained shear strength with time (Chapter 2) may be greater than the gain in strength because of consolidation near the drainage boundaries.

Example

Design a strip footing to carry the loading system, shown in Fig.4.8, in a saturated clay.

Data:

Minimum depth of footing	= 1 m
Undrained shear strength	= 100 kN/m^2
Required factor of safety	= 2
Bulk unit weight	= 20 kN/m^3
Eccentricity	= 0.2 m
Vertical component, P_v	= 400 kN/m
Horizontal component, P_h	= 75 kN/m

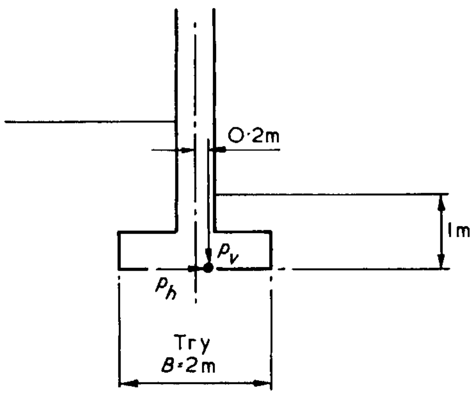

Fig.4.8 Example of bearing capacity calculations for inclined and eccentric loading

Table 4.2 Approximate allowable bearing values, after CP 2004:1972

Group	Types of rocks and soils	Approximate bearing value (kN/m^2)	Remarks
1 Rocks	Hard igneous and gneissic rocks in sound condition	10 000	These values are based on the assumption that the foundations are carried down to unweathered rock
	Hard limestones and hard sandstones	4 000	
	Schists and slates	3 000	
	Hard shales, hard mudstones and soft sandstones	2 000	
	Soft shales and soft mudstones	600 to 1000	
	Hard sound chalk, soft limestone	600	
	Thinly bedded limestones, sandstones, shales)	To be assessed after inspection	
	Heavily shattered rocks)		
2 Non-cohesive soils	Compact gravel, or compact sand and gravel	>600	Width of foundation (B) not less than 1 m. Ground water level assumed to be a depth not less than B below the base of the foundation
	Medium dense gravel, or medium dense sand and gravel	200 to 600	
	Loose gravel, or loose sand and gravel	<200	
	Compact sand	>300	
	Medium dense sand	100 to 300	
	Loose sand	<100	
3 Cohesive soils	Very stiff boulder clays and hard clays	300 to 600	Group 3 is susceptible to long-term consolidation settlement
	Stiff clays	150 to 300	
	Firm clays	75 to 150	
	Soft clays and silts	<75	
	Very soft clays and silts	Not applicable	

Calculation:

$B' = B - 2e = 2 - 2 \times 0.2 = 1.6$ m

$N_c = 6.0$ (for $D/B = (1.0/1.6) = 0.625$, Fig.4.4)

Safe foundation pressure $= N_c \,.\, s_u/F + \gamma D$

$$= \frac{6.0 \times 100}{2} + 20 \times 1$$

$$= 320 \text{ kN/m}^2$$

Equivalent applied pressure $= \dfrac{P_v + \lambda \,.\, P_h}{A}$ (λ from Table 4.1)

$$= \frac{400 + 1.4 \times 75}{1.6 \times 1}$$

$$= 316 \text{ kN/m}^2.$$

This is satisfactory.

The resistance to sliding along the base may be assessed as follows, neglecting the passive resistance of the soil which may be affected by softening, etc.

Sliding resistance = base area × adhesion between base and clay

$= 2 \times 1 \times 100 \times 0.75$

$= 150$ kN

This assumes that the adhesion between the underside of the base and the clay is 0.75 times the undrained shear strength. For further discussion on adhesion between clay and concrete, see Chapter 6.

Factor of safety against sliding = 150/75 = 2. This is satisfactory.

2.3 Side adhesion for footings in clay

Additional support to a footing at depth in clay may be obtained from side adhesion of the clay to the foundation. Particular care must be taken when making an allowance for tension or shrinkage cracks. Because of the difficulty of estimating the depth of such cracks, side adhesion is generally neglected for shallow foundations.

In the case of a bridge pier, for example, extending deep into a clay layer, a considerable contribution to the load-carrying capacity will derive from side adhesion and this should be allowed for in design. The problem is similar to the design of a large diameter pile which is considered in Chapter 6.

2.4 Allowable bearing pressures

Approximate allowable bearing pressures, for preliminary design only, are given in Table 4.2, taken from CP 2004:1972.

5 Settlement analysis

1 Introduction

This chapter deals with the prediction of the settlement of structures, and concentrates on factors affecting significantly the accuracy of such predictions.

Initial, undrained settlement has been covered in Chapter 3, and settlements related to volume change are discussed below.

There may be a temptation to believe that settlement prediction has become an exact science, because of the advances that have been made in recent years, and the availability of the powerful finite element method of analysis. This is not true and the following quotation, Terzaghi (1936), is particularly relevant and valid.

'Whoever expects from soil mechanics a set of simple, hard-and-fast rules for settlement computation will be deeply disappointed. He might as well expect a simple rule for constructing a geological profile from a single test boring record. The nature of the problem strictly precludes the possibility of establishing such rules. If a supervising or construction engineer wants to enjoy the benefits of recent developments in this field he should first of all study the rules for securing reliable settlement records, and then start to observe the buildings of his district. After he has done this for a certain period he will discover for himself the value of the information which he can obtain from soil mechanics.'

2 Consolidation settlements of clays

It should be made clear that although initial, primary consolidation and secondary settlements are discussed separately, this does not imply that they are separate components taking place at different times. The settlement at the end of construction is sometimes taken as being equal to the initial settlement but, even if the construction period is short, this will include some part of the primary consolidation settlement. Secondary settlement also, considered to be the settlement occurring after changes in effective stress have taken place, will also develop during the primary consolidation period as the pore-water pressure dissipates and the effective stresses increase.

2.1 Terzaghi's theory of consolidation

The process of consolidation is illustrated by the piston and spring analogy shown in Fig.5.1. At the instant the load is applied, because the system is not allowed to drain, the spring cannot deform and the loading is carried by the excess pore-water pressure. If, now, slow drainage is allowed, water will leak out and the load will be transferred from the water to the spring until finally, after sufficient time has elapsed and the spring has deformed sufficiently to carry the applied loading, the deformation ceases and the excess pore-water pressure is zero. In the corresponding soil element, the spring is replaced by the soil structure, and the rate of water expulsion is governed by the permeability of the soil and the length of the drainage path.

It is necessary, then, to calculate both the magnitude and the rate of the consolidation settlement and in practice, use is generally made of the Terzaghi theory of one-dimensional consolidation, which considers the situation shown in Fig.5.2.

The main assumptions on which the theory is based are:

- The soil is saturated
- The water and the clay particles are incompressible
- D'arcy's law is valid
- For a change in voids ratio corresponding to a given increment in effective stress, the permeability, k, and the coefficient of volume change, m_v, remain constant
- The time taken for the clay to consolidate depends entirely on the permeability of the clay
- The clay is laterally confined
- The flow of water is one-dimensional
- Effective and total stresses are uniformly distributed over any horizontal section.

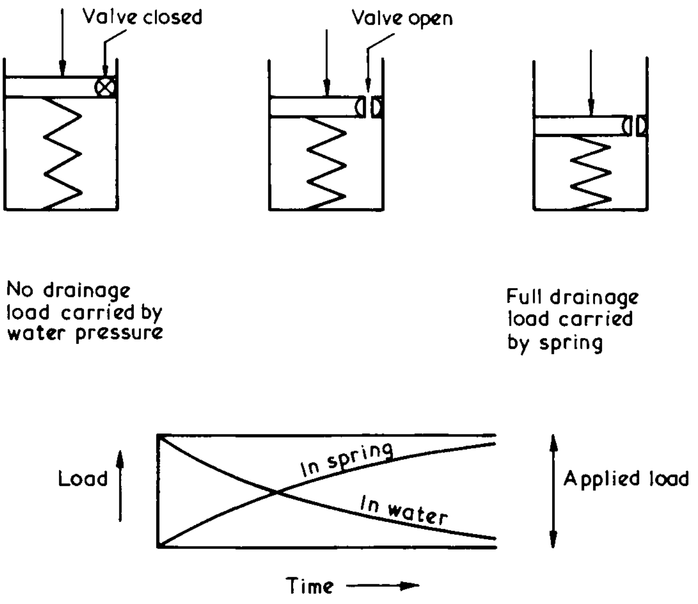

Fig.5.1 Piston and spring analogy

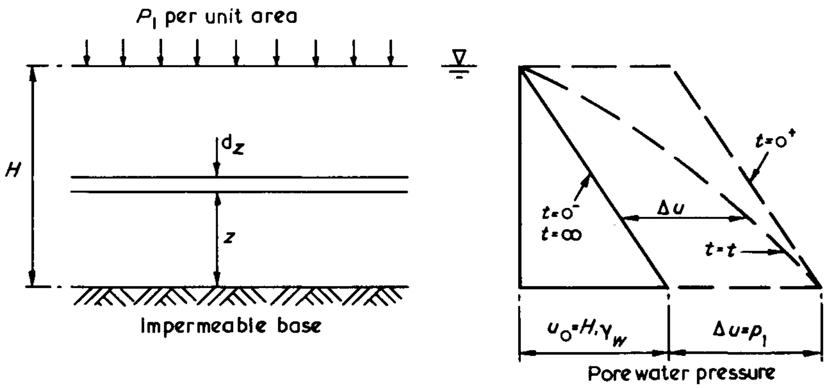

Fig.5.2 Key figure for one-dimensional consolidation

These assumptions correspond to the oedometer test in the laboratory and to a clay layer in the field subjected to uniform global loading, that is, a uniformly distributed loading applied over an infinite area.

Based on these assumptions, the governing differential equation relating excess pore-water pressure, position and time can be derived as

$$\frac{\partial u}{\partial t} = c_v \cdot \frac{\partial^2 u}{\partial z^2} \tag{5.1}$$

where

$$c_v = \frac{k}{m_v \gamma_w} = \text{coefficient of consolidation}$$

and

$$m_v = \frac{\Delta V}{V} / \Delta p$$

$$= \frac{\Delta H}{H} / \Delta p = \text{coefficient of volume compressibility.}$$

Equation 5.1 must be solved for the following boundary conditions:

$\Delta u = p_1$ for $t = 0$ and $0 \leqslant z \leqslant H$

$\Delta u = 0$ for $t > 0$ and $z = \mathrm{H}$

$\Delta u = 0$ for $t = \infty$ and $0 \leqslant z \leqslant H$

The solution may be expressed in the form:

$$\Delta u = \frac{4p_1}{\pi} \sum_{N=0}^{N=\infty} \frac{(-1)^N}{2N+1} \cdot \mathrm{e}^{-(2N+1)^2 \cdot \pi^2 (T_v/4)} \cdot \cos\left[\frac{(2N+1)\pi z}{2H}\right] \tag{5.2}$$

where

$$T_v = \frac{c_v \cdot t}{H^2} \, ,$$

an independent dimensionless variable known as the *time factor.*

It follows that the degree of consolidation, $\bar{U}$, at any time (equal to the settlement at that time, δ_t, expressed as a percentage of the total final settlement, δ_c, at the end of consolidation) is given by:

$$\bar{U} = \frac{\delta_t}{\delta_c} = 1 - \frac{8}{\pi^2} \sum_{N=0}^{N=\infty} \frac{1}{(2N+1)^2} \cdot \mathrm{e}^{-(2N+1)^2 \cdot \pi^2 T_v/4} \tag{5.3}$$

Solutions relating $\bar{U}$ and T_v for various distributions of initial excess pore-water pressure, and single and double drainage are given in Fig.5.3. Using these solutions, it should be noted that the total thickness of the consolidating layer is always used in the computations. The solution relating $\bar{U}$ and T_v is then taken, corresponding to the drainage conditions of the particular problem.

2.2 Further points on consolidation

2.2.1.

A typical relationship between voids ratio and effective pressure is shown on Fig.5.4(a) and between voids ratio and the logarithm of effective pressure on Fig.5.4(b).

2.2.2.

The final consolidation settlement can be calculated using any of the following expressions:

$$\delta_c = \frac{\Delta e}{1 + e_0} \, . \, H \tag{5.4}$$

$$\delta_c = m_v \, . \, H \, . \, \Delta p \tag{5.5}$$

$$\delta_c = \frac{C_c}{1 + e_0} \, . \, H \, . \, \log_{10} \frac{p'_o + \Delta p}{p'_o} \tag{5.6}$$

where C_c = compression index and is the slope of the $e - \log p'$ line.

It is convenient to use C_c when dealing with normally consolidated clays and m_v for over-consolidated clays.

2.2.3.

It can be seen from Fig.5.4 that the settlement for a given load increment is much greater for a normally consolidated clay than for an over-consolidated clay. It is vital therefore to determine whether or not a clay is over-consolidated. This can be determined from:

- A knowledge of the geological history of the clay, that is, whether previous overburden has been removed or the ground water table is now higher than in the past,
- The Casagrande construction, illustrated in Fig.5.5, which gives the pre-consolidation pressure p'_c, (the greatest effective pressure the clay has carried in the past). If $p'_c > p'_o$, the clay is over-consolidated. If $p'_c = p'_o$, the clay is normally consolidated,
- Comparing the measured undrained shear strength with that to be expected for a normally consolidated clay having a similar plasticity index, see Fig.2.17. If the measured strength is greater than that anticipated for a normally consolidated clay the clay is probably over-consolidated,
- Comparing C_c corresponding to p'_o with the value predicted for a normally consolidated clay, $C_c = 0.009$ (LL-10). If C_c at p'_o is less than that expected for a normally consolidated clay, the clay is probably over-consolidated,
- A determination of the liquidity index (LI), of the clay where

  $$\mathrm{LI} = \frac{w_c - \mathrm{PL}}{\mathrm{LL} - \mathrm{PL}}$$

  and LL is the liquid limit and PL is the plastic limit, determined according to BS 1377. Normally consolidated clays have a liquidity index varying from about 0.6 to 1.0, and over-consolidated clays have a liquidity index varying from 0 to about 0.6. This gives a rough guide only.

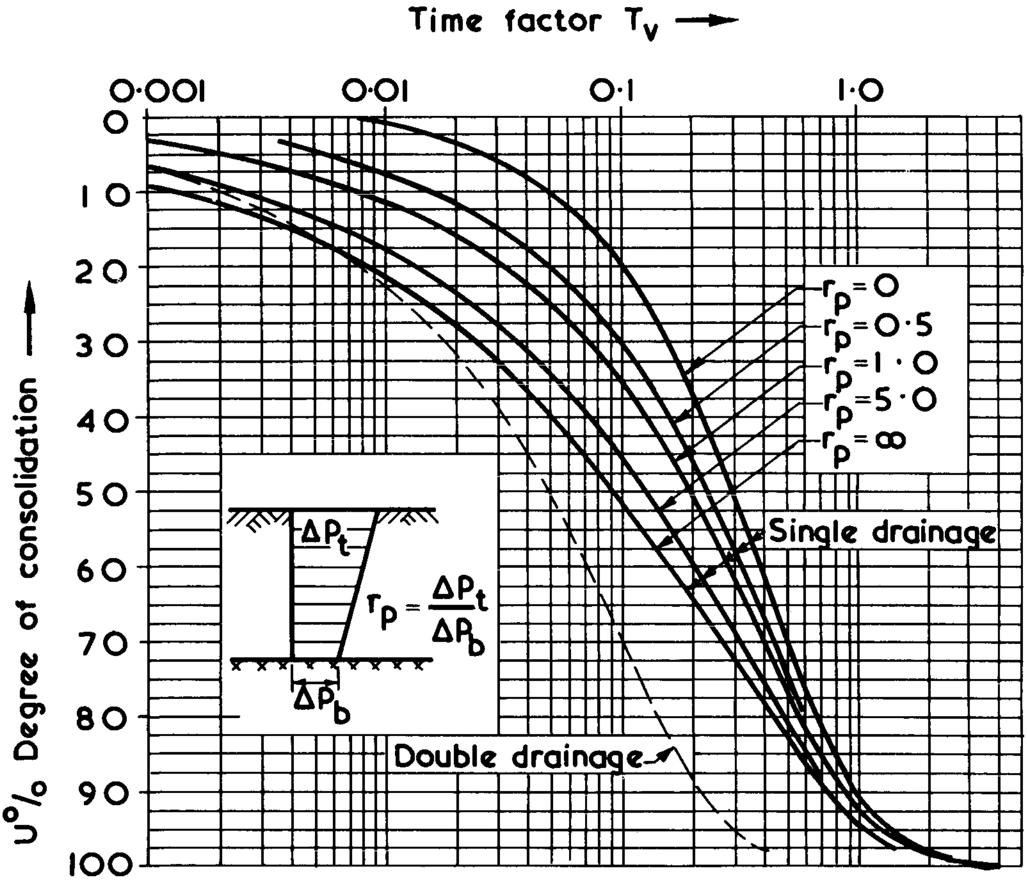

Fig.5.3 Relationship between degree of consolidation and time factor, after Janbu, Bjerrum and Kjaernsli (1956)

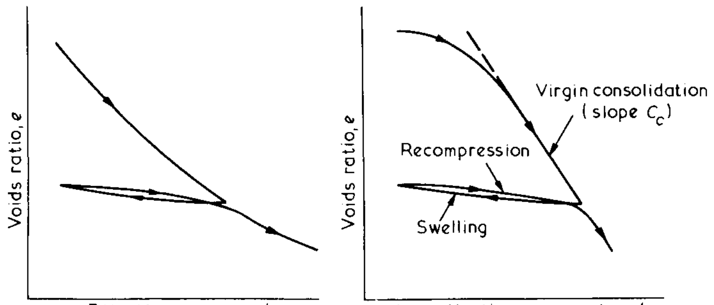

Fig.5.4 (a) Relationship between voids ratio and effective pressure; (b) relationship between voids ratio and the logarithm of effective pressure

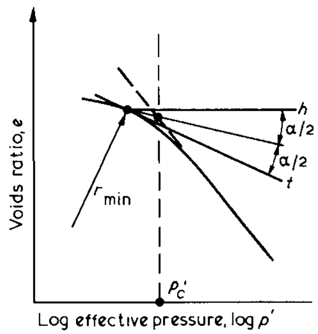

Fig.5.5 Construction for determining the preconsolidation pressure, p'_c, after Casagrande (1936)

2.2.4.

The coefficient of consolidation is calculated using either the square root of time plot or the logarithm of time plot; the procedures are illustrated in Fig.5.6.

2.2.5.

It is important, particularly for stiff clays having low compressibilities, to correct the measured compressibility for the initial compression in the oedometer, otherwise values very much on the high side may result, that is, the deformation ($d_o - d_s$) must be excluded when determining m_v; d_o is the corrected zero reading and d_s is the observed initial reading.

2.3 Example of settlement calculation

The problem is to calculate the total primary consolidation settlement for the example shown in Fig.5.7, and to determine the time for 50% and 90% of this settlement to develop.

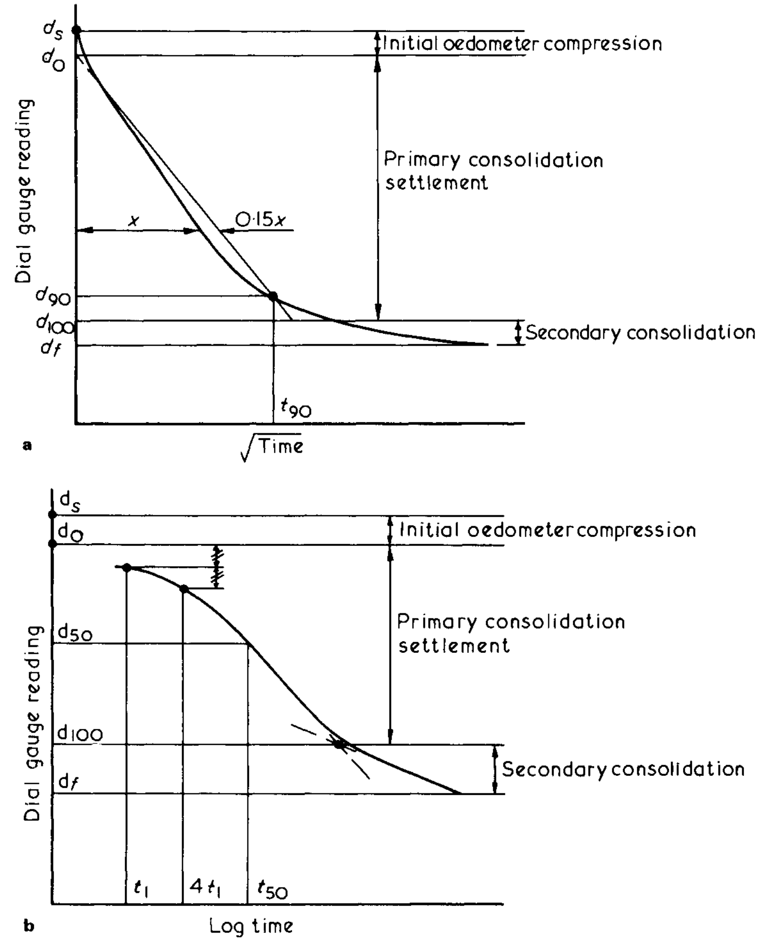

Fig.5.6 Determination of the coefficient of consolidation, c_v; (a) square root of time method, $c_v = T_{90} . H^2/t_{90} = 0.212\ H^2/t_{90}$ (H = sample thickness); (b) logarithm of time method, $c_v = T_{50} . H^2/t_{50} = 0.0492\ H^2/t_{50}$ (H = sample thickness)

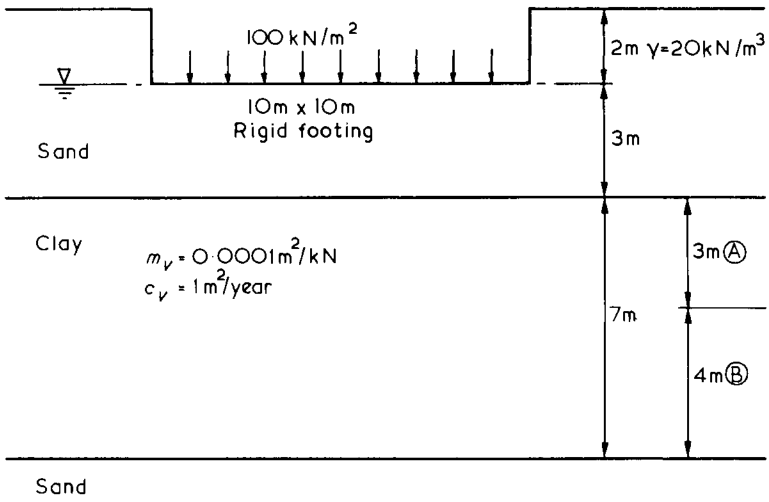

Fig.5.7 Example of calculation of primary consolidation settlement

Table 5.1 Observed vertical movements of compensated foundations, after Bjerrum and Eide (1966)

Structure	Date completed	Undrained shear strength (kN/m^2)	Net foundation pressure (kN/m^2)	Heave (mm)	Total settlement (mm)
Håndverk Industri, Drammen	1958	7–15	1	26	34
Werringgården, Drammen	1956	6–15	0	29	30
Norløff, Drammen	1955	6–15	0	–	c.30
Park Hotel, Drammen	1961	10–15	0	–	40
Idunbygg, Drammen	1963	30	0–5	–	45

For the purposes of settlement calculation, the clay will be subdivided into two layers, *A* and *B*, of thickness 3 m and 4 m respectively.

The net increase in foundation stress at foundation level is $100 - 2 \times 20 = 60$ kN/m². The net increase in vertical stress under the centre of *layer A* = $60 \times 0.75 = 45$ kN/m² (for z/B = 4.5/10, Fig.3.3) and *layer B* = $60 \times 0.46 = 27.6$ kN/m² (for $z/B = 8/10$, Fig.3.3)

$$\delta_c = m_v \, . \, H_A \, . \, \Delta\sigma_A + m_v \, . \, H_B \, . \, \Delta\sigma_B \text{ (equation 5.5)}$$

$$= (0.0001 \times 3000 \times 45 + 0.0001 \times 4000 \times 27.6) \text{ mm}$$

$$= (13.5 + 11.0) \text{ mm} = 24.5 \text{ mm}$$

Making an allowance for the rigidity of the footing by taking a rigidity factor of 0.8, the total consolidation settlement of the rigid footing is $0.8 \times 24.5 = 19.6$ mm.

For $U = 50\%$, $T_v = 0.049$, from Fig.5.3 therefore $t_{50} = (0.049 \times 7^2)/1 = 2.4$ years.

For $U = 90\%$, $T_v = 0.21$, from Fig.5.3 therefore $t_{90} = (0.21 \times 7^2)/1 = 10.3$ years.

3 Prediction of primary consolidation settlement

Prediction of the magnitude and rate of the primary consolidation settlement of saturated clay strata was first made possible by Terzaghi about 50 years ago when the theory of one-dimensional consolidation was developed. In addition, an oedometer was designed which allowed the determination of the parameters, c_v and m_v or C_c, necessary for the calculation procedure.

Considerable progress has been made in refining the computation process, and the authors have attempted to isolate some of the factors of particular importance which influence the accuracy of settlement predictions.

3.1 Net increase in stress

Consolidation settlement calculations are based on the assumption that the settlement is a function of the *net* increase in foundation pressure; if this net increase is zero, it is assumed that the consolidation settlement will be zero. The view has been expressed that, because the changes in pore-water pressure for equal unloading and loading stages may well be different (Bishop and Henkel, 1953), it is possible that residual pore-water pressures could be set up owing to an unloading and reloading cycle, particularly in cases when the factor of safety against a bottom heave failure during excavation is small, which is very often the case. It appears, however, that there is a considerable body of evidence to show that only very small settlements are experienced with fully floating foundations (Casagrande and Fadum, 1942; Aldrich, 1952; Bjerrum, 1964; Golder, 1965; Bjerrum and Eide, 1966; Bjerrum, 1967; D'Appolonia and Lambe, 1971). The data given by Bjerrum and Eide (1966) are summarized in Table 5.1.

It can be seen that the settlement during reloading was approximately equal to the heave. In addition, it was noted that the settlements terminated a short time after the end of construction. It can therefore be concluded that it is satisfactory to perform consolidation settlement calculations based on net increases in foundation pressure only.

3.2 Sample disturbance

The importance of sample disturbance has been recognized for many years, for example, Terzaghi, 1941; Rutledge, 1944; Schmertmann, 1953 and 1955; and procedures have been suggested to correct laboratory stress–strain relationships for such disturbance. For normally consolidated clays, sample disturbance will lead to measured oedometer compressibilities which are too low, while for over-consolidated clays, the measured compressibilities may be too high.

Bjerrum (1967) pointed out that the measurement of the preconsolidation pressure was particularly sensitive to sample disturbance and that only the highest standards of sampling and laboratory technique would result in consistent and reliable determinations.

Berre, Schjetne and Sollie (1969) compared values of $C_c/(1 + e_o)$ and p'_c/p'_o obtained from a new 95 mm piston sampler and from the 54 mm piston sampler (itself a very high quality instrument) which has been in use for many years. They found more scatter in the results from the 54 mm sampler, and, in addition, the average value of p'_c/p'_o derived from the 95 mm sampler was some 5% higher than that obtained from the smaller tube. In addition, they noted that chemical changes may take place in a clay if stored for several months in steel sampling tubes, and that these changes could well alter the geotechnical properties of the soil.

Bjerrum (1973) noted that several types of soft and sensitive clays at very small strain show a critical shear stress which in many cases governs their behaviour. This small strain behaviour is destroyed if the clay is subjected to even relatively small strains either during the sampling operations or during handling in the laboratory. Furthermore, sample disturbance leading to redistribution of moisture content, may lead to significant errors in measured parameters.

A method of correcting an e-$\log p'$ curve for sample disturbance is shown in Fig.5.8 (Schmertmann, 1953).

Considering first a normally consolidated clay, the correction for sample disturbance is outlined on Fig.5.8(a). The straight line through e_o, p'_o intersecting the straight line portion of the

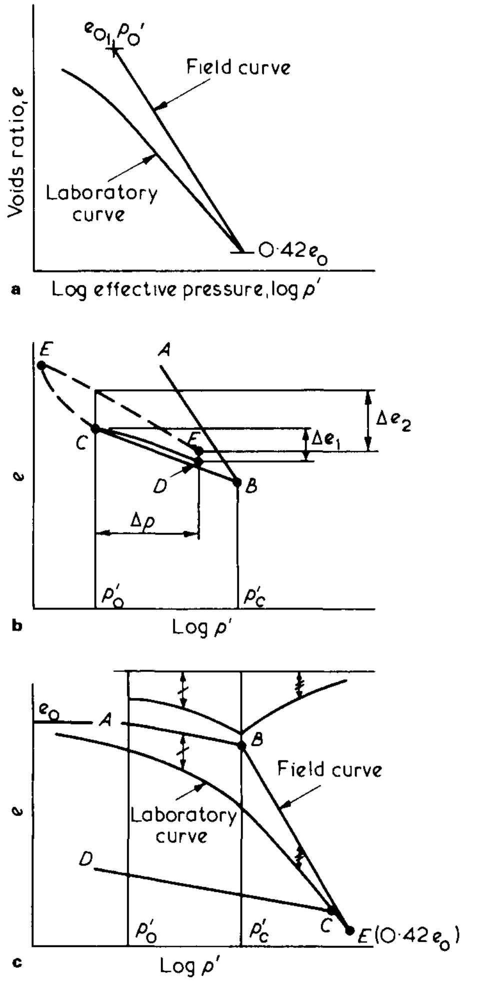

Fig.5.8 Correction of voids ratio–log effective pressure curve for sample disturbance, after Schmertmann (1953)

laboratory curve at $e = 0.42\ e_o$ is taken as representing the field relationship between voids ratio and log pressure. It should be noted that if the correction for sample disturbance is not made, then the calculated settlements would underestimate the true field settlement.

If the clay is over-consolidated, however, a different situation exists. Referring to Fig.5.8(b), allow a clay to first be consolidated to a higher pressure p_c', point B, and then as a consequence of the removal of glaciers or surface erosion, for example, let it swell to a smaller pressure, p_o', point C which represents the condition of the over-consolidated soil in the field. If a loading of Δp is applied to the soil in the field, it will consolidate along the full line curve to point D, and the change in void ratio will be Δe_1. If the soil is sampled at C, and a standard oedometer test carried out, the sample will swell to point E under the first loading increment in the oedometer and then consolidate along line EF. If this curve is used to predict settlement, the change in voids ratio will be Δe_2, which is greater than Δe_1, and thus the field settlement will be over-estimated. A better test procedure, which should be applied to all clays, either normally consolidated or over-consolidated, is not to add water to the sample until the applied loading is approximately equal to p_o'. Care must be taken, however, to ensure that the sample cannot dry out. Even if this procedure is followed, it will still be necessary to correct for sample disturbance, and Schmertmann's procedure is as follows, (referring to Fig.5.8(c)):

- Plot (e_o, p'_o), point A
- Determine p'_c, the maximum pre-consolidation pressure
- Through A draw a straight line AB parallel to the rebound curve, CD, to intersect the vertical line through p'_c at B
- Through B draw a straight line BE to intersect the straight line portion of the laboratory curve at E, where $e = 0.42\ e_o$.

The curve ABE then represents the field relationship between voids ratio and pressure.

The determination of p'_c is clearly of great importance and Schmertmann has suggested that the use of 'voids ratio reduction patterns' gives a more precise estimate of p'_c than the Casagrande construction. A voids ratio reduction pattern is simply the difference in voids ratio between the laboratory curve and any estimate field curve plotted against log pressure. Evidence suggests that the voids ratio reduction pattern is symmetrical about p'_c. Various values for p'_c are assumed, the *field* curves are constructed, and the value which gives the most symmetrical voids ratio reduction pattern is most probably the correct field pre-consolidation pressure.

In his paper, Schmertmann (1953) shows, first, that for good undisturbed samples, the slope of the e-log p' curve in the range of over-consolidation is approximately equal to the slope of the rebound curve, and this has often been confirmed in the laboratory. Second, the slope of the rebound curve is not very sensitive to the amount of sample disturbance. These two factors form the basis of Schmertmann's construction.

There can be no doubt that high standards of sampling and testing must be adopted if reliable settlement predictions are to be obtained.

3.3 Induced pore-water pressures under a structure

A most important contribution to settlement analysis was made by Skempton and Bjerrum (1957) who pointed out that an element of soil underneath a foundation undergoes lateral deformation as a result of applied loading and that the induced pore-water pressure is, in general, less than the increment in vertical stress on the element, because it is dependent on the A value. The consolidation of a clay results from the dissipation of pore-water pressure. But a given set of stresses will set up different pore-water pressures in different clays, if the A values are different. Thus two identical foundations carrying identical loads, resting on two clays with identical compressibilities, will experience different consolidation settlement if the A values of the clay are unequal. This is true despite the fact that no difference would be seen in oedometer test results. For the special case of the oedometer test, however, where the sample is laterally confined, then, irrespective of the A value, the pore-water pressure set up is equal to the increment in vertical stress (Simons and Menzies, 1974). Skempton and Bjerrum (1957) proposed that a correction factor should be applied to the settlement, calculated on the basis of oedometer tests and showed that the factor was a function of the geometry of the problem and the A value, the smaller the A value, the smaller the correction factor. The factor μ is shown in Fig.5.9 and the field settlement is then equal to μ times the settlement calculated on the basis of oedometer tests (see equation 5.14).

For heavily over-consolidated clays, A values less than 1 would be expected and the Skempton–Bjerrum correction factor is usually applied in such cases. It should be noted that in the working range of stress for normally consolidated clays, particularly when there is no question of over-stressing occurring, A values less than 1 can arise, and the correction factor should then be applied.

3.4 Stress path settlement analysis

As discussed above, Skempton and Bjerrum (1957) recognized that an element of soil underneath a foundation undergoes lateral deformation as a result of applied foundation loading and that the subsequent consolidation would be a function of the excess pore-water pressures set up

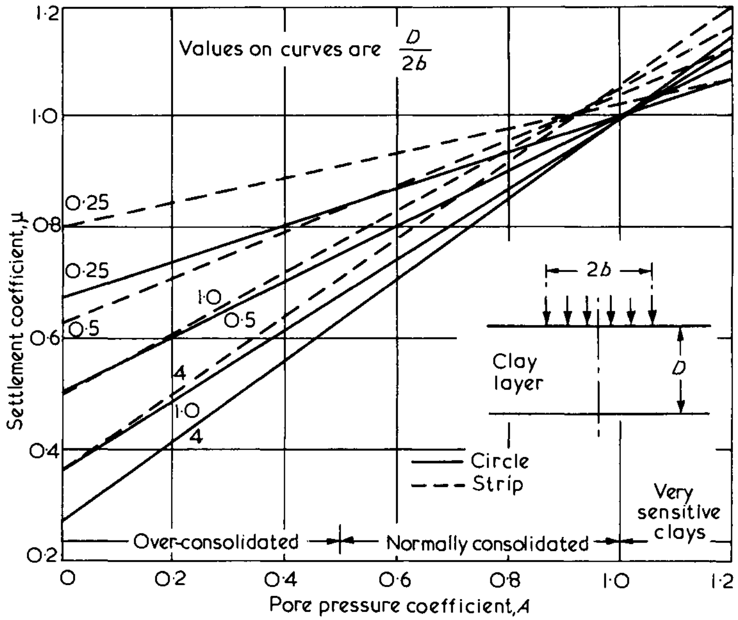

Fig.5.9 Correction factor for pore pressures set up under a foundation, after Skempton and Bjerrum (1957)

in situ. It was assumed, however, that the relationship between axial compressibility and effective stress could be determined in the standard oedometer, that is, the influence of lateral stresses on the stress deformation characteristics of the soil was not taken into account. A better laboratory procedure to predict the deformation of a soil under a given foundation loading, would be to test the soil by applying as closely as possible the same stress changes as those to which the soil will be subjected in the field. Moreover, because soil behaviour is generally non-linear, deformation properties, such as the undrained elastic modulus, Poisson's ratio, and the drained compressibility, will vary with stress level. It is also desirable that a soil specimen, after sampling, be first brought back to the stress system initially prevailing in the ground, before subjecting it to the stress changes it is likely to undergo on loading. Thus the concept of stress path testing (Simons and Som, 1969 and 1970; Simons, 1971) logically follows.

A stress path is essentially a line drawn through points on a plot of stress changes and shows the relationship between components of stress at various stages in moving from one stress point to another. Stress paths can be plotted in a variety of ways, and in studying the deformation of soils, a simple plot of vertical stress (effective or total) has been found to be convenient. It should also be noted that in this discussion, consideration is only given to cases where, by virtue of symmetry, the intermediate and minor principal stresses are equal and where the vertical and horizontal stresses are the principal stresses.

Consider how an element of over-consolidated clay under the centre line of a circular loaded area may be stressed. Before the application of the surface loading, the *in situ* vertical and horizontal effective stresses will be p' and $K_o \cdot p'$, respectively, where K_o is greater than unity (Skempton, 1961). The *in situ* effective stresses (p' and $K_o \cdot p'$) are represented by the point A and the corresponding total stresses by A_1 in Fig.5.10. Owing to the applied foundation pressure, q, the stresses on the element will increase by $\Delta\sigma_v$ and $\Delta\sigma_{h1}$. If the foundation pressure is applied sufficiently quickly so that no drainage occurs during the load application, the element will deform without any volume change and any vertical compression will be associated with a lateral expansion.

Now, the increase in stresses $\Delta\sigma_v$ and $\Delta\sigma_{h1}$ will set up an excess pore-water pressure in the element of saturated clay, (B = 1) (Skempton, 1954), where

$$\Delta u = \Delta\sigma_{h1} + A(\Delta\sigma_v - \Delta\sigma_{h1}) \tag{5.7}$$

Therefore, immediately after load application, the effective stresses are:

$$(\sigma'_v)_o = p' + \Delta\sigma_v - \Delta u \tag{5.8}$$

$$(\sigma'_h)_o = K_o \cdot p' + \Delta\sigma_{h1} - \Delta u \tag{5.9}$$

Since for most clays, and certainly for London clay, the value of A is positive and less than unity in the range of stresses normally encountered in practice, Δu is greater than $\Delta\sigma_{h1}$ consequently, the effective vertical stress increases and the effective horizontal stress decreases during load application, and the stress point moves from A to B. The vertical strain during undrained loading is, therefore, a function of the stress path, AB. The element now begins to consolidate. During the early stages, the increase in effective horizontal stress is a re-compression until the original value $K_o \cdot p'$ is restored, beyond which the further increase of effective horizontal stress is net, while the element is subjected to a net increase in effective vertical stress during the entire process of consolidation.

During load application under undrained conditions, a saturated clay behaves as an incompressible medium with Poisson's ratio equal to 0.5. As the excess pore-water pressure dissipates, however, Poisson's ratio decreases and finally falls to its fully drained value at the end of consolidation. This change in Poisson's ratio is unlikely to affect significantly the vertical stress (for an elastic, isotropic, homogeneous medium, the vertical stress increases are independent of the material parameters) but the horizontal stress will decrease by an amount δ to a new value $K_o \cdot p' + \Delta\sigma_{h2}$, where,

$$\Delta\sigma_{h2} = \Delta\sigma_{h1} - \delta \tag{5.10}$$

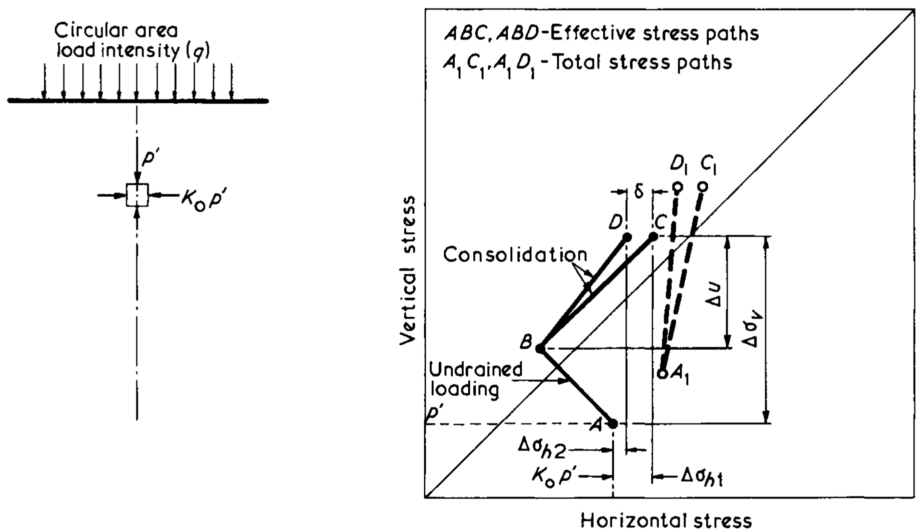

Fig.5.10 Stress path during undrained and drained loading, after Simons and Som (1969)

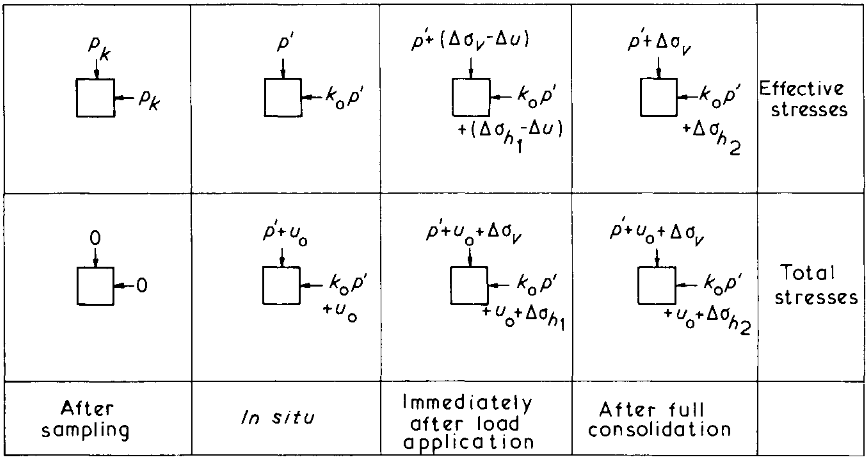

Fig.5.11 Idealized experimental programme for predicting settlement, after Simons and Som (1969)

Therefore during consolidation, the element will follow the effective stress path *BD*, which will govern the vertical strain during drained loading.

An ideal settlement analysis should take into account the complete patterns of stress changes to which typical elements of soil will be subjected in the field, and a summation of the corresponding vertical strains would give the predicted settlement of the structure. The stages of an idealized experimental programme are outlined in Fig.5.11. When a sample is removed from the ground without significant mechanical disturbance or change in water content, the total stresses are reduced to zero and a negative pore-water pressure is set up (Skempton and Sowa, 1963). In the first stage, therefore, the *in situ* stresses should be restored to obtain the condition before sampling. Then a set of stresses equal to those to which the sample will be subjected owing to the foundation loading, should be applied under undrained conditions, and both the vertical strain and the pore-water pressure measured. The sample should then be allowed to consolidate against a back-pressure equal to the equilibrium pore-water pressure u_o, and, at the same time, the horizontal stress should be decreased to its final value. The vertical strain recorded during this final stage together with that observed during the undrained loading, gives the total strain of the element in the field and the total settlement can be obtained by summation.

The stress path method of settlement analysis has been applied to London clay (Som, 1968, Simons and Som, 1969 and 1970; Simons, 1971).

The most important conclusions resulting from this work are:

- The actual stress path for an element of soil beneath a foundation in the field is in general quite different from that implied in standard methods of settlement computation based on the oedometer test. Because the axial deformation of an element of soil is dependent on the stress path followed, standard methods of settlement analysis cannot be expected to yield accurate predictions.

- In a foundation problem, the elastic modulus of the soil varies with depth as a consequence of increasing effective stresses before construction, and also because of different stress levels that are imposed by the applied foundation pressure. To measure correctly the variation of the elastic modulus with depth, it is necessary that an undisturbed sample be first brought back to the stress system prevailing in the ground before sampling and then be subjected under undrained conditions to the actual stress increments that are likely to be applied in the field. For London clay, the elastic modulus so obtained differs considerably from, and is generally larger than, that determined from standard undrained tests.

- The *volumetric* compressibility of London clay is primarily a function of effective vertical stress and is largely independent of the lateral stresses, at least within the range of stresses covered by the testing programme. However, the *vertical strain* is greatly influenced by the relative magnitude of the vertical and lateral stress increments during consolidation. Direct use of oedometer test results will not therefore result in accurate predictions of settlement, even if account is taken of the different excess pore-water pressures set up in the oedometer and in the field.
- The volumetric compressibility of London clay can, for practical purposes, be determined from either triaxial or oedometer tests, the latter giving satisfactory results only when initial swelling is positively prevented, and apparatus and bedding errors are eliminated. It is then possible to use the oedometer volume compressibility, together with a relationship between K' ($=\Delta\sigma_3'/\Delta\sigma_1'$) and ϵ_1/ϵ_v (the ratio of the axial to volume strain) to calculate the settlement of a structure. This relationship can be predicted with sufficient accuracy by assuming the soil to be a cross-anisotropic elastic material.

3.4.1 Example of settlement calculation

It has been shown that both the undrained and drained deformation moduli vary with the stress path followed and, therefore, significant errors in settlement calculations can develop if procedures are adopted which do not satisfactorily take into account the influence of stress path. Purely as an illustrative example, the settlement of a typical foundation on London clay has been calculated by three different methods, and the results are compared below.

The example is a circular, flexible, smooth footing, 12.2 m in diameter and founded at a depth of 6.1 m at a site for which the soil profile has been assumed to be the same as at Bradwell, Skempton (1961), and settlement analyses have been made for the centre of this circular foundation. The Bradwell data have been chosen simply because the effective stress–depth relationships, necessary for the stress path method of analysis, have been established to a considerable depth at this site.

From a knowledge of bearing capacity, a net foundation pressure of 140 kN/m^2, gross pressure 198 kN/m^2, has been adopted, to give a factor of safety against failure of more than three. The buried footing effect has not been taken into account in the comparative analyses that follow.

The immediate undrained settlement has been calculated in the conventional manner using an average Young's modulus of 38 500 kN/m^2 obtained from stress–strain relationships of standard undrained tests, and the equation:

$$\delta_i = \frac{q \cdot B \cdot \mu_o \cdot \mu_1}{E} \tag{5.11}$$

where q = net foundation pressure, 140 kN/m^2; B = diameter of circle = 12.2 m; μ_o, μ_1 = dimensionless influence factors, obtained from Fig.3.6.

The immediate undrained settlement following the stress path method is given by:

$$\delta_i = \Sigma \frac{\Delta\sigma_v - \Delta\sigma_h}{E(z)} \cdot \mathrm{d}z \tag{5.12}$$

where $\Delta\sigma_v$ and $\Delta\sigma_h$ are the increments in total vertical and horizontal stresses at any depth z, respectively, and $E(z)$ is the corresponding deformation modulus, taking into account the initial and final (under undrained conditions) vertical and horizontal effective stresses.

The results of the calculations are given in Table 5.2 and show an immediate settlement of 32.7 mm by the conventional method and 17.2 mm by the stress path method.

The consolidation settlement, δ_c, has been calculated using the conventional method, the Skempton and Bjerrum (1957) approach, and the stress path method.

Table 5.2 Example of settlement calculations, after Simons (1971)

Type of settlement	Conventional method (mm)	Skempton and Bjerrum's method (mm)	Stress path method (mm)
Immediate	32.7	32.7	17.2
Consolidation	109.0	75.1	40.9
Total	141.7	107.8	58.1

In the conventional method, the settlement is given by:

$$\delta_c = \int_0^z (m_v)_1 \,.\, \Delta\sigma_v \,.\, dz \qquad (5.13)$$

where $(m_v)_1$ is the volume compressibility determined in the standard oedometer test, and $\Delta\sigma_v$ the increase in total vertical stress.

Following the Skempton and Bjerrum method, the settlement is:

$$\delta_c = \mu \int_0^z (m_v)_1 \,.\, \Delta\sigma_v \,.\, dz \qquad (5.14)$$

where $(m_v)_1$ and $\Delta\sigma_v$ are as before and μ is a function of the soil type and the geometry of the foundation.

In the present case, μ is 0.69, corresponding to $A = 0.55$ and $z/B = 1.5$, from Fig.5.9.

For the stress path method, the settlement is:

$$\delta_c = \int_0^z \lambda \,.\, (m_v)_3 \,.\, \Delta u \,.\, dz \qquad (5.15)$$

where Δu is the increase in pore-water pressure under undrained loading which dissipates, resulting in the consolidation settlement; $(m_v)_3$ is the coefficient of volume compressibility for three-dimensional strain, which has been shown to be independent of the type of test for practical purposes; λ is the ratio of vertical strain to the volumetric strain which has been shown to be highly sensitive to the stress increment ratios.

The results of the calculations are given in Table 5.2 and show δ_c = 109 mm by the conventional method, δ_c = 75.1 mm by Skempton and Bjerrum's method, and δ_c = 32.7 mm by the stress path method.

The conventional method gives the highest calculated settlement, because it assumes that $\Delta u = \Delta\sigma_v$ and that the relationship between axial compressibility and effective vertical stress is given by the standard oedometer. The Skempton and Bjerrum method takes into account the fact that Δu is not equal to $\Delta\sigma_v$ in the field, although it is in the oedometer, but assumes again that the relationship between axial compressibility and effective vertical stress can be obtained from the oedometer test.

The relative magnitudes of the settlements as calculated by the different methods depend on the conditions existing at any particular site, and are not, therefore, in general, the same as those indicated by the example above. It is clear that the Skempton and Bjerrum approach is a great improvement on the conventional method, but will not necessarily give a precise estimate of the true field settlement.

The stress path method represents an improvement on the Skempton and Bjerrum procedure, but suffers from the practical disadvantage that very sophisticated time-consuming and expensive laboratory techniques are required. Because, however, it has been shown (Som, 1968; Simons and Som, 1969) that, for practical purposes, the volumetric compressibility can be determined from either triaxial or oedometer tests, it is possible to use the oedometer volume compressibility together with a relationship, which can be obtained experimentally or predicted theoretically, between the ratio of the axial to the volumetric strain and the ratio of applied effective horizontal to vertical stress.

3.5 Pre-consolidation pressure

An excellent example of the importance in practice of determining the pre-consolidation pressure is given by Vargas (1955) who showed from settlement observations of a number of buildings in Sao Paulo that:

- Where the applied foundation stress did not exceed the difference between the pre-consolidation pressure and the *in situ* effective pressure, the observed settlements were generally less than 10 mm, and were very much smaller than those computed directly from oedometer curves, on occasions equalling only 10% of the computed values.
- Where the applied foundation stress exceeded $p'_c - p'_o$, albeit only marginally, much larger settlements were measured. Reasonable agreement between calculated and observed settlement was obtained only if the calculations were based on stress increases in excess of p'_c, not p'_o.

Detailed studies of the properties of various clays by a number of investigators have shown that there are different factors which can give rise to a pre-consolidation pressure greater than the present effective overburden pressure, for example:

- Removal of overburden
- Fluctuations in the groundwater table
- Cold-welding of mineral contact points between particles
- Exchange of cations
- Precipitation of cementing agents
- Geochemical processes caused by weathering
- Delayed compression.

It is well known that the determination of p'_c is partly a function of the test procedure adopted in the laboratory, for example, the rate of loading adopted, whether or not rest periods have been permitted, and the effects of sample disturbance. The value of p'_c determined in the laboratory may well be different from that which can be relied upon in the field.

The development of pre-consolidation pressure resulting from delayed compression and the effects of such pre-consolidation on the settlements of structures has been discussed in detail by Bjerrum (1967 and 1973).

The concept of instant and delayed compression as proposed by Bjerrum is illustrated in Fig.5.12; instant compression is the settlement which would result if the excess pore-water pressures set up by a foundation loading could dissipate instantaneously with load application; delayed compression is the settlement then developing at constant effective stress.

A clay which has recently been deposited and come to equilibrium under its own weight but has not undergone significant secondary consolidation may be classified as a *young* normally consolidated clay. Such a clay is characterized by the fact that it is just capable of carrying the

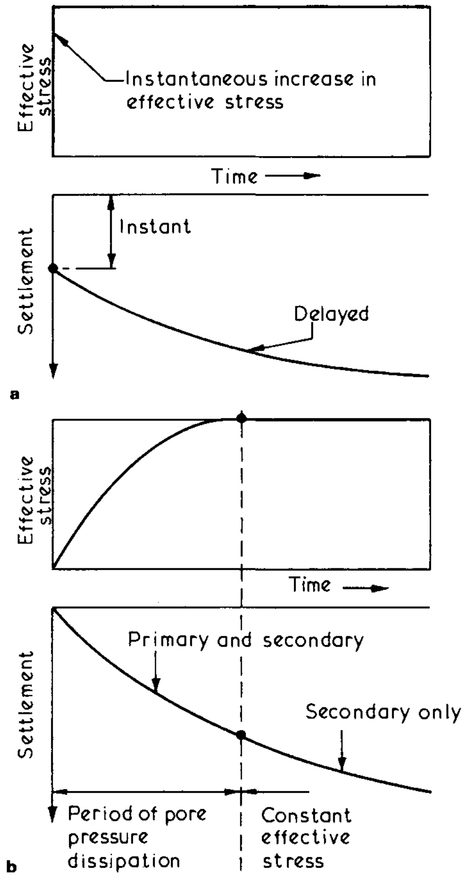

Fig.5.12 Instant and delayed compression, after Bjerrum (1967)

overburden weight of soil, and any additional load will result in relatively large settlements. If an undisturbed sample of a young clay is tested in an oedometer, the resulting e-log$p$ curve will show a sharp bend exactly at the effective overburden pressure p_o', which the sample carried in the field. A consolidation curve of this type is shown in Fig.5.13 marked young, being characterized by the fact that $p_c' = p_o'$. Thus, to this group of clays belongs only the clays which are geologically recent. A clay which has just consolidated under an additional load as, for instance, a fill, will also be classified with respect to its compressibility as a young clay deposit.

If a young clay is left under constant effective stresses for hundreds or thousands of years, it will continue to settle. The result of this secondary or delayed consolidation is a more stable configuration of the structural arrangement of the particles which means greater strength and reduced compressibility. With time, a clay undergoing delayed consolidation will thus develop a reserve resistance against a further compression. It can carry a load in addition to the effective overburden pressure without significant volume change. If an undisturbed sample of such an *aged* normally consolidated clay is subjected to a consolidation test, the resulting e-log$p$ curve will follow the curve marked *aged* on Fig.5.13. The curve shows an abrupt increase in compressibility at a pressure p_c' which is greater than p_o'.

As pointed out by Bjerrum (1972), considerable patience is required to determine experimentally in the laboratory the basic information necessary for constructing such a diagram as Fig.5.13. The only diagrams existing originate from areas where long-term observations of settlement are available.

A p'_c effect developed as a result of a delayed consolidation is characterized by the fact that the developed value of p'_c increases proportionally with p'_o, the effective overburden pressure the clay carried in the period it experienced delayed consolidation. In a homogeneous clay deposit, the ratio p'_c/p'_o is consequently constant with depth and this ratio can conveniently be used to describe the effect. The p'_c/p'_o ratio of clay deposits of the same age will increase with the amount of secondary consolidation which the clay has undergone under the existing overburden pressure. Because secondary consolidation increases with the plasticity of the clay, the p'_c/p'_o ratio will increase with the plasticity index. Fig.5.14 shows the correlation between p'_c/p'_o ratio and the plasticity index observed in some normally consolidated clays, which have all aged over a period of thousands of years.

It is of considerable importance to distinguish between pre-consolidation pressure owing to (a) over-consolidation as a result of removal of overburden pressure, or ground-water level fluctuations or chemical and weathering effects and (b) delayed consolidation. There is some evidence to indicate that for the first category, clays can be loaded up very close to the pre-consolidation pressure with small resulting settlements, for example, Vargas (1955), but if p'_c is due to delayed compression, then significant settlements, probably too large to be considered acceptable, develop when the applied pressure exceeds 50% of $p'_c - p'_o$ (Bjerrum, 1967), and as shown in Table 5.3.

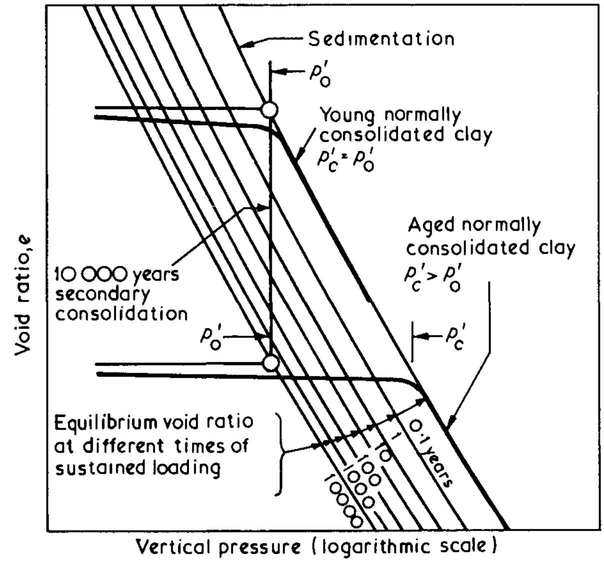

Fig.5.13 Relationships between voids ratio–log effective pressure–time, after Bjerrum (1967)

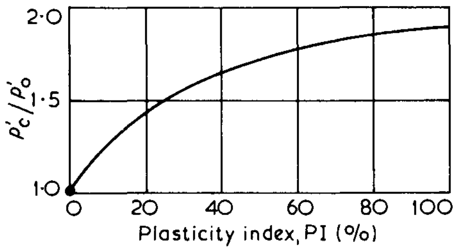

Fig.5.14 Relationship between p'_c/p'_o and plasticity index, after Bjerrum (1967)

Table 5.3 Observed 20 year settlements for structures in Norway, related to $\Delta p/p_c' - p_o'$ and $\Delta p/s_u$, after Simons (1974)

Structure	Settlement at 20 years (mm)	$\dfrac{\Delta p}{p_c' - p_o'}$	$\dfrac{\Delta p}{s_u}$
Skoger Sparebank	40	37%	0.6
Scheitliesgate 1	200	58%	0.9
Skistadbygget	c.230	72%	1.0
Konnerudgate 12	250	74%	1.6
Turnhallen. Light	360	68%	1.8
Konnerudgate 16	400	80%	1.8
Danvikgate 3	460	80%	1.8
Turnhallen. Heavy	600	123%	3.5

It can be seen from Table 5.3 that settlements after 20 years amounting to about 200 mm may be expected for values of $\Delta p/(p_c' - p_o')$ of 58% (Scheitliesgate 1), increasing to 400 to 460 mm (Konnerudgate 16 and Danvikgate 3) for $\Delta p/(p_c' - p_o')$ about 80%.

A completely different picture emerges from the original studies carried out in Sweden by Nordin and Svensson (1974). At Margretelund, Lidköping, the measured settlement is less than 9 mm (and appears to be virtually complete) with a $\Delta p/(p_c' - p_o')$ value of about 0.5, while at Lilla Torpa, Vänersborg, the observed settlements are up to 16 mm, with very little more expected, and here the net increase in stress due to the building loads and anticipated ground-water lowering, is nearly equal to $p_c' - p_o'$. At the present time, laboratory studies alone will not allow accurate settlement predictions to be made. Long term regional studies are vitally necessary to determine, in particular:

- Whether in the field, primary consolidation and/or secondary settlements will develop over a long period of time, and
- Whether a threshold level exists, below which acceptable settlements develop and above which large and potentially dangerous settlements will be experienced.

Regional studies of the type reported by Vargas (1955) for the Sao Paulo clay; Bjerrum (1967) for the Drammen clay; Jarrett, Stark and Green (1974) for the Grangemouth area; and Nordin and Svensson (1974) for Lidköping and Vänersborg, are therefore of considerable significance.

It should be stressed that, at the present time, it has been shown that very few clays exhibit a pre-consolidation pressure due to delayed consolidation (Brown, 1968).

Berre and Bjerrum (1973) have shown from a series of triaxial and simple shear laboratory tests that the development of a quasi pre-consolidation pressure may be associated with a critical shear stress; if the applied shear stress together with the initial shear stress is less than this value, then only relatively small deformations will be experienced. If the critical stress is exceeded, however, appreciable deformations will occur. This concept is confirmed by the behaviour of test embankments at Åsrum, Mastemyr and Sundland, in Norway.

Further confirmation is given by the settlement observations of various structures in Drammen and the relevant data are summarized in Table 5.3. It can be seen that there is a correlation between the 20 year observed settlement and the ratio of $\Delta p/s_u$ (Δp being the net applied foundation pressure on the surface of the clay layer, and s_u the undrained shear strength); the greater $\Delta p/s_u$, the greater the observed settlement.

3.6 Rate of settlement

The observed rate of settlement of structures is almost invariably very much faster than that calculated using one-dimensional consolidation theory based on oedometer tests carried out on small samples. Rowe (1968 and 1972) showed that the drainage behaviour of a deposit of clay depends on the fabric of the soil. Thin layers or veins of sand and silt, or rootholes, can result in the overall permeability of the clay *in situ* being many times greater than that measured on small samples. An hydraulic oedometer (Rowe and Barden, 1966), was developed to enable more reliable measurements of c_v to be made. Sample diameters of up to 250 mm with heights of up to 125 mm can be accommodated, with either vertical or horizontal drainage. The loading is applied hydraulically, and pore-water pressures, volume changes and axial deformations can be measured.

In situ permeability measurements, coupled with laboratory measurements of compressibility (which are not so sensitive to sample size) give values of c_v in fair agreement with field performance, and with the results from large samples tested in the hydraulic oedometer at similar stress levels. Reference can be made to the proceedings of the conference on '*In situ* Investigations in Soils and Rocks', held in London (1970), and to the symposium on 'Field Instrumentation in Geotechnical Engineering', held in London (1973).

Recourse to theories of three-dimensional consolidation, coupled with reliable determinations of c_v taking account of orientation and stress level, is necessary if it is important to obtain reasonably accurate predictions of rates of settlement.

In situ permeability tests have to be conducted at relatively low stress levels and therefore at least a few laboratory consolidation tests on large samples should be carried out to investigate the influence of stress level on c_v. The field rate of consolidation is of particular importance when the design of road, rail or runway embankments on soft clay is being considered.

4 Secondary settlement

Secondary settlement is generally considered to be the settlement which develops following changes in effective stress. After many years of research work into secondary consolidation, no reliable method is yet available for calculating the magnitude and rate of such settlement, for which the necessary soil parameters can be obtained fairly simply, and which also takes into account the various factors, for example the principal effective stress ratio, the load increment ratio, temperature, and time effects, which are known to affect significantly secondary settlement. For this reason, if estimates of secondary consolidation are required in practice, they are generally based on empirical procedures.

Table 5.4 Observed 20 year settlements greater than 200 mm, after Simons (1974)

Structure	δ_{20} (mm)	Reference
Skistadbygget, Drammen	c.230	Engesgaar (1972)
Konnerudgate 12, Drammen	250	Bjerrum (1967)
Masonic Temple, Chicago	250	Skempton, Peck & McDonald (1955)
Cold Stores, Grimsby	c.300	Cowley, Haggar and Larnach (1974)
Silo, Russi	c.300	Vefling (1974)
Konnerudgate 16, Drammen	400	Bjerrum (1967)
Monadnock Block, Chicago	450	Skempton, Peck & MacDonald (1955)
Danvikgate 3, Drammen	460	Bjerrum (1967)
Skabo Office Block, Oslo	460	Simons (1957)
Jernbanetollsted, Drammen	500	Andersen & Frimann Clausen (1974)
Auditorium Tower, Chicago	540	Skempton, Peck & MacDonald (1955)
Turnhallen, Drammen	600	Simons (1957)
Tower City Hall, Drammen	670	Bjerrum (1967)
Apartment Building, Oslo	c.700	Hutchinson (1963)
Residential Building, Nantua	c.1200	Sanglerat, Girousse & Gielly (1974)

Note: δ_{20} = observed or extrapolated maximum settlement at 20 years.

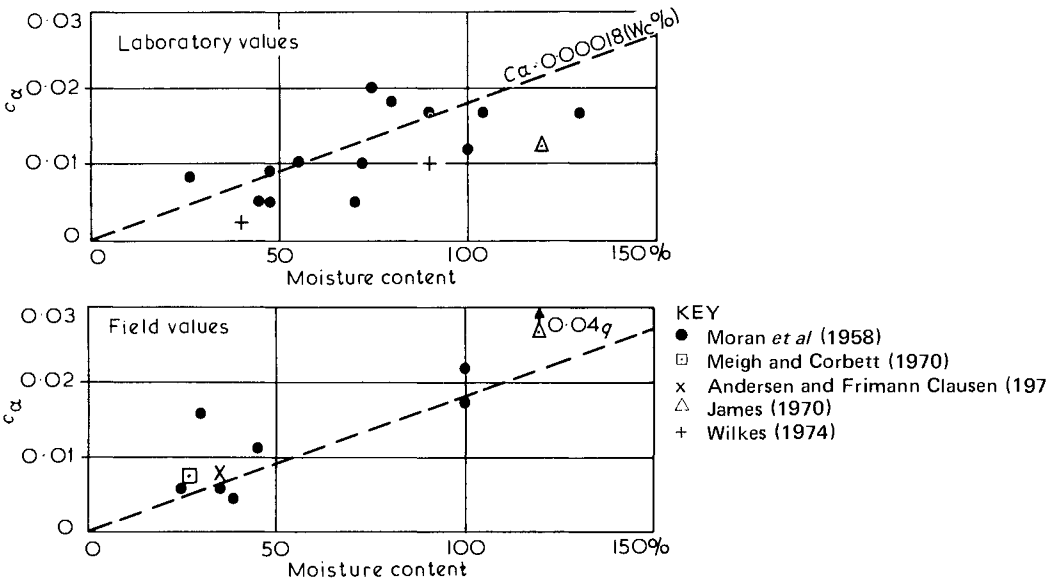

Fig.5.15 Values of c_α, the coefficient of secondary consolidation plotted against moisture content, after Simons (1974)

Contrary to the view which has sometimes been expressed that secondary settlement is often of little practical consequence so far as structures are concerned, several case records are available which show clearly that in certain circumstances a large part of the observed settlement has occurred after full dissipation of excess pore-water pressure, for example, Foss (1969). Satisfactory prediction of secondary settlement is therefore certainly a matter of practical importance.

When considering secondary settlement it should be noted that two different factors may influence this process. The first is reduction in volume at constant effective stress and the second is vertical strain resulting from lateral movements in the ground beneath the structure. Terzaghi (1948) pointed out that these two factors may be expected to result in completely different types of settlement. The relative importance of these factors will vary from structure to structure, depending on the stress level, type of clay, and the geometry of the problem, and for any given structure will vary with the location of any deforming soil element, and with time.

No great accuracy can therefore be expected from predictions of secondary settlement and caution should be exercised when attempting to extrapolate the results from one particular investigation to another set of conditions.

Investigations into secondary settlement can be considered to fall into three categories:

- Laboratory work
- Empirical approaches based on field and laboratory results
- Theoretical analyses based on rheological models.

4.1 Laboratory work

Many workers have carried out various types of laboratory test to investigate various aspects of secondary consolidation behaviour. Important points to emerge are that:

- Organic soils show pronounced secondary effects
- Many soils exhibit a linear relationship between settlement and log time for a considerable period, although this relationship cannot hold indefinitely
- Isotropic consolidation results in less secondary effect than consolidation with no lateral yield
- Secondary settlement is more pronounced at stresses below the pre-consolidation pressure, for small load increment ratios, with increasing temperature, with decrease in the length of the drainage path, and for small factors of safety

- Instability may occur, that is, the rate of settlement may increase temporarily after a long period of time.

4.2 Empirical approaches

Generally, these approaches are based on the assumption that secondary settlements can be approximated by a straight line on a settlement versus logarithm of time plot (Buisman, 1936; Koppejan, 1948; Zeevaert, 1957, 1958). While there is much evidence to indicate that such a simple extrapolation cannot in general be expected to give reliable predictions in field problems, this approach is often adopted in practice and, it must be admitted, there is as yet no theoretical solution available which takes into account all the factors which are known to affect secondary compression and in which the relevant soil parameters can be fairly easily obtained.

Use has been made of c_a, the coefficient of secondary consolidation, defined as the secondary settlement per unit height per log cycle of time.

Values of c_a are shown in Fig.5.15.

Bjerrum (1967) presented his model to represent instant and delayed compression on a plot of void ratio versus the logarithm effective vertical pressure, Fig.5.13, and Foss (1969) applied this approach to predicting the secondary settlements of four structures in Drammen. It must be noted, however, that the predictions are based on the assumptions that:

- The relative positions of the lines representing field void ratios at different loading times from 24 hours to 3000 years are available,
- If $\Delta p < p'_c - p'_o$, no primary consolidation settlement will occur, and
- The clay under a structure will follow these relationships.

While Foss found good agreement between calculated and observed rates of secondary settlement, further comprehensive laboratory data for other clays are an urgent requirement. The data should be similar to those available for Drammen, and supported by settlement records of structures on these clays.

4.3 Theoretical approaches

A helpful summary of various theoretical approaches has been made by Clayton (1973). Possibly the most useful contribution of these approaches has been to study the effects of variables in order to suggest – qualitatively – differences between laboratory testing and field performance of clays. Garlanger's mathematical model (Garlanger, 1972) combined with finite difference techniques appears at the present time, to be the most powerful tool available in the prediction of the time-settlement behaviour of loaded soil in the field. This model takes into account the effects of drainage path length on the stress–strain behaviour of clays, and it can be adapted to reflect the effects of the variation of pressure increment that occurs beneath structures on deep deposits.

4.4 Long term settlement records

Although secondary settlements are of significance for many structures, there are also a number of cases where settlement records show small or negligible secondary effects. Three such illustrative examples are, the apartment building at Økernbråten, Oslo (Simons, 1963), the trial embankment at Avonmouth (Murray, 1971), and the multi-storey buildings in Glasgow (Somerville and Shelton, 1972). Typical settlement-log time curves are shown in Fig.5.16.

At Økernbråten, a nine-storey block of flats founded on strip foundations transmitting 226 kN/m^2 to the underlying firm to stiff, becoming soft with depth, clays, at least 20 m thick, experienced a maximum settlement of 18 mm and the settlements stopped completely about 3.5 years after the end of construction.

At Avonmouth, the square embankment with a maximum height of 9.2 m, a width at the base of 67 m and side slopes of 1 in 2, constructed of pulverized fuel ash of average bulk unit

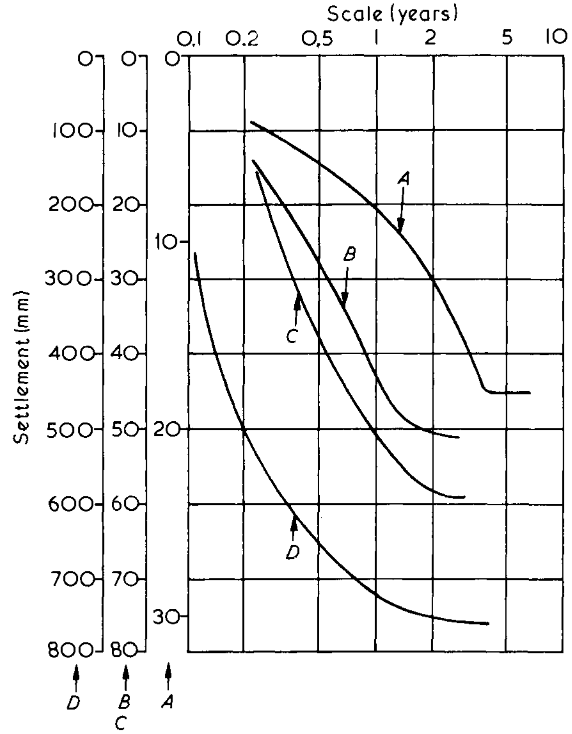

Fig.5.16 Settlement–log time curves indicating terminating settlement, after Simons (1974).
CASE A. Økernbråten, Oslo, Simons (1963)
CASE B. Point 9, Block C, Bridgeton, Somerville and Shelton (1972)
CASE C. Point 19, Block C, Parkhead, Somerville and Shelton (1972)
CASE D. Avonmouth, Murray (1971)

weight 13.4 kN/m^3 on highly compressible alluvial soils containing peat, about 13 m in thickness, with undrained shear strengths ranging generally from about 40 kN/m^2 to about 90 kN/m^2, experienced a maximum settlement of about 780 mm some 1000 days after the start of construction of the embankment, 90% of primary consolidation occurring 300 days after the start of construction. The rate of movement is now quite small and appears to be reducing with time.

At Glasgow, six blocks of fifteen-storey flats were constructed in the Parkhead and Bridgeton districts, which are underlain by deep alluvial deposits of firm laminated clays and silts with deeper deposits of sands, gravels and glacial drifts, followed by productive coal measures. Raft foundations were adopted, with net bearing pressures of about 53.5 kN/m^2. The time-settlement curves show very slow rates of settlement only 1 to 2 years after the end of construction, with maximum settlements ranging from 30 to 60 mm.

Clearly, there is a need to be able to distinguish between cases where settlement continues over many years, as illustrated in Fig.5.17 for Norwegian and Swedish clays, and cases where the rate of settlement virtually stops a few years after the end of construction, as shown in Fig.5.16.

The complexity of the problem is shown in Fig.5.18, which gives the settlement-log time plots for the three well-known Chicago structures, namely, the Masonic Temple, the Monadnock Block, and the Auditorium Tower (Skempton, Peck and MacDonald, 1955). The behaviour of the Masonic Temple is quite different from that of the other two, with more than 90% of the total final settlement developed after five years. The corresponding figures for the Monadnock Block and the Auditorium Tower are 47% and 62%. Furthermore, after 10 years the settlement of the Masonic Temple was virtually complete, but for the other two structures, settlements were still taking place after 30 years.

Investigations into the geochemistry of the soils, work on micropaleontology, or electron microscope analysis, might be necessary, as well as the determination of engineering properties, in order to classify clays with regard to their long term settlement behaviour.

Settlement observations taken on structures and embankments should be continued over a sufficient period of time for the long term trends to be indicated. To halt observations at a time when excess pore-water pressures have just dissipated, for example, may well result in an incomplete picture emerging of the true settlement time performance.

A final point to be noted is that structures subjected to large variations in live load, for example, silos, storage tanks and high structures under wind action, may be expected to experience appreciably larger secondary settlements than would be the case for non-varying loading conditions (Bjerrum, 1964 and 1968).

5 Other methods of predicting settlement

Some other approaches which have been suggested for predicting the deformations of structures are outlined below.

5.1 Centrifugal models

Recent developments in testing centrifugal models indicate that this method of predicting ground displacements may well be a practical tool in the near future. The results obtained by Wroth

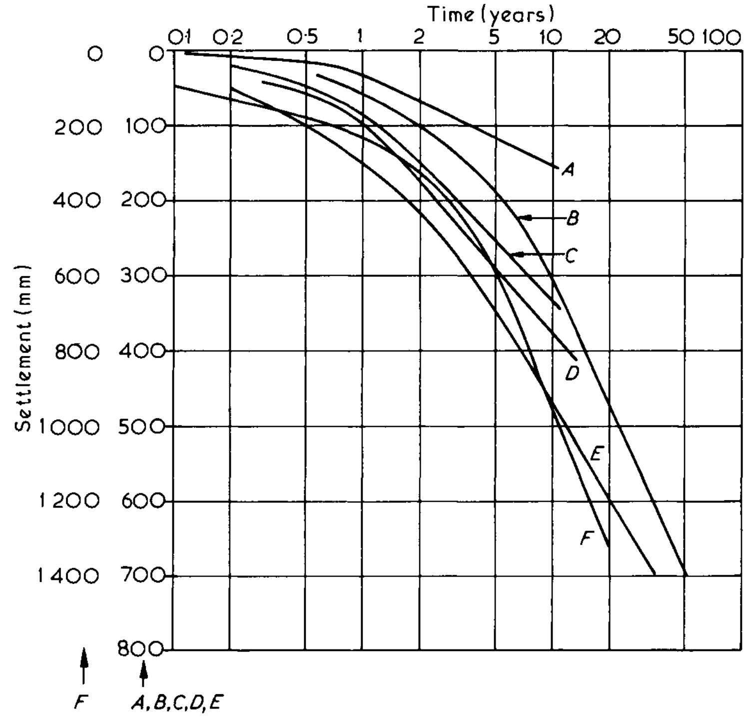

Fig. 5.17 Settlement–log time curves indicating non-terminating settlement, after Simons (1974)
Case A. Scheitliesgate 1, Drammen, Bjerrum (1967)
Case B. Jernbanetollsted, Oslo, Anderson and Frimann Clausen (1974)
Case C. Konnerudgate 16, Drammen, Bjerrum (1967)
Case D. Skabo office block, Oslo, Simons (1957)
Case E. Turnhallen, Drammen, Simons (1957)
Case F. Test fill. Vasby, Sweden, Chang, Broms and Peck (1973)

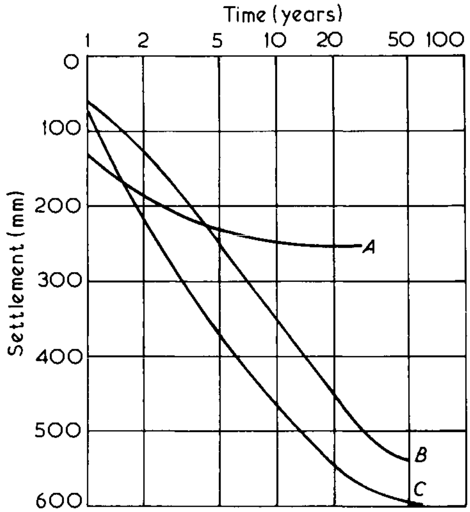

Fig.5.18 Settlement–log time curves for three structures in Chicago, after Skempton, Peck and MacDonald (1955)
CASE A – Masonic temple; Case B – Monadnock block; Case C – Auditorium Tower

and Simpson (1972) in predicting the deformations of the trial embankment at King's Lynn (Wilkes, 1974) are particularly encouraging.

5.2 Janbu's deformation modulus

Settlement calculations are usually based on the parameters C_c or m_v. Janbu (1963 and 1969) proposed basing computations on the tangent modulus, being equal to $d\sigma/d\epsilon$, as a suitable measure of the compressibility of soils, ranging from sound rock to plastic clays. The tangent modulus depends on stress conditions and stress history and can be considered to represent a resistance against deformation. As the calculation procedure based on the tangent modulus concept is very simple, and virgin loading, unloading and reloading conditions can be taken into account, this approach seems worthy of consideration.

5.3 Dutch cone sounding apparatus

As an approximate method to estimate settlement, the use of the static cone sounding apparatus has been proposed (Gielly, Lareal and Sanglerat, 1970; Sanglerat, 1972) based on correlations between compressibility and the cone resistance. No accurate settlement forecast can be expected for reasons which have been discussed, but it appears that the cone resistance can give a useful first approximation of compressibility (Meigh and Corbett, 1970).

5.4 Correlation of compression index with moisture content

Another first approximation to compressibility for normally consolidated clays is based on correlations between $C_c/(1 + e_o)$ and the moisture content. Various such correlations have been plotted on Fig.5.19 and a fairly narrow band results only for moisture contents less than about 70%.

5.5 Elastic method

Butler (1974) describes the use of the so-called elastic method to predict the consolidation settlement of structures founded on the heavily over-consolidated London clay. By assuming that $E' = 130\, s_u$, and taking Poisson's ratio = 0.1, reasonably good agreement between calculated and observed settlements was obtained. Use of this method, however, for general application to any clay requires a knowledge not only of Poisson's ratio, ν, and the elastic modulus E_v in the vertical direction, but also the elastic modulus, E_h, in the horizontal direction. This latter value is known to affect very significantly the value of the vertical displacement. For example, Simons, Rodriques and Hornsby (1974) found that for $E_h = 1.8\ E_v$ (a typical value for London clay) the calculated settlements amounted to about 60% of those calculated for $E_h = E_v$. Use of the elastic method must therefore be restricted to those cases where reliable knowledge of E_h, E_v and ν is available and where comparisons between predicted and observed settlements can be made.

6 The prediction of settlements on granular deposits

6.1 Introduction

For granular soils, it has been indicated in Chapter 4, that apart from very narrow, shallow footings on loose materials with a high water table, the allowable pressure which may be applied to a foundation will be governed by considerations of settlement, rather than of the shear strength of the soil. For this reason, accurate prediction of the settlement of structures founded on granular materials is of considerable practical importance.

Because of the high permeability of granular materials, most of the settlement will develop during application of the foundation loading. After the end of construction, therefore, only minor settlements due to creep are likely to occur, unless very large foundations are concerned or the granular soil is silty, or the foundation is subjected to fluctuating loads, for example, wind, machinery vibrations, and the filling and emptying of silos and oil tanks.

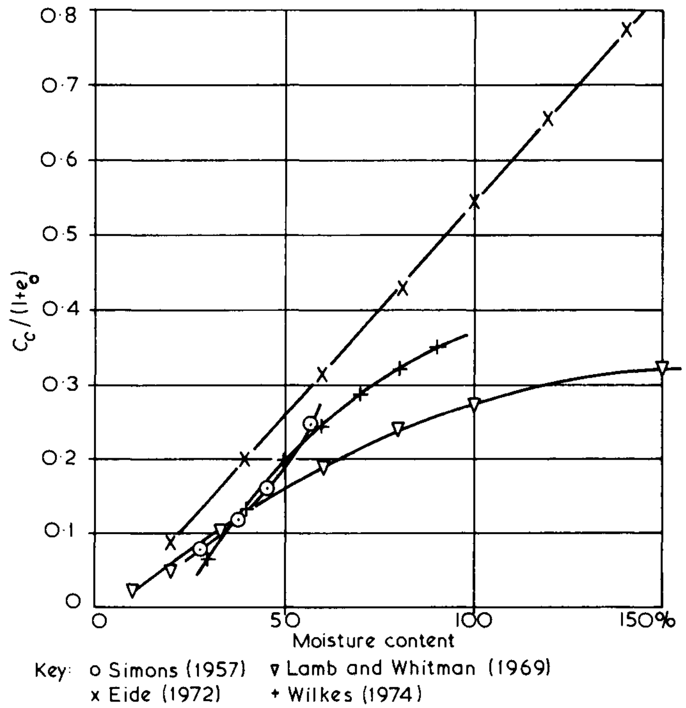

Fig.5.19 Relationship between $C_c/(1 + e_o)$ and natural moisture content, after Simons (1974)

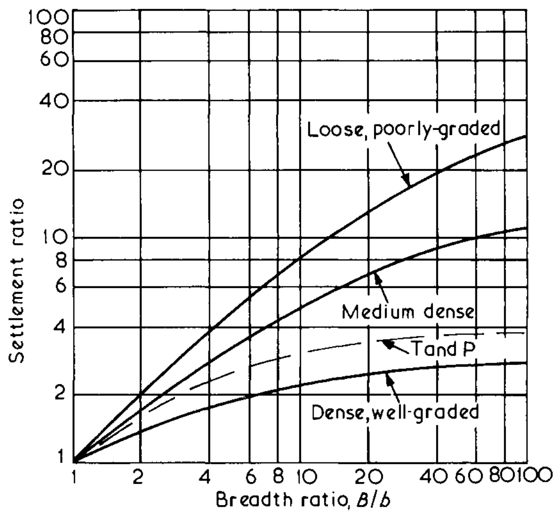

Fig.5.20 Relationship between settlement ratio and foundation to plate size ratio, after Terzaghi and Peck (1948) and Bjerrum and Eggestad (1963)

It is known from studies of case records of structures founded on granular soils that the differential settlement between adjacent footings can on occasions approach the total settlement, see Fig.5.36, (Skempton and MacDonald, 1956; Bjerrum, 1963; Terzaghi and Peck, 1967) partly because granular soils tend to be less homogeneous than clays. On average, however, the differential settlements are about 2/3 the maximum settlement, while for clays the corresponding figure is about 1/3. Thus for clays, for a given maximum settlement, a relatively smaller differential settlement will generally be experienced.

It is expensive and difficult, and in many cases impossible, to obtain undisturbed samples of granular soils. Even recompacting granular soil back to exactly the same relative density as in the field will not guarantee that stress–strain relationships obtained in the laboratory will be equal to those pertaining in the field because the effects of over-consolidation, if any, lateral stresses in the field, and the structural arrangement of the grains will not be properly reproduced. Therefore, the methods generally used to predict settlements are based on field tests, namely, the plate loading test, the standard penetration test and the dutch cone test. Very occasionally, laboratory tests have been used, for example, oedometer tests and stress-path triaxial tests (D'Appolonia *et al*, 1968).

6.2 Plate loading tests

For plate loading tests to be applicable at all, they must be carried out on soil which is representative of the soil to be stressed by the prototype foundation. Thus, plate tests should ideally be carried out at different depths and at different locations and the position of the groundwater table will have to be taken into consideration. Care must be taken to avoid disturbing the soil immediately below the plate, and to reduce bedding errors to a minimum.

Local minor variations in density will greatly affect the results of plate tests, but will have lesser influence on the settlement of the full-size foundation. A sufficient number of tests should be carried out in order to obtain a reliable average value. Preferably, plates of different size should be used, so that a better extrapolation up to full size can be made.

An interesting development of the plate loading test is the screw plate, which can be rotated into the ground, a loading test carried out, and rotated further to a greater depth for another loading test. In this way, no excavation is required and tests can be carried out without difficulty below the water table (Kummeneje, 1955).

It is then necessary to extrapolate from the results of the plate loading tests to the settlement of the prototype foundation.

Terzaghi and Peck (1948) proposed the following relationship between the settlement of a footing of width B m and the settlement, δ_b, of a 0.3 m square test plate, loaded to the same loading intensity.

$$\frac{\delta_B}{\delta_b} = \left(\frac{2B}{B+0.3}\right)^2 \tag{5.16}$$

It should be noted that for large B, the ratio tends to a maximum value of four. The relationship is plotted in dimensionless form in Fig.5.20.

Bjerrum and Eggestad (1963), from a study of case records, indicated that there can be an appreciable scatter in the correlation between settlement and the dimension of the loaded area, and, more important, that settlement ratios very much larger than four could occur. They suggested that the correlation was also dependent on density, and made the proposals shown in Fig.5.20. It has been suggested that the correlation is also influenced by the grading of the sand (Meigh, 1963); coarse, well-graded soils have low settlement ratios, and fine uniformly graded soils, have high settlement ratios.

D'Appolonia *et al* (1968) found settlement ratios greater than 10 for dense fine uniformly graded sands.

6.3 Dutch cone test

In this test, a 60° degree cone with a cross-sectional area of 10 cm^2 is forced into the ground at a reasonably constant rate of strain, and provision is made to measure independently the point resistance, and the resistance due to side friction. The test was first devised to assess the bearing capacity of piles, but is now used to predict the settlement of structures on sands. Originally, prediction procedures were developed by de Beer and his co-workers, but more recently Schmertmann has proposed a different approach. A practical problem associated with the test is that on occasions it is difficult to penetrate overlying harder layers.

If C_r is the static cone point resistance and p'_o the effective overburden pressure at the depth the test is carried out, then de Beer and Martens (1957) proposed that the compressibility coefficient, C, is given by

$$C = \frac{1.5\, C_r}{p'_o} \tag{5.17}$$

The settlement is then given by

$$\delta = \frac{H}{C} \cdot \log_e \frac{p'_o + \Delta p}{p'_o} \tag{5.18}$$

where Δp is the increase in stress due to the net foundation pressure at the centre of the layer of thickness H under consideration.

It has been found that this procedure generally overestimates the observed settlement. For example, de Beer (1965) found by comparing calculated and observed settlements for about 50 bridges that, on average, the calculated settlements were about twice as high as those observed. Because of this overestimate, the less conservative relationship of

$$C = \frac{1.9\, C_r}{p'_o} \tag{5.19}$$

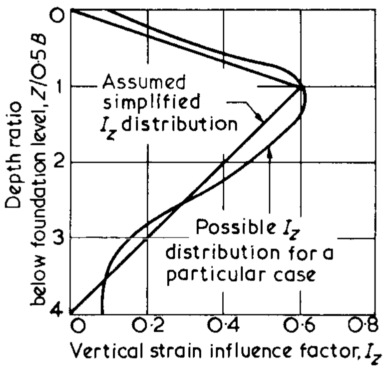

Fig.5.21 Variation of strain influence factor with depth, after Schmertmann (1970)

suggested by Meyerhof (1965) has been more widely used. These methods strictly only apply to normally loaded sands; if a sand has been preloaded, subsequent settlements will be small, but it is, of course, difficult to determine the degree of over-consolidation of a granular deposit.

Schmertmann (1970) proposed a different approach to the use of cone penetration tests in the calculation of the settlement of footings on sands. He made the point that the distribution of vertical strain under the centre of a footing on a uniform sand is not qualitatively similar to the distribution of the increase in vertical stress, the greatest strain occurring at a depth of about $B/2$.

Schmertmann gives the following equation for calculating settlement:

$$\delta = C_1 \,.\, C_2 \,.\, \Delta p \sum_{0}^{2B} \left(\frac{I_z}{E}\right) . \Delta z \qquad (5.20)$$

where, Δp = increase in effective overburden pressure at foundation level; Δz = thickness of layer under consideration; C_1 = depth embedment factor; I_z = strain influence factor given in Fig.5.21.

$$C_1 = 1 - 0.5\left[\frac{p'_o}{\Delta p}\right], \quad p'_o = \text{initial effective overburden pressure at foundation level} \qquad (5.21)$$

C_2 = empirical creep factor based on work by Nonweiller (1963)

$$= 1 + 0.2 \log_{10}\left[\frac{t}{0.1}\right] \qquad (5.22)$$

where t is the period in years for which the settlement is to be calculated; E = deformation modulus

$$E = 2 \,.\, C_r \qquad (5.23)$$

Schmertmann claims that not only is his method simple to apply but also that its use leads to more accurate estimates of settlement than the de Beer procedure; on average for 16 sites where a comparison has been made, settlements calculated using de Beer's method were about 50% greater than those obtained by the Schmertmann method.

The method is best illustrated by a worked example.

6.3.1 Numerical example

Calculate the settlement for the loading condition illustrated in Fig.5.22. The calculations are given below.

Net increase in pressure at foundation level is:

$182 - 2 \times 16 = 150$ kN/m².

Layer	Δz (mm)	C_r (kN/m²)	E (=2 C_r)	I_z	$\dfrac{I_z . \Delta z}{E}$
A	1000	2500	5000	0.23	0.0460
B	300	3500	7000	0.53	0.0227
C	1700	3500	7000	0.47	0.1141
D	500	7000	14000	0.30	0.0107
E	1000	3000	6000	0.185	0.0308
F	700	8500	17000	0.055	0.0023
					Sum = 0.2266

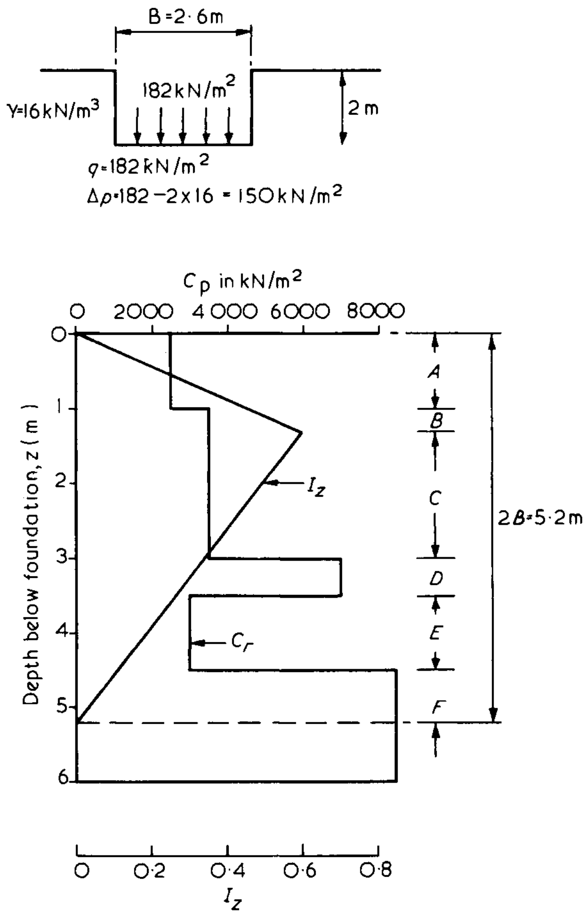

Fig.5.22 Example of settlement calculation following Schmertmann (1970)

$$C_1 = 1 - 0.5\left(\frac{p'_o}{\Delta_p}\right), \text{ from equation 5.21,}$$

$$= 1 - 0.5\left(\frac{32}{150}\right)$$

$$= 0.89$$

Taking a five year creep period,

$$C_2 = 1 + 0.2\log_{10}\left(\frac{t}{0.1}\right), \text{ from equation 5.22,}$$

$$= 1 + 0.2\log_{10} 50$$

$$= 1.34$$

$$\delta = C_1 \,.\, C_2 \,.\, \Delta_p \,.\, \Sigma\frac{I_z \,.\, \Delta z}{E}, \text{ from equation 5.20}$$

$$= 0.89 \times 1.34 \times 150 \times 0.2266$$

$$= 40.1 \text{ mm}$$

6.4 Correlation between standard penetration test (SPT) and Dutch cone tests

On occasions, it can be useful to estimate the equivalent SPT 'N' value from the results of Dutch cone point resistance, and *vice versa.*

Meyerhof (1956) attempted to correlate the results of the two tests and suggested the following relationship:

$$C_r = 4N \tag{5.24}$$

where, C_r = static cone point resistance in ton/ft^2 or kg/cm^2.

Further work (Meigh and Nixon, 1961; Rodin, 1961; Sutherland, 1963) showed that this simple relationship was not in general sufficiently accurate for all granular soils and that the

Table 5.5 Ratio of cone point resistance to SPT N value, after Meigh and Nixon (1961)

Soil description	C_r/N
Sandy silt	250
Fine sand and silty fine sand	400
Fine to medium sand	480
Sand with some gravel	800
Medium and coarse sand	800
Fine to medium sand	1000
Gravelly sand	800–1800
Sandy gravel	1200–1600

Table 5.6 Correlation of SPT N value with relative density for granular soils after Terzaghi and Peck (1948)

SPT N value	Relative density
0–4	Very loose
4–10	Loose
10–30	Medium dense
30–50	Dense
50	Very dense

correlation depended on grain size as shown in Table 5.5; in this case the units of C_r are in kN/m^2.

6.5 Standard penetration test

The standard penetration test (SPT) is an empirical dynamic penetration test, developed in the USA in the 1920s, and was usually carried out in 50 to 100 mm diameter wash borings. In the UK it is almost always performed in shell borings of diameter 150 mm to 200 mm. This procedure increases the risk of disturbance of the soil immediately below the borehole due to suction as the shell is withdrawn. To minimize this effect, it is considered good practice to require that the outside shell diameter shall not be more than 90% of the internal diameter of the casing and that it should be withdrawn slowly from the hole.

The test consists of driving into the ground a standard split spoon sampler by a 63.6 kg weight falling 762 mm. The spoon sampler has a 50 mm outside diameter, a 35 mm inside diameter and a length of 0.8 m. After proper cleaning of the hole, the penetrometer on the end of the boring rods is lowered to the bottom of the hole and driven an initial 150 mm and the blow count recorded. The penetrometer is then driven a further 300 mm and the blow count for this latter drive is called the SPT N value. It is considered good practice to record the blow count for each of six 75 mm increments, as this allows a better assessment of the depth of any disturbance. In very dense materials, the blow count necessary to achieve full penetration may be excessive and tests are often terminated after reaching a blow count of 50 and the penetration achieved is recorded.

Tests are generally carried out at depth intervals of 1.5 m. In gravel, a special solid 60° cone is used to avoid damage to the spoon, and work by Palmer and Stuart (1957) and Rodin (1961) showed that the solid cone tended to give slightly higher results.

If the soil consists of very fine or silty sand below the water table, a correction is made when the measured N is greater than 15, because excess pore-water pressures set up during driving cannot dissipate. The results are affected as follows:

$$N_{\text{corrected}} = 15 + 0.5\,(N_{\text{measured}} - 15) \tag{5.25}$$

A granular deposit can be classified as shown in Table 5.6.

An approximate correlation between the N value and the angle of shearing resistance has been proposed by Peck, Hanson and Thornburn (1974) and is shown in Fig.5.23.

Terzaghi and Peck (1948) were the first to propose a correlation between the N value and allowed pressure, by presenting a relationship between the size of a footing, the N value, and the applied pressure to give a settlement of 25 mm for a deep groundwater table (depth greater than $2B$ below the underside of a footing of width B). This correlation is shown in Fig.5.24. If the groundwater table is at foundation level, the allowable pressure should be halved. A further correction factor, C_D, for the depth of embedment of the footing was also introduced. C_D varies from 1 to 0.75 as the level of the base of the footing varies between ground level and a depth B below ground level, thus the deeper the footing the less the settlement.

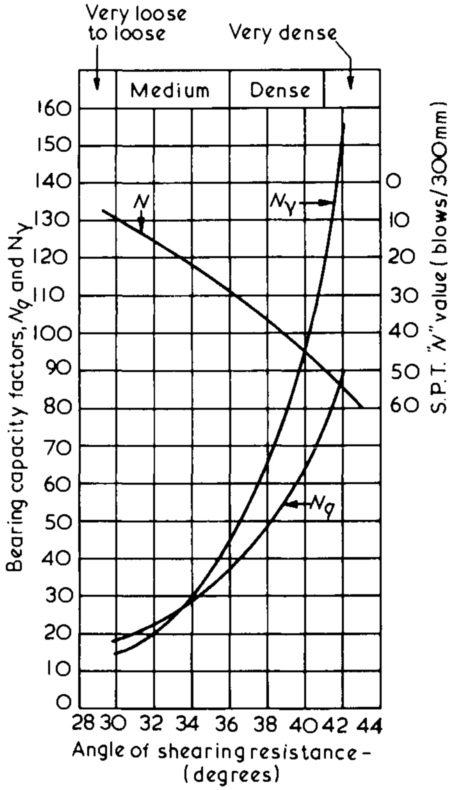

Fig.5.23 Relationship between SPT 'N' value and ϕ', N_q and N_γ, after Peck, Hanson and Thornburn (1974)

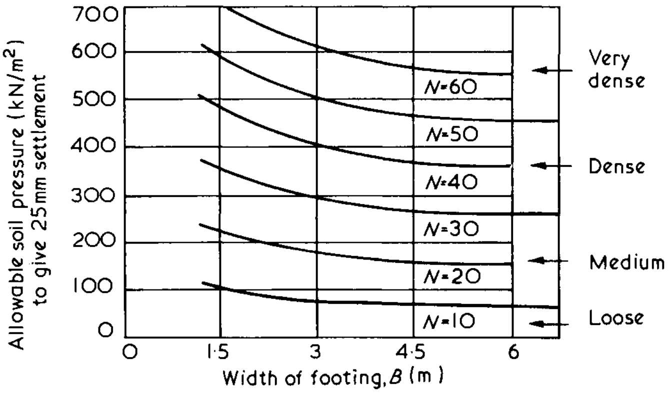

Fig.5.24 Correlation of allowable bearing pressure to give 25 mm settlement to SPT 'N' value, after Terzaghi and Peck (1948)

This standard Terzaghi and Peck procedure is generally recognized as being conservative and as experience was gained, various different procedures have been proposed to predict the settlements of structures founded on granular materials, based on N values. Some of these procedures are outlined below.

Following Meyerhof (1965), settlements can be calculated using the following relationships:

- $\delta = \dfrac{1.9\, q}{N}$ for $B < 1.25$ m

- $\delta = \dfrac{2.84\,.\,q}{N}\left[\dfrac{B}{B + 0.33}\right]^2$ for $B > 1.25$ m

- $\delta = \dfrac{2.84\, q}{N}$ for large rafts,

where q = applied foundation pressure.

N is averaged over a depth equal to the width of the footing. These equations correspond roughly to the standard Terzaghi-Peck settlement chart, given in Fig.5.24.

Meyerhof (1965) also suggested that no allowance need be made for the groundwater table, as its presence should be reflected by the SPT results, and, in addition, that the allowed pressures can be increased by 50%. Meyerhof's proposals have been confirmed by the work of D'Appolonia *et al* (1968).

The penetration resistance reflects both the *in situ* relative density and the effective stress at the depth at which the test is carried out, and therefore an infinite number of combinations of stress level and relative density will result in the same measured N value, and relationships have been developed to correct the measured blow count for the *in situ* vertical effective stress. A simple correction chart has been proposed by Tomlinson (1969) based on the work by Gibbs and Holtz (1957) and is reproduced in Fig.5.25. The differences between the corrected and

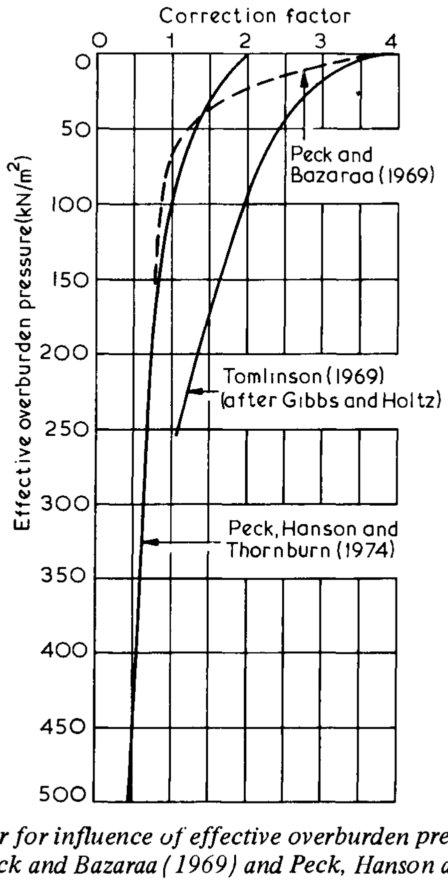

Fig.5.25 Correction factor for influence of effective overburden pressure on SPT 'N' value, after Tomlinson (1969), Peck and Bazaraa (1969) and Peck, Hanson and Thornburn (1974)

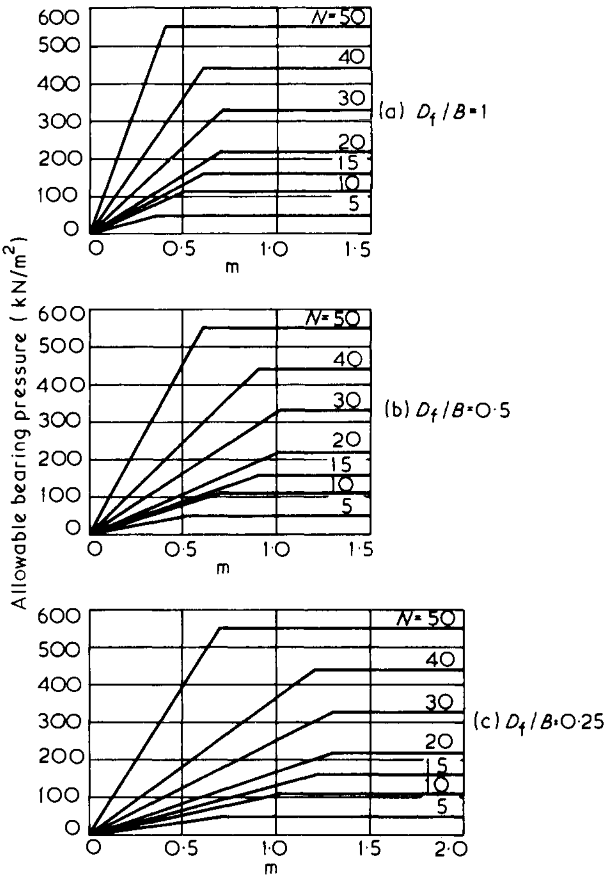

Fig.5.26 Correlation of allowable bearing pressure to give 25 mm settlement to SPT 'N' value, after Peck, Hanson and Thornburn (1974)

measured blow counts are most marked for tests carried out at shallow depths. Tomlinson's chart indicates that the measured N should be increased up to four times for very shallow depths, but a correction of this magnitude should be applied with caution.

Peck and Bazaraa (1969) recognized that the original Terzaghi and Peck proposals were too conservative, and proposed three modifications. First, the allowable soil pressures indicated in Fig.5.24 should be increased by 50% as proposed by Meyerhof (1965). Second, they agreed that the measured N values should be corrected for overburden pressure, but considered that the application of the Gibbs and Holtz values lead to overcorrection, and, therefore proposed the curve marked Peck and Bazaraa in Fig.5.25. This leads to smaller correction factors than do Tomlinson's proposals. Third, they proposed a slightly different correction for the groundwater position. They recommended that when the water table is at a distance D_w below the base of a shallow footing of width B, then the settlement δ' may be estimated from $\delta' = K \cdot \delta$, where δ is the settlement of the same footing when the sand is dry. K is the ratio of the effective overburden pressure at a depth 0.5 B below the base of the footing when the sand is dry to that at the same depth when the water table is present.

A further approach to the calculation of the settlements of footings on granular soils, again based on the work of Bazaraa (1967) is outlined by Peck, Hanson and Thornburn (1974). The influence of the effective overburden pressure on the measured N value is taken into account using the curve marked Peck, Hanson and Thornburn in Fig.5.25. A correction for the water table position is given as:

$$C_w = 0.5 + 0.5\left(\frac{D_w}{D_f + B}\right) \tag{5.26}$$

where D_f is the depth of the footing and D_w the depth of the groundwater table, both measured from the ground surface. A maximum value for C_w of unity should be taken for D_w greater than $(D_f + B)$. These values are then used in a new chart relating N values, breadth of footings and allowable bearing pressure to give 25 mm settlement, shown in Fig.5.26.

Parry (1971) proposed a simple empirical method for calculating settlement assuming that settlement is a function of the width of the loaded area, the magnitude of the bearing pressure and the deformation modulus of the soil. The equation to be used is:

$$\delta = \frac{a \,.\, q \,.\, B}{N} \,.\, C_D \,.\, C_W \,.\, C_T \tag{5.27}$$

where δ = settlement in mm; a = constant = 200 in SI units; q = applied pressure in MN/m^2; B = foundation width in m; N = measured average N value; C_D = factor for the influence of excavation; C_W = factor for the influence of the water table; C_T = factor for the thickness of the compressible layer.

N is taken as the measured value at a depth equal to $3\,B/4$ below foundation level if the N values vary consistently with depth. If otherwise, then:

- Take the average value of N between foundation level and a depth of $3\,B/4$ and multiply by three giving $3\,N_1$.
- Take the average value of N between depths $3\,B/4$ and $3\,B/2$ and multiply by two giving $2\,N_2$.
- Take the average value of N between $3\,B/2$ and $2\,B$ giving N_3. Then,

$$N = \frac{3\,N_1 + 2\,N_2 + N_3}{6} \tag{5.28}$$

C_D takes into account the fact that excavation for the foundation alters the stress system in the ground and hence the N values measured before excavation require modification. C_D is obtained from Fig.5.27. C_D is unity if the foundation is placed on a completely backfilled excavation.

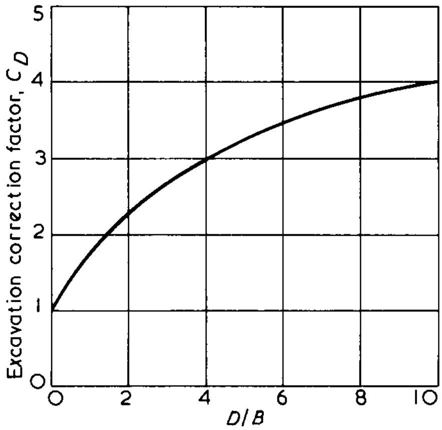

Fig.5.27 Excavation correction factor, C_D, after Parry (1971)

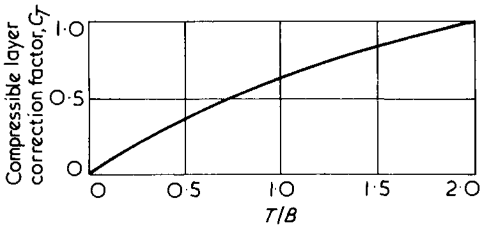

Fig.5.28 Correction factor for thickness of compressible material, after Parry (1971)

Table 5.7 Shape factor, m, after Alpan (1964)

L/B	1	1.5	2	3	5	10
m	1	1.21	1.37	1.60	1.94	2.36

C_W corrects for the influence of the water table. Assuming that the water table has an influence only within a depth of 2 B below foundation level, and taking D as the depth of the excavation and D_W the depth of the water table below ground surface.

$$C_W = 1 + \frac{D_w}{D + 3\,B/4} \text{ for } 0 < D_w < D \tag{5.29}$$

or,

$$C_w = 1 + \frac{D_w(2B + D - D_w)}{2B(D + 0.75\,B)} \text{ for } D < D_w < 2B \tag{5.30}$$

No correction is applied for surface footings or footings in backfilled excavations if the water table does not rise after the site excavation and during the life of the structure. If it is expected to rise, the measured N values should be reduced in direct proportion to the change in effective overburden pressure in the field.

The thickness, T, of the compressible sand stratum below the foundation is taken into account using the factor C_T, given in Fig.5.28. When deriving the curve for C_T, it was assumed that in a uniform soil, half the settlement occurs within a depth 3 $B/4$ below foundation level and the remaining half within a depth range 3 $B/4$ to $2B$ below foundation level.

The method proposed by Alpan (1964) is based on predicting the settlement, δ_p, of a plate 0.3 m square at foundation level using measured N values corrected for effective overburden pressure and then extrapolating this predicted settlement up to the settlement of the full scale structure, δ_B, using the Terzaghi and Peck correlation,

$$\delta_B = \delta_p \left[\frac{2B}{B + 0.3} \right]^2 \tag{5.31}$$

According to Alpan,

$$\delta_p = a_o \, . \, q \tag{5.32}$$

and therefore,

$$\delta_B = a_o \cdot q \cdot \left[\frac{2B}{B + 0.3} \right]^2 \tag{5.33}$$

$$= q \cdot a_B \tag{5.34}$$

where, q = applied foundation pressure; B = foundation width; a_o = reciprocal of the modulus of subgrade reaction for a 0.3 m plate. For other than square or circular foundations, δ_B is multiplied by a shape factor, m, given in Table 5.7.

The procedure is as follows.

The value of N at foundation level is corrected for the effective overburden pressure, p', at foundation level using Fig.5.29 by determining the relative density corresponding to N and p' and following the relative density curve to the Terzaghi–Peck curve and reading-off the corrected N value.

The corrected N is used in Fig.5.30 for low N values, or Fig.5.31 for high N values to give a_o, checking for lower N values, that the proposed applied pressure, q, is less than that defining the limit of the linear range. The ratio a_B/a_o is obtained from Fig.5.32, corresponding to the

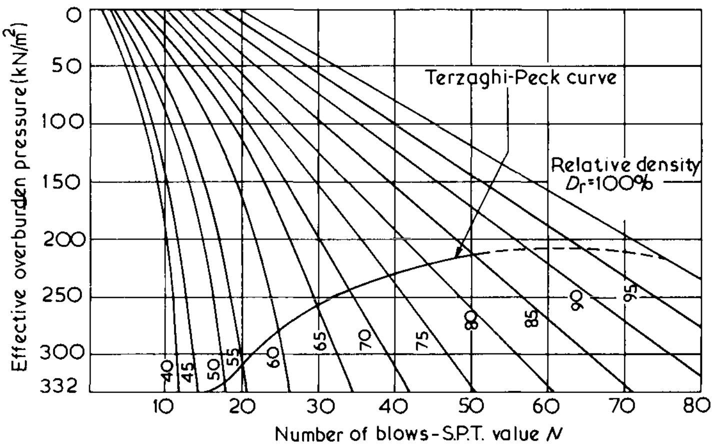

Fig.5.29 Correction factor for effective overburden pressure, after Alpan (1964)

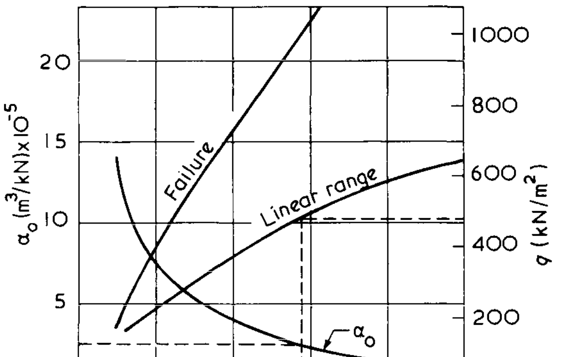

Fig.5.30 Determination of a_o, for low SPT 'N' values, after Alpan (1964)

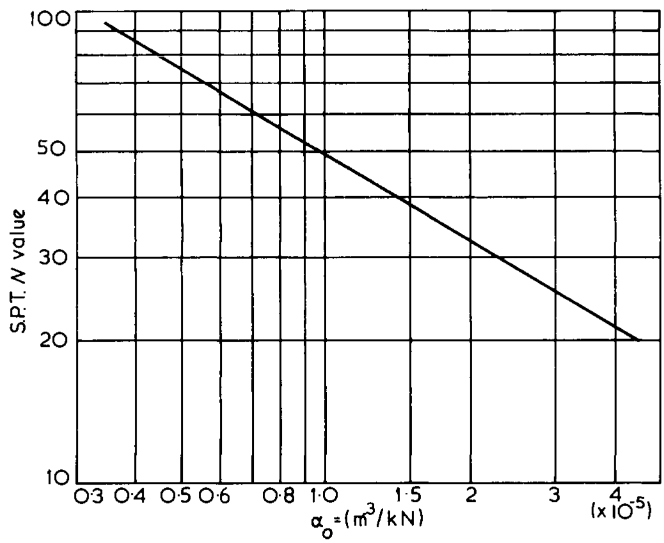

Fig.5.31 Determination of a_o, for high SPT 'N' values, after Alpan (1964)

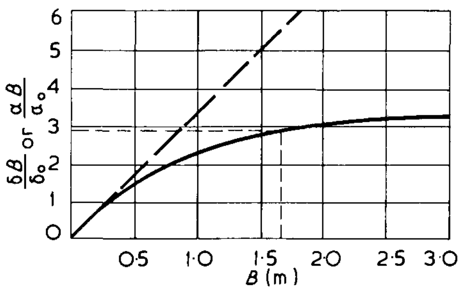

Fig.5.32 'Relationship between settlement ratio and foundation width, after Alpan (1964)

footing width, B. The settlement is then obtained from equation 5.34, applying the shape factor, m, if necessary.

The procedure can be criticized on the grounds that it is based on:

- N at foundation level and not on N averaged over the depth influenced by the foundation
- The Terzaghi and Peck relationship between settlement and foundation size is known to be subject to errors; see Fig.5.20.

6.5.1 Example following Alpan's procedure

Determine the settlement of a rectangular footing of length 3.4 m, and breadth 1.7 m, placed on a sand layer at a depth of 1.5 m. The applied pressure is 300 kN/m^2, the groundwater table is deep, N at foundation level is 10, and the bulk unit weight of the sand is 18.5 kN/m^3.

The effective overburden pressure at foundation level is $1.5 \times 18.6 = 27.9$ kN/m^2, from Fig.5.29, for $N = 10$, the relative density is 64% and the corresponding N on the Terzaghi–Peck curve is 29.

From Fig.5.30, for $N = 29$, $a_o = 0.25 \times 10^{-4}$ m^3/kN and since the linear range extends to about 470 kN/m^2, the applied pressure of 300 kN/m^2 is well below this.

From Fig.5.32, $a_B/a_o = 2.9$ for $B = 1.7$ m, and from Table 5.7, $m = 1.37$ for $L/B = 2$.

Hence,

$$\delta_B = m \,.\, q \,.\, a_B, \text{ from equation 5.34}$$

$$= 1.37 \times 300 \times 0.25 \times 10^{-4} \times 2.9$$

$$= 0.0298 \text{ m}$$

$$= 29.8 \text{ mm}$$

6.5.2 Example using various methods of predicting settlement

The various methods outlined above have been used to calculate the settlement for the example illustrated in Fig.5.33. The footing is founded on sand.

1. *de Beer and Martens*

$$\delta = \frac{H}{C} \log_e \frac{p'_o + \Delta_p}{p'_o}, \text{ equation 5.18}$$

The calculations are given in Table 5.8.

2. *de Beer and Martens,* but taking

$$C = 1.9 \frac{C_r}{p'_o}$$

The calculated settlement is $36.2 \times \frac{1.5}{1.9} = 28.6$ mm

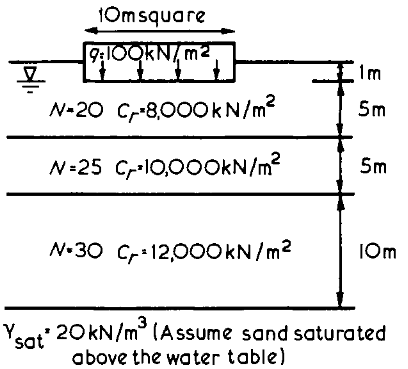

Fig.5.33 Example of settlement calculations

Table 5.8 Results of settlement calculations, following de Beer and Martens (1957)

Layer (m)	C_r (kN/m²)	p'_o (kN/m²)	$C = \frac{3}{2}\frac{C_r}{p'_o}$	$p'_o + \Delta_p$	$\frac{p_o + \Delta_p}{p'_o}$	$\log_e \frac{B'_o + \Delta_p}{p'_o}$	H (mm)	δ (mm)
0–5	8 000	45	267	119.8	2.66	0.978	5 000	18.3
5–10	10 000	95	158	133.4	1.40	0.336	5 000	10.6
10–20	12 000	170	106	184.4	1.08	0.077	10 000	7.3
						Total = 36.2 mm		

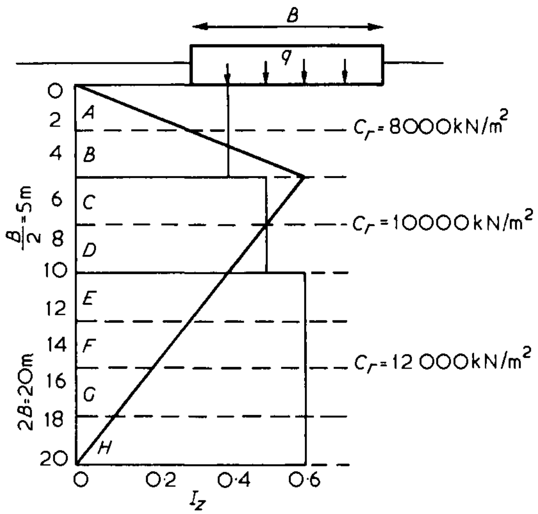

Fig.5.34 Determination of Schmertmann's influence factor

Table 5.9 Results of settlement calculations, following Schmertmann (1970)

Layer	H (mm)	C_r (kN/m²)	$E = 2\,C_r$	I_z	$\frac{I_z}{E} \cdot H$
A	2500	8 000	16 000	0.15	0.0234
B	2500	8 000	16 000	0.45	0.0703
C	2500	10 000	20 000	0.545	0.0681
D	2500	10 000	20 000	0.45	0.0562
E	2500	12 000	24 000	0.35	0.0365
F	2500	12 000	24 000	0.25	0.0260
G	2500	12 000	24 000	0.15	0.0156
H	2500	12 000	24 000	0.05	0.0052
					Sum = 0.3013

3. *Schmertmann.* The influence factor I_z is obtained from Fig.5.34.

$$\delta = C_1 C_2 \Delta_p \, \Sigma \, \frac{I_z}{E} \, . \, H, \text{ equation 5.20.}$$

The calculations are given in Table 5.9

$$C_1 = 1 - 0.5 \left[\frac{p'_o}{\Delta_p} \right] = 1 - 0.5 \, \frac{20}{80} = 0.875$$

$$C_2 = 1 + 0.2 \log_{10}\left[\frac{t}{0.1}\right] = 1 + 0.2 \log_{10} 50 = 1.34 \text{ assuming five year creep period.}$$

Therefore

$$\delta = 0.875 \times 1.34 \times 80 \times 0.3013 = 28.3 \text{ mm}$$

4. *Terzaghi–Peck original proposal* (from Fig.5.24).

N	B(m)	q for 25 mm (kN/m^2)	δ (mm)
22.5	10	95 (high groundwater table)	26.3

5. *Meyerhof (1955)*

$$= \frac{2.84 \,.\, q}{N}\left[\frac{B}{B + 0.33}\right]^2$$

$$= \frac{2.84 \times 100}{22.5}\left[\frac{10}{10.33}\right]^2$$

$= 11.8$ mm

6. *Terzaghi–Peck modified by Meyerhof (1965)*

N	B (m)	q for 25 mm (kN/m^2)	δ (mm)
22.5	10	190×1.5	$\frac{25 \times 100}{285} = 8.8$

7. *Terzaghi–Peck using Tomlinson's correction for p_o'*

N	p_o' (kN/m^2)	Correction factor	$N_{cor.}$	q for 25 mm (kN/m^2)	δ (mm)
22.5	70	2.2	49.5	450	5.6

8. *Peck and Bazaraa*

N	p_o' (kN/m^2)	Factor for p_o'	Factor for water table	q for 25 mm (kN/m^2)	δ (mm)
22.5	70	1.0	$\frac{6 \times 20}{20 + 5 \times 10} = 1.7$	$190 \times 1.5 = 285$	$\frac{100}{285} \times 1.7 \times 25 = 14.9$

9. *Parry*

$$\delta = \frac{aqB}{N_m} C_D C_w C_T, \text{ equation 5.27.}$$

N_m	B (m)	T (m)	D (m)	C_D	C_T	q (kN/m^2)
25	10	20	1.0	1.1	1.0	0.1

$$D_w = 1.0 \text{ m}, C_w = 1 + \frac{D_w}{D + 3\,B/4} = 1 + 0.118 = 1.118$$

$$\delta = \frac{200 \times 0.1 \times 10}{25} \times 1.1 \times 1.118 \times 1.0 = 9.8 \text{ mm}$$

10. *Alpan*

p_o' f.l. (kN/m^2)	N_m	D_r (%)	N_C	a_o (m^3/KN)	B (m)	a_B/a_o	q (kN/m^2)	Shape factor	δ (mm)
20	20	92	60	0.72×10^{-5} (linear)	10	3.77	100	1	2.71

For a high groundwater table the predicted settlement is increased by 100%. Therefore, δ = 5.4 mm.

The calculated settlements according to the various methods are collected together in Table 5.10.

It can be seen that widely differing predictions result from the various methods. It must be stressed that in other situations, while a scatter in predicted settlements must be expected, the relative differences between the methods may well be quite different.

Simons, Rodriques and Hornsby (1974) used eight of the above methods to predict the settlements of six structures for which settlements have been observed. The results are summarized in Table 5.11. It can be seen that while Alpan's method, based on the SPT and Schmert-

Table 5.10 Calculated settlements by 10 methods for example in Fig.5.33

Method	Calculated settlement	Field test
de Beer and Martens	36	Cone test
de Beer and Martens with $C = 1.9\ C_r/p_o'$	29	Cone test
Schmertmann	28	Cone test
Terzaghi–Peck	26	SPT
Meyerhof	12	SPT
Terzagi–Peck modified by Meyerhof	9	SPT
Terzaghi–Peck modified by Tomlinson	6	SPT
Peck and Bazaraa	15	SPT
Parry	10	SPT
Alpan	5	SPT

Table 5.11 Calculated settlements by eight methods for six structures where settlements have been observed

Method	$\frac{\delta_{calc.}}{\delta_{obs.}}$ average	$\frac{\delta_{calc.}}{\delta_{obs.}}$ range
de Beer and Martens	3.22	1.0–4.8
Schmertmann	1.48	0.2–4.0
Terzaghi and Peck	1.89	0.5–3.2
Terzaghi and Peck, modified by Meyerhof	0.70	0.2–1.1
Terzaghi and Peck, modified by Tomlinson	0.31	0.1–0.6
Peck and Bazaraa	0.63	0.3–1.4
Alpan	0.95	0.1–2.4
Parry	0.72	0.1–1.3

mann's method using the Dutch static cone give the best agreement with observed settlements on average, the ranges of calculated to observed settlement are very wide indeed and hence in any single case, the calculated settlement may be quite different from that actually experienced.

This is perhaps not surprising as neither the SPT nor the Dutch cone test measures soil compressibility directly, and in particular, the test results will not indicate whether a granular deposit is normally or over-consolidated, and this is one important factor which will influence the settlement which will develop. The use of *in situ* plate loading tests which at least measure soil compressibility would seem to lead to more reliable predicted settlements.

7 Allowable settlements

The allowable settlement of a structure, that is, the amount of settlement a structure can tolerate, depends on several factors, for example the type of structure, its height, rigidity, function, and location; and the magnitude, rate and distribution of settlement.

It is important to distinguish between:

- Total settlement, which may cause damage to the services of the structure
- Differential settlement as a result of tilt which may be noticeable in high buildings
- Differential settlement due to shear distortion, which may lead to structural damage.

The foundation engineer, ideally, is required to predict the amount of differential settlement, due to tilt or distortion, which a structure can tolerate, and then to predict the differential settlement which will actually occur resulting from the structural loading and the ground conditions.

In reality it is difficult – if not impossible – to predict either because of the difficulty of taking into account the interaction of the various structural elements, the redistribution of load as the structure settles differentially, and the time factor. The slower the settlements develop, the greater will be the settlements a structure is able to withstand without damage, because of creep in the structure, hence the settlement criteria are different for buildings on sand and on clay. In addition, it is not possible in practice to determine with any degree of accuracy the variations in thickness and compressibility of the various strata underlying a structure. Finally, it is necessary to take into account that types of cracks inevitably appear in all buildings due to other causes, requiring maintenance expenses independent of whether or not cracks result from settlement.

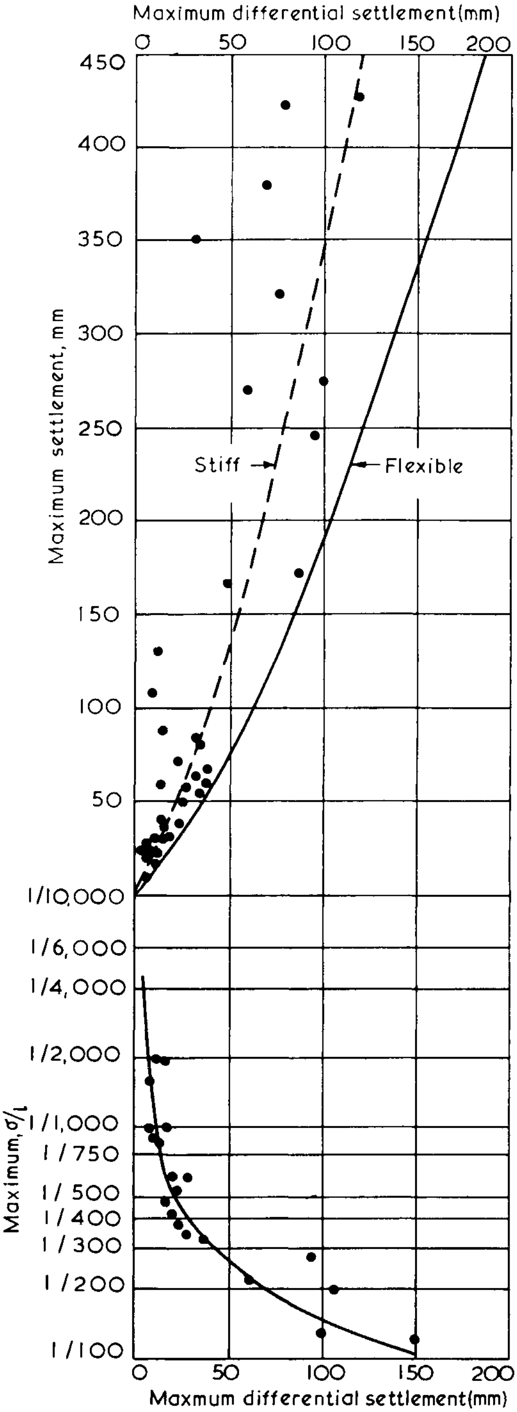

Fig.5.35 Relationship between maximum settlement, maximum differential settlement and maximum angular distortion for clays, after Bjerrum (1963a)

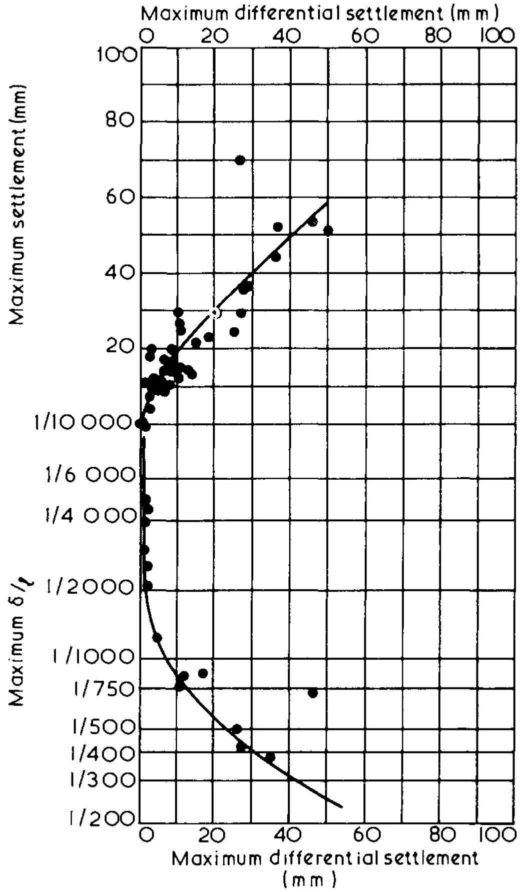

Fig.5.36 Relationship between maximum settlement, maximum differential settlement and maximum angular distortion for sands, after Bjerrum (1963a)

For these reasons, observation has been used as a basis for suggesting tolerable limits to settlements (Skempton and MacDonald, 1955; Bjerrum, 1963a, b).

Because maximum settlements can be predicted with some accuracy (but not differential settlements) it is usual to relate allowable settlements to maximum settlements.

Skempton and MacDonald (1955) suggested the following design limits for maximum settlements:

Isolated foundations on clay	65 mm
Isolated foundations on sand	40 mm
Rafts on clay	65 mm to 100 mm
Rafts on sand	40 mm to 65 mm

The smaller limits placed on foundations on sand are due partly to the time factor discussed previously, and also to the fact that granular soils tend to be less homogeneous than clays.

Bjerrum (1963a, b), taking into account additional information, made proposals to relate allowed maximum settlements to angular distortion, defined as the settlement difference between two points divided by the horizontal distance apart.

Table 5.12 shows the types of damage which can be expected for various values of the angular distortion, and it can be seen that damage to structural elements will occur at larger distortions than will cause trouble to machinery.

Table 5.12 Suggested correlation between type of structural problem and angular distortion, after Bjerrum (1963b)

Type of problem	δ/L
Difficulties with machinery sensitive to settlement	1/750
Danger for frames with diagonals	1/600
Limit for buildings where cracking is not permissible	1/500
Limit where first cracking in panel walls is to be expected, or where difficulties with overhead cranes are to be expected	1/300
Limit where tilting of high buildings may be noticeable	1/250
Considerable cracking in panel and brick walls. Safe limit for flexible brick walls where $h/L < 1/4$	1/150
Limit where structural damage may occur	

Bjerrum (1963b) related maximum settlements to maximum observed differential settlements and then to corresponding maximum angular distortions for clays, Fig.5.35, and for sands, Fig.5.36.

The procedure is to estimate the maximum settlement a structure is likely to experience, using the procedures outlined in this chapter and then, using Fig.5.35 for structures founded on clays and Fig.5.36 for structures founded on granular soils, read of the likely maximum angular distortion. Table 5.12 then indicates the type of damage which may be expected.

An interesting point to note is that many structures have been subjected to settlements of considerable magnitude, apparently without experiencing sufficient damage to render them unserviceable. Table 5.4 shows observed or extrapolated maximum settlements greater than 200 mm, at an arbitrary time of 20 years, for a number of structures. Oil tanks have not been included in Table 5.4, although many have experienced maximum settlements greater than 200 mm without damage.

6 Piled foundations

1 Introduction

The following aspects of pile design are considered:

(a) Types of pile
(b) Piles in cohesive soils
(c) Piles in granular soils
(d) Group action of piles
(e) Negative skin friction
(f) Piles under lateral loads
(g) Testing of piles.

Three design criteria should be kept in mind:

(a) The pile material itself must not be over-stressed
(b) There must be an adequate factor of safety against a shear failure
(c) The settlements must be within tolerable limits.

It should be noted that piles may be required for a variety of reasons, for example, to:

(a) Transfer load to a stronger and/or less compressible stratum
(b) Carry horizontal forces from bridge abutments or retaining walls
(c) Increase the stability of tall buildings
(d) Carry uplift forces
(e) Avoid scour damage
(f) Compact loose sands.

In any situation, the type of pile chosen and the design method used will be influenced by the factors which governed the decision to use piles in the first place.

It should be emphasized that although in the following sections the methods outlined for predicting the bearing capacity of piles are based on field and laboratory tests, pile loading tests should be carried out whenever circumstances permit, as a check on the computations.

2 Types of pile

Piles may be classified in a number of ways. Following the Code of Practice for Foundations, CP 2004:1972, which is based on the effect the pile has on the soil during installation, piles are considered to fall into three main classes: very large displacement, small displacement, and non-displacement, with further sub-divisions as shown in Fig.6.1.

There are numerous types of pile, either proprietary or non-proprietary, in the above groups. Considering the technical factors listed below narrows the choice to two or three types and the final choice is generally made on overall cost, although the reputation of a particular piling contractor may well prove to be a decisive influencing factor.

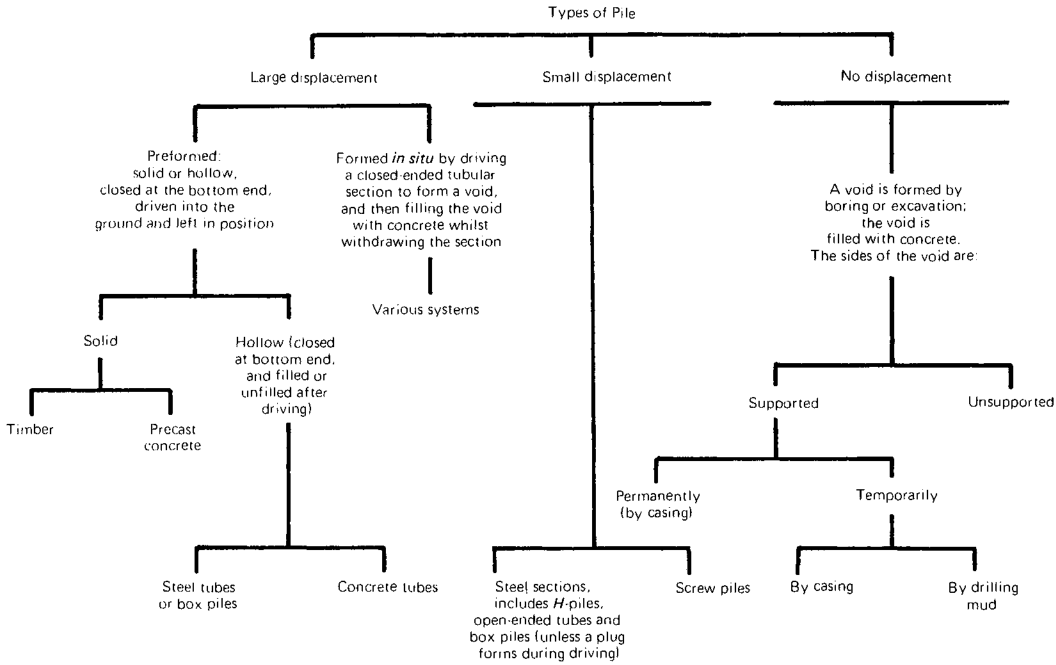

Fig. 6.1 Classification of piling systems

2.1 Factors governing the choice of pile type

Vital factors to be taken into consideration when determining the type of pile to be used are:

- The location and type of structure
- Ground conditions, including the position of the ground water table
- Durability in the long term. Timber piles are subject to decay, particularly above the water table, and to attack by marine borers. Concrete is liable to chemical attack in the presence of salts and acids in the ground, and steel piles may suffer from corrosion, if the specific resistivity of the clay is low and the degree of depolarization is high
- Overall cost to the client. The cheapest form of piling is not necessarily the cheapest pile per metre run. Delays to the contract owing to lack of experience or lack of appreciation of a particular problem by the piling contractor may add considerably to the total cost of a project. The cost of pile testing should be considered if the piling contractor has insufficient experience to establish the required pile length or diameter. In particular, heavy additional costs to the contract may be incurred if piles fail under test load. It is advantageous to use a reputable firm with good local experience. It should be stressed that most delays and troubles on piling contracts can be avoided by carrying out a thorough site investigation at as early a stage as possible.

2.2 Large displacement piles

2.2.1 Driven and cast-in-place

The advantages are:

- Can be driven to a predetermined set
- Pile lengths are readily adjustable
- An enlarged base can be formed which can increase the relative density of a granular founding stratum leading to much higher end bearing capacity
- Reinforcement is not determined by the effects of handling or driving stresses

- Can be driven with a closed end so excluding the effects of ground water
- Noise and vibration can be reduced in some types, for example by driving on a plug at the bottom of the pile.

The disadvantages are:

- Heave of neighbouring ground surface, which could affect nearby structures or services
- Disturbance of the soil, which could lead to reconsolidation and the development of negative skin friction forces on piles
- Displacement of nearby retaining walls
- Lifting of previously driven piles, where the penetration at the toes of the piles into the bearing stratum has not been sufficient to develop the necessary resistance to upward forces
- Tensile damage to unreinforced piles or piles consisting of green concrete, where forces at the toe have been sufficient to resist upward movements
- Damage to piles consisting of uncased or thinly cased green concrete due to the lateral forces set up in the soil, for example, necking or waisting
- Concrete cannot be inspected after completion
- Concrete may be weakened if artesian flow pipes up shaft of piles when tube is withdrawn
- Light steel sections or precast concrete shells may be damaged or distorted by hard driving
- Limitation in length owing to lifting force required to withdraw casing
- Noise, vibration and ground displacement may cause a nuisance or may damage adjacent structures
- Cannot be driven with very large diameters nor can very large end bulbs be formed
- Cannot be driven where headroom is limited.

Pile lengths of up to 24 m and pile loads of about to 1500 kN are common.

2.2.2 *Driven precast reinforced or prestressed concrete piles*

The advantages are:

- Can be driven to a predetermined set
- Stable in squeezing ground, for example, soft clays, silts and peats
- Pile material can be inspected before piling
- Can be redriven if affected by ground heave
- Construction procedure unaffected by ground water
- Can be driven in long lengths
- Can be carried above ground level, for example, through water for marine structures
- Can increase the relative density of a granular founding stratum.

The disadvantages are:

- Heave and disturbance of surrounding soil may cause difficulties, as discussed above for driven and cast-in-place piles
- Cannot readily be varied in length
- May be damaged due to hard driving
- Reinforcement may be controlled by handling and driving requirements rather than by stresses caused by structural loads
- Cannot be driven with very large diameters or in conditions of limited headroom
- Noise, vibration and ground displacements may cause difficulties.

Pile lengths up to 27 m and pile loads up to 1000 kN are usual.

2.2.3 *Timber piles*

Timber piles are light, easy to handle and, in some countries, cheap. They can be joined together and can be provided with driving points. Timber piles are liable to decay and attack by marine borers and generally are only used below the water table but can be pressure impregnated to provide protection above the water table. They are usually used as friction piles but, on occasions, as point bearing piles. In this case, care must be taken to avoid damage owing to overdriving. The danger of damaging the pile during driving can be reduced by limiting the drop and the number of blows of the hammer. The weight of the hammer should at least be equal to the weight of the pile for hard driving conditions and not less than half the weight of the pile for easy driving. Pile lengths up to 20 m and loads up to 600 kN are usual.

2.3 Small displacement piles

Examples of these piles are rolled steel sections, screw piles, or open-ended tubes and hollow sections where the soil is removed during penetration. Some of the remarks listed under Section 2.2 apply.

Rolled steel section piles are easily handled and can be driven hard. They can be driven in very long lengths and the pile length can be readily varied. They can carry heavy loads and can be successfully anchored in steeply sloping rock surfaces (Bjerrum, 1957). The piles are liable to corrosion which can be allowed for in design or can be treated using cathodic protection, or the piles can be coated.

Screw piles are valuable in marine works because they can resist both tensile and compressive forces.

In general, small displacement piles are particularly useful if ground displacements and disturbance must be severely curtailed.

Rolled steel section piles are used up to 36 m in length with pile loads of up to 1700 kN, and with screw piles, lengths of up to 24 m with working loads up to 2500 kN are possible.

2.4 Bored and cast-in-place non-displacement piles

2.4.1 Advantages

- No risk of ground heave
- Length can be readily varied
- Soil can be inspected and compared with site investigation data
- Can be installed in very long lengths, with very large diameters, and end enlargements of up to two or three pile diameters are possible in clays and soft rocks
- Reinforcement is not dependent on handling or driving conditions
- Can be installed without appreciable noise or vibration, and under conditions of limited headroom.

2.4.2 Disadvantages

- Boring methods may loosen sandy or gravelly soils or change soft rocks to a slurry, for example, chalk or marl
- Susceptible to waisting or necking in squeezing ground
- Difficulties with concreting under water. The concrete cannot subsequently be inspected
- An inflow of water may cause damage to the unset concrete in the pile or may cause a disturbance to the surrounding ground leading to reduced pile bearing capacity
- Enlarged ends cannot be formed in granular soils.

Concrete should be placed as soon as possible after boring the hole, to avoid softening of the ground. It is important to have adequate workability, so that the concrete can flow against the walls of the shaft. In practice, this means that the concrete slump should be in the range of 100 mm to 150 mm. To avoid segregation, honeycombing, bleeding and other defects resulting from high water content, the use of a plasticizing additive may be beneficial. In general, the concrete should contain not less than 300 kg of cement per cubic metre.

Pile lengths of up to 45 m with loads of up to 10 000 kN are not unusual.

3 Piles in cohesive soils

Piles in cohesive soils, apart from short under-reamed piles of large diameter, generally carry most of the load on the pile shaft. The bearing capacity is usually predicted on the basis of undrained shear strength data, although an effective stress approach has been proposed (Burland, 1973).

The failure load Q_f, of a pile is given by:

$$Q_f = \text{load carried on the shaft} + \text{load carried on the base}$$

$$= s \,.\, c_s \,.\, A_s + (N_c \,.\, A_b \,.\, s_u + \gamma D A_b) \tag{6.1}$$

where A_s = area of pile shaft; A_b = area of base of pile; s_u = undrained shear strength at base of pile; c_s = average adhesion between shaft and clay; N_c = bearing capacity factor; D = length of pile; γ = bulk unit weight of clay; s = shape factor, =1.0 for a plain shaft, =1.2 for a tapered pile.

The weight of a pile is approximately equal to $\gamma \,.\, D \,.\, A_b$. Thus, the load, P_f, causing failure of a pile is given by:

$$P_f = N_c \,.\, A_b \,.\, s_u + s \,.\, c_s \,.\, A_s \tag{6.2}$$

The allowable load, P_a, is given by:

$$P_a = \frac{N_c \,.\, A_b \,.\, s_u}{F_1} + \frac{s \,.\, c_s \,.\, A_s}{F_2} \tag{6.3}$$

or

$$P_a = \frac{N_c \,.\, A_b \,.\, s_u}{F_1} + \frac{s \,.\, \bar{s}_u \,.\, a \,.\, A_s}{F_2} \tag{6.4}$$

where $\bar{s}_u$ = average undrained shear strength over the length of the pile and,

$$a = \text{adhesion factor}$$

$$= c_s / \bar{s}_u \tag{6.5}$$

The first term presents no difficulty because N_c can be taken as being equal to nine (for large diameter short piles a reduced value from Fig.4.4 can be used) and the undrained shear strength can be obtained with sufficient accuracy if the factors outlined in chapter 2 are taken into account. In addition, the load carried on the base is generally small compared with that carried on the shaft and so an error in the estimation of the base load is of less significance.

The major problem, therefore, is the determination of the adhesion mobilized between the shaft and the clay.

3.1 Driven piles

Driving piles into cohesive soils causes radical changes to the soil strength, and phenomena like remoulding, ground heave, the formation of an enlarged hole, and strain softening affect the adhesion developed between pile and clay.

With the passage of time, reconsolidation of the clay around the pile will occur and hence the adhesion will depend on the time elapsed between pile driving and pile loading or testing. Experience has shown that at least 30 days should elapse between driving and testing in order to allow equilibrium conditions to be re-established in the clay. With some clays, 90 days may

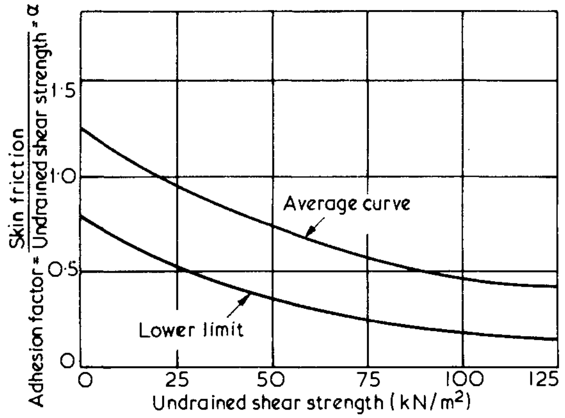

Fig. 6.2 Relationship between adhesion factor for driven piles and undrained shear strength of clay, after Tomlinson (1969)

be more suitable. It should also be noted that on any one site the adhesion factor may vary to a certain extent from pile to pile.

The problem of the variation of the adhesion factor has been studied by Tomlinson (1957), Peck (1958), Nordlund (1959), Woodward, Lundgren and Boitano (1961), Flaate (1968), Tomlinson (1970 and 1971).

Fig.6.2, after Tomlinson (1969), shows the variation of the adhesion factor with the undrained shear strength of the clay. The drop in adhesion factor with increasing strength of the clay is most marked.

It should be stressed that Fig.6.2 can only be expected to give an approximate indication of the failure load of a driven pile in clay, because of the large variation in the adhesion factors for any given shear strength.

Flaate (1968), after a comprehensive analysis of a number of pile loading tests suggested that α depended not only on the average undrained shear strength of the clay, but also on the plasticity index and made the proposals shown in Fig.6.3. It should be noted that very few tests were analysed in the firm to stiff range of clay strength.

The work of Tomlinson (1957, 1970, 1971), has greatly clarified the position regarding adhesion factors for piles driven into stiff clays. Piles driven into stiff to hard cohesive soils without any soft or loose overburden cause a heave of the ground surface around the pile. Radial cracks develop and a gap is formed between the pile and the soil. Tomlinson (1957) noted the significance of this gap in reducing the skin friction of piles in clays and stated that it was probably due to lateral vibrations or 'whip' of the piles during driving. Perhaps even more important, Tomlinson (1970, 1971), showed that the adhesion factor is influenced by the presence of other soils overlying the stiff London clay. Overlying soft clay results in smaller adhesion factors, while overlying granular soils give greater factors. He observed that driven piles generally give higher adhesion factors than jacked piles.

Important conclusions resulting from Tomlinson's work are as follows:

- Where piles are driven through sands or sandy gravels, these soils are carried down to a limited depth forming a skin of compacted sand or sand/clay mixture around the shaft. This skin has a high skin friction value such that piles driven to penetrations of less than 20 diameters into the stiff cohesive soils can have an ultimate skin frictional resistance exceeding 1.25 times the undrained shear strength of the soil. For greater penetrations, the effect of the skin of granular material becomes progressively less and the adhesion factor tends to decrease with increasing shear strength of the soil.

- Where piles are driven through soft clays or silts into stiff to very stiff cohesive soils, a soft skin is carried down, again to a limited depth, but the skin gains somewhat in shear strength owing to consolidation. The soft skin has a considerable weakening effect on the frictional resistance on the shaft where the pile penetrates the stiff cohesive soil by less than 20 diameters. An adhesive factor of 0.4 should be used for these conditions subject to a minimum penetration of 8 diameters. Beyond 20 diameters penetration, the adhesion factor appears to be fairly constant for undrained shear strengths between 70 and 140 kN/m^2 at an average value of 0.70.

Piles driven into stiff to very stiff cohesive soils extending from the surface downwards cause a gap to form around the upper part of the shaft such that skin friction cannot be assumed to act over this part. The gap is of considerable significance where piles are driven to a penetration of less than 20 diameters, where an adhesion factor of 0.4 may be adopted for penetrations between 8 and 20 diameters. For piles driven deeper than 20 diameters the adhesion factor is governed by the shear strength of the soil, decreasing from unity for undrained shear strengths up to 90 kN/m^2 to 0.4 at a strength of 170 kN/m^2.

For the case of steel *H* piles, the adhesion is usually calculated on a perimeter equal to twice the flange width plus twice the web depth, and the end bearing on the gross cross-sectional area, that is, the flange width times the web depth.

An overall factor of safety of 2.5 is often used, and it has been suggested that partial factors of safety are appropriate, for example, 3 on end bearing and, say, 1.5 on shaft resistance. This is in an attempt to take into account the fact that the shaft resistance may be fully mobilized at a deformation of the order of 2–7 mm, whereas the base resistance requires a greater deformation for full mobilization.

The material of the pile does not appear to be of any great significance, although it is commonly believed that timber and concrete piles should have higher adhesion factors than smooth steel piles. For examples, the Code of Practice of the Danish Society of Engineers (1966) suggests multiplying the calculated adhesion by unity for timber and concrete piles and by 0.7 for steel piles. If the pile material is coated by bitumen, for example, greatly reduced adhesion will result. An interesting case has been described by Hutchinson and Jensen (1968). Reinforced concrete test piles driven into soft silty clays at Khorramshar failed to reach their predicted carrying capacity by quite a wide margin. In a subsequent investigation of the difficulties, Hutchinson and Jensen made the interesting observation that the skin friction at the pile/soil

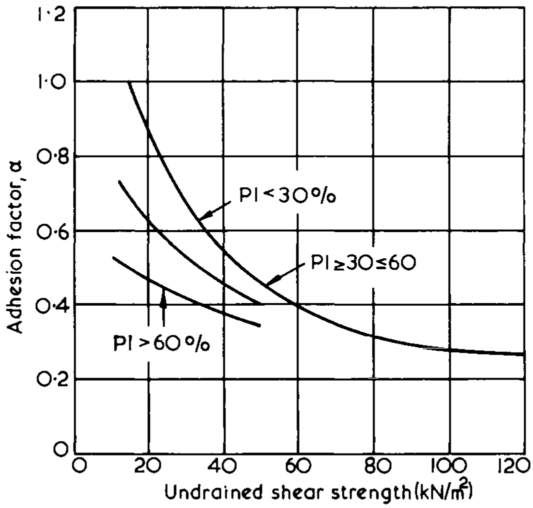

Fig. 6.3 Relationship between adhesion factor for driven piles and undrained shear strength of clay, after Flaate (1968)

interface had been considerably weakened by the 1–2 mm thick coating of soft bitumen applied to the piles to protect them from acid attack. The skin friction developed on the coated piles was only 30 to 80% of that on the uncoated piles.

3.2 Cast *in situ* bored piles

The process of boring a hole for a pile seriously disturbs the clay in the immediate neighbourhood of the hole. Placing the concrete causes water to be absorbed by the clay surrounding the pile, leading to softening and reduced strength. The base resistance and adhesion of bored piles in the London clay has been extensively studied (Skempton, 1959; Burland, Butler and Dunican, 1966; Whitaker and Cooke, 1966; Butler and Morton, 1971; Burland and Cooke, 1974).

Skempton (1966) has suggested *first approximation design rules*, which are given below.

The load on the shaft, P_s, is given by:

$$P_s = A_s \times 0.45 \times \bar{s}_u \tag{6.6}$$

The load on the base, P_b, is given by:

$$P_b = A_b \times 9 \times w \times s_u \tag{6.7}$$

where $w = 0.8$ for $B < 1$ m and 0.75 for $B > 1$ m; A_s = area of shaft; A_b = area of base; $\bar{s}_u$ = average undrained shear strength along the shaft; s_u = undrained shear strength at the base.

These undrained shear strengths are based on traditional 38 mm diameter triaxial tests on $U-4$ open drive samples using average values. If the strength is measured in a different way, that is, using plate loading tests or larger samples, then different coefficients of correlation will result.

The working load (WL) is then given as follows:

$$\text{For plain shafts, WL} = \frac{\text{Total}}{2} \tag{6.8}$$

For belled piles

$$\text{(i) WL} = \frac{\text{Total}}{2.5} \text{ with } B < 2 \text{ m} \tag{6.9}$$

$$\text{or (ii) WL} = \frac{\text{Shaft}}{1.5} + \frac{\text{Base}}{3} \tag{6.10}$$

For $B > 2$ m, the working load is to be evaluated from settlement considerations. Finally, the settlements of the structure should be checked.

For the case of short bored piles in London clay, where the clay may be heavily fissured at a shallow depth, the adhesion factor should be taken as 0.3.

It must be stressed that the adhesion factor of 0.45 is an average value and may vary from site to site and may also vary on any one site, if the workmanship and the method of construction is allowed to vary. The adhesion factor may be lower for belled piles because of the greater time involved in constructing such piles. The time elapsed between drilling and correcting is important. Generally, piles should be concreted immediately after they are drilled. Water added to assist the drilling operations may lead to lower values of the adhesion factor.

For belled piles, it has been suggested that the shaft resistance should be ignored for a distance of two base diameters above the top of the under-ream.

Based on research carried out by the Building Research Station, UK, Burland and Cooke (1974) have proposed a simple and logical method for determining the allowable working loads for piles in stiff clays having a wide range of dimensions. Using their approach, the corresponding settlements are likely to be acceptable for most common structures and they further indicate how the immediate settlements for a single pile can be estimated with tolerable accuracy. The discussion which follows draws heavily on their paper.

The significance of pile geometry on pile behaviour was not appreciated until tests on bored piles were carried out in which the shaft and base components of resistance were separated. Whitaker and Cooke (1966) have tested bored piles with load cells incorporated in each shaft immediately above the base, and so it was possible to measure separately the development of shaft and base forces as the applied load was increased and the pile settled. The results presented by Whitaker and Cooke show that the two components are mobilized at entirely different rates of settlement. For most practical purposes the load settlement relationships for the shaft and the base are independent of each other. The frictional resistance on the shaft develops rapidly and almost linearly with settlement and is generally fully mobilized when the settlement is about 0.5% of the shaft diameter. Thereafter, it either remains sensibly constant, or decreases slightly as the settlement is increased further. On the other hand, the base resistance is seldom fully mobilized until the pile settlement reaches 10 to 20% of the base diameter. The load settlement relationship is normally far from linear although it is often convenient to assume that it is linear for loads less than about 1/3 of the ultimate base resistance.

The shape of the total load settlement curve for a bored pile depends on the relative load contributions of the shaft and the base. A test on a long straight shafted pile will result in a total settlement curve of the form shown in Fig.6.4(a), while relatively short piles with large under-reams exhibit behaviour of the form illustrated in Fig.6.4(b).

If piles are designed to carry a working load equal to 1/3 to 1/2 the total failure load, it can be seen from Fig.6.4(b) that for piles with large under-reams there is every likelihood of the shaft resistance being fully mobilized at the working load. This has an important bearing on design which is discussed later.

It has been shown that the behaviour of a bored pile can lie anywhere between that of a friction pile (i.e. long straight shafted pile) and that of a deep footing (i.e. a short under-reamed pile). A load factor criterion for design is therefore required which is applicable over the complete range. It has already been stressed that the deflections required to mobilize end bearing are much larger than those required to mobilize the full shaft adhesion. Thus, if the base is operating at a reasonable factor of safety, the shaft adhesion will be at, or very close to, its ultimate value. Therefore, Burland, Butler and Dunican (1966) suggested two simple stability criteria which impose a minimum overall load factor, F, with the additional proviso that a factor of safety in end bearing, F_b, is not exceeded. This proviso will normally only apply when the shaft friction is fully mobilized. These conditions may be written:

$$P_a \leqslant \frac{L_B + L_s}{F} \tag{6.11}$$

and

$$P_a \leqslant L_s + \frac{L_B}{F_B} \tag{6.12}$$

where P_a = working load; L_B = ultimate base load; L_s = ultimate shaft load; F = overall load factor, often taken as 2.0; F_B = factor of safety in end bearing, usually taken as three.

Methods for evaluating L_B and L_s have already been described. Put simply, equation 6.11 ensures overall stability while equation 6.12 guards against local over-stressing. Equation 6.12 only applies when the base diameter, D, is large compared with the shaft diameter, d.

To predict the short term undrained behaviour of a bored pile, the procedure outlined by Burland, Butler and Dunican (1966) is suggested. It is based on the assumption that the load settlement curve for the pile shaft is linear up to full mobilization which takes place at a settlement of 0.5% of the shaft diameter. As far as the base is concerned, Burland, Butler and Dunican found that, to a good approximation,

$$\frac{\delta}{D} = K \cdot \frac{q}{q_s} \tag{6.13}$$

where δ = settlement of the base; D = base diameter; q = applied pressure; q_s = ultimate pressure; K = factor varying from 0.01 to 0.02.

In any problem, K can be determined from a large *in situ* plate loading test, or if this is not possible, can be taken conservatively as 0.02.

The method of design is illustrated by an example which is reproduced from Burland and Cooke (1974).

Example: Test pile, P, Whitaker and Cooke (1966)

Details: Length of shaft = 14.5 m
Diameter of shaft = 0.94 m
Diameter of base = 1.86 m
$\bar{s}_u = 128\ \text{kN/m}^2$
$s_u = 150\ \text{kN/m}^2$

Required: With $F = 2$ and $F_b = 3.0$, find the maximum safe working load and draw the load settlement diagram up to working load. It is assumed that the shear strength values quoted are representative for the clay *in situ*.

$$L_s = a \cdot \bar{s}_u \cdot A_s$$

$$= 0.45 \times 128 \times \pi \times 0.94 \times 14.5$$

$$= 2466\ \text{kN}$$

$$L_B = 9 \times s_u \times A_b$$

$$= 9 \times 150 \times \pi/4 \times 1.86^2$$

$$= 3668\ \text{kN}$$

Now, from equation 6.11 (overall stability),

$$P_a = \frac{2466 + 3660}{2} = 3063\ \text{kN}$$

And, from equation 6.12 (over-stressing of base),

$$P_a = 2466 + \frac{3660}{3} = 3686\ \text{kN}$$

Therefore, the working load is 3063 kN.

It is assumed that the settlement will be large enough to mobilize the full shaft adhesion i.e. $L_s = 2466$ kN.

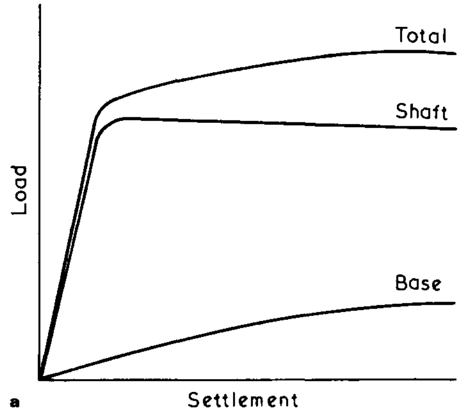

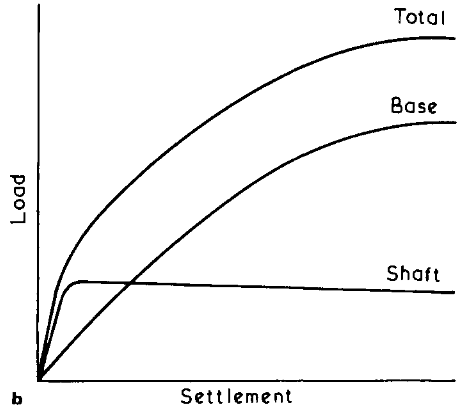

Fig.6.4 (a) Load settlement relationship for long straight shafted bored pile in London clay; (b) load settlement relationship for short under-reamed bored pile in London clay, after Burland and Cooke (1974)

Therefore, the load on the base is (3063 – 2466) = 597 kN.
Now, from equation 6.13,

$$\delta = D \times \frac{Q}{Q_u} \times K$$

$$= 1.86 \times \frac{597}{3668} \times 0.02$$

$$= 6 \text{ mm.}$$

The settlement required to mobilize fully the shaft friction is $(0.5/100) \times 940 = 4.7$ mm. Thus the assumption of full mobilization is valid.

Fig.6.5 shows the load settlement curves for the shaft, the base and the complete pile (being the sum of the previous two), together with the results of an incremental load test. The analysis is in remarkable agreement with the observations, and this must to some extent be considered fortuitous.

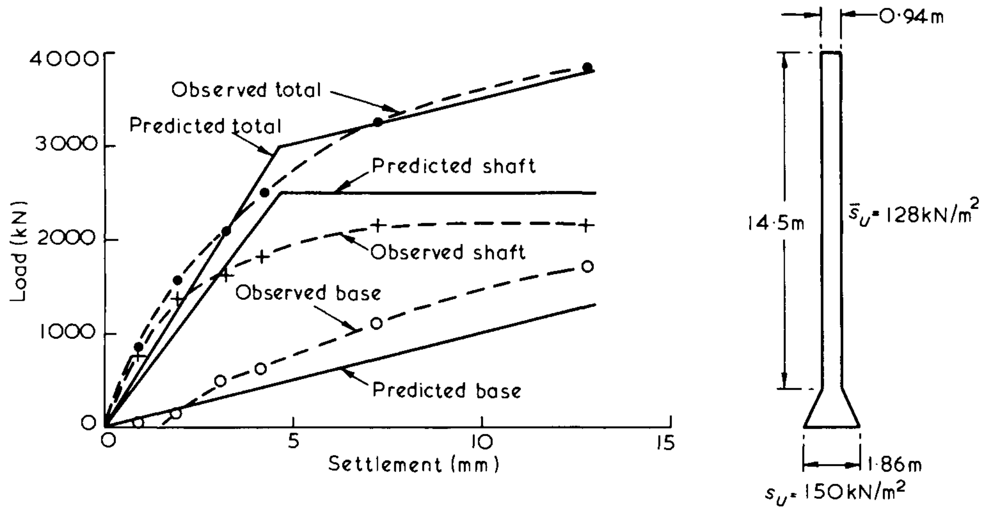

Fig. 6.5 Predicted load settlement relationship for a bored pile in London clay, after Burland and Cooke (1974)

Burland and Cooke (1974) also describe a method for preparing simple design charts which greatly facilitate design decision making because the effects of changing pile dimensions, founding levels or working levels can be determined at a glance.

There is little published data on adhesion factors appropriate to other types of clay. Tomlinson (1969) quotes 0.1 in very stiff to hard Lias clay, while Woodward, Lundgren and Boitano (1961) have quoted values of 0.49 to 0.52 for clays in California having shear strengths of about 100 kN/m^2.

In all cases, of course, the most reliable estimates of pile bearing capacity will result from pile loading tests. It is, however, vital that the test piles are bored and constructed in the same way as the piles under the structure. Account must also be taken of time effects.

4 Piles in granular soils

Parallel sided piles in granular soils act mainly as end bearing piles, with only a relatively small proportion of the load being carried on the shaft.

Pile bearing capacity can be predicted on the basis of:

- Bearing capacity theory
- Dutch cone test
- Standard penetration test
- Pile driving formulae
- Correlation with special sounding tests, for example, driving rods, pushing and pulling rods, rotating rods.

4.1 Bearing capacity theory

$$P_f = A_b \cdot p' \cdot (N_q - 1) + A_s \cdot K \cdot p'_{ave} \cdot \tan\delta' \qquad (6.14)$$

where p' = effective overburden pressure at base of pile; p'_{ave} = average effective overburden pressure over the length of pile; K = a coefficient of earth pressure; δ' = angle of wall friction; A_b = base area of pile; A_s = shaft area of pile; N_q = bearing capacity factor; P_f = failure load on pile.

The above expression neglects the $\frac{1}{2}\gamma' B N_\gamma$ term since it is small compared with the N_q term, and assumes that the bulk unit weight of the soil is equal to the unit weight of the pile.

There are many relationships which have been proposed between N_q and ϕ'. Tomlinson (1969) has suggested, for pile design, using the work of Berezantsev (1961) and this relationship is given in Fig.6.6. It should, however, only be used provided the pile can be driven into the granular stratum for a depth equal to about five times the pile width. For shallow penetrations, the values approach Terzaghi's solution for shallow foundations.

Since N_q is sensitive to ϕ', a relatively small error in estimating ϕ' will lead to a much larger error in N_q. Of particular difficulty is the assessment of the effect of pile driving operations on ϕ'. Meyerhof (1959) suggests that the bearing capacity of piles driven into loose sands can be doubled owing to compaction.

Broms (1965b) suggested the following values for K in granular soils:

Type of pile	*Loose*	*Dense*
Steel	0.5	1.0
Concrete	1.0	2.0
Timber	1.5	3.0

Aas (1966) proposed the following values of δ', which are perhaps somewhat on the safe side:

Steel piles	$\delta' = 20°$
Concrete piles	$\delta' = 3/4\ \phi'$
Timber piles	$\delta' = 2/3\ \phi'$

4.2 Dutch cone test

The failure load on the base of the pile is simply

$$P_b = A_b \, . \, C_{KD} \tag{6.15}$$

where C_{KD} is the cone point resistance averaged over a distance extending from about $4B$ above the pile tip to $1B$ below. With a factor of safety of 2½, the pile is unlikely to settle more than 12 mm under working load. The skin friction can either be calculated from bearing capacity, theory, section 4.1 above, or as follows, (Meyerhof, 1965).

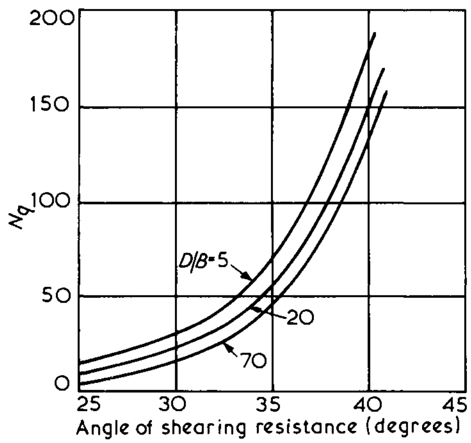

Fig.6.6 Relationship between N_q and ϕ', after Berezantsev (1961)

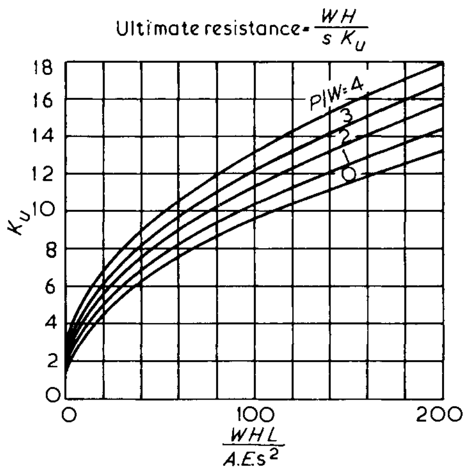

Fig. 6.7 Design chart for the Janbu pile driving formula

For displacement piles, the ultimate unit skin friction

$$c_s = \frac{C_{KD\ ave}}{200}\ \mathrm{kN/m^2} \tag{6.16}$$

or for H piles, the ultimate unit skin friction

$$c_s = \frac{C_{KD\ ave}}{400}\ \mathrm{kN/m^2} \tag{6.17}$$

where $C_{KD\ ave}$ = average cone point resistance over the length of the pile in kN/m^2.

4.3 Standard penetration test

This can only be used in an indirect manner as follows:

- Estimating ϕ' from N and then using bearing capacity theory
- Estimating C_{KD} from N and then proceeding as in section 4.2.

4.4 Pile driving formulae

Many attempts have been made to determine the relationship between the dynamic resistance of a pile during driving and the static load carrying capacity of the pile. These intended relationships are called pile driving formulae and have been established empirically or theoretically. Much discussion has been generated, for example, American Soc. Civ. Eng. (1951), Chellis (1941), Cummings (1940), and Greulich (1941). Conflicting opinions have been expressed.

The relationship between dynamic and static resistance of a pile as expressed by a pile driving formula should be independent of time if the formula is to have any validity. This is clearly not the case with clays and, therefore, pile driving formulae should not, in general, be applied to cohesive soils, but only to granular soils, that is, sands and gravels.

Of the many pile driving formulae which have been proposed, the authors suggest that the Janbu formula and the Hiley formula are convenient to use and give reasonable predictions of the ultimate bearing capacity of driven piles in granular soils.

4.4.1 The Janbu formula (Janbu, 1953)

$$Q_u = \frac{1}{K_u} \cdot \frac{\eta WH}{s} \tag{6.18}$$

where Q_u = ultimate load capacity; WH = input energy; s = final set (penetration/blow)

$$K_u = C_d \left[1 + \left(1 + \frac{\lambda_e}{C_d} \right)^{1/2} \right] \tag{6.19}$$

$$C_d = 0.75 + 0.15 \frac{W_p}{W} \tag{6.20}$$

$$\lambda_e = \frac{\eta W . H . L}{A . E . s^2} \tag{6.21}$$

L = length of pile; A = cross-sectional area; E = modulus of elasticity of pile material; W = weight of hammer; W_p = weight of pile; H = drop of hammer. Fig.6.7 eases the computation.

The efficiency factor, η, is dependent on the pile driving equipment, the driving procedure adopted, the type of pile, and the ground conditions. Values of η can be chosen as follows:

η = 0.70 for good driving conditions
η = 0.55 for average driving conditions
η = 0.40 for difficult or bad conditions

4.4.2 The Hiley formula (Hiley, 1925)

$$Q_u = \frac{K . W . H . \eta}{s + c/2} \tag{6.22}$$

where η = efficiency of the blow; K = hammer coefficient; c = sum of the temporary elastic compression of the pile, c_p, the pile head, c_c, and the ground c_q.

Values of K, η, c_c, c_p and c_q can be obtained from Table 6.1 and Figs 6.9 to 6.13, although it is preferable to measure c_p and c_q directly in the field.

It should be noted that η depends on the coefficient of restitution, e, which is given in Table 6.2, η then being obtained from Fig.6.8.

Table 6.1 Values of hammer coefficient K, after BSP Pocket Book (1969)

Hammer	K
Drop hammer, winch operated	0.8
Drop hammer, trigger release	1.0
Single-acting hammer	0.9
BSP double-acting hammer	1.0*
McKiernan–Terry diesel hammers	1.0†

* Instead of *WH* in the Hiley formula use manufacturers rated energy per blow, at actual speed of operation of hammer, the hammer speed must be checked when taking the final set.

† For *WH* substitute manufacturer's rated energy per blow, corresponding to the stroke of the hammer at the final set.

Table 6.2 Values of the coefficient of restitution, e, after BSP Pocket Book (1969)

Type of pile	Head condition	Single-acting or drop-hammer or diesel hammer	Double-acting hammer
Reinforced concrete	Helmet with composite plastic or Greenheart dolly, and packing on top of pile	0.4	0.5
	Helmet wtth timber dolly (not Greenheart) and packing on top of pile	0.25	0.4
	Hammer directly on pile with pad only	–	0.5
Steel	Driving cap with composite plastic or Greenheart dolly	0.5	0.5
	Driving cap with timber (not Greenheart) dolly	0.3	0.3
	Hammer directly on pile	–	0.5
Timber	Hammer directly on pile	0.25	0.4

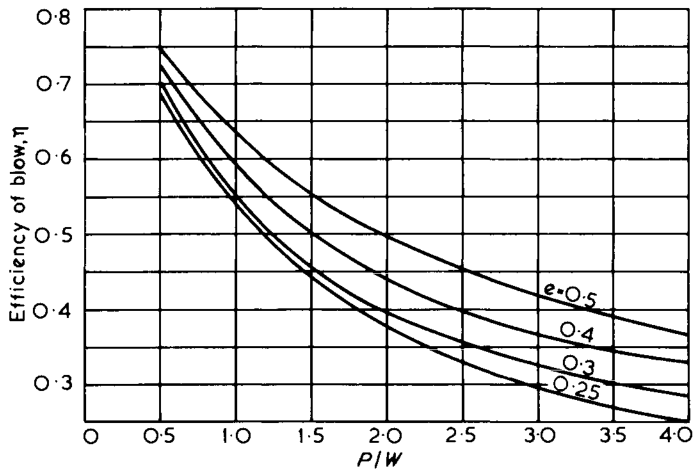

Fig. 6.8 Determination of efficiency factor, η, for use in the Hiley pile driving formula, after BSP Pocket Book (1969)

4.4.3 Comparison of formulae

A detailed investigation into the validity of pile driving formulae in granular soils (Flaate, 1964) suggests that there is little to choose between the Hiley and the Janbu formulae. In order to obtain a minimum factor of safety of 1.75 for any one pile, Flaate showed that it is necessary to use $F = 2.7$ with the Hiley formula and $F = 3.0$ with the Janbu procedure. Janbu's formula gave a slightly better correlation between tested and calculated bearing capacity and also the lowest arithmetic mean value of the factor of safety.

An example on the use of these formulae is given below:

Example

A 400 × 400 mm reinforced concrete pile 20 m long is driven through loose materials and then into dense gravel to a final set of 3 mm/blow, using a 30 kN single-acting hammer with a stroke of 1.5 m. Determine the ultimate driving resistance of the pile if it is fitted with a helmet, plastic dolly and 50 mm of packing on top of the pile. The weight of the helmet and dolly is 4 kN.

Weight of pile = 74 kN
Weight of helmet and dolly = 4 kN
Total weight, P = 78 kN
Weight of hammer, W = 30 kN

Therefore, $P/W = 78/30 = 2.6$

Using the Hiley formula

$e = 0.4$ (Table 6.2), hence $\eta = 0.39$ (Fig.6.8).

H = effective height of fall of hammer

$= 0.9 \times 1.5$ m (Table 6.1)

$= 1.35$ m $= 1350$ mm

Assume a value for the ultimate driving resistance $Q'_u = 1250$ kN. Then

$$\text{overall driving stress} = \frac{1250}{0.4 \times 0.4}$$

$$= 7813 \text{ kN/m}^2$$

$$= 7.8 \text{ MN/m}^2$$

$c_c = 5.8$ mm (Fig.6.9, $2/3\,A + B$), $c_p = 11.0$ mm (Fig.6.10), $c_q = 2.8$ mm (Fig.6.13).
Total $c = c_c + c_p + c_q = 19.6$ mm

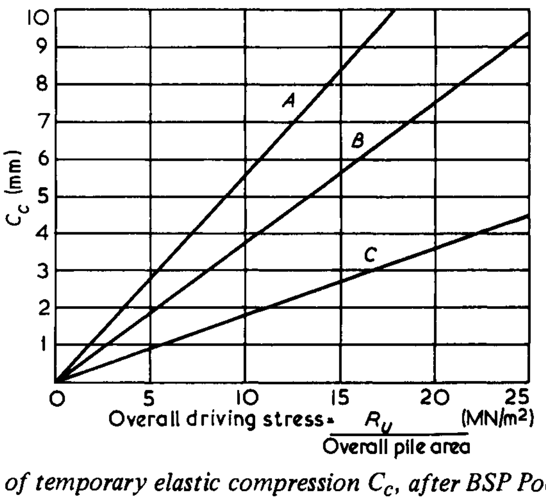

Fig.6.9 Determination of temporary elastic compression C_c, after BSP Pocket Book (1969)
Key: A = concrete pile, 75 mm packing under helmet; B = concrete or steel pile, helmet with dolly or head of timber pile. C = 25 mm pad only on head of RC pile

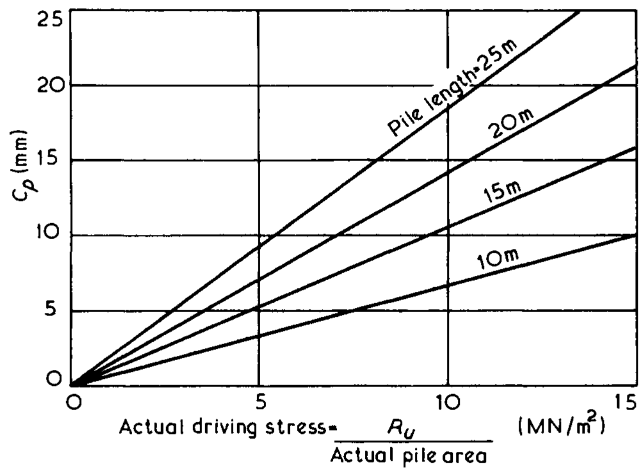

Fig.6.10 Determination of temporary elastic compression C_p, for concrete piles, after BSP Pocket Book (1969)

$$Q_u = \frac{W.H.\eta}{s + c/2} = \frac{30 \times 1350 \times 0.39}{3 + ½ \times 19.6}$$

$$= 1234 \text{ kN}$$

This is nearly equal to the assumed value of 1250 kN and hence the calculation need not be repeated.

Using the Janbu formula

$$\frac{\eta WHL}{A \,.\, E \,.\, s^2} = \frac{0.70 \times 30 \times 1.5 \times 20}{0.16 \times 14\,000\,000 \times 0.003^2} = 0.3$$

$$K_u = 7.1$$

Then

$$Q_u = \frac{\eta WH}{s \,.\, K_u}$$

$$= \frac{0.70 \times 30 \times 1.5}{0.003 \times 7.1} = 1479 \text{ kN.}$$

It can be seen that in this case the Janbu formula predicts a greater ultimate pile capacity than the Hiley formula.

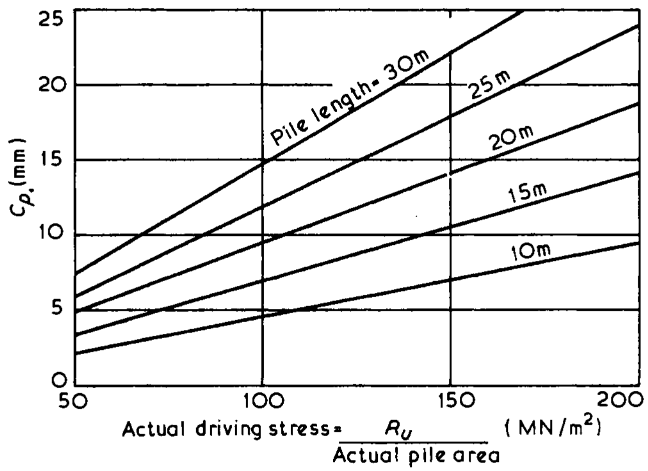

Fig. 6.11 Determination of temporary elastic compression C_p, for steel piles, after BSP Pocket Book (1969)

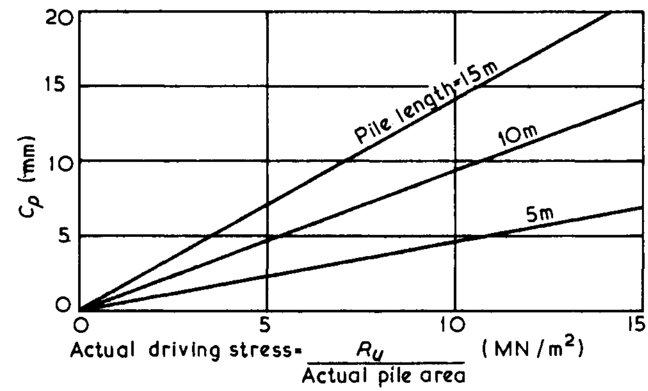

Fig. 6.12 Determination of temporary elastic compression C_p, for timber piles, after BSP Pocket Book (1969)

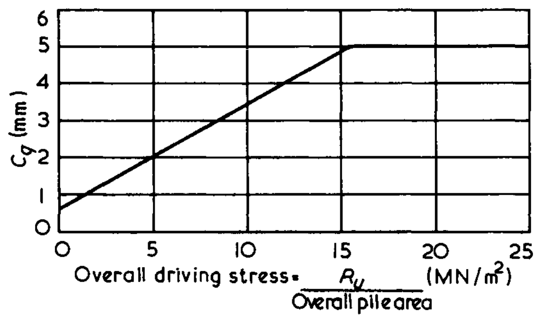

Fig. 6.13 Determination of temporary elastic compression C_q, after BSP Pocket Book (1969)

The corresponding working loads are:

- for the Hiley formula, $\dfrac{1234}{2.7} = 457$ kN
- for the Janbu formula, $\dfrac{1479}{3} = 493$ kN

4.5 Correlation with special sounding tests

Provided sufficient experience is available, that is, comparisons with pile loading tests, special sounding tests can be extremely useful, for example, driving rods, pushing and pulling rods, rotating rods, light Swedish rotary sounding apparatus.

4.6 Overdriving of piles

It is sometimes necessary to drive piles through dense sands and gravels, for example, either to penetrate an underlying clay layer, or because of the possibility of scour in river beds. Damage to the pile due to over-driving must be avoided, both when penetrating an overlying hard layer or when driving into the bearing stratum to develop the full bearing capacity. In this connection, it should be remembered that a penetration of up to five pile diameters into dense granular material may be necessary to develop fully the end bearing capacity.

The Hiley formula can be used to determine the failure, load, Q_u, and then the peak driving stress, P_d, is given by:

$$P_d = \frac{Q_u}{A}\left(\frac{2}{\sqrt{\eta}} - 1\right) \tag{6.23}$$

Janbu (1953) suggests that the driving energy, $(WH)_c$, needed to avoid damage is limited by:

$$(WH)_c = \left(\frac{\mathrm{L}}{2500} + 2s\right) . \sigma_o . A \tag{6.24}$$

where L = pile length; s = set; A = cross-sectional area of the pile; σ_o = half-compressive strength.

5 Group action of piles

5.1 Spacing

Upheaval of the ground surface caused by driving closely spaced piles into dense or incompressible material should be minimized and hence a minimum pile spacing is necessary. If the spacing is too large, on the other hand, uneconomic pile caps may result. When driving piles in sands or gravels, it is advisable to start driving at the centre of a group and then to work outwards, in order to avoid difficulty with 'tightening-up' of the ground.

C.P.2004:1972 suggests the following minimum pile spacing:

Type of pile	*Minimum spacing*
Friction	Perimeter of the pile
End bearing	Twice the least width
Screw piles	1½ times diameter of screw blades

The Norwegian Code of Practice on Piling, Den Norske Pelekomite (1973), gives the following minimum pile spacing:

Length of pile	Friction piles in sand	Friction piles in clay	Point bearing piles
Less than 12 m	3 *d*	4 *d*	3 *d*
12 to 24 m	4 *d*	5 *d*	4 *d*
Greater than 24 m	5 *d*	6 *d*	5 *d*

Note: 1. *d* is the pile diameter or largest side
2. the pile spacing is measured at pile cut-off level, unless raking piles are used, in which case the spacing is measured at an elevation 3 m below pile cut-off level.

5.2 Settlement of pile groups in clays

It is clear that settlement of a group of piles in clay cannot be predicted from the results of a loading test on a single pile, because time effects, remoulding of the soil owing to pile driving and scale effects are quite different for the single test pile and the pile group. The action of the piles is to transfer the load to some lower stratum and various suggestions have been proposed as to how to include this load transfer in settlement calculations. Once a load transfer is assumed, then settlement calculations can be made in the usual manner.

The following assumptions have been used:

1. An equivalent raft at two thirds the pile length over the area enclosed by the piles at that depth.
2. An equivalent raft at two thirds the pile length over a larger area, because of side friction on the group of piles. A spread of one horizontal to four vertical may be reasonable.
3. An equivalent raft at the base of the piles over the area enclosed by the piles at this depth.
4. An equivalent raft at the base of the piles over a larger area.

The differences between these assumptions are clearly appreciable. Comparing (1) and (3) above, which appear to be those in most common use, a design using assumption (1) would provide piles 50% longer than one using assumption (3) for the same allowable maximum settlement. This is clearly illogical. For displacement piles, assumption (1) would seem to be a suitable choice, as it would, in general, give a greater computed settlement than (3), and so would in some measure allow for the disturbance caused by pile driving. For bored piles, particularly if they are closely spaced, assumption (3) seems realistic.

5.3 Settlement of pile groups in granular soils

It should be possible to calculate the settlement of a group of piles in granular soils in a manner similar to that employed for pile groups in clay, that is, to assume some form of distribution of load and then to calculate the settlements using the results of Dutch cone or standard penetration tests. This procedure is not generally adopted, however, and it is usual to base settlement predictions for pile groups on the results of loading tests on individual piles.

Skempton (1953) has compared the settlements of a number of pile groups with the settlements of corresponding individual piles and has proposed the following relationship between the settlement, δ_B, of a pile group of width B m, and the observed settlement δ_s, of a single pile at the same load intensity.

$$\frac{\delta_B}{\delta_s} = \left(\frac{4B + 3}{B + 4}\right)^2 \tag{6.25}$$

Care should be taken when piles are driven into sands and gravels which are underlain by clays, if the stresses transferred to the clays from the pile group may result in over-stressing or excessive consolidation. The factor of safety against a bearing capacity failure in the clay can be assessed by assuming a spread of load onto the surface of the clay in a similar manner as indicated in Fig.4.5. The settlement in the underlying layer can be computing in the normal way by first determining the distribution of stress throughout the clay layer, using, for example, Fig.3.3.

An interesting case record has been described by Terzaghi (1939). Timber piles for a hospital in New Orleans were driven through clay to virtual refusal into a sand deposit. There were no measurable settlements under a pile test load of 15 tons, and the piles were designed to carry this loading. During construction, a settlement of 100 mm occurred, which increased to 300 mm after 2 years. This was due to a compressible clay layer underlying the sand.

5.4 Bearing capacity of pile groups in clay

It has been recognized for some time that a group of piles may fail as a block under a loading less than the sum of the bearing capacity of the individual piles.

In an interesting series of model experiments carried out at the Building Research Station (Whitaker, 1970), it was shown that a group of piles in clay could either fail as individual piles or as a block. A block failure occurred for pile spacings of the order of two diameters, and for wider spacings the piles failed individually but the efficiency ratio (equal to the average load per pile in the group at failure divided by the failure load of a single comparable pile) only reached unity at a spacing of about eight diameters.

The stability of a group of piles may be checked using Terzaghi and Peck's block failure hypothesis, where the failure load of a pile group, Q_g, is given by:

$$Q_g = N_c \times A_b \times s_u + A_s \,.\, \bar{s}_u \tag{6.26}$$

where, N_c = bearing capacity factor; A_b = base area enclosed by the pile group; s_u = undrained shear strength at base of pile group; A_s = perimeter area of pile group; $\bar{s}_u$ = average undrained shear strength around the perimeter of the piles.

In addition to checking block failure, Tomlinson (1969) has suggested taking an efficiency ratio of 0.7 for a spacing of 2 diameters increasing to unity at a spacing of 8 diameters.

5.6 Bearing capacity of pile groups in granular soils

The action of driving pile groups into granular soils will tend to compact the soil around the piles. In addition, because of the greater equivalent width of a pile group as compared with a single pile, the ultimate failure load will tend to increase. For these reasons, the efficiency ratio of a group of piles in granular soils will be greater than unity, or for large pile spacings equal to unity.

It is unusual to take this into account in design.

Care must be taken, of course, to ensure that no weaker or more compressible soil layers occur within the zone of influence of the pile group.

When driving piles into dense granular soils, care must be taken to ensure that previously driven piles are not lifted by the driving of other piles.

For further discussion on group action, reference can be made to Tomlinson (1969) and Whitaker (1970).

6 Negative skin friction

When piles are driven through strata of soft clay into firmer materials, they will be subjected to loads caused by negative skin friction in addition to the structural loads, if the ground settles relative to the piles. Such settlement may be due to the weight of superimposed fill, to groundwater lowering, or a result of disturbance of the clay caused by pile driving (particularly large displacement piles in sensitive clays leading to reconsolidation of the disturbed clay under its own weight).

This additional loading due to negative skin friction may be so large as to cause over-stress of the pile material or may lead to large settlements, or even failure, in the underlying supporting soil.

An interesting example of the development of negative skin friction forces has been described by Johannessen and Bjerrum (1965). A hollow steel pile was driven through about 40 m of soft blue clay to rock, and 10 m of fill was placed around the pile. After 2½ years, the ground surface had settled nearly 2 m and the pile had shortened by 15 mm. The compressive stress induced at the pile point, resulting only from negative skin friction, was 200 MN/m^2. It was also found that the adhesion developed between the clay and the steel pile was equal to 0.2 × (the effective vertical stress) and was also approximately equal to the undrained shear strength of the clay, measured by the *in situ* vane test, before pile driving.

The load transferred to the pile depends on:

- The pile material
- The type of soil
- The amount and rate of relative movement between the soil and the pile.

It appears that only a small relative movement, of the order of 10 mm, is necessary for full negative skin friction to occur.

The maximum extra load per pile in a pile group due to negative skin friction, Q_{ns}, is given by:

$$Q_{ns} = A_s \times \bar{s}_u \times a \tag{6.27}$$

or

$$Q_{ns} = \frac{A_g \times \bar{s}_u + W}{n} \tag{6.28}$$

whichever is smaller, where A_s = circumferential area of a pile; A_g = circumferential area of the pile group; s_u = average undrained shear strength along length of pile; a = adhesion factor; W = buoyant weight of soil within pile group; n = number of piles

To reduce negative skin friction, the following measures have been used:

- In Holland, for example, using precast concrete piles with shafts of small cross-sectional area compared with the points (Plantema and Nolet, 1957)
- Driving piles inside a casing with the space between pile and casing filled with a viscous material and the casing withdrawn (Golder and Willeumier, 1964)
- Coating the piles with bitumen.

An example of the successful use of bitumen coating on piles has been given by Bjerrum, Johannessen and Eide (1969). At Sørenga, Norway, three test piles *C, D, E* were installed in 1966 through about 15 m of fill consisting of rock fill and boulders placed in 1964, overlying about 40 m of soft marine clay. The test piles were full-scale steel tube piles with a diameter of 500 mm and a wall thickness of 8 mm.

Pile *C*, see Fig.6.14, was the reference untreated pile, while piles *D* and *E* were both coated by a 1 mm thick layer of bitumen and were driven with an enlarged point of diameter 690 mm. In order to protect the bituminous coating on pile *D* from being damaged during driving through the fill, an outer casing of diameter 630 mm was driven down through the fill with the pile section, and the space between the pile and the casing was filled with bentonite slurry. No precautions other than the enlarged point were undertaken to protect the bitumen on pile *E* when it was driven through the fill.

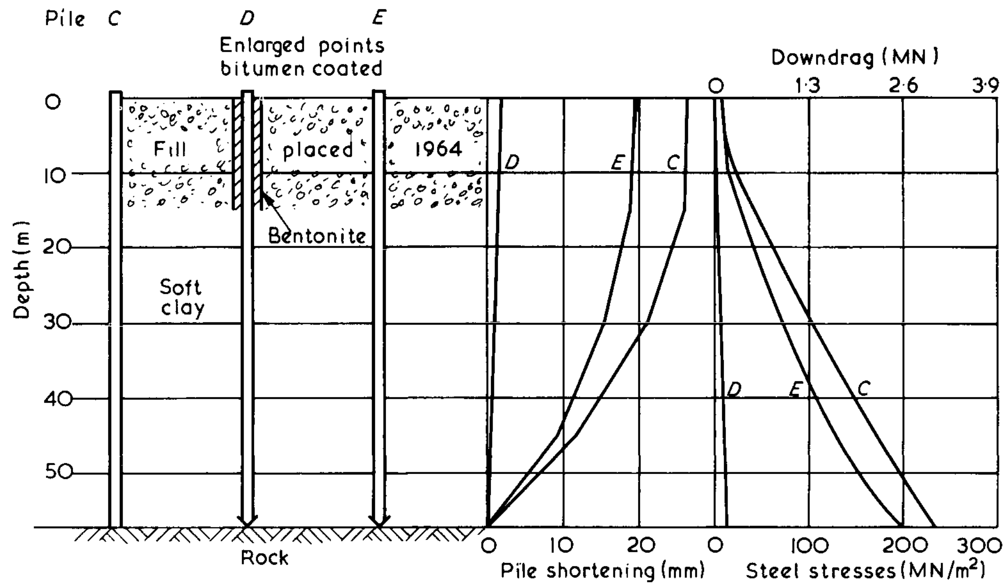

Fig. 6.14 Examples of the effects of negative skin friction on the behaviour of piles, after Bjerrum, Johannessen and Eide (1969)

About a year after driving the test piles, the negative friction on the reference pile, pile C, amounted to about 3000 kN just above the point with a corresponding steel stress of 226 MN/mm^2. The pile top had settled more than 50 mm of which 25 mm was due to the penetration of the pile point into rock. Pile D, was coated with bitumen and driven with the outer casing as protection against the fill, and showed at that time a negative skin friction load of about 150 kN. The necessity of using a casing through the fill to protect the bitumen was clearly illustrated by the observations on pile E. In spite of its bitumen coating, the load due to negative skin friction amounted to 2600 kN. These results are illustrated in Fig.6.14. It can be concluded that a bitumen coating provides a most efficient means of reducing negative skin friction loads, provided the integrity of the coating is ensured when driving the pile through coarse overlying fill material.

Results of measurements of negative skin friction on piles have been presented by Gant, Stephens and Moulton (1958), Fellenius and Broms (1969), Endo, Minau, Kawaski and Shibata (1969), Walker and Darval (1973). Theoretical expressions for the design of pile foundations taking into consideration negative skin friction have been developed by Buisson, Ahu and Habib (1960), Zeevaert (1960), Brinch Hansen (1968), Paulos and Mattes (1969) and Sawaguchi (1971).

Bjerrum (1973) drew attention to the fact that the adhesion developed between a pile and clay was dependent not only on the pile material, the type of clay, the time elapsed between installing the pile and testing it, and the presence or otherwise of other material overlying the clay, but also on the rate of relative deformation between the pile and the soil. For soft compressible clays, it is known that the lower the rate of relative deformation, the smaller will be the developed adhesion. For cases where the rate of relative movement is high, the procedure outlined above may be used to estimate the magnitude of the negative skin friction forces. When the rate movement is small, Bjerrum suggested that the negative skin friction, s_a, could be estimated from the simple equation:

$$s_a = Kp'_o \tag{6.29}$$

where,

K = 0.25 for very silty clay
= 0.20 for low plasticity clays
= 0.15 for clays of medium plasticity
= 0.10 for highly plastic clays

Although a bitumen coating on piles can lead to great reductions in negative skin friction forces, it must be ascertained that the integrity of the coating will be maintained during the period of the relative movement between soil and pile. A case in Perth, Western Australia was discussed by Simons (1971b). The ground conditions consisted of about 20 m of soft, normally consolidated clay on which embankments up to 18 m high were placed, leading to settlements of up to 7 m. Four unloaded steel test piles were put down, two coated with bitumen and two were uncoated. The uncoated piles soon picked up a large negative skin friction load, while the bitumen coated piles initially showed little load pick-up. After some months, the loads on the coated piles began to increase, eventually reaching the same order of magnitude as the loads on the uncoated piles. This was apparently due to bacteriological action in the clay attacking the bitumen coating. Caution must therefore be exercised when transferring experience from one part of the world to another.

If piles subjected to negative skin friction forces are founded in granular material, then not only must the additional pile loading be taken into account in design, but also the reduction in bearing capacity of the granular material, due to the decrease in the effective overburden pressure on the surface of the granular soil, brought about by the transfer of load to the pile.

Based on a bearing capacity equation put forward by Brinch Hansen (1968), which takes into consideration the penetration of a foundation into the bearing stratum, Simons and Huxley (1975) have presented a series of solutions incorporating as variables:

- Pile diameter
- Pile penetration into the granular material
- Angle of shearing resistance of the granular material
- Effective overburden pressure on the surface of the granular material.

These solutions allow the bearing capacity of a pile to be read-off, once the friction angle and reduction in effective overburden pressure on the surface of the granular material due to negative skin friction, have been assessed.

An example is given in Fig.6.15, and it can be seen that for small penetrations and small

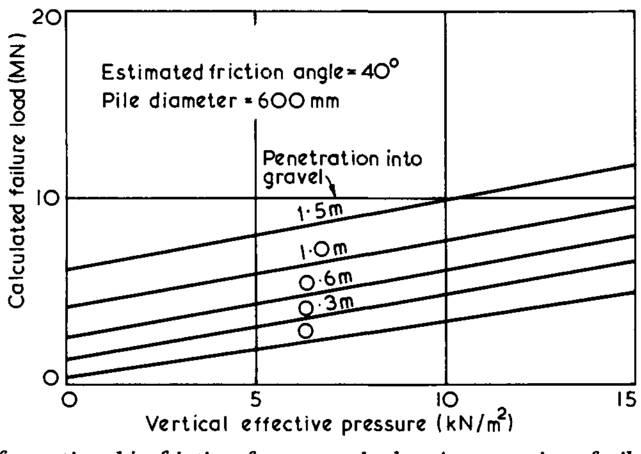

Fig.6.15 Effect of negative skin friction forces on the bearing capacity of piles founded in granular soils, after Simons and Huxley (1975)

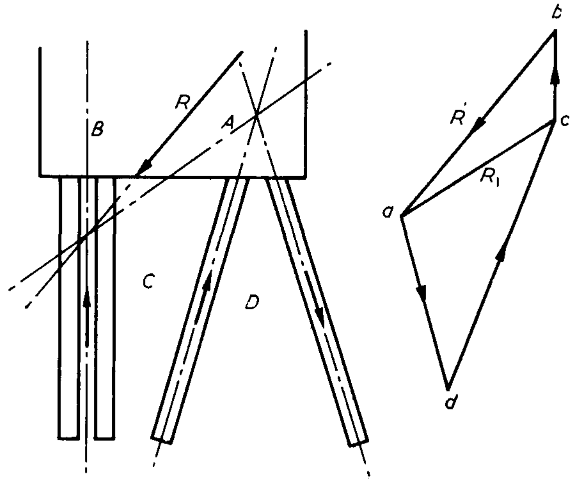

Fig. 6.16 Graphical procedure for determining the distribution of loads for a group of vertical and raking piles

effective overburden pressures, the calculated failure load in the granular material is less than the allowable load which the concrete in the pile can carry.

It should be noted that a solution to this problem was proposed by Zeevaert (1960). This solution did not consider the effect of pile penetration into the bearing stratum and is somewhat unrealistic since it follows logically from this limitation that the bearing capacity of any pile driven into granular material occurring at the ground surface, is zero.

The Norwegian Code of Practice on Piling, Den Norske Pelekomite (1973) recommends:

- That negative skin friction be calculated to a depth, D, where the ground settles 5 mm more than the piles.
- If displacement piles are driven at close centres leading to ground displacements and the establishment of excess pore-water pressures, and the subsequent ground settlement is due only to these factors, and not due to nearby filling, then a reduced value of negative skin friction load can be adopted, for example by using half the undrained shear strength for soft clays, or assuming the adhesion is equal to 0.1 times the vertical effective stress.
- An upper limit to the submerged weight of soil which can be transferred to a group of piles of plan area $B \times L$ is obtained by considering a volume of soil equal to $D \times (B + D/4) \times (L + D/4)$.
- It is considered satisfactory to operate with the minimum calculated value for negative skin friction load.
- Bitumen coating of piles leads to significant reduction in negative skin friction forces. Measurements show that bitumen coatings have reduced adhesions of 50 to 60 kN/m^2 for uncoated piles to 5 to 15 kN/m^2 for coated piles.
- For steel piles, a bitumen coating thickness of 1 mm should be used, and for concrete piles, a thickness of 2 mm is suggested.
- Provision must be made to avoid damage to the coating during pile driving, using, for example, enlarged pile points or driving inside a casing if overlying granular material is present.

7 Lateral loads on piles

Lateral loads applied to groups of piles can be carried either by the horizontal components of raking piles or by the lateral resistance of the soil surrounding vertical piles. If vertical piles are subjected to substantial horizontal forces, then the upper levels of the ground should be able to resist these forces without excessive lateral movement occurring. It may be necessary to connect pile caps with horizontal beams to obtain sufficient resistance. If these measures are insufficient, then raking piles should be used.

7.1 Lateral loads on raking piles

The computation of the forces and moments transmitted to a group of vertical and raking piles presents an extremely difficult problem to which no satisfactory solution exists at present.

It is usual to base the analysis on severe simplifying assumptions, for example, that the piles are axially loaded, that Hooke's law is obeyed, that the lateral restraint to the piles from the soil can be ignored, and that the piles are hinged top and bottom.

A simple graphical procedure is illustrated in Fig.6.16.

7.2 Lateral loads on vertical piles

A guide to the allowable horizontal forces which may be applied at ground level to the tops of vertical piles is given in Table 6.3 for short term loading of timber and concrete piles in clay, while Table 6.4 gives allowable long term loads for timber and concrete piles in clay, silt and sand. For the short term case, the maximum bending moment occurs at a depth of between 0.5 and 1.5 m, and for the long term case the critical depth is between 1 and 1.5 m.

There are three design considerations:

- The pile must be able to carry the bending moments
- The soil must be able to support the loading
- The lateral deflections must be tolerable.

Table 6.3 Guide to allowable horizontal force applied to the top of a timber or concrete pile for short term loading, in clays, after Den Norske Pelekomitė (1973)

		Allowable short term lateral load in clays (kN)		
Pile area (m^2)	Max bending moment (m . kN)	s_u = 10 kN/m^2	s_u = 25 kN/m^2	s_u = 50 kN/m^2
0.04	4.5	7	15	20
0.06	8.5	10	20	30
0.09	15.0	15	30	40

Table 6.4 Guide to allowable horizontal force applied to the top of a timber or concrete pile for long term loading, after Den Norske Pelekomitė (1973)

		Allowable long term lateral load (kN)		
Pile area (m^2)	Max bending moment (m . kN)	Clay, tan ϕ' = 0.5	Silt, tan ϕ' = 0.7	Sand, tan ϕ' = 0.9
0.04	4.5	5	6	7
0.06	8.5	8	10	12
0.09	15.0	13	16	19

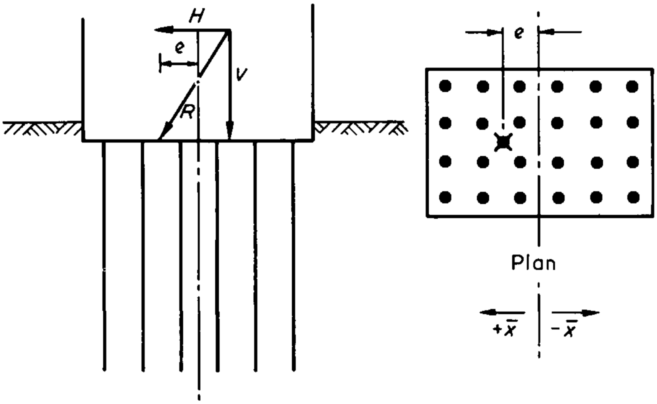

Fig. 6.17 Group of vertical piles under an inclined eccentric load

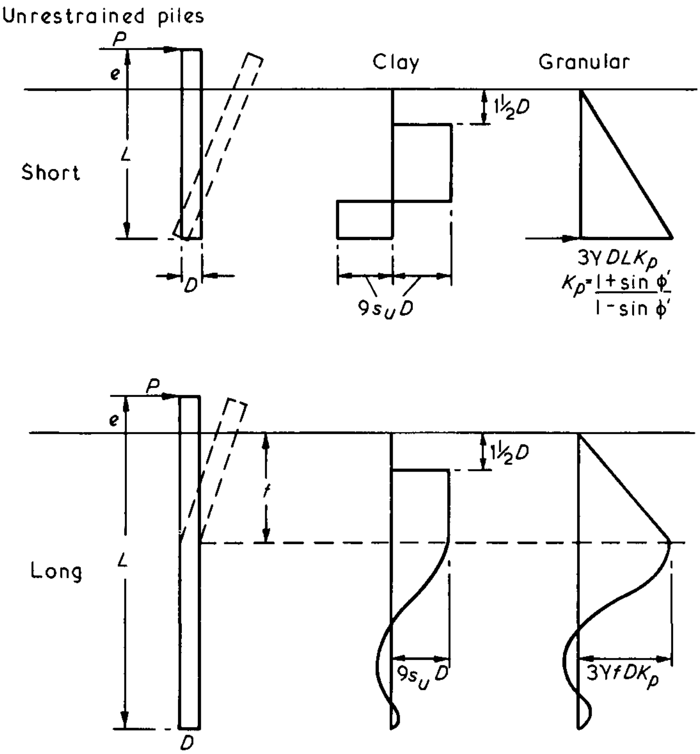

Fig. 6.18 Failure mechanisms for short and long unrestrained piles, after Broms (1965)

For a group of vertical piles carrying an inclined eccentric load, R, as shown in Fig.6.17, the vertical load, P_v, on any one pile is given by:

$$P_v = \frac{V}{n} + \frac{V.\,e.\,\bar{x}}{\bar{x}^2} \tag{6.30}$$

where, V = total vertical load on the group; n = number of piles in the group; e = eccentricity of the load; $\bar{x}$ = distance from centre line of a pile to the neutral axis of the pile group; it is positive when measured in the same direction as e, and negative when in the opposite direction.

The procedures outlined below, to calculate horizontal loads on vertical piles, follow the proposals suggested by Broms (1964a, 1964b, 1965a) which are based on simplifying assumptions which are questionable. The reasonably good agreement obtained between the methods proposed and the results of field tests indicates, however, that the assumptions are justified.

7.2.1 Single piles in cohesive soils

7.2.1.1 Ultimate lateral resistance. Possible failure mechanisms for short and long unrestrained piles are shown in Fig.6.18 and for short and long restrained piles in Fig.6.19. Short piles imply that failure is governed by the soil strength, and with long piles, failure is governed by the moment of resistance of the pile. The ultimate value of soil resistance against a laterally loaded pile appears to vary between 8 and 12 times s_u, and there is some evidence to suggest that the value is somewhat smaller to a depth of about three pile diameters below the surface. Broms suggested, therefore, an assumed distribution of soil reaction of zero from the surface to a depth of 1.5 pile diameters and a constant value of 9 s_u below this depth, as required.

Based on these assumptions, solutions are given in dimensionless form in Fig.6.20 for short piles and Fig.6.21 for long piles. For the case of restrained piles, it should be noted that the solutions imply that moment restraint from the pile cap, equal to the moment in the pile just below the cap, is available. In any particular case, the procedure is to determine from Fig.6.20 that adequate penetration into the soil is obtained and then from Fig.6.21 to check that the available moment of resistance of the pile section is not exceeded.

7.2.1.2 Lateral deflections. The calculation of lateral deflections is based on the coefficient of subgrade reaction, k, defined by the equation:

$$p = k \cdot y \tag{6.31}$$

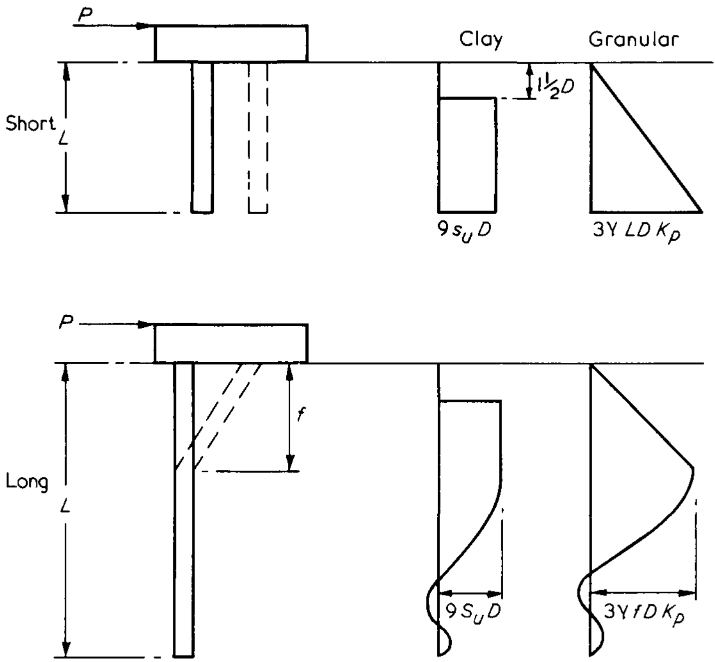

Fig.6.19 Failure mechanisms for short and long restrained piles, after Broms (1965)

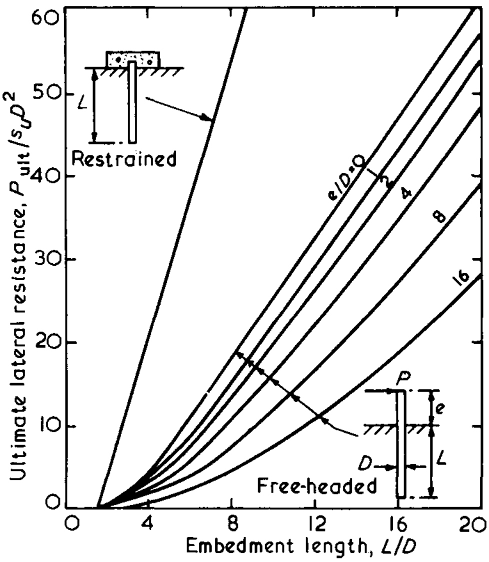

Fig. 6.20 Ultimate lateral resistance for short piles in cohesive soils, after Broms (1965)

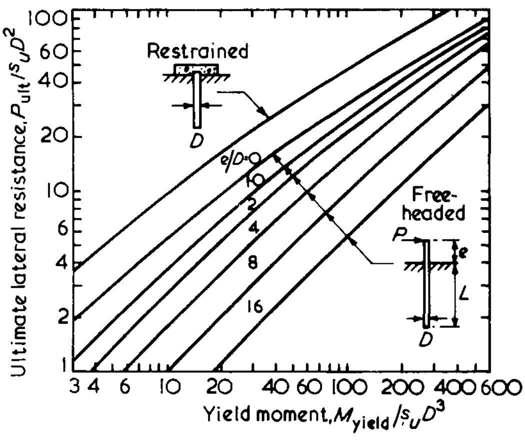

Fig. 6.21 Ultimate lateral resistance for long piles in cohesive soils, after Broms (1965)

where p is the applied pressure causing a deflection y.

It should be noted that the value of k depends not only on the nature of the soil but also on the size, shape and stiffness of the foundation which carries the load. It is extremely difficult to obtain reliable values for k and hence only very approximate predictions of the magnitude of the lateral deflections of a laterally loaded pile can be expected.

The deflections depend primarily on the dimensionless length βL where

$$\beta = \left(\frac{k_h \cdot B}{E_p \cdot I_p}\right)^{1/4} \tag{6.32}$$

where $E_p \cdot I_p$ is the stiffness of the pile section, B is the diameter or width of the laterally loaded pile in metres and k_h is the coefficient of horizontal subgrade reaction for the pile and depends on the deformation properties of the soil and on the dimensions and stiffness of the laterally loaded pile.

For long piles, $\beta L > 2.25$, the value of k_h to be used is obtained from:

$$k_h = 0.4 \cdot \frac{k}{B} \tag{6.33}$$

where k is the coefficient of subgrade reaction, applicable to a square plate of breadth equal to 1 m.

Values of k can be estimated from Table 6.5.

For short piles, $\beta L < 2.25$, the value of k_h may be taken equal to:

$$k_h = \left(\frac{2L + 3B}{5L}\right) \cdot \frac{k}{B} \tag{6.34}$$

Preferably, the coefficient of horizontal subgrade reaction may be estimated from the results of lateral load tests on piles.

The lateral deflection at ground surface, y_o, is obtained from Fig.6.22.

It is sufficient to consider variations in k_h to a depth of $\beta L = 2$ for restrained piles and $\beta L = 1$ for free-headed, when the piles are long.

For short piles, if k increases with depth, the value at a depth of 0.25 L for a free-headed pile, and at a depth of 0.5 L for a restrained pile, may be taken as the equivalent uniform value.

7.2.2 Single piles in granular soils

7.2.2.1 Ultimate lateral resistance. Possible failure mechanisms for unrestrained piles are shown in Fig.6.18 and for restrained piles in Fig.6.19. The following assumptions are made in the

Table 6.5 Values of k, for cohesive soils

Undrained strength of clay, s_u (kN/m^2)	50 to 100	100 to 200	200 to 400
k (kN/m^3)	8000	16 000	32 000

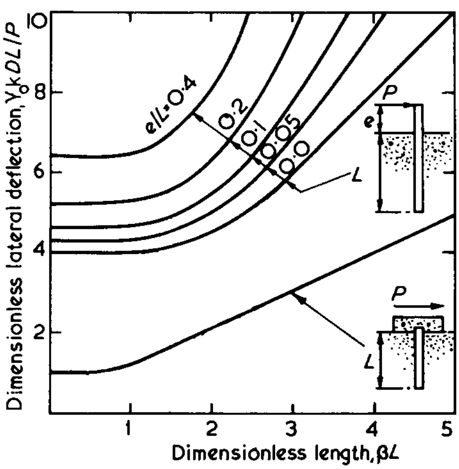

Fig.6.22 Lateral deflections at ground surface for piles in cohesive soils, after Broms (1965)

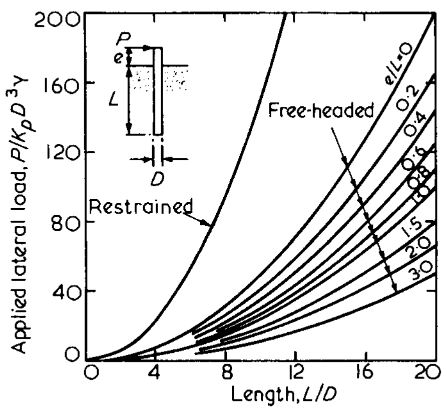

Fig.6.23 Ultimate lateral resistance for short piles in granular soils, after Broms (1965)

analysis:

- The active earth pressure acting on the back of a laterally loaded pile may be neglected
- The distribution of passive pressure along the front of the pile is equal to three times the calculated Rankine earth pressure
- The shape of the pile section has no influence on the ultimate lateral resistance or the earth pressure distribution
- The full lateral resistance is mobilized at the movements considered.

Based on these assumptions, solutions are given in Fig.6.23 for short piles and Fig.6.24 for long piles.

K_p is the coefficient of passive pressure

$$= \frac{1 + \sin\phi'}{1 - \sin\phi'}$$

and γ is the unit weight (submerged for high groundwater table).

7.2.2.2 Lateral deflections. The solution is again based on the use of a coefficient of subgrade reaction k_h which is assumed to be proportional to depth,

$$k_h = n_h \cdot \frac{z}{B} \tag{6.35}$$

The deflections depend on the dimensionless length, ηL, where

$$\eta = \left(\frac{n_h}{E_p \cdot I_p}\right)^{1/5} \tag{6.36}$$

and values of n_h are given in Table 6.6.

The dimensionless lateral deflection $y_o \cdot (E_pI_p)^{3/5} \cdot (n_h)^{2/5}$ is plotted against the dimensionless length ηL in Fig.6.25.

It should be noted that the lateral deflections may be larger than those indicated in Fig.6.25, if jetting has been used.

The lateral deflections at ground surface for relatively short piles have been found to be mainly a function of the penetration depth and the deformation properties of the surrounding soil, whereas the lateral deflections at the ground surface of a relatively long pile are independent of the penetration depth but dependent on the stiffness of the pile section.

The ultimate lateral resistance of short piles has been found to be governed by the penetration depth of the pile and to be independent of the pile section. The ultimate lateral resistance of long piles is governed by the ultimate bending resistance of the pile section and is independent of the penetration depth.

It should be pointed out that the ultimate lateral resistance of a pile group may be less than the ultimate lateral resistance calculated as the sum of the ultimate resistances of the individual

Table 6.6 Values of n_h, for granular soils

Relative density of sand	Loose	Medium	Dense
n_h (dry or moist) (kN/m^3)	750	2250	6000
n_h (submerged) (kN/m^3)	400	1500	3600

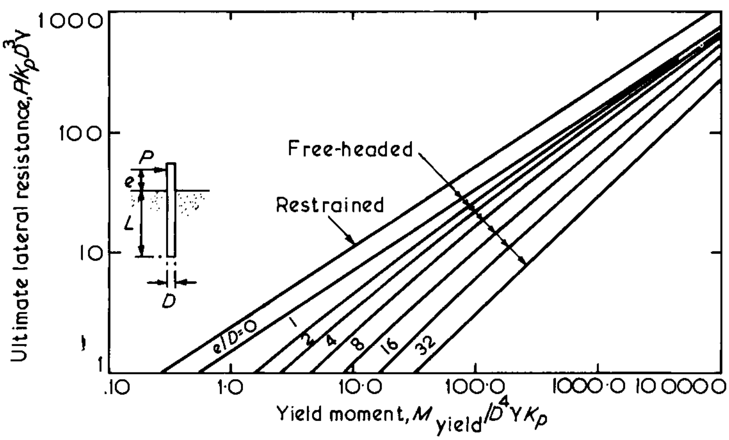

Fig. 6.24 Ultimate lateral resistance for long piles in granular soils, after Broms (1965)

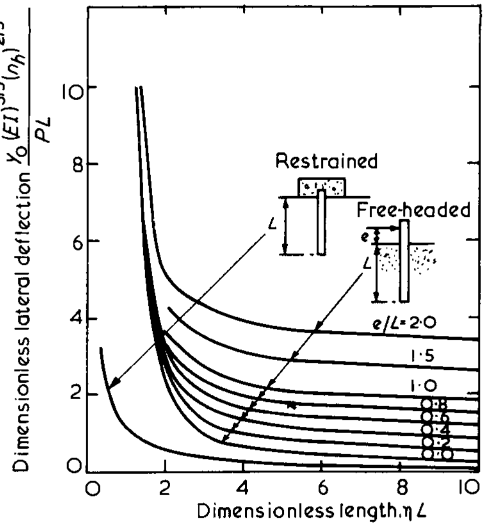

Fig. 6.25 Lateral deflections at ground surface for piles in granular soils, after Broms (1965)

piles. This effect is likely to be more pronounced for clays than for sands. Little or no reduction may be expected when the pile spacing is greater than four pile diameters. If the pile spacing is two pile diameters, then the piles and the soil within the pile group may behave as a unit.

7.3 General comments

1. If raker piles have to be placed at the perimeter of a heavily loaded area in soil subject to significant settlement, then the risk of over-stressing these piles is considerable, and heavy reinforcement may be necessary. Under such conditions, it may well be preferable to avoid using raking piles.
2. It should be emphasized that because of variations in alignment of raker piles, the effects of differential settlement of a pile group, the stiffness of the pile cap, and the difficulty in determining with any precision the magnitude of the horizontal loads to be carried, the loads on individual raking piles may well vary quite substantially from those obtained by analysis. A conservative approach should therefore be used.
3. The performance of a vertical pile when subjected to a horizontal load is mainly controlled by the properties of the soil near the surface, for example, the upper three to five metres. Seasonal variations in moisture content may therefore be of significance. It may be beneficial to remove poor surface soil and replace it with well compacted gravel.
4. Repeated load applications may increase the lateral deflection to about twice that for constant loading.
5. If piles are driven into granular soils the soil stiffness is increased and thus the lateral soil resistance is increased.
6. There is considerable interaction between closely spaced piles in a group. For maximum lateral restraint, widely spaced piles are advisable, up to eight pile diameters in the direction of the load and about four pile diameters normal to the load.
7. The lateral deflections resulting from restrained piles are much smaller than those from similar free headed piles.
8. Further reference can be made to McNulty (1956), Clapham (1963), Reese and Matlock (1956), Broms (1964 a, b), Broms (1965a), Poulos (1971).

8 Pile testing

In this section, a brief review is given of methods which can be used to test piles. Pile loading tests are first discussed, followed by integrity testing.

8.1 Pile loading tests

Pile loading tests are carried out for the following reasons:

- To determine the settlement under working load
- To determine the ultimate bearing capacity
- As proof of acceptability.

There are two types of loading test which can be carried out, viz., the maintained load (ML) test, in which the loading is applied incrementally, and the constant rate of penetration (CRP) test.

In the ML test, the maximum load to be applied should be determined in advance, and the stages of the incremental loading, and unloading, should be prescribed. It is convenient to use increments of about 25% of the working load up to working load, with smaller increments thereafter. Each increment of load should be applied as smoothly and expediently as possible and simultaneous readings of time, and the load and settlement gauges are taken at convenient intervals as the load increases. For each loading increment, the loading should be held constant, and settlement readings taken at intervals of time which may be made progressively longer. A plot of settlement against time should be made as the test proceeds and the trend of the curve will indicate when movement has decreased to an acceptably small rate, which according to CP 200 4:1972 may be taken as 0.1 mm in 20 minutes. It is usual to include unloading stages in the programme and one unloading stage, from the working load, is often specified. It is desirable to hold the working load for a period of 24 hours.

The results of a maintained load test are shown in Fig.6.26, giving the curves of load and settlement versus time and of load versus the maximum settlement reached at each stage. The unloading stage is also plotted.

The maintained load test is commonly used to determine the ultimate bearing capacity of a pile. In practice, a well-defined failure load is not necessarily obtained and the following definitions of failure are often adopted:

- The failure load is that which causes settlement equal to 10% of the pile diameter, making allowance for the elastic shortening of the pile itself which may be significant for long piles
- The failure load is that at which the rate of settlement continues undiminished without further increment of load, unless, of course, the rate is so slow as to indicate that it is due to consolidation of soil
- The failure load is the load where the load settlement curve has its minimum radius of curvature
- Drawing tangents to the initial and final portions of the load settlement curve and taking the point of intersection as the failure load
- The failure load is that load which gives double the settlement for 0.8 of the failure load.

The ML test is time-consuming (because of having to wait until the rate of settlement drops to an acceptable value) and often the failure load is not clearly defined.

The CRP test has the advantage that it is quick and often results in a well-defined failure load. It has the disadvantage that it does not give the elastic settlement under the working load, which is of significance in determining whether or not there has been plastic yield of the soil at working load.

In the CRP test, the pile is jacked continuously into the soil, with the load being adjusted to give a constant rate of penetration. In this connection a pacing ring has been used to advantage. Failure is defined either as the load at which the pile continues to move downward without further increase in load, or the load at which the penetration reaches a value equal to 10% of the pile base diameter. It is important that the jack should have a travel greater than the sum of the final penetration of the pile and the upward movement of the reaction system. The movement

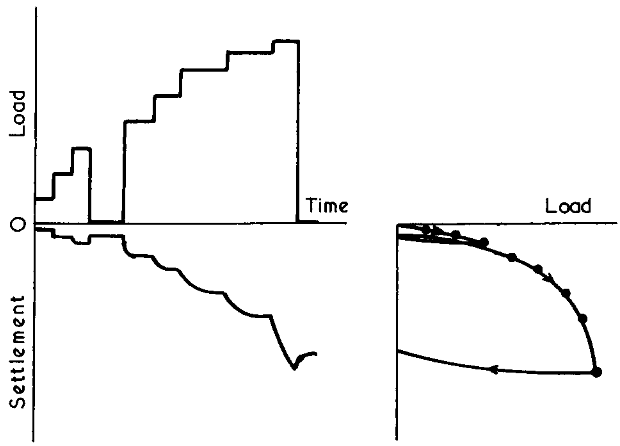

Fig. 6.26 Results of a maintained load pile test

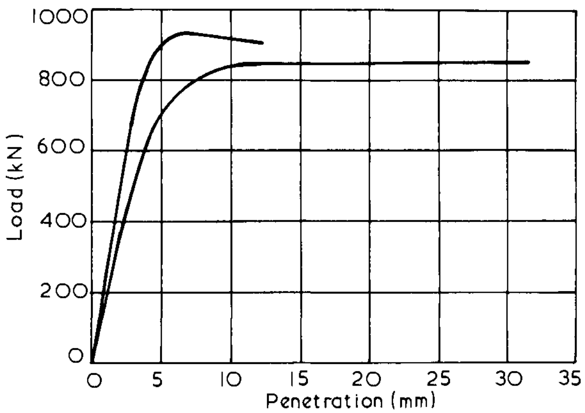

Fig.6.27 Load settlement curve for a friction pile

of the reaction system may be about 75 mm if kentledge is used and about 25 mm with tension piles. In an end bearing pile the penetration in a test may reach as much as 25% of the pile base diameter and for a friction pile about 10% of the shaft diameter. A rate of penetration of about 0.75 mm/min has been found suitable for friction piles in clay, for which the penetration to failure is likely to be less than 25 mm, while for end bearing piles in granular soils, where larger movements are necessary, rates of penetration of 1.5 mm/min may be required. Tests have shown that the actual rate of penetration, provided it is steady, may be half or twice these values without significantly affecting the result.

During the test, a plot of load against settlement should be made. The curve for a friction pile will be similar to those shown in Fig.6.27, usually a well-defined failure load at a small penetration, and for an end bearing pile as shown in Fig.6.28, a poorly-defined failure load at a large penetration.

The reaction for the loading can be applied either (a) using kentledge applied directly to the pile, or (b) by jacking against kentledge supported above the pile, or (c) by jacking against a beam tied down to tension piles. The supports in method (b) should be preferably more than 1.25 m away from the test pile, and in method (c) any anchor pile should be at least four test pile diameters from the test pile, centre to centre, and in no case less than 1.5 m. When testing piles with enlarged bases, the spacing should be twice the base diameter or four times the test pile shaft diameter, whichever is larger, from the centre of the test pile to the centre of any anchor pile.

With kentledge, loads of up to 5000 kN can be applied. It is important to ensure that the arrangement is stable and safe. The set-up should be properly designed, and inspected regularly during load application for signs of distress. Observations of horizontal movement of the system may give an early indication of instability. Kentledge normally cannot be used to test raking piles, and care should be taken when building up kentledge on sloping ground.

Using tension piles, loads of up to 15 000 kN have been applied, and for large loads in particular, tension piles may well provide a more economical solution than kentledge. It is difficult to line-up accurately two tension piles with a test pile, but the system may be stabilized by cross-braces. It may be preferable to use three or four tension piles per test pile. Working piles are not normally used as tension piles.

When measuring loads, it is advisable to use an hydraulic capsule (up to 4500 kN) or a load measuring column (up to 10 000 kN) or a proving ring. The height of the load measuring system should be kept as small as possible and the loading must be applied concentrically to the pile. A check on the load, for gross errors, may be obtained from the pressure gauge reading of the jack. Bourdon gauges are of low accuracy and should be regularly calibrated in a testing machine.

The settlements may be measured in the following ways:

(a) Direct levelling using a surveyor's level and staff to determine the movement of the pile head with reference to fixed datum. Preferably a check to a second datum should be carried out. A precision of reading of at least 1 mm is generally required
(b) Using dial gauges, measuring-off glass plates related to a reference beam supported on two foundations which are sufficiently far from the test pile and the reaction system to be unaffected by ground movement; the distance should not be less than 3 test pile diameters, or in no case less than 2 m. Readings should be taken to an accuracy of 0.02 mm and observations taken on at least two or preferably four points to check on any tilting.
(c) Using a strained high tensile wire, which is positioned against a scale fixed to the pile and the movement of the scale relative to the wire is determined to any accuracy of 0.5 mm.

Where methods (b) and (c) are used, protection of the beam or wire from sun and wind should be made. Regular temperature observations during the loading test should be carried out.

It is important that test piles are representative of the working piles, that is, they should be constructed in exactly the same manner as working piles. Furthermore, when evaluating test pile results, the fact that the soil conditions may well vary across the site should be considered. Finally, attention must be paid to time effects; sufficient time must be allowed between installation and testing for the soil conditions to be re-established around the pile, and it should be remembered that pile load tests are short-term, undrained tests, while working piles are loaded much more slowly. In this connection, reference can be made to Eide, Hutchinson and Landva (1961) who discussed the results of a long-term test loading of a friction pile in clay.

8.2 Integrity testing

There is increasing interest in methods which have been used to test the integrity of piles. Basically, methods are available which either test the pile material itself, or test the pile and soil together. Again, some methods require prior measures, while others do not. Some of the methods which are available are described in this section.

8.2.1 Pile loading tests

These have been discussed in some detail in section 8.1. From the point of view of integrity testing, they suffer from the following disadvantages (Davis and Dunn, 1974):

(a) They are expensive and time-consuming.

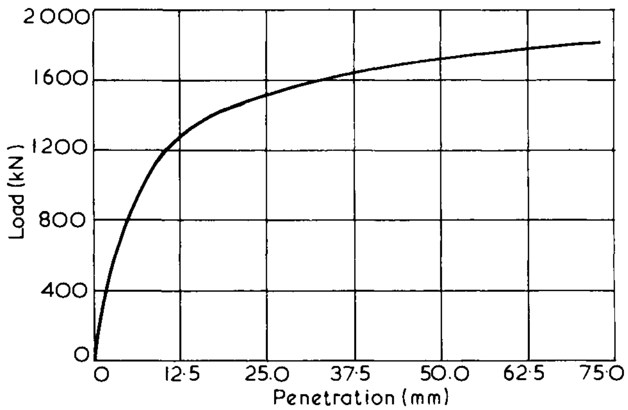

Fig. 6.28 Load settlement curve for an end bearing pile

(b) Because of (a), only a small number of piles is usually tested and this number is often not large enough to give statistically significant results.
(c) Because of (b), load tests can be regarded as measuring the performance of test piles only and do not serve to locate faulty piles.
(d) Test piles are seldom loaded up to failure.
(e) They are seldom carried out to determine the relative contributions of end resistance and skin friction.
(f) The test yields no information as to the actual dimensions of the pile under the ground; it only confirms that the pile is structurally strong enough to carry the test load without giving any measure of concrete quality.
(g) More care may be taken by the contractor in installing test piles than other piles so that results can be misleading.
(h) The pile is usually discarded after test and not included as part of the foundation.

8.2.2 Pile coring

Coring is the traditional method to check a suspect pile, by drilling using a diamond drill. Cores are collected from the axis of the pile and the composition of the cores examined to establish structural homogeneity. The process requires highly skilled and systematic workmanship and is expensive both in terms of time and money. To core drill a 10 m length of pile takes about two days. A caliper log of the drilled hole can also be made.

A much faster method, nowadays often used, is to drill holes in the pile by percussion equipment and then to examine the inner structure physically by lowering a television camera and watching the transmission on a screen. A 100 mm diameter hole, or perhaps a clean 50 mm diameter hole, is required. During drilling, the integrity of the pile can be roughly determined by the drill resistance and the composition and colour of the material blown out. The camera is necessary for confirmation and for those cases when the extent of discontinuity is small. The method is quick and about six 10 m long piles can be drilled and tested in a day.

8.2.3 Excavation

A well-established method used to examine piles is to set up headings under a foundation slab and observe the piles *in situ*. Timbering is required and care must be taken not to damage piles during excavation. A major disadvantage is that in general piles are only exposed down to the groundwater level. If groundwater lowering is contemplated, thought must be given to possible effects of settlement or negative skin friction, which may be induced. Exposed piles should be measured and photographed and the pile material thoroughly examined.

8.2.4 Stressing internally cast rods or cables (Moon, 1972)

In principle, the method is that of applying a compressive force over the length of the pile by the stressing of internally cast, and recoverable, rods or cables. If the pile is significantly weakened by any form of fault, this becomes apparent by a downward movement of the top, in the case of a fault near the top, or by greater elongation of the stressing element than that due to stressing alone, indicating an upward movement of a lower section in the case of faulting nearer the base. A pile may have imperfections, but satisfactory application of a test load equal to or greater than the required capacity would prove them insufficient to require the condemning of the pile. It has been estimated that the test would increase the cost of a bored pile by some 12%.

8.2.5 Vibration testing (Gardner and Moses, 1973; Davis and Dunn, 1974)

Vibration testing of piles has been developed by the Centre Experimental de Recherches et d'Etudes du Batiment et des Travaux Publics (CEBTP) of France and the technique has been used on a number of sites in the UK.

A generator supplies a sinusoidal current of frequency f which can be varied from 0 to

1000 Hz. This current drives an electrodynamic motor of mass M which is installed at the head of the pile. The motor vibrates vertically and exerts a force F on the head of the pile.

$$F = F_o \,.\, \sin wt = M \,.\, \gamma \qquad (6.37)$$

where $\gamma = \gamma_o \,.\, \sin wt$ being the acceleration of the mass M. A signal from the motor feeds a regulator which keeps γ_o constant. The head of the pile vibrates at the same frequency as the motor. The force constant F_o can be determined by measuring the amplitude of F at a known frequency f. If the instantaneous velocity of the pile head V is measured continuously, the value of the velocity constant V_o for any frequency can be determined from:

$$V = V_o \sin wt + K \qquad (6.38)$$

V_o/F_o is called the modulus of mechanical admittance.

During the test, the frequency is varied from 20 to 1000 Hz and an automatic plotter records the variation of V_o/F_o with f. The shape of the resulting graph depends upon the soundness of the pile, the rigidity of the end bearing and also the lateral restraint provided by the soil surrounding the pile.

The vibration method does not require any special provision to be made in the piles during casting. The pile heads require some preparation; the pile head must be level with the ground surface, and must be horizontal and smooth. The test will not detect minor defects but it is claimed that it will establish that a sound end bearing has been achieved and that the pile is free from major defects. Limitations on the use of the vibration test include a limiting length to diameter ratio of 20 and the requirement for the pile to be a right cylinder, although end bearing piles through soft alluvial deposits can be successfully tested with L/d ratios up to 30. It is necessary to test with no extraneous vibrations caused by site plant, which means testing at night on some sites. Also, if bulbs are formed at depth, it is usually impossible to learn anything about the state of the pile concrete below the bulb. The testing schedule need not interrupt the site programme, because between 25 and 40 piles can be tested per day, from pile ages of 4 days upwards.

It is claimed that the method can check or give a measure of:

- The pile length, or depth to first major discontinuity
- The weighted average pile cross-section
- The mass of the pile
- The damping effect of the soil surrounding the pile
- The apparent stiffness of the pile.

8.2.6 Sonic testing (Levy, 1970; Gardner and Moses, 1973)

The test is based on the measurement of time taken to pass sonic pressure waves horizontally between a transmitter and receiver. The transmitter and the receiver, which are made of piezo-electric ceramics, move within two (or three, for large piles) parallel, vertical, 42 mm diameter tubes cast into the pile. The tubes are first filled with water to ensure acoustic coupling and the transducers are raised within the tubes by a winch to keep them in the same horizontal plane. The difference in propagation times of the sound waves between the two tubes is represented as a linear trace on the oscilloscope. A zone of weak concrete is detected by a marked fainting of the signals and a sudden lengthening of the travel time. A Polaroid camera attached to the oscilloscope is used to obtain a permanent record of the results.

8.2.7 Radiometric logging (Forrester, 1974)

These techniques give information on properties of materials at the atomic level. Measurements are unaffected by the way in which constituent atoms are bound together. It is possible by the measurement of attenuation or scattering of gamma-rays that arise from radioactive sources to derive the density of concrete. The water content can be determined by the amount of moderation of fast neutrons by hydrogen.

Assuming that instrumental errors are small and that they can be kept to within 1%, the precision of density measurements by gamma-ray attenuation through concrete thicker than 200 mm depends on the distance of the source from the detector, the thickness of the concrete, the magnitude of the reading and the compaction of the concrete.

The measurement of the density of the concrete in a pile is a measure of its integrity. Measurement by attenuation of a gamma-ray involves the positioning of two vertical parallel tubes in the pile on a diameter. A source and a detector are lowered to the same level and the amount of attenuation of the radiation in the concrete is measured. This attenuation can be related to the density of the concrete. A 3% error in the density can arise from the variability of the source intensity and compositional changes in the solid component of the concrete examined can produce an apparent density error of 24%.

With the back-scatter technique the source and deduction are separated in a tubular probe by a lead block. The probe is lowered into a single tube pre-positioned vertically in the pile. Radiation from the source only reaches the detector by being scattered back from the tube and the concrete surrounding it. A sphere of concrete 100–150 m in diameter is surveyed by this technique and the errors in the estimation of the density can be up to 10%.

Excess water in the concrete can affect the estimation of the density because the attenuation and scattering of the gamma-rays by hydrogen is not in the same relative proportion as for other elements.

Water measurements by neutron moderation are carried out by a probe in a single tube. A radioactive isotope–light metal source generates fast neutrons and the slow neutrons produced by the interaction with hydrogen are measured by a selective detector. The probe has the generator and detector in one piece and the volume of concrete examined is a sphere of between 100–150 m in diameter. The precision of measurement can be within 10%.

Safety in handling these devices is covered by their having to comply with the standards prescribed in the Ionising Radiations (sealed sources) Regulations, 1969.

Bibliography

Aas, G., (1966). 'Baereevne av peler i frisksjonsjordarter'. Norsk Geoteknisk Forening Stipendium, (1956–66). Oslo, N.G.I.

Aldrich, H. P. (1952). 'Importance of net load to the settlement of buildings in Boston'. Contributions to S.M., (1941–53). Boston Society of Civil Engineers.

Alpan, I. (1964). 'Estimating the settlements of foundations on sand'. *Civ. Eng. and Public Works Rev.* Volume 59, pp.1415–1418.

Anderson, K. H. and Frimann Clausen, C. J. (1974). 'A 50 year settlement record of a heavy building on compressible clay'. Proceedings Conference on Settlement of Structures, Cambridge. pp.71–78.

Arthur, J. R. F. and Menzies, B. K. (1968). Correspondence on: 'A new soil testing apparatus'. *Geotechnique* Vol.18 pp.271–272.

Arthur, J. R. F. and Menzies, B. K. (1972). 'Inherent anisotropy in a sand'. *Geotechnique* Vol.22 No.1 pp.115–128.

Arthur, J. R. F. and Phillips, A. B. (1972). Discussion on: 'Inherent anisotropy in a sand'. *Geotechnique* Vol.22 pp.537–538.

A.S.C.E. (1941). The Committee on the Bearing Value of Pile Foundations. Pile Driving Formulae. Progress Report, A.S.C.E. Proceedings Vol.67, No.5, pp.853–866.

Atkinson, J. H. (1973). 'The deformation of undisturbed London clay'. Ph.D. Thesis. University of London.

Atkinson, J. H. (1974). Discussion on Session 4: 'The interpretation of field observations. Field instrumentation in geotechnical engineering'. Part 2, pp.677–679. Butterworths, London.

Bauer, C. E. A., Scott, J. D., and Shields, D. H. (1973). 'The deformation properties of a clay crust'. 8th Int. Conference Soil Mech. & Found. Eng., 1.1, pp.31–38.

Bazaraa, A. R. S. S. (1967). 'Use of the standard penetration test for estimating settlement of shallow foundations on sand'. Ph.D. Thesis, University of Illinois.

Berezantsev, U. G. (1961). 'Load bearing capacity and deformation of piled foundations.' 5th I.C.S.M.F.E., Paris, Vol.2, pp.11–12.

Berre, T. (1973). Sammenheng Mellom Tid, Deformasjoner og Spenninger for Normal-Konsoliderte Marine Leirer. Norwegian Geotechnical Institute, Publication No.97, pp.1–14.

Berre, T. and Bjerrum, L. (1973). 'Shear strength of normally consolidated clays.' 8th I.C.S.M.F.E., Moscow, Vol.1.1, pp.39–49.

Berre, T., Schjetne, K., and Sollie, S. (1969). 'Sampling disturbance of soft marine clays'. 7th I.C.S.M.F.E., Mexico, Special Session 1, pp.21–24.

Bishop, A. W. (1958). 'Test requirements for measuring the coefficient of earth pressure at rest'. Conference on earth pressure problems, Brussels Vol.1.

Bishop, A. W. (1959). 'The principle of effective stress.' Text of lecture to N.G.I. 1955, Teknisk Ukeblad 106: No.39, pp.859–863.

Bishop, A. W. (1966). Sixth Rankine Lecture: 'The strength of soils as engineering materials'. *Geotechnique* Vol 16, pp.89–130.

Bishop, A. W. (1966). 'Soils and soft rocks as engineering materials'. Inaugural lecture, Imperial College of Science and Technology.

Bishop, A. W. (1973). 'The influence of an undrained change in stress on the pore pressure in porous media of low compressibility'. *Geotechnique* Vol 23, No.3, pp.435–442.

Bishop, A. W. and Henkel, D. J. (1953). 'Pore pressure changes during shear in two undisturbed clays.' 3rd I.C.S.M.F.E., Zurich, Vol.1, pp.94–99.

Bishop, A. W. and Henkel, D. H. (1962). *The Measurement of Soil Properties in the Triaxial Test.* Edward Arnold (Publishers), Ltd, London.

Bishop, A. W., Garga, C. E., Andresen, A., and Brown, J. D. (1971). 'A new ring shear apparatus and its application to the measurement of residual strength.' *Geotechnique* Vol 21, pp.273–328.

Bjerrum, L. (1957). 'Norwegian experiences with steel piles to rock. *Geotechnique,* Vol.7, pp.1–24.

Bjerrum, L. (1963a). Generelle Krav til Fundamentering av Forskjellige Byggverk; Tillatte Setninger. N.I.F. Kurs in Fundamentering, Oslo. 17 p.

Bjerrum, L. (1963b). Discussion on Section 6. Euro. Conference S.M.F.E., Wiesbaden, Vol.2, pp.135–137. (Also N.G.I., Publication No.98.)

Bjerrum, L. (1964). Relasjon Mellom Målte og Beregnede Setninger av Byggverk på Leire og Sand. N.G.F. Foredraget, 1964. Norwegian Geotechnical Institute, Oslo 92 p.

Bjerrum, L. (1967). 'Engineering geology of Norwegian normally consolidated marine clays as related to settlements of buildings'. 7th Rankine Lecture, *Geotechnique,* Vol.17, pp.81–118.

Bjerrum, L. (1968). 'Secondary settlements of structures subjected to large variations in live load'. N.G.I. Publication No.73.

Bjerrum, L. (1972a). 'Embankments on soft ground'. A.S.C.E. Specialty conference on performance of earth and earth supported structures, Purdue University, 2, Lafayette, Indiana, pp.1–54.

Bjerrum, L. (1972b). 'The effect of rate of loading on the p_c' value observed in consolidation tests on soft clay.' Norwegian Geotechnical Institute Publication No.95.

Bjerrum, L. (1973). 'Problems of soil mechanics and construction on soft clays'. 8th I.C.S.M.F.E., Moscow, Vol.3, pp.111–159.

Bjerrum, L. and Eggestad, A. (1963). 'Interpretation of loading tests on sand'. Euro. C.S.M.F.E., Wiesbaden, Vol.1, pp.199–204.

Bjerrum, L. and Eide, O. (1966). Anvendelse av Kompensert Fundamentering i Norge. N.G.I., Publication No.70.

Bjerrum, L. and Simons, N. E. (1960). 'Comparison of shear strength characteristics of normally consolidated clays'. Proceedings of research conference on shear strength of cohesive soils, pp.711–724. Boulder, Colorado.

Bjerrum, L. and Øverland, A. (1957). 'Foundation failure of an oil tank in Frederikstad, Norway'. 4th I.C.S.M.F.E., London, Vol.I, pp.287–290.

Bjerrum, L., Johannessen, I. J., and Eide, O. (1969). 'Reduction of negative skin friction on steel piles to rock'. 7th I.C.S.M.F.E., Mexico, Vol.2, pp.27–34.

Bjerrum, L., Simons, N. E., and Torblaa, I. (1958). 'The effect of time on the shear strength of a soft marine clay.' Proceedings of Brussels conference on earth pressure problems, Vol.1, pp.148–158.

Boussinesq, J. (1885). *Application des Potentiels a l'etude de l'equilibre et du Mouvement des Slides Elastiques* Gauthier-Villard Paris.

Bratchell, G. E., Leggatt, A. J., and Simons, N. E. (1974). 'The performance of two large oil tanks founded on compacted gravel at Fawley, Southampton, Hampshire'. Proceedings of conference on settlement of structures, Cambridge, pp.3–9.

Brinch, Hansen J. (1955). 'Simpel Beregning of Fundamenters Baereevne'. *Ingeniøren,* Vol.4, pp.95–100.

Brinch, Hansen J. (1968). 'A revised and extended formula for bearing capacity'. Bulletin No.28, Danish Geotechnical Institute.

British Steel Piling Company, Ltd. (1969). The B.S.P. pocket book.

Broms, B. B. (1964a). 'Lateral resistance of piles in cohesive soils'. P.A.S.C.E., J.S.M.F.D., S.M.2, pp.27–63.

Broms, B. B. (1964b). 'Lateral resistance of piles in cohesionless soils'. P.A.S.C.E., J.S.M.F.D., S.M.3, pp.123–156.

Broms, B. B. (1965a). 'Design of laterally loaded piles'. P.A.S.C.E., J.S.M.F.D., S.M.3, pp.79–99.

Broms, B. B. (1965b). 'Methods of calculating the ultimate bearing capacity of piles: a summary.' *Sols-Soils,* Vol.5, No.18–19, pp.21–32.

Brown, J. D. (1968). General Report. Proceedings Bolkesjø Symposium on shear strength and consolidation of normally consolidated clays, pp.2–8.

Buisman, A. S. K. (1936). 'Results of long duration settlement tests'. 1st I.C.S.M.F.E., Rotterdam, Vol.1, pp.100–106.

Buisson, M., Ahee, J., and Habil, P. (1960). Le Frottement Négatif. Institut Technique de bâtiment et des Travaux Publics. Annales, Vol.13, No.145, Supplement, pp.30–46.

Burland, J. B. (1973). 'Shaft friction of piles in clay – a simple fundamental approach.' *Ground Eng.,* Vol.6, No.3, pp.30–42.

Burland, J. B. and Cooke, R. W. (1974). 'The design of bored piles in stiff clays.' *Ground Eng*., Vol.7, No.4, pp.28–35.

Burland, J. B. and Wroth, C. P. (1974). General Report – session 5. Conference on settlement of structures, Cambridge.

Burland, J. B., Butler, F. G., and Dunican, P. (1966). 'The behaviour and design of large diameter bored piles in stiff clay. Large bored piles.' I.C.E., London, pp.51–71.

Burland, J. B., Sills, G. C., and Gibson, R. E. (1973). 'A field and theoretical study of the influence of non-homogeneity on settlement.' 8th I.C.S.M.F.E., 1.3, pp.39–46.

Butler, F. G. (1974). General Report and State of the Art Review, Session 3: 'Heavily over-consolidated clays'. Proceedings of conference on settlement of structures, Cambridge.

Butler, F. G. and Morton, K. (1971). 'Specification and performance of test piles in clay'. Conference on behaviour of piles, I.C.E., London, pp.17–26.

Calhoon, M. L. (1972). Discussion on D'Appolonia, Poulos and Ladd (1971). J.S.M.F.D., A.S.C.E., 98 S.M.3. pp.306–308.

Carrier, W. D., and Christian, J. T. (1973). 'Rigid circular plate resting on a non-homogeneous elastic half-space'. *Geotechnique* Vol.23, pp.67–84.

Casagrande, A. (1936). 'The determination of the pre-consolidation load and its practical significance'. 1st C.S.M.F.E., Volume 3 Cambridge.

Casagrande, A. and Carillo, N. (1944). 'Shear failure of anisotropic materials'. Proc. Boston Soc. of Civ. Eng., Vol.31, pp.74–87.

Casagrande, A. and Fadum, R. E. (1942). 'Application of soil mechanics in designing building foundations'. A.S.C.E. Proc., Vol.68, pp.1487–1520.

Chang, Y. C. E., Broms, B., and Peck, R. B. (1973). 'Relationship between the settlement of soft clays and excess pore pressure due to imposed loads.' 8th I.C.S.M.F.E., Vol.1.1, pp.93–96.

Chellis, R. D. (1941). 'Discussion on pile driving formulae'. Progress Report, Committee on the bearing value of pile foundations. A.S.C.E., Proceedings, Vol.67, No.8, pp.1517–1537.

Clapham, H. G. (1963). 'The effect of lateral loads on embedded piles'. D.I.C. Dissertation, University of London. 117 p.

Clayton, C. R. I. (1973). 'The secondary compression of clays.' M.Sc. Thesis, Imperial College, London.

Cole, K. W. and Burland, J. B. (1972). 'Observations of retaining wall movements associated with a large excavation'. Proc. 5th European conference, S.M. & F.E., Madrid 1, pp.445–453.

Cowley, B. E., Haggar, E. G. and Larnach, W. J. (1974). A comparison between the observed and estimated settlements of three large cold stores in Grimsby'. Conference on settlement of structures, Cambridge, pp.79–90.

Cummings, A. E. (1940). 'Dynamic pile driving formulae.' Contributions to soil mechanics, (1925–1940). *J. Boston Soc of Civ Eng,* pp.392–413.

D'Appolonia, D. J. and Lambe, T. W. (1971). 'Floating foundations for control of settlement.' J.S.M.F.D., A.S.C.E., Vol.97, S.M.6, pp. 899–915.

D'Appolonia, D. J., D'Appolonia, E., and Brisette, R. F. (1968). 'Settlement of spread footings on sand'. A.S.C.E., J.S.M.F.D., S.M.3, pp.735–760.

Davis, A. G. and Dunn, C. S. (1974). 'From theory to field experience with the non-destructive vibration testing of piles'. Seminar on concrete pile testing. C and CA, Fulmer.

Davis, E. H. and Poulos, H. G. (1968). 'The use of elastic theory for settlement prediction under three-dimensional conditions'. *Geotechnique* Vol.18, pp.67–91.

de Beer, E. E. (1965). 'Bearing capacity and settlement of shallow foundations on sand.' Proc. Symposium on bearing capacity and settlement of foundations, Duke University, pp.15–33.

de Beer, E. E. and Martens, A. (1951). Method of computation of an upper limit for the influence of heterogeneity of sand layers on the settlement of bridges'. 4th I.C.S.M.F.E., London, Vol.1, pp.275–281.

D'Elia, B. and Grisolia, M. (1974). 'On the behaviour of a partially floating foundation on normally consolidated silty clays.' Proc. conference on settlement of structures, Cambridge, pp.91–98.

Den Norske Pelekomite (1973). Veiledning ved pelefundamentering. Norwegian Geotechnical Institute, Veiledning No.1.

Eide, O. (1972). Personal communication.

Eide, O., Hutchinson, J. N., and Landva, A. (1961). 'Short and long term test loading of a friction pile in clay.' 5th I.C.S.M.F.E., Paris.

Endo, M., Minau, A., Kawaski, T., and Schibata, T. (1969). 'Negative skin friction acting on steel pipe pile in clay'. 7th I.C.S.M.F.E., Mexico, Vol.2, pp.85–92.

Engesgaar, H. (1970). *Resultater av to Belastningsforsøk på Sundland i Drammen.* Norwegian Geotechnical Institute Publication No.84.

Engesgaar, H. (1973). '15 storey building on plastic clay in Drammen, Norway'. 8th I.C.S.M.F.E., Moscow, Vol.1.3, pp.75–80.

Fadum, R. E. (1948). 'Influence values for estimating stresses in elastic foundations'. 2nd I.C.S.M.F.E., Rotterdam, Vol.3, pp.77–84.

Fellenius, B. H. and Broms, B. B. (1969). 'Negative skin friction for long piles driven in clay'. 7th I.C.S.M.F.E., Mexico, Vol.2, pp.92–98.

Flaate, K. (1964). *An investigation of the Validity of Three Pile Driving Formulae in Cohesionless Materials.* N.G.I. Publication No.56, pp.11–22.

Flaate, K. (1968). Baereevne av Friksjonspeler i Leire; om Beregning av Baereevne på grunnlag av Geotekniske Undersøkelser. Oslo, Veglaboratoriet, 38 p., mimeographed.

Forrester, J. (1974). 'Radiometric logging'. Seminar on concrete pile testing, C and CA, Fulmer.

Foss, I. (1969). 'Secondary settlements of buildings in Drammen', Norway, 7th I.C.S.M.F.E., Mexico, Vol.2, pp.99–106.

Fox, E. N. (1948). 'The mean elastic settlement of uniformly loaded area at a depth below ground surface.' 2nd I.C.S.M.F.E., Rotterdam, Vol 1, pp.129.

Frimann Clausen, C. J. (1969). 'Loading test, Mastemyr'. Proc. Bolkesjø symposium on shear strength and consolidation of normally consolidated clays, pp.42–44.

Frimann Clausen, C. J. (1970). *Resultater av et Belastningsforsøk på Mastemyr i Oslo.* Norwegian Geotechnical Institute Publication No.84, pp.29–40.

Gant, E. V., Stephens, J. E., and Moulton, L. K. (1958). 'Measurement of forces produced in piles by settlement of adjacent soil'. Highway Research Board Bulletin 173, pp 20–45.

Gardner, R. P. M. and Moses, G. W. (1973). 'Testing bored piles formed in laminated clays.' *Civ. Eng. and Public Works Rev.*, pp.60–63.

Garlanger, J. E. (1972). 'The consolidation of soils exhibiting creep under constant effective stress'. *Geotechnique,* Vol.2, No.2, pp.141–161.

Gibbs, H. J. and Holtz, W. G. (1957). 'Research on determining the density of sands by spoon penetration testing'. 4th I.C.S.M.F.E., London, Vol.1, pp.35–39.

Gibson, R. E. (1967). 'Some results concerning displacements and stresses in a non-homogeneous elastic half-space'. *Geotechnique* Vol.17, pp.58–67.

Gibson, R. E. (1974). Fourteenth Rankine lecture: 'The analytical method in soil mechanics'. *Geotechnique* Vol 24 No.2. pp.113–140.

Gibson, R. E. and Sills, G. C. (1971). 'Some results concerning the plane deformation of a non-homogeneous elastic half-space'. Proc. Roscoe Memorial conference on stress–strain behaviour of soils, pp.564–572.

Gielly, L., Lareal, P., and Sanglerat, G. (1970). 'Correlations between *in situ* penetrometer tests and the compressibility characteristics of soils'. Proc. conference on *in situ* invest. in soils and rocks, London, pp.167–172.

Golder, H. Q. (1965). 'State of the art of floating foundations'. J.S.M.F.D., A.S.C.E., Vol.31, S.M.2, Proceeding Paper 4278, pp.81–88.

Golder, H. Q. and Willeimier, G. C. (1964). 'Design of the main foundations of the Port Mann Bridge', *Eng. J. Canad*, Vol.47, No.8, pp.22–29.

Greulich, G. G. (1941). 'Discussion on pile driving formulae,' Progress report, Committee on the bearing value of pile foundations, Proc., Vol.67, No.7, pp.1391–1396.

Hiley, A. E. (1925). 'A rational pile driving formula and its application in practice explained'. Eng., Vol 119, p.657.

Hobbs, N. B. (1971). 'The Menard pressuremeter – *in situ* loading tests in soils and rocks.' Summer school in foundation engineering, University of Surrey.

Hutchinson, J. N. (1963). 'Settlements in soft clay around a pumped excavation in Oslo'. Euro. C.S.M.F.E., Wiesbaden, Vol.1, pp.119–126.

Hutchinson, J. N. and Jensen, E. V. (1968). 'Loading tests on piles driven into estuarine clays at Port of Khorramshav, and observations on the effect of bitumen coatings on shaft bearing capacity'. N.G.I., Publication No.78.

Høeg, K., Andersland, O. B., and Rolfsen, E. N. (1969). 'Undrained behaviour of quick clay under load tests at Åsrum . *Geotechnique* Vol 19, pp.101–115.

James, P. M. (1970). 'The behaviour of a soft recent sediment under embankment loadings.' *J. of Eng. Geology*, Vol.3, pp.41–53.

Janbu, N. (1953). 'Une analyse energetique du battage des pieux a l'aide de paramtres sans dimension'. Institut Technique du Batiment et des Travoux Publics. Annales, No.63–64. (also N.G.I. Publication No.3).

Janbu, N. (1963). 'Soil compressibility as determined by oedometer and triaxial tests'. European conference S.M.F.E., Wiesbaden, Vol.1, pp.19–25.

Janbu, N. (1969). 'The resistance concept applied to deformations of soils'. Proc. 7th I.C.S.M.F.E., Mexico, Vol.1, pp.191–196.

Janbu, N. and Senneset, K. (1973). 'Field compressometer – principles and applications'. Proc. 8th I.C.S.M.F.E., 1.1, pp.191–198.

Janbu, N., Bjerrum, L., and Kjaernsli, B. (1956). Veiledning ved Løsning av Fundamenteringsoppgaver. N.G.I. Publication No.16. 93 p

Jarrett, P. M., Stark, W. G., and Green, J. (1974). 'A settlement study within a geotechnical investigation of the Grangemouth area'. Conference on settlement of structures, Cambridge, pp.99–105.

Johannessen, I. J. and Bjerrum, L. (1965). 'Measurement of the compression of a steel pile to rock due to settlement of the surrounding clay.' 6th I.C.S.M.F.E., Montreal, Vol.2, pp.261–264.

Koppejan, A. W. (1948). 'A formula combining the Terzaghi load-compression relationship and the Buisman secular time effect'. 2nd I.C.S.M.F.E., Vol.3, pp.32–37.

Kummeneje, O. (1955). 'Fundamentering av oljetank i Drammen'. *Bygg*, Vol.3, No.9, pp.239–243. (also N.G.I. Publication No.12).

Ladd, C. C. (1964). 'Stress–strain modulus of clay in undrained shear'. A.S.C.E. Proceedings 90, S.M.5, pp.103–132.

Ladd, C. C. (1969). 'The prediction of *in-situ* stress–strain behaviour of soft saturated clays during undrained shear. Bolkesjø symposium on shear strength and consolidation of normally consolidated clays, pp.14–19. Norwegian Geotechnical Institute, Oslo.

Lambe, T. W. (1964). 'Methods of estimating settlement'. J.S.M.F.D., A.S.C.E., 90, No.SM5, pp.43–67.

Lambe, T. W. (1973a). 'Predictions in soil engineering'. *Geotechnique* Vol.23, pp.151–202.

Lambe, T. W. (1973b). 'Up-to-date methods of investigating the strength and deformability of soils. (Laboratory and field testing of soils for their strength, deformative and rheological properties). Proceedings 8th I.C.S.M.F.E., 3, pp.3–43.

Lambe, T. W. and Whitman, R. V. (1969). *Soil Mechanics.* John Wiley and Sons, Inc. 553 p.

Levy, J. F. (1970). Sonic pulse method of testing cast *in situ* concrete piles'. *Ground Eng.*, Vol.3, No.3, pp.17–19.

Liu, T. K. and Dugan, J. P. (1974). Elastic settlement behaviour of three steel storage tanks' Conference on Settlement of Structures, Cambridge, pp.106–109.

Lo, K. Y. (1965). 'Stability of slopes in anisotropic soils'. Proceedings A.S.C.E., 91, S.M.4, pp.85–106.

Lysmer, J. and Duncan, J. M. (1972). *Stresses and Deflections in Foundations and Pavements.* Department of Civil Engineering, University of California, Berkeley, 5th Edition.

Madhloom, A. A. W. A. (1973). 'The undrained shear strength of a soft silty clay from Kings Lynn, Norfolk'. M.Phil. Thesis, University of Surrey.

Marsland, A. (1971,a). 'Large *in situ* tests to measure the properties of stiff fissured clays.' Proceedings First Australia–New Zealand Conference on geomechanics, Melbourne, pp.180–189.

Marsland, A. (1971,b). 'The shear strength of stiff fissured clays'. Proceedings of Roscoe Memorial symposium on stress–strain behaviour of soils, Cambridge, pp.59–68.

Marsland, A. (1971,c). 'Laboratory and *in situ* measurements of the deformation moduli of London clay.' Proceedings symposium on the interaction of structure and foundation, Midland Soil Mechanics and Foundation Engineering Society, Department of Civil Engineering, University of Birmingham, pp.7–17.

McNulty, J. F. (1956). 'Thrust loading on piles'. A.S.C.E., J.S.M.F.D., Proceedings Paper 940, No.SM2.

Meigh, A. C. (1963). 'Discussion on settlements on granular soils'. Euro. C.S.M.F.E., Wiesbaden, Volume 2, pp.71–72.

Meigh, A. C. and Corbett, B. O. (1970). 'A comparison of *in situ* measurements on a soft clay with laboratory tests and the settlement of oil tanks'. Proceedings of Conference *in situ* investigations in soil and rocks, pp.173–179.

Meigh, A. C. and Nixon, I. K. (1961). 'Comparison of *in situ* tests for granular soils'. 5th I.C.S.M.F.E., Paris, Vol.1, pp.499.

Meyerhof, G. G. (1953). 'The bearing capacity of foundations under eccentric and inclined loads'. 3rd I.C.S.M.F.E., Zurich, Vol.1, pp.440–445.

Meyerhof, G. G. (1956). 'Penetration tests and bearing capacity of cohesionless soils'. A.S.C.E., J.S.M.F.D., Vol 82, S.M.1.

Meyerhof, G. G. (1959). 'Compaction of sands and bearing capacity of piles.' A.S.C.E., J.S.M.F.D., S.M.6, pp.1–29.

Meyerhof, G. G. (1965). 'Shallow foundations'. A.S.C.E., J.S.M.F.D., Vol.91, S.M.2, pp.21–31.

Moon, M. R. (1972). 'A test method for the structural integrity of bored piles'. *Civ. Eng. and Public Works Rev.*, pp.476–480.

Moran, Proctor, Meuser, and Rutledge (1958). 'Study of deep soil stabilization by vertical sand drains'. Report for Bureau of Yards and Docks. Department of the Navy.

Murray, R. T. (1971). 'Embankments constructed on soft foundations; settlement study at Avonmouth.' Report No.419, Crowthorne, 26 p.

Newmark, N. M. (1942). 'Influence charts for computation of stresses in elastic soils.' University of Illinois, Eng. Experimental Station Bull. No.338.

Nordin, P. Q. and Svensson, L. (1974). 'Settlements of buildings founded on lightly over-consolidated clay in Western Sweden'. Conference on settlement of structures, Cambridge, pp.116–122.

Nordlund, R. L. (1959). 'Bearing capacity of piles in cohesionless soils'. P.A.S.C.E., J.S.M.F.D., S.M.3, pp.1–35.

Palmer, D. J. and Stuart, J. G. (1957). 'Some observations on the standard penetration test and a correlation of the test with a new penetrometer'. 4th I.C.S.M.F.E., Vol.1, pp.231–236.

Parry, R. H. G. (1971). 'A direct method of estimating settlements in sands from SPT values.' Proceedings symposium interaction of structure and foundations, Midlands S.M.F.E. Society, Birmingham, pp.29–37.

Peck, R. B (1958). 'Study of comparative behaviour of friction piles'. Highway Research Board, Special Report 36, 72 p.

Peck, R. B. (1962). 'Art and science in subsurface engineering'. *Geotechnique,* Vol.12, pp.60–68.

Peck, R. B. and Bazaraa, A.R. S. S. (1969). Discussion. A.S.C.E., J.S.M.F.D., Vol.95, S.M.3, pp.305–309.

Peck, R. B., Hanson, W. E., and Thornburn, T. H. (1974). *Foundation Engineering,* John Wiley and Sons, Inc., 514 p.

Plantema, G., and Nolet, C. A. (1957). 'Influence of pile driving on the sounding resistances in a deep sand layer'. 4th I.C.S.M.F.E., London, Vol.2, pp.52–55.

Poulos, H. G. (1971). 'Behaviour of laterally loaded piles'. Proceedings A.S.C.E., J.S.M.F.D., S.M.5, pp.711–731 (Part 1. single piles); pp.733–751 (Part 2, pile groups).

Poulos, H. G. and Davis, E. H. (1974). *Elastic Solutions for Soil and Rock Mechanics.* John Wiley & Sons, Inc.

Poulos, H. G. and Mattes, N. S. (1969). 'The analysis of downdrag in end bearing piles. 7th I.C.S.M.F.E., Mexico, Vol.2, pp.203–209.

Raymond, G. P., Townsend, D. L., and Lojkasek, M. J. (1971). 'The effect of sampling on the undrained soil properties of a Leda soil'. *Canadian Geotechnical J.*, Vol.8, pp.546–557.

Reese, L. C. and Matlock, H. (1956). 'Non-dimensional solutions for laterally loaded piles with soil modulus assumed proportional to depth.' 8th Texas C.S.M.F.E., Special Publication No.29, University of Texas.

Rodih, S. (1961). 'Experiences with penetrometers with particular reference to the standard penetration test'. 5th I.C.S.M.F.E., Paris, Vol.1, p.517.

Rodriques, J. S. (1975). 'The development and application of a finite element program for the solution of geotechnical problems'. Ph.D. Thesis, University of Surrey.

Rowe, P. W. (1968). 'The influence of geological features of clay deposits on the design and performance of sand drains'. I.C.E. London Proceedings, Supplement Paper 70585, 72 p.

Rowe, P. W. (1972). 'The relevance of soil fabric to site investigation practice'. 12th Rankine lecture. *Geotechnique,* Vol.22, No.2, pp.195–300.

Rowe, P. W. and Barden, L. (1965). Closure to discussion on: 'Importance of free ends in triaxial testing' *J. Soil Mechanics and Foundation Div.* A.S.C.E.91, pp.105–106.

Rowe, P. W. and Barden, L. (1966). 'A new consolidation cell'. *Geotechnique,* Vol.16, pp.162–170.

Rutledge, P. C. (1944). 'Relation of undisturbed sampling to laboratory testing'. *Trans. A.S.C.E.,* Vol.109.

Sanglerat, G. (1972). *The Penetrometer and Soil Exploration.* Elsevier-North Holland, 464 p.

Sanglerat, G., Girousse, H., and Gielly, J. (1974). 'Usual settlements of a building at Nantua (France)'. Conference on settlement of structures, Cambridge, pp.123–131.

Sawaguchi, M. (1971). 'Approximate calculation of negative skin friction of a pile'. *Soils and Foundations,* Vol.2, No.3, pp.31–49.

Schmertmann, J. H. (1953). 'Estimating the true consolidation behaviour of clay from laboratory test results'. Proceedings A.S.C.E., Vol.79, Separate No.311.

Schmertmann, J. H. (1955). 'The undisturbed consolidation behaviour of clay.' Trans. A.S.C.E. No.120, Paper 2775, pp.1201–1233.

Schmertmann, J. H. (1970). 'Static cone to compute static settlement over sand.' A.S.C.E., J.S.M.F.D., Vol.98, S.M.3, pp.1011–1043.

Serota, S. and Jennings, R. A. J. (1959). 'The elastic heave of the bottom of excavations'. *Geotechnique* Vol.9 No.1, pp.62–70.

Simons, N. E. (1957). 'Settlement studies on two structures in Norway.' 4th I.C.S.M.F.E., London, Vol.1, pp.431–436.

Simons, N. E. (1963). 'Settlement studies on a nine storey apartment building at Økernbråten, Oslo.' Euro. Conference S.M.F.E., Wiesbaden, Vol.1, pp.179–191.

Simons, N. E. (1967). Discussion, proc. geotechnical conference Oslo, Session 2: shear strength of stiff clay, pp.159–160.

Simons, N. E. (1971a). 'The stress path method of settlement analysis applied to London clay.' Proceedings Roscoe Memorial symposium on stress–strain behaviour of soils, Cambridge, pp.241–252.

Simons, N. E. (1971b). Discussion, Conference on behaviour of piles, I.C.E., London, p.94.

Simons, N. E. (1974). General Report, Session 2, Conference on settlement of structures, Cambridge, (Proceedings to be published).

Simons, N. E. and Huxley, M. A. (1975). 'The effect of negative skin friction on the bearing capacity of piles in granular soils.' (to be published).

Simons, N. E. and Menzies, B. K. (1974). 'A note on the principle of effective stress.' *Geotechnique* Vol.24, pp.259–261.

Simons, N. E. and Som, N. N. (1969). 'The influence of lateral stresses on the stress deformation characteristics of London clay.' 7th I.C.S.M.F.E., Mexico City, Vol.1, pp.369–377.

Simons, N. E. and Som, N. N. (1970). 'Settlement of structures on clay with particular emphasis on London clay.' Constr. Industry Research Institute Assoc. Report 22, 51 p.

Simons, N. E., Rodrigues, J., and Hornbsy, P. A. (1974). Discussion, Conference on settlement of structures, Cambridge.

Skempton, A. W. (1951). 'The bearing capacity of clays.' Building Research Congress, England.

Skempton, A. W. (1953). Discussion, 3rd I.C.S.M.F.E., Zurich, Vol.3, p.172.

Skempton, A. W. (1954). The pore pressure coefficients *A* and *B*. *Geotechnique* Vol 4, pp.143–147.

Skempton, A. W. (1959). 'Cast *in situ* bored piles in London clay.' *Geotechnique,* Vol.9, No.4, pp.153–173.

Skempton, A. W. (1961). 'Horizontal stresses in over-consolidated eocene clay.' 5th I.C.S.M.F.E., Vol.1, pp.351–357.

Skempton, A. W. (1964). Fourth Rankine lecture: 'Long-term stability of clay slopes'. *Geotechnique* Vol 14, pp.77–101.

Skempton, A. W. (1966). Summing-up. Proceedings symposium on large bored piles, I.C.E., London, pp.155–157.

Skempton, A. W. and Bishop, A. W. (1954). 'Soils', Chapter 10 of *Building Materials, their Elasticity and Inelasticity.* North Holland Publishing Company, Amsterdam.

Skempton, A. W. and Bjerrum, L. (1957). 'A contribution to the settlement analysis of foundations on clay.' *Geotechnique,* Vol.7, No.4, pp.168–178.

Skempton, A. W., and MacDonald, D. H. (1956). 'The allowable settlement of buildings'. *Proc. I.C.E.,* Vol.5, No.3, Pt.3, pp.737–784.

Skempton, A. W., and Sowa, V. A. (1963). 'The behaviour of saturated clays during sampling and testing.' *Geotechnique* Vol 13, pp.269–290.

Skempton, A. W., Peck, R. B., and MacDonald, D. H. (1955). 'Settlement analyses of six structures in Chicago and London.' *Proc. I.C.E.,* Part 1, Vol.4, No.4, p.525.

Som, N. N. (1968). 'The effect of stress path on the deformation and consolidation of London clay.' Ph.D. Thesis, University of London.

Somerville, S. H. and Shelton, J. C. (1972). 'Observed settlement of multi-storey buildings on laminated clays and silts in Glasgow.' *Geotechnique*, Vol.22, pp.513–520.

Steinbrenner, W. (1934). Tafeln zur Setzungberechnung. Die Strasse, Vol.1, p.121.

Sutherland, H. B. (1963). 'The use of *in situ* tests to estimate the allowable bearing pressure of cohesionless soils.' *Struct. Eng.,* Vol.41, No.3.

Sutherland, J. B. (1974). General Report. Session 1, Conference on settlement of structures, Cambridge.

Teng, W. C. (1962). *Foundation Design.* Prentice Hall, New Jersey.

Terzaghi, K. (1936). 'Settlement of structures'. 1st I.C.S.M.F.E., Vol.3, pp.79–87.

Terzaghi, K. (1939). 'Soil mechanics – a new chapter in engineering science'. James Forrest Lecture. *Journal I.C.E.,* No.7, pp.106–141.

Terzaghi, K. (1941). 'Undisturbed clay samples and undisturbed clays. *J. Boston Soc of Civ. Eng,* Vol.28, No.3, pp.211–231.

Terzaghi, K. (1943). *Theoretical Soil Mechanics.* John Wiley and Sons Ltd., 510 p.

Terzaghi, K. (1948). Closing Discussion on; 'Foundation pressure and settlements of buildings on footings and rafts. 2nd I.C.S.M.F.E., Rotterdam, Vol.6, p.118.

Terzaghi, K. and Peck, R. B. (1948). *Soil Mechanics in Engineering Practice.* 1st edition, New York, Wiley.

Terzaghi, K. and Peck, R. B. (1967). *Soil Mechanics in Engineering Practice.* 2nd edition, New York, Wiley, 729 p.

Timoshenko, S. and Goddier, J. N. (1951). *Theory of Elasticity*, McGraw Hill.

Tomlinson, M. J. (1957). 'The adhesion of piles driven in clay soils.' 4th I.C.S.M.F.E., London, Vol.2, pp.66–71.

Tomlinson, M. J. (1969). *Foundation Design and Construction.* Pitman Publishing, 2nd edition, p.785.

Tomlinson, M. J. (1970). 'Research on the skin friction of piles driven into stiff clays.' C.I.R.I.A. research report.

Tomlinson, M. J. (1971). 'Some effects of pile driving on skin friction.' Conference on behaviour of piles, I.C.E., London, pp.107–114.

Vargas, M. (1955). 'Foundation of structures on over-consolidated clay layers in Sao Paulo.' *Geotechnique,* Vol.5, pp.253–266.

Vefling, G. (1974). 'Settlements of three heavy sugar silos in Italy.' Conference on settlement of structures, Cambridge, pp.132–138.

Walker, L. K. and Darval, P. L. P. (1973). 'Dragdown on coated and uncoated piles.' 8th I.C.S.M.F.E., Moscow, Vol.2.1, pp.257–262.

Ward, W. H. (1961). 'Displacements and strains in tunnels beneath a large excavation in London.' 5th I.C.S.M.F.E., Paris Vol2, pp.749–753.

Ward, W. H. (1971). 'Some field techniques for improving site investigations and engineering design.' Proc. Roscoe Memorial symposium on stress strain behaviour of soils, pp.676–682.

Ward, W. H., Burland, J. B., and Gallois, R. W. (1968). 'Geotechnical assessment of a site at Mundford, Norfolk, for a large proton accelerator'. *Geotechnique* Vol.18, pp.399–431

Whitaker, T. (1970). *The Design of Piled Foundations.* Pergamon Press, 188 p.

Whitaker, T. and Cooke, R. W. (1966). 'An investigation of the shaft and base resistance of large bored piles in London clay'. Large bored piles. I.C.E., London, pp.7–49.

Wilkes, P. F. (1974). 'A geotechnical study of a trial embankment at Kings Lynn.' Ph.D. Thesis, University of Surrey.

Woodward, R. J., Lundgren, R., and Boitano, J. D. (1961). 'Pile loading tests in stiff clays. 5th I.C.S.M.F.E., Paris, Vol.2, pp.177–184.

Wroth, C. P. and Simpson, B. (1972). 'An induced failure of a trial embankment. Part 2: finite element computations. Purdue conference on performance of earth and earth supported structures, Vol.1.1, pp.65–79.

Zeevaert, L. (1957). 'Foundation design and behaviour of Tower Latino Americana in Mexico City.' *Geotechnique*, Vol.7, pp.115–133.

Zeevaert, L. (1958). 'Consolidation of Mexico City's volcanic clay.' Proceedings of conference on soils for engineering purposes, A.S.T.M. – S.T.P., No.232, p.28.

Zeevaert, L. (1960). 'Reduction of point bearing capacity of piles because of negative friction.' Proceedings 1st Pan American C.S.M., Mexico, Vol.3, pp.1145–1152.

Index